

SEISMIC MARGIN REVIEW
MIDLAND ENERGY CENTER PROJECT

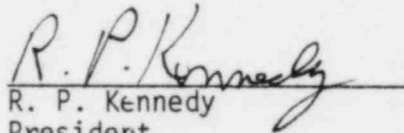
VOLUME I

METHODOLOGY AND CRITERIA

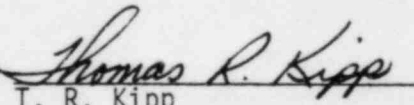
by

D. A. Wesley
R. D. Campbell
R. P. Kennedy
R. H. Kincaid
P. S. Hashimoto

Approved:


R. P. Kennedy
President

Approved:


T. R. Kipp
Manager of
Quality Assurance

prepared for

CONSUMERS POWER COMPANY
Jackson, Michigan

February, 1983

B302170309 B30228
PDR ADOCK 05000329
A PDR



STRUCTURAL
MECHANICS
ASSOCIATES
A Calif. Corp.

REVISIONS

Document Number SMA 13701.05R003(Volume I)

Title Seismic Margin Review
Midland Energy Center Project
Volume I, Methodology and
Criteria

Rev.	Description	QA	Project Manager
7-30-1982	Draft for Review	<i>Thomas R. Kipp</i> 7/30/82	<i>Dawesley</i> 7/30/82
2-2-1983	Initial Issue	<i>Thomas R. Kipp</i> 2/3/83	<i>Dawesley</i> 2-3-83

SEISMIC MARGIN REVIEW
MIDLAND ENERGY CENTER PROJECT

TABLE OF CONTENTS

<u>VOLUME NO.</u>	<u>TITLE</u>
I	METHODOLOGY AND CRITERIA
II	REACTOR CONTAINMENT BUILDING
III	AUXILIARY BUILDING
IV	SERVICE WATER PUMP STRUCTURE
V	DIESEL GENERATOR BUILDING
VI	BORATED WATER STORAGE TANK
VII	ELECTRICAL, CONTROL, INSTRUMENTATION AND MECHANICAL EQUIPMENT
VIII	NSSS EQUIPMENT AND PIPING
IX	BALANCE-OF-PLANT CLASS 1, 2 AND 3 PIPING, PIPE SUPPORTS AND VALVES
X	MISCELLANEOUS SUBSYSTEMS AND COMPONENTS

TABLE OF CONTENTS

VOLUME I

<u>Section</u>	<u>Title</u>	<u>Page</u>
1	INTRODUCTION	I-1-1
	1.1 Scope of Evaluation	I-1-2
	1.1.1 Structures and Components Evaluated	I-1-2
	1.1.2 Analytical Approach	I-1-3
	1.2 Deviations from FSAR Design Bases	I-1-4
2	SEISMIC INPUT	I-2-1
	2.1 Site Specific Ground Response Spectra	I-2-1
	2.2 SME Ground Response Spectra	I-2-1
	2.3 SME and SSE Design Earthquakes	I-2-2
	2.4 SME Artificial Earthquakes	I-2-2
3	MIDLAND SITE SOIL PROPERTIES	I-3-1
	3.1 Site Conditions	I-3-1
	3.2 Soil Characteristics	I-3-1
	3.3 Strain Degradation Effects	I-3-2
	3.4 Uncertainty Range on Shear Modulus	I-3-5
4	SOIL-STRUCTURE INTERACTION	I-4-1
	4.1 Effective Shear Moduli with Layering	I-4-1
	4.2 Energy Entrapment Due to Layering	I-4-5
	4.3 Development of Upper and Lower Bound Shear Moduli	I-4-8
	4.4 Soil Stiffnesses	I-4-9
	4.5 Soil Energy Dissipation	I-4-11
5	STRUCTURE ANALYTICAL MODELS	I-5-1
	5.1 SME Structures Model Approach	I-5-1
	5.2 Structure Model Description	I-5-2
6	STRUCTURES SEISMIC RESPONSE	I-6-1
	6.1 Seismic Analysis Procedure	I-6-1
	6.2 Composite Modal Damping	I-6-2
	6.3 Structure Seismic Loads	I-6-5
	6.4 Determination of Number of Modes	I-6-5

TABLE OF CONTENTS (Continued)

VOLUME I

<u>Section</u>	<u>Title</u>	<u>Page</u>
	6.5 Combination of Modal Responses	I-6-6
	6.6 Combination of the Three Components of Motion	I-6-7
	6.7 Distribution of Loads to Structure Elements	I-6-7
7	MARGIN EVALUATION OF STRUCTURES	I-7-1
	7.1 Load Combinations	I-7-1
	7.2 Acceptance Criteria	I-7-2
	7.2.1 Concrete Structures	I-7-2
	7.2.2 Steel Structures	I-7-3
8	INPUT TO EQUIPMENT	I-8-1
	8.1 Development of In-Structure Response Spectra	I-8-1
	8.2 In-Structure Floor Response Spectra Smoothing and Broadening	I-8-5
	8.3 Vertical Amplification of Floor Slabs	I-8-5
9	SME SEISMIC MARGIN EVALUATION METHODS AND ACCEPTANCE CRITERIA FOR EQUIPMENT AND SUPPORTS	I-9-1
	9.1 Selection of Equipment	I-9-2
	9.1.1 NSSS System (Piping, Vessels, Supports and Reactor Internals	I-9-2
	9.1.2 ASME Code Class 1, 2 and 3 Balance- of-Plant Piping and Supports	I-9-3
	9.1.3 ASME Code Class 1 Balance-of- Plant Equipment	I-9-3
	9.1.4 ASME Code Class 2 and 3 Balance- of-Plant Equipment and Supports	I-9-3
	9.1.5 Emergency Power Supplies	I-9-3
	9.1.6 Cable Trays and Supports	I-9-3
	9.1.7 HVAC Ducting and Supports	I-9-4
	9.1.8 Electrical Conduit and Supports	I-9-4
	9.1.9 Component Support Anchorage	I-9-5

TABLE OF CONTENTS (Continued)

VOLUME I

<u>Section</u>	<u>Title</u>	<u>Page</u>
9.1.10	Electrical, Instrumentation and Control Equipment	I-9-4
9.2	Procedures Used to Compute Margins . . .	I-9-5
9.2.1	Procedures Used for New Analysis	I-9-5
9.2.1.1	Damping	I-9-6
9.2.1.2	Combination of Modal Responses	I-9-6
9.2.1.3	Combination of Earth- quake Components	I-9-7
9.2.1.4	Analytical Procedures	I-9-7
9.2.1.4.1	NSSS System	I-9-7
9.2.1.4.2	BOP Piping Systems	I-9-8
9.2.1.4.3	Cable Tray Systems	I-9-8
9.2.1.4.4	HVAC Systems	I-9-9
9.2.1.5	Multiple Support Equipment and Sybsystems	I-9-10
9.2.2	Procedures Used for Existing Design Analyses	I-9-10
9.2.3	Procedure Used for Equipment Qualified by Test	I-9-12
9.2.3.1	Equipment Qualified by Dynamic Testing	I-9-12
9.2.3.2	Equipment Qualified by Static Testing	I-9-14
9.3	Load Combinations and Acceptance Criteria	
9.3.1	ASME Code Class 1 NSSS and Balance-of-Plant Piping	I-9-14
9.3.2	ASME Code Class 2 and 3 Balance-of-Plant Piping	I-9-15
9.3.3	ASME Class 1 Vessels, Pumps and Valves	I-9-15

TABLE OF CONTENTS (Continued)

VOLUME I

<u>Section</u>	<u>Title</u>	<u>Page</u>
9.3.4	ASME Code Class 2 and 3 Equipment	I-9-16
9.3.6	Component Supports for ASME Code Class 2 and 3 Piping and Equipment	I-9-17
9.3.7	Cable Trays and Supports	I-9-18
9.3.8	HVAC Ducting and Supports	I-9-19
9.3.9	Component Support Anchorage . . .	I-9-19

REFERENCES

APPENDICES

1. INTRODUCTION

The seismic design input for the Midland Energy Center Project is 0.12g peak horizontal ground acceleration for the Safe Shutdown Earthquake (SSE) and 0.6g peak horizontal ground acceleration for Operating Basis Earthquake (OBE), Reference 1. Corresponding input for vertical ground motion was taken as two-thirds of the horizontal. The ground response spectra used for the design are the Housner spectra (Reference 2) with spectral accelerations increased by 50 percent in the 0.2 to 0.6 second period range.

Recently, the expected seismic input at the Midland site has been reevaluated using current methodology (References 3, 4 and 5). Seismic inputs for the site were determined in terms of site specific response spectra applicable at both the original ground surface and at the top-of-fill. These site specific response spectra exceed the design spectra over a broad frequency range. The purpose of the Seismic Margin Review (SMR) is to assure the adequacy of the essential Midland plant structures and equipment to withstand the higher postulated seismic excitation. This assurance is demonstrated by showing that there are margins in the design of the structures, systems and components, such that, under the normal operating conditions if the plant is subjected to the postulated higher seismic input, the plant can be brought to safe shutdown condition. An evaluation was conducted to determine the seismic margins compared to current code allowables for a representative sampling of structural elements and piping and equipment items. If necessary, provision is made to compute the seismic margins to failure. The results of this evaluation are presented in this report. Volume I of the report consists of the methodology and criteria employed in this evaluation, and Volumes II through X present the results for the individual structures and equipment.

1.1 SCOPE OF EVALUATION

1.1.1 Structures and Components Evaluated

The seismic margin review was performed on those structures and equipment necessary to achieve a safe shutdown of the reactors. The seismic input for the SMR is referred herein as the Seismic Margin Earthquake (SME). The Seismic Category I structures and systems necessary for safe shutdown are identified in the Midland FSAR (Reference 1). Representative critical structural elements and equipment items essential for safe shutdown were included in the SMR. The following Category I structures were chosen for review.

- a. Reactor Containment Building and Concrete Internals Structures
- b. Auxiliary Building
- c. Service Water Pump Structure
- d. Diesel Generator Building
- e. Borated Water Storage Tank
- f. Buried Structures

The structural elements selected for review for each of the above structures are listed in subsequent volumes of this report. Selected mechanical and electrical components and distribution systems were evaluated to determine the safety margins for the SME. The sampling was based on criticality of function, vulnerability of equipment, high seismic stress levels, and location in the structures. Components of mechanical and electrical equipment in both the Nuclear Steam Supply System (NSSS) and Balance-of-Plant (BOP) that were evaluated in detail include:

- a. Piping
- b. Pipe Supports
- c. Active Valves
- d. Switchgear, and Instrumentation and Control Equipment

- e. Pumps and their Supports
- f. Heat Exchangers and their Supports
- g. Vessels and their Supports
- h. Station Batteries and Racks
- i. Diesel Generator
- j. Cable Trays and Supports
- k. HVAC Ducts and Supports
- l. Conduits and Supports

The specific items evaluated together with their locations in the structures and SME inputs are listed in subsequent volumes.

1.1.2 Analytical Approach

Existing analytical models of structures and equipment were used to the extent possible consistent with the current state-of-the-art of seismic analysis. Analytical models developed for the structure design analyses were reviewed for adequacy and used as appropriate. Design models for the reactor building, auxiliary building-control tower, service water pump structure, and the diesel generator building were used to generate new seismic responses for the SME as discussed in Section 6. These models are representative of current structural design models and incorporated the soils-related remedial designs for the auxiliary building-control tower and the service water pump structure. New soil compliance functions for these structures were generated as part of the SMR in order to reflect a somewhat broader range of soil properties than was used in design as well as the effects of the variation of site characteristics with depth.

For vendor supplied equipment, the vendor seismic qualification analyses or tests were reviewed and vendor computed responses were scaled for the SME to determine the margins against code and, if necessary, the margin against failure. No independent analyses were conducted for vendor supplied components. For BOP piping, cable tray and HVAC systems

designed by the Architect/Engineer (Bechtel Corporation), independent analyses of selected systems were conducted to determine margins against code or against failure.

For NSSS piping and equipment including reactor internals, the vendor, Babcock and Wilcox, was commissioned by Consumers Power Company to conduct seismic response analyses using SME input to the various NSSS dynamic models and to provide details of design loading and associated design basis stress response. SME response loading and corresponding design basis stresses were scaled to determine SME margins.

Using the seismic responses developed for the SME input, margins to code allowable values of selected structural elements and equipment items were computed. For any results where the code margin is less than unity, provision is made to conservatively compute the margin to failure.

1.2 DEVIATIONS FROM FSAR DESIGN BASES

The criteria and methodology used in the evaluation of the seismic margins is not a redefinition of the criteria used in design. The behavior limits defined in the FSAR (Sections 3.7, 3.8, 3.9, and 3.10) were not intended for use in evaluating a realistic seismic design margin, but rather to establish the basis for a safe and adequate seismic design. Consequently, several deviations from the FSAR design bases are implemented in the SMR in order to develop more rational results. Among the more important differences are:

- a. Seismic input was defined by the site specific response spectra.
- b. A broader range of soil properties was used.
- c. Parametric variations were used to establish conservative loads.
- d. Composite modal damping was based on more realistic limits.
- e. Load combinations correspond to the criteria of achieving safe shutdown, when the plant, under normal operating condition, is subjected to SME.

In many cases, the approach used in the SMR results in a conservatively broader range of parameters than were used in design. The specific analysis methods and criteria used in the SMR are discussed in the following sections of this report.

2. SEISMIC INPUT

2.1 SITE SPECIFIC GROUND RESPONSE SPECTRA (SSRS)

The site specific ground response spectra developed for the Midland site were determined from real time histories from earthquakes of magnitudes and epicentral distances similar to those expected for Midland (Reference 3). The initial data base included earthquakes with epicentral distances less than 40 km and M_L magnitudes from 4.5 to 6.0. A subset of these records was selected based on a determination that the local geology at their recording stations was similar to Midland.

Response spectra for these time histories were then computed together with the mean, median, and 84th percentile spectra. The 84th percentile spectra were selected as the site specific response spectra for the Midland Plant. The peak ground acceleration (PGA) is approximately 0.133g for the original ground surface location. These spectra are applicable for the reactor building, auxiliary building and the service water pump structure which are all founded below the original ground surface. A similar approach was used to develop site specific response spectra applicable at the top-of-fill spectra as was used for the original ground spectra (Reference 4). The top of the fill SSRS has a PGA of approximately 0.15g. These spectra are applicable for structures founded near the surface of the approximately 30 foot of fill such as the diesel generator building and borated water storage tanks.

2.2 SME GROUND RESPONSE SPECTRA

The original Housner response spectra exceed the site specific response spectra in the 2 Hz and less range for the original ground surface. A similar effect is evident for the top-of-fill spectra although spectra cross at somewhat lower frequencies. In order to provide a conservative basis for the SMR, an envelope of the site

specific response spectra for the original ground surface or top-of-fill, as applicable, together with the Housner spectra anchored to 0.12g peak acceleration was used. Figure I-2-1 shows the resulting spectra for the original ground and Figure I-2-2 shows the corresponding top-of-fill spectra. Inclusion of the Housner spectra is expected to provide adequate additional conservatism in the low-frequency range to account for a distant, high magnitude earthquake. These two sets of spectra are referred to as the Seismic Margin Earthquake (SME) spectra. Two-thirds of the corresponding horizontal input was used for the vertical input for the original ground surface and top of fill locations.

2.3 SME AND SSE DESIGN EARTHQUAKES

The FSAR SSE earthquake used for design consisted of the Housner response spectra anchored to a 0.12g peak ground acceleration but increased by 50 percent in the 0.2 to 0.6 second period range. The 50 percent amplification was introduced to provide increased conservatism in the fundamental period range for most of the Seismic Category I structures. A comparison of the SME original ground surface and FSAR SSE ground response spectra is shown in Figure I-2-3 for 5 percent damping. At frequencies above 4 Hz, the SME response spectrum indicates higher seismic response may be expected, assuming the same damping. Figure I-2-4 shows a similar comparison of the FSAR SSE spectrum with the 5 percent damped top-of-fill SME spectrum.

2.4 SME ARTIFICIAL EARTHQUAKES

In order to develop the in-structure response spectra necessary to describe the seismic input for equipment, time history analyses of the structures were conducted. Synthetic time histories consistent with the SME ground response spectra were developed to provide the seismic input to the structures. These synthetic time histories were generated by Program STUF (Reference 7). STUF creates synthetic time histories through an iterative process that operates on the Fourier series representation of a natural or synthetic earthquake used as input. It is based on the method proposed in Reference 53. Separate time histories were developed

for the original ground surface and for the top-of-fill. Figure I-2-5 shows the acceleration, velocity, and displacement traces for the original ground surface. The synthetic time histories were baseline corrected and have a duration of approximately 10 seconds. Figure I-2-6 shows the response spectra developed by the original ground surface synthetic time history. Figures I-2-7 through I-2-10 show comparisons of the response spectra developed by the synthetic time history with the corresponding SME ground response spectra for the original ground surface for 5, 10, 20 and 40% of critical damping.

The ground acceleration, velocity, and displacement time history traces for the top-of-fill synthetic time history are shown in Figure I-2-11. The corresponding response spectra for the top-of-fill as generated by the synthetic time history, are shown in Figure I-2-12. Figures I-2-13 through I-2-16 show the comparisons of the spectra developed by the synthetic time history and the SME top-of-fill response spectra.

In general, the synthetic time histories produce spectra which exceed the SME ground response spectra. The few locations where the synthetic time history response spectra are lower than the ground spectra are considered acceptable since the in-structure response spectra used in the SMR of equipment are generated from an envelope of a broad range of soil parameters. Thus, even if the in-structure response spectra for a given soil case and structure may be influenced by a "valley" in the synthetic time history input, conservative in-structure response spectra are assured by using an envelope of the responses from other soil cases which will shift the structure response from the "valleys" to the "peaks."

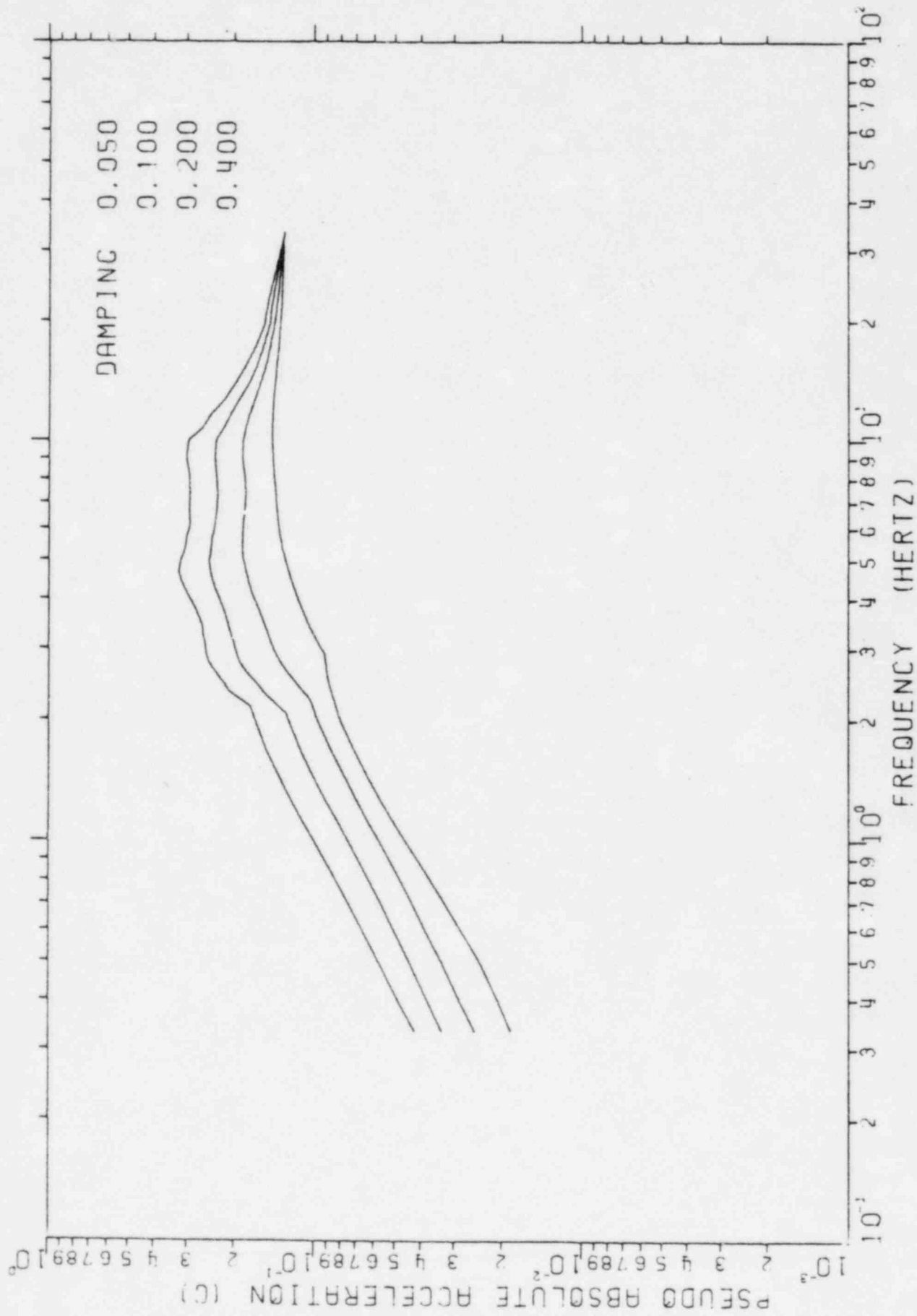


FIGURE I-2-1. SEISMIC MARGIN EARTHQUAKE ORIGINAL GROUND SURFACE ENVELOPE RESPONSE SPECTRA

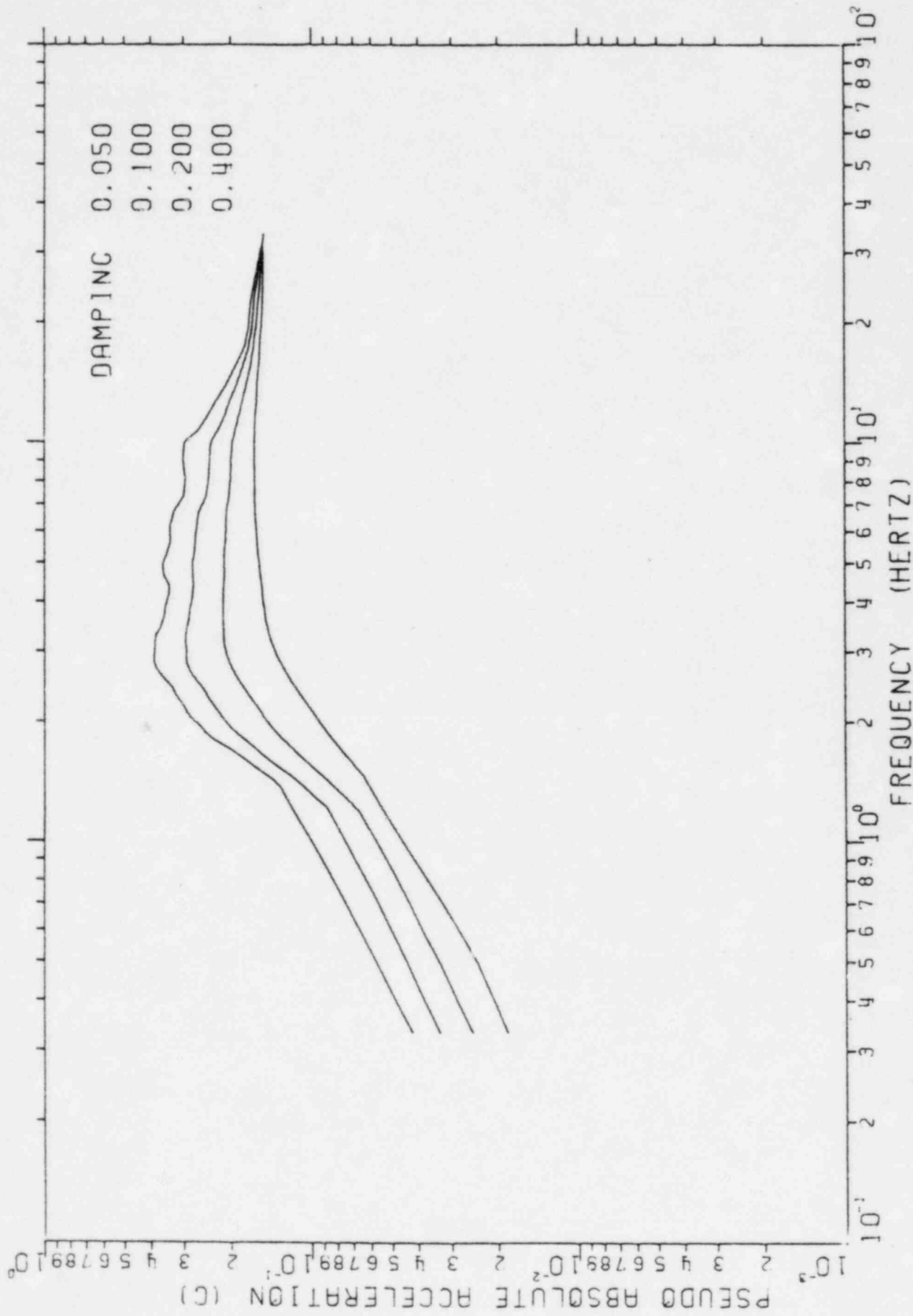


FIGURE I-2-2. SEISMIC MARGIN EARTHQUAKE TOP OF FILL ENVELOPE RESPONSE SPECTRA

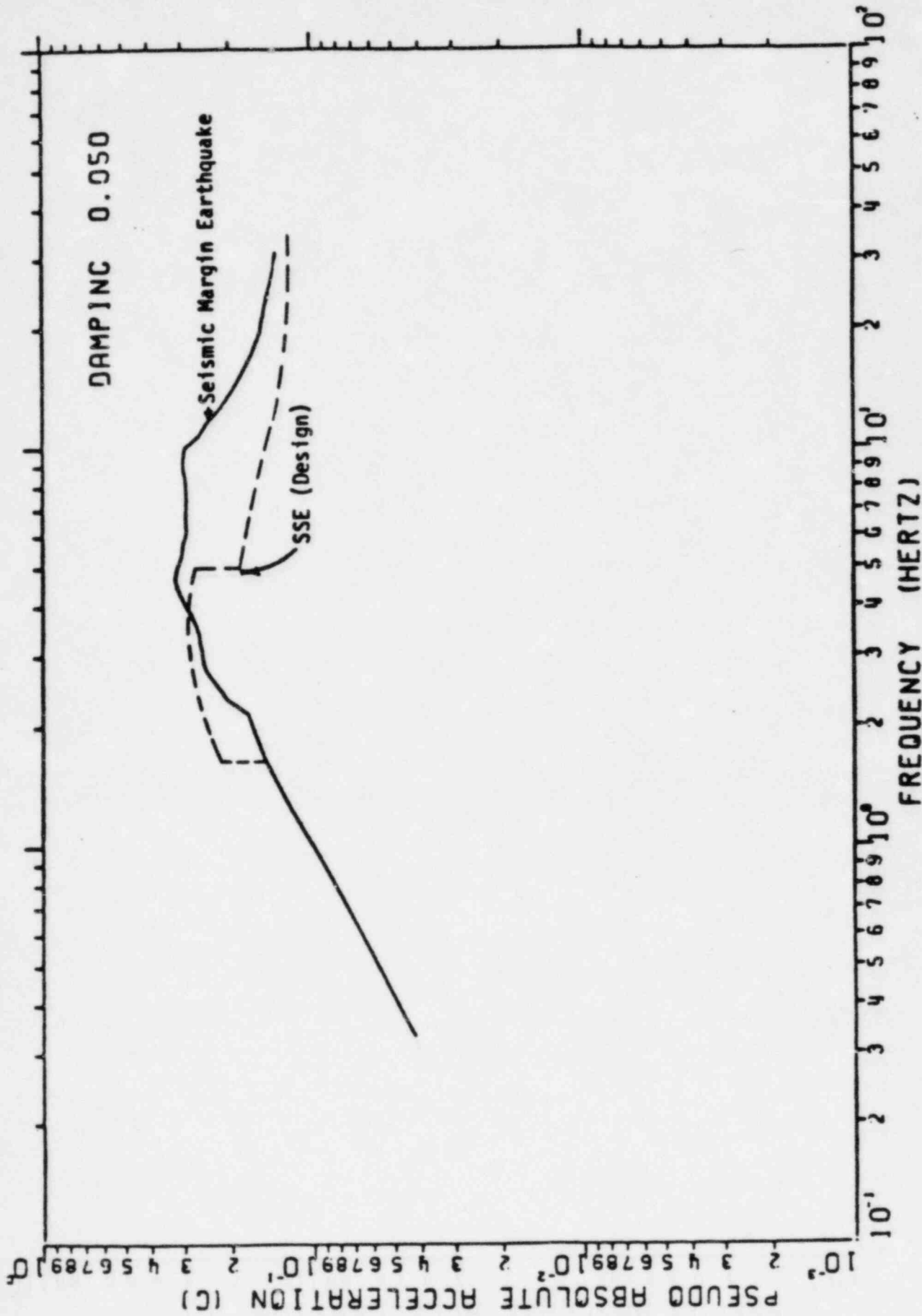


FIGURE I-2-3. COMPARISON OF SME AND FSAR (SSE) ORIGINAL GROUND SURFACE RESPONSE SPECTRA

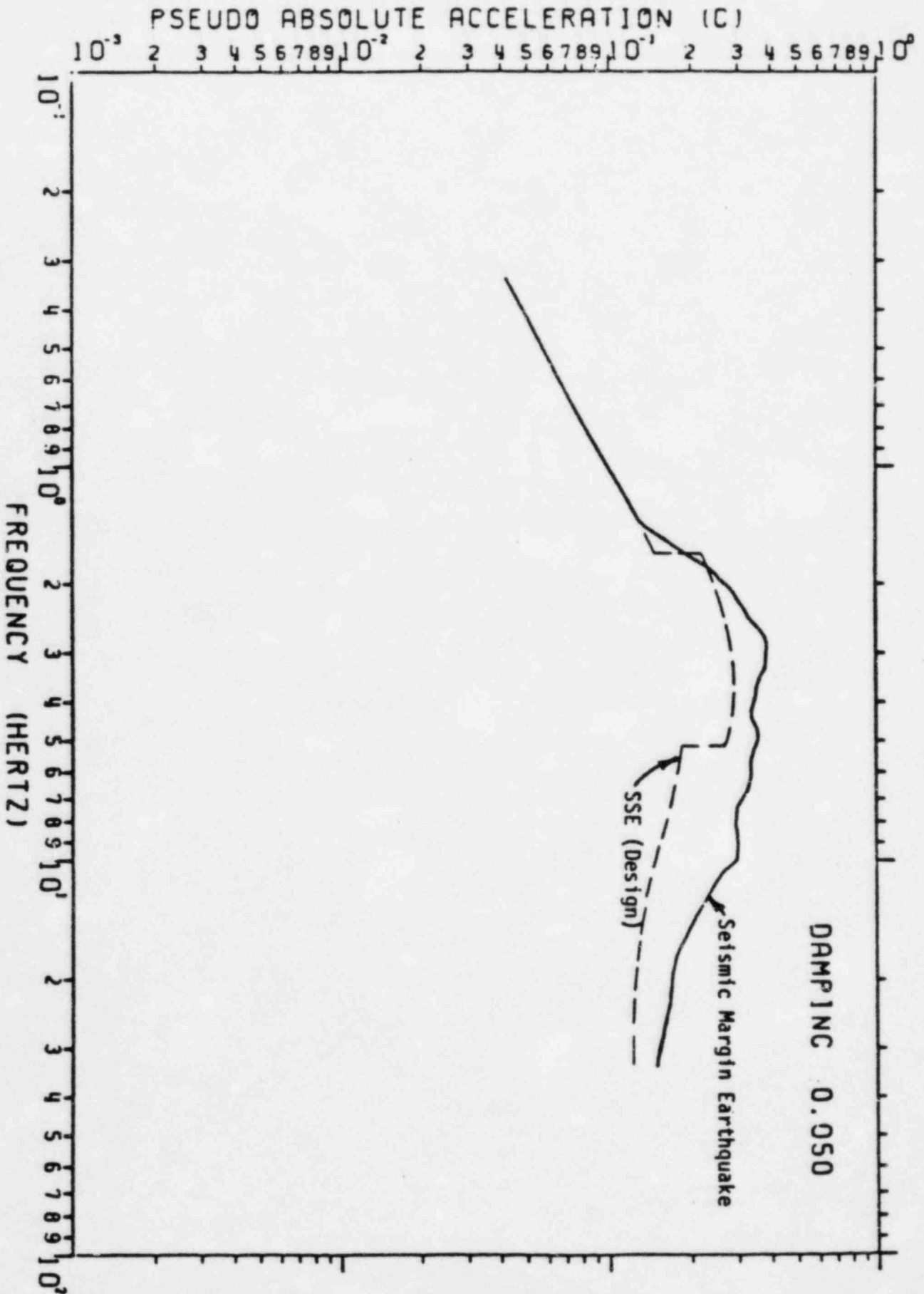


FIGURE I-2-4. COMPARISON OF SME AND FSAR (SSE) TOP OF FILL RESPONSE SPECTRA

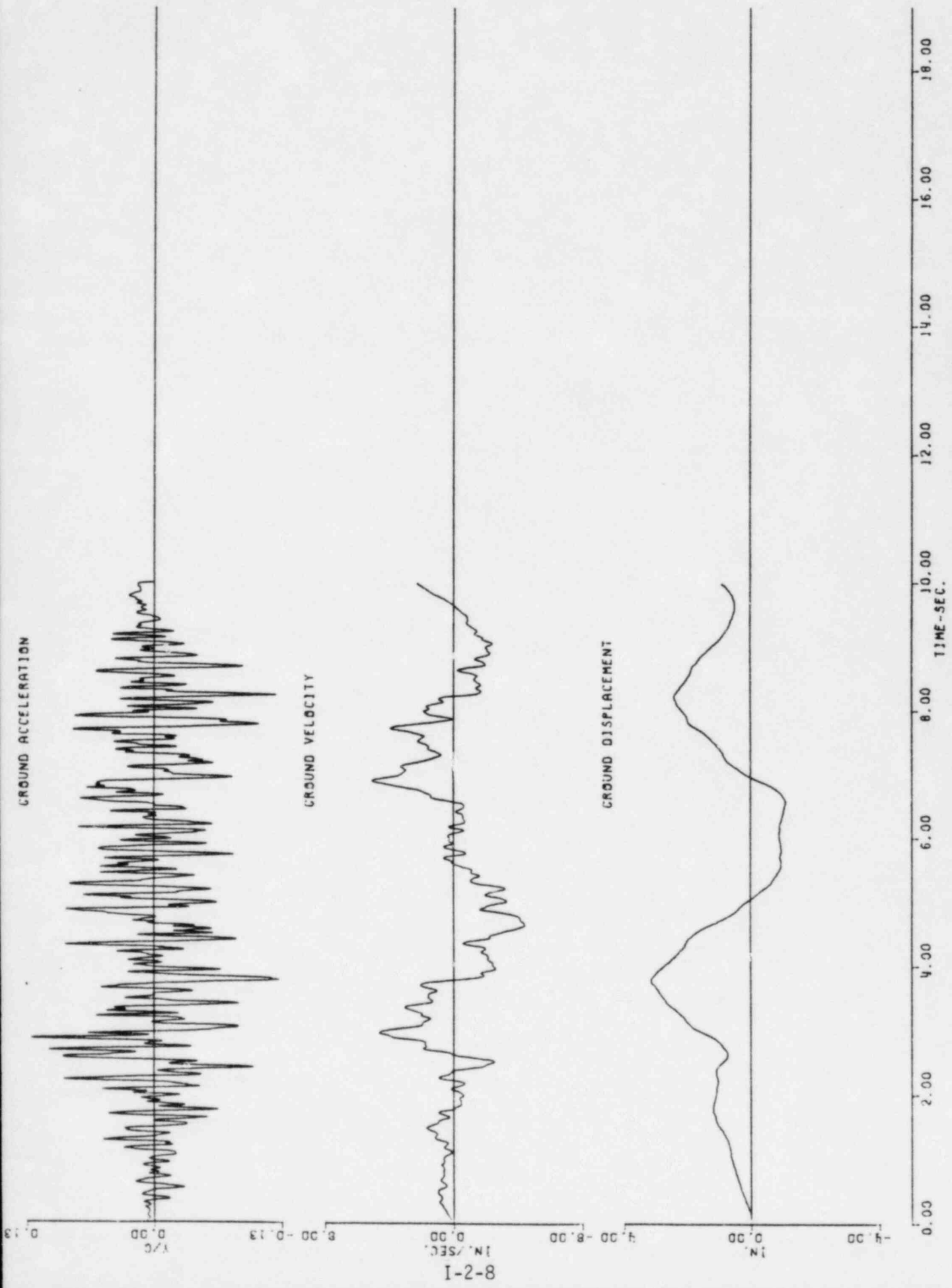


FIGURE I-2-5. SME SYNTHETIC TIME HISTORY - ORIGINAL GROUND SURFACE

8-2-1

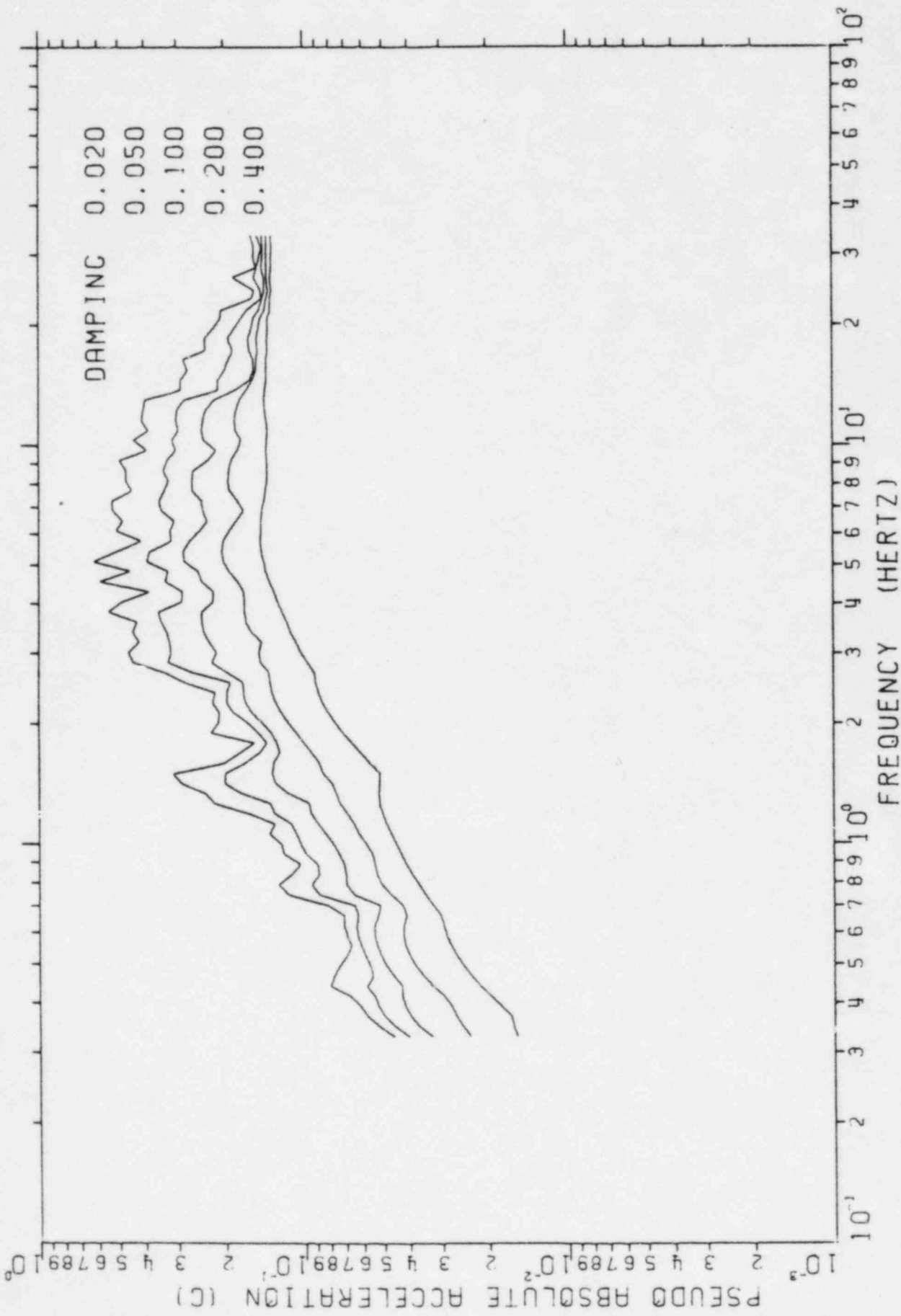


FIGURE I-2-6. SME SYNTHETIC TIME HISTORY RESPONSE SPECTRA - ORIGINAL GROUND SURFACE

I-2-10

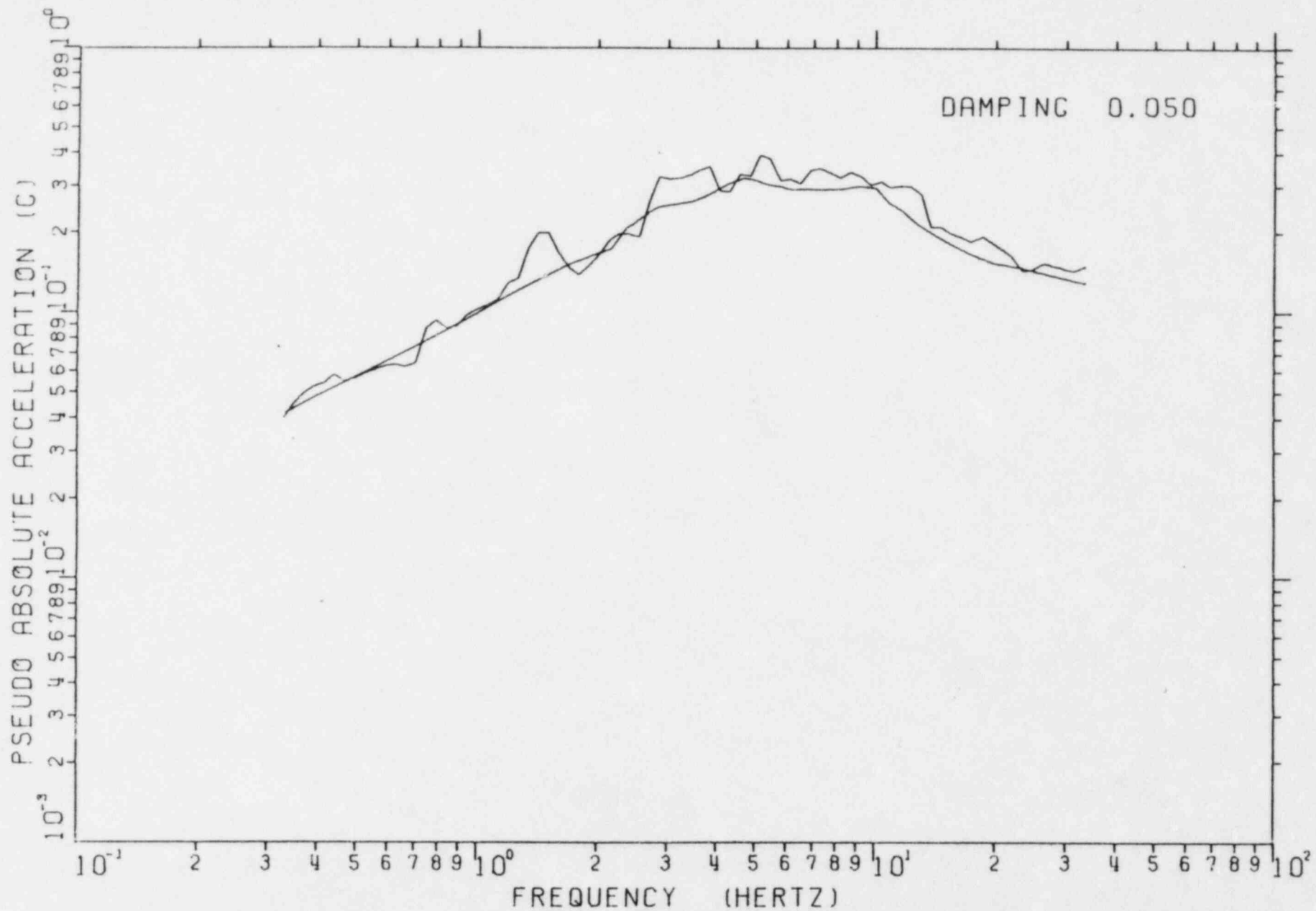


FIGURE I-2-7. COMPARISON OF SYNTHETIC TIME HISTORY AND SME ENVELOPE RESPONSE SPECTRA
ORIGINAL GROUND SURFACE - 5% DAMPING

I-2-11

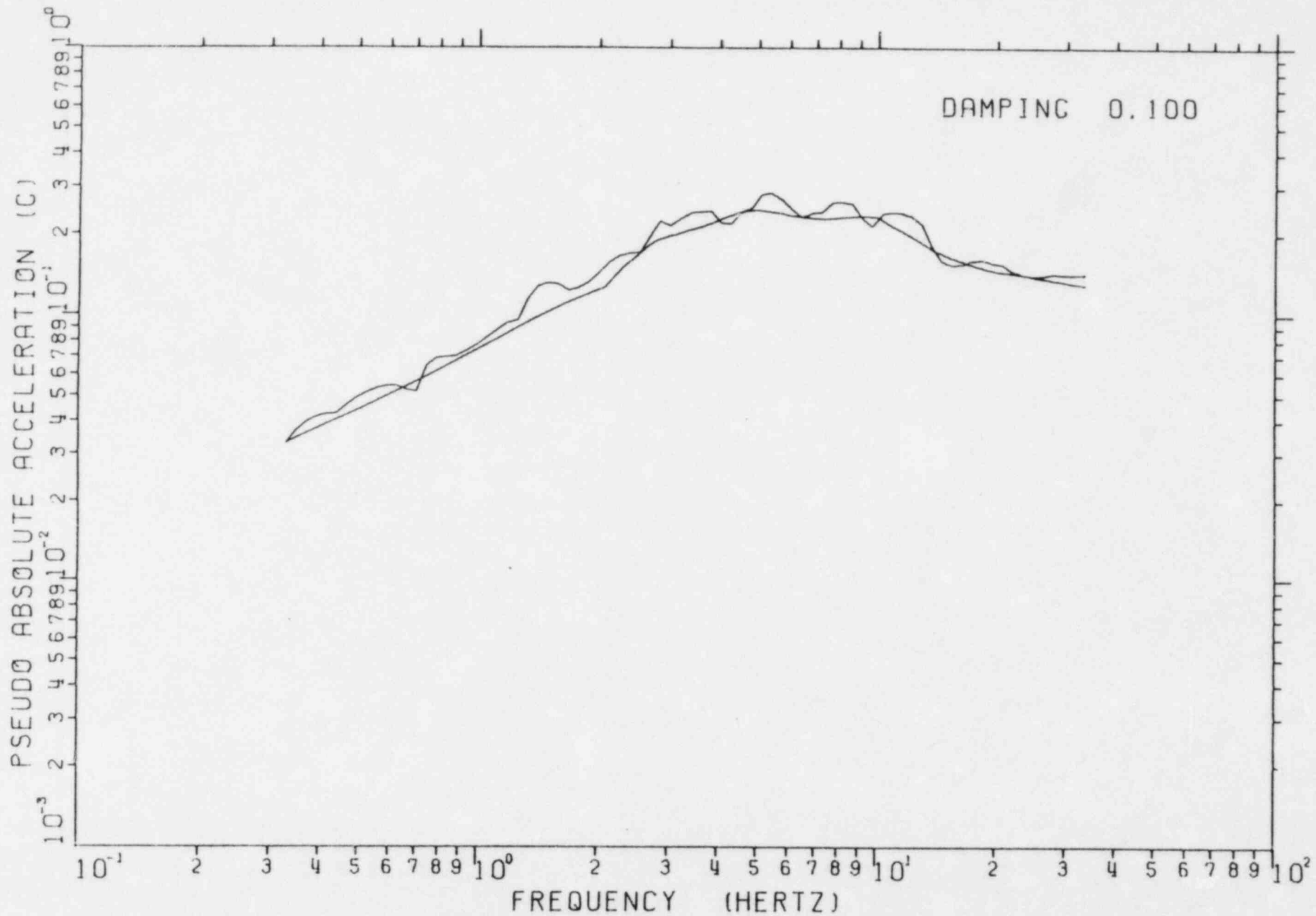


FIGURE I-2-8. COMPARISON OF SYNTHETIC TIME HISTORY AND SME ENVELOPE RESPONSE SPECTRA ORIGINAL GROUND SURFACE - 10% DAMPING

1-2-12

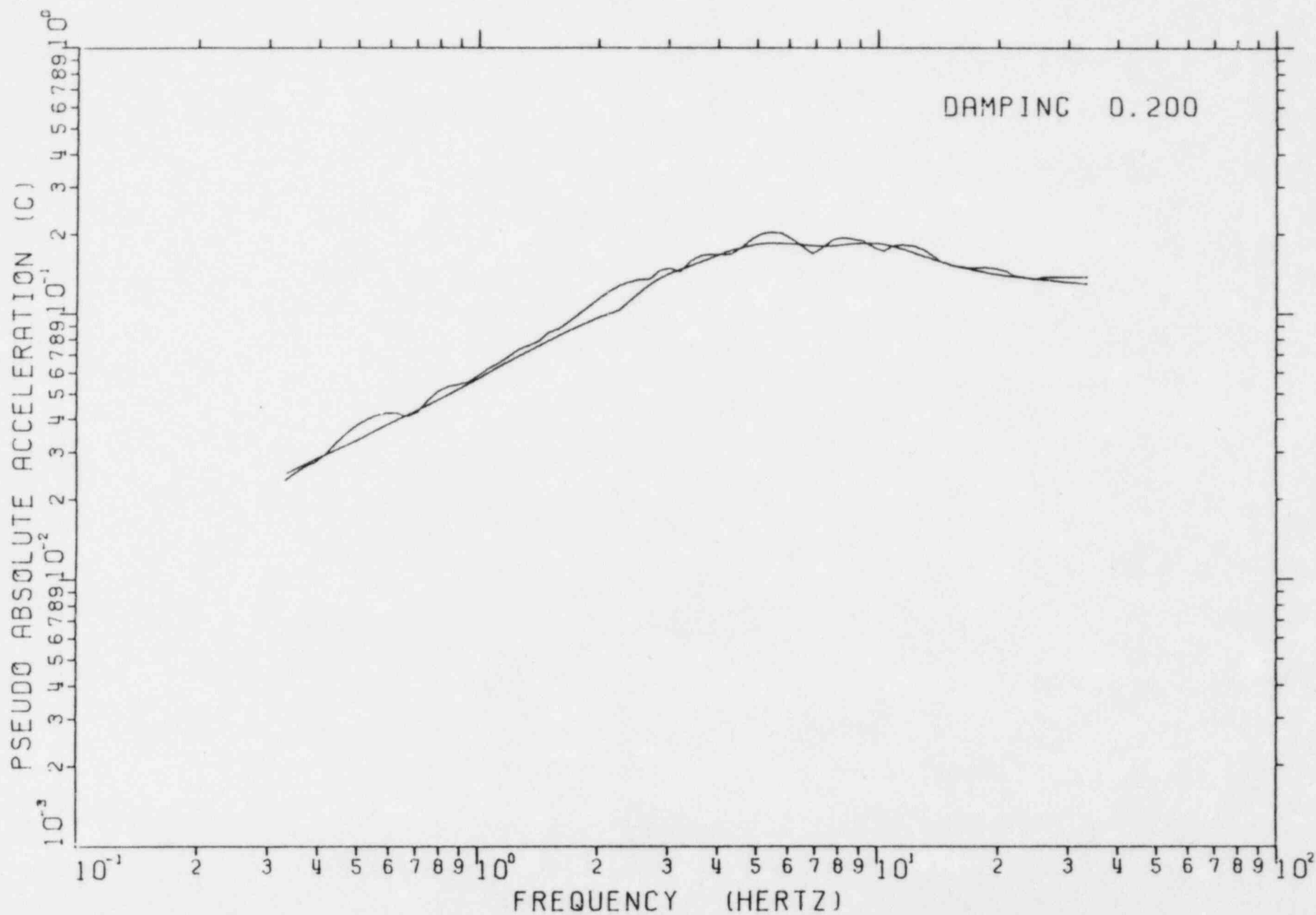


FIGURE I-2-9. COMPARISON OF SYNTHETIC TIME HISTORY AND SME ENVELOPE RESPONSE SPECTRA ORIGINAL GROUND SURFACE - 20% DAMPING

I-2-13

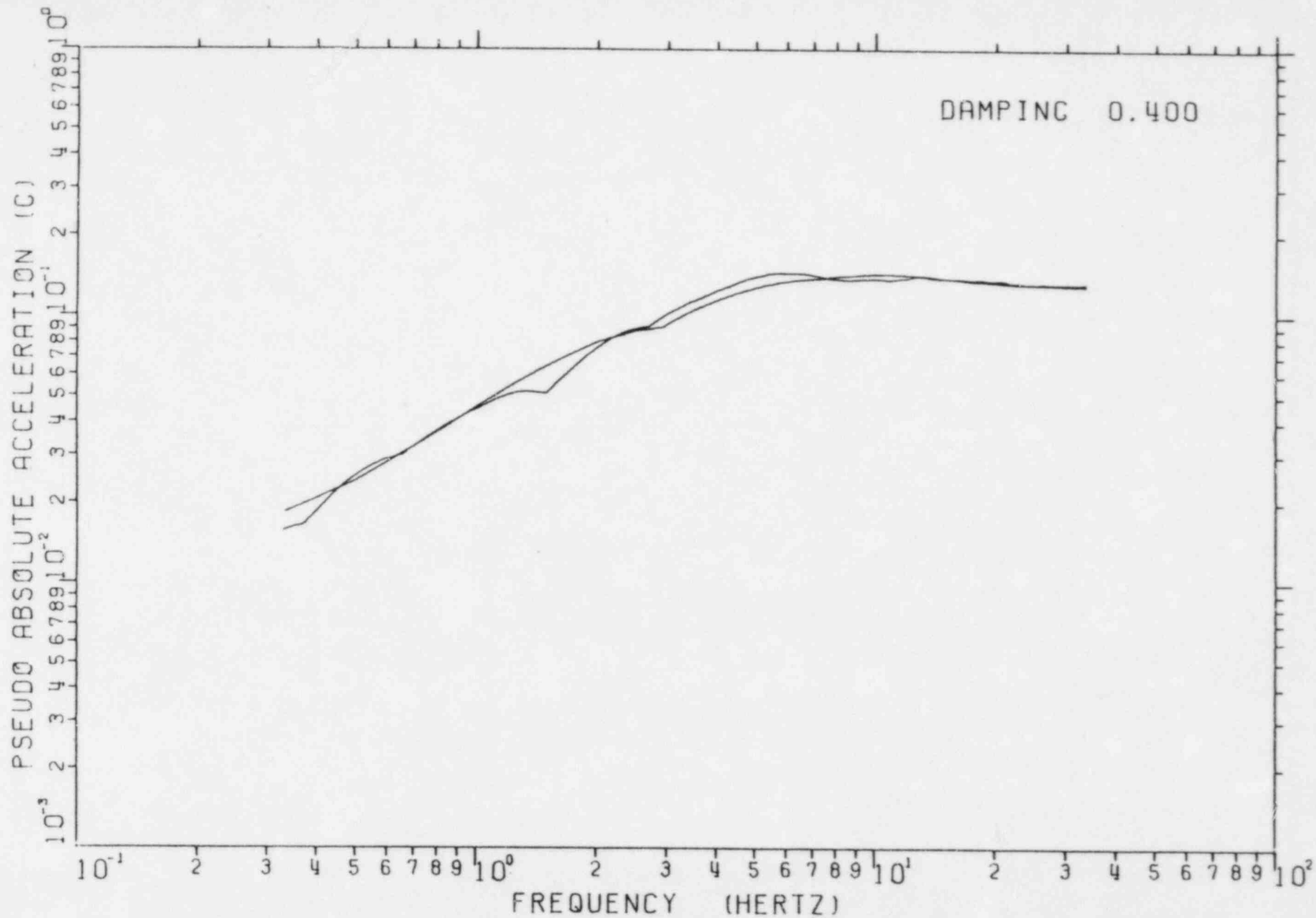
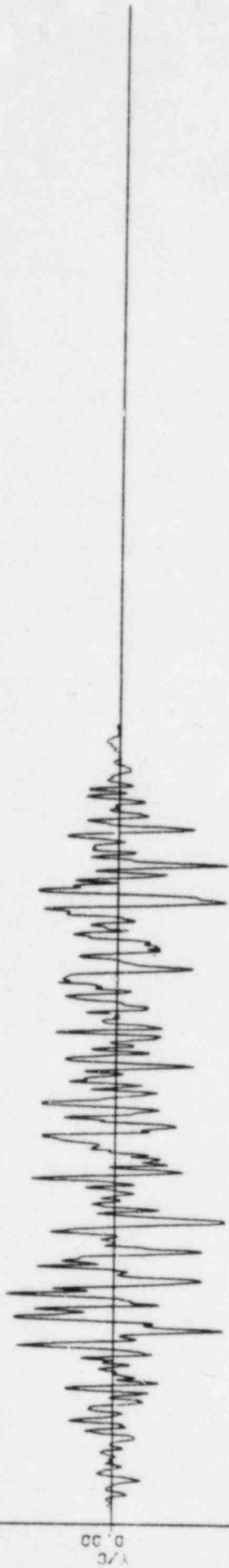
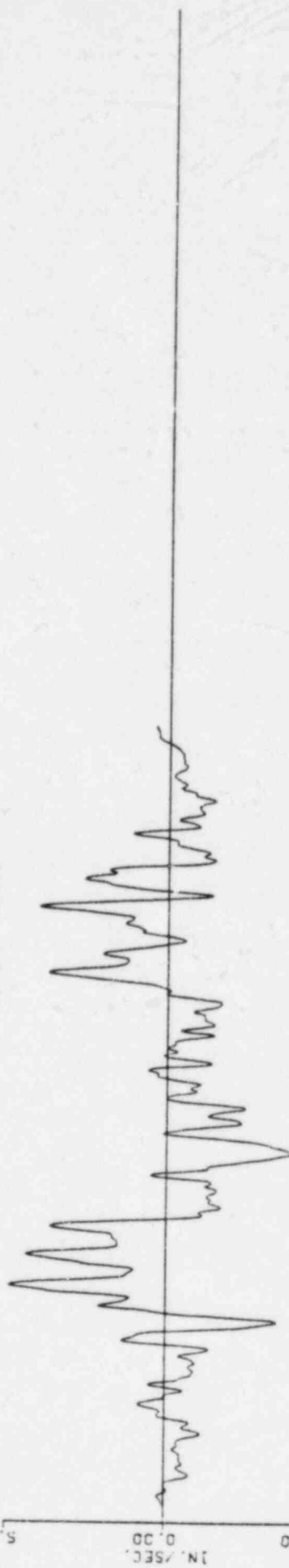


FIGURE I-2-10. COMPARISON OF SYNTHETIC TIME HISTORY AND SME ENVELOPE RESPONSE SPECTRA ORIGINAL GROUND SURFACE - 40% DAMPING

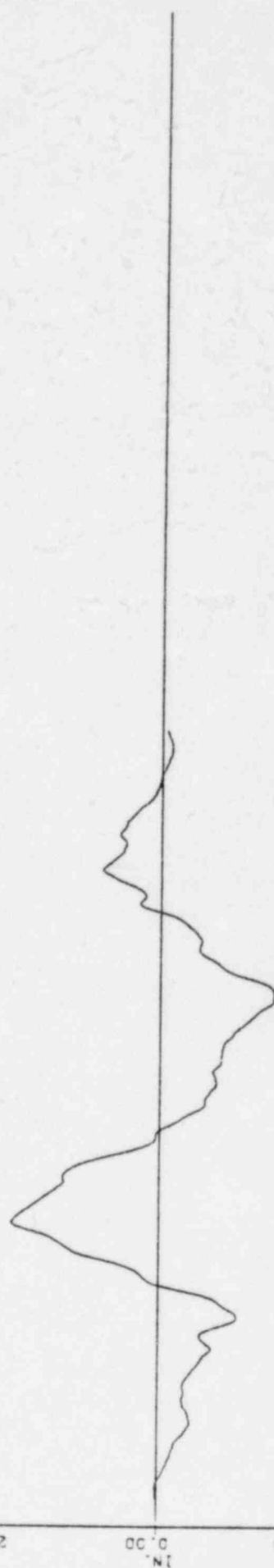
GROUND ACCELERATION



GROUND VELOCITY



GROUND DISPLACEMENT



0.00 2.00 4.00 6.00 8.00 10.00 12.00 14.00 16.00 18.00
TIME-SEC.

FIGURE I-2-11. SME SYNTHETIC TIME HISTORY - TOP OF FILL

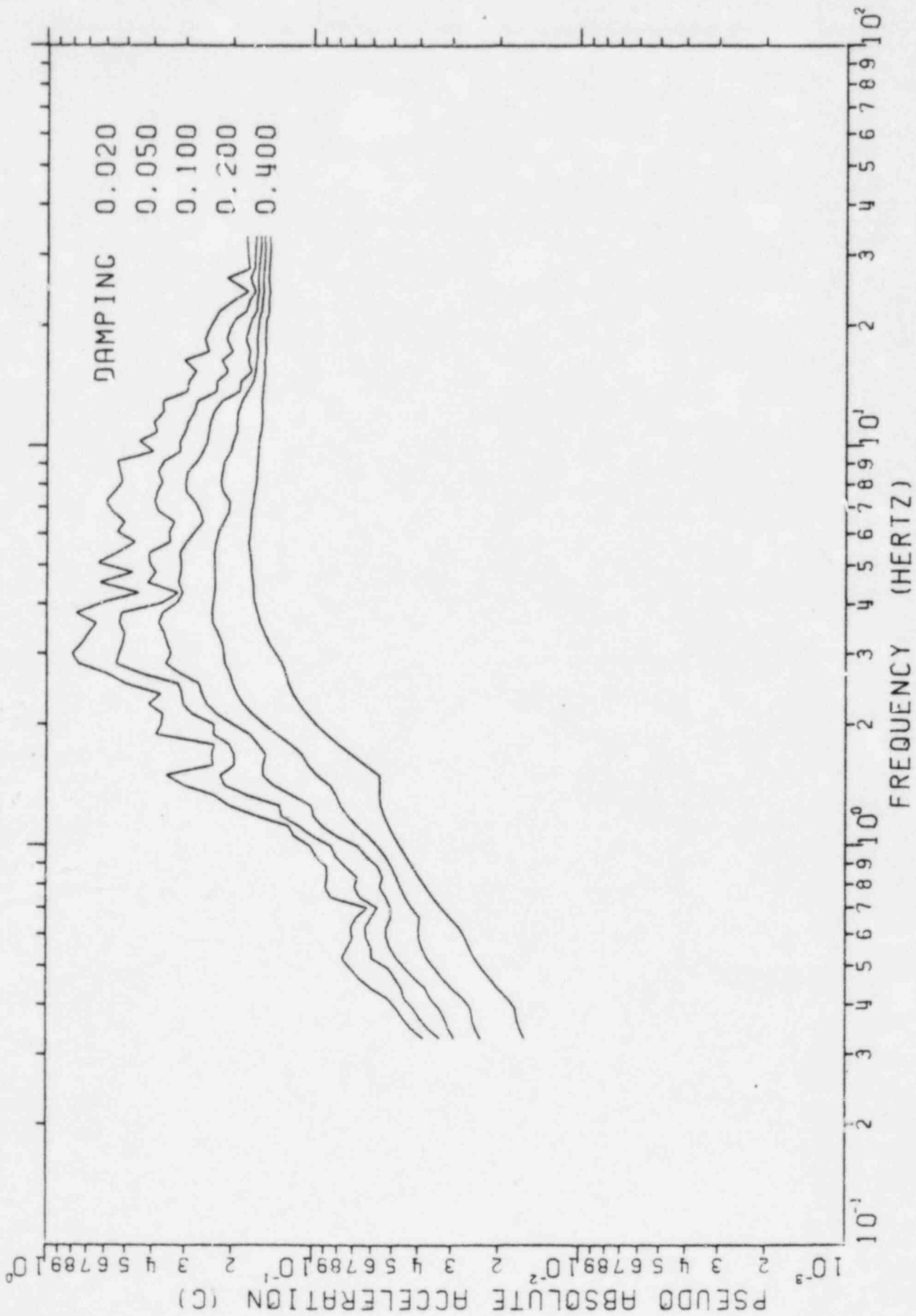


FIGURE I-2-12. SME SYNTHETIC TIME HISTORY RESPONSE SPECTRA - TOP OF FILL

I-2-16

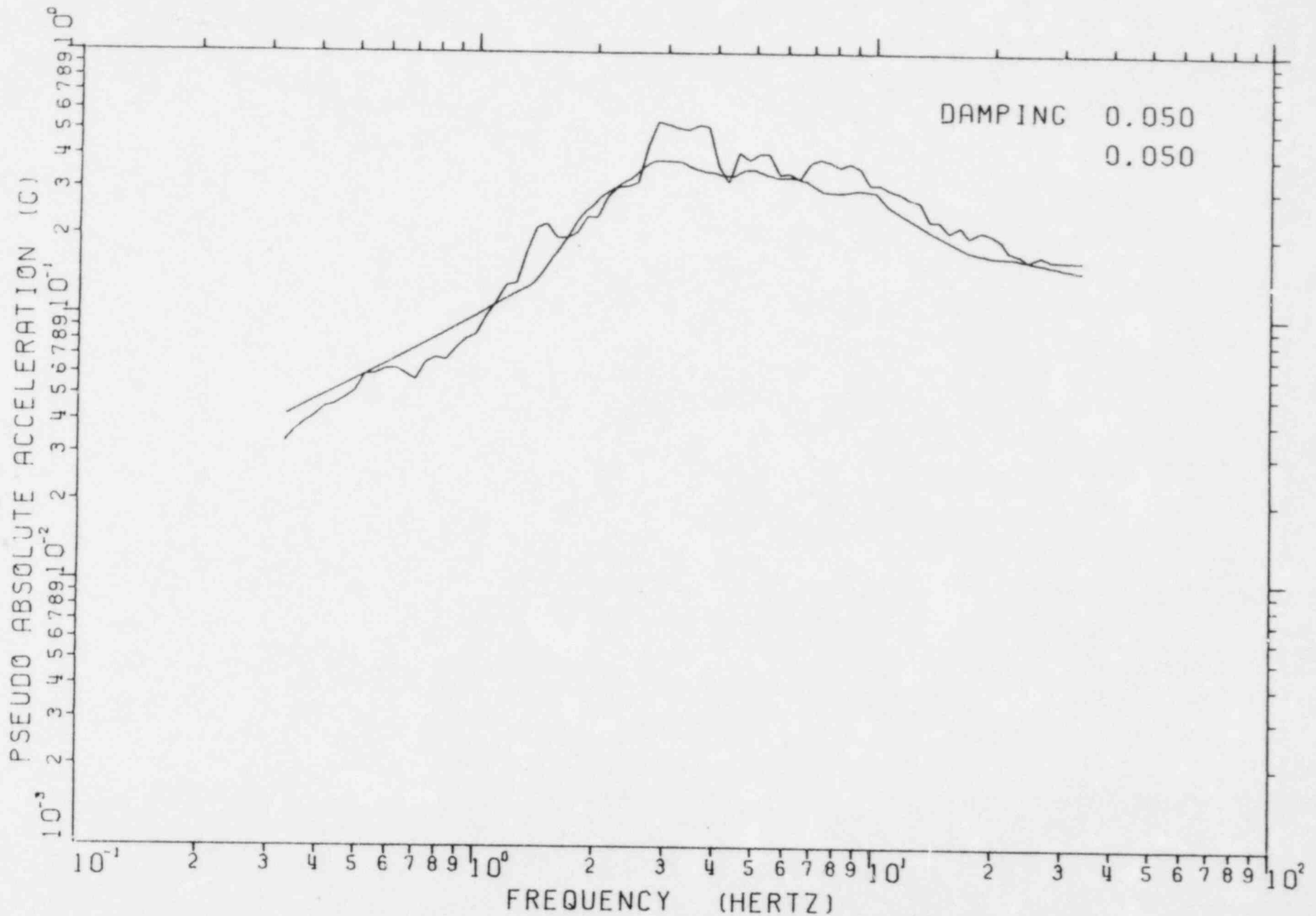


FIGURE I-2-13. COMPARISON OF SYNTHETIC TIME HISTORY AND SME ENVELOPE RESPONSE SPECTRA
TOP OF FILL - 5% DAMPING

I-2-17

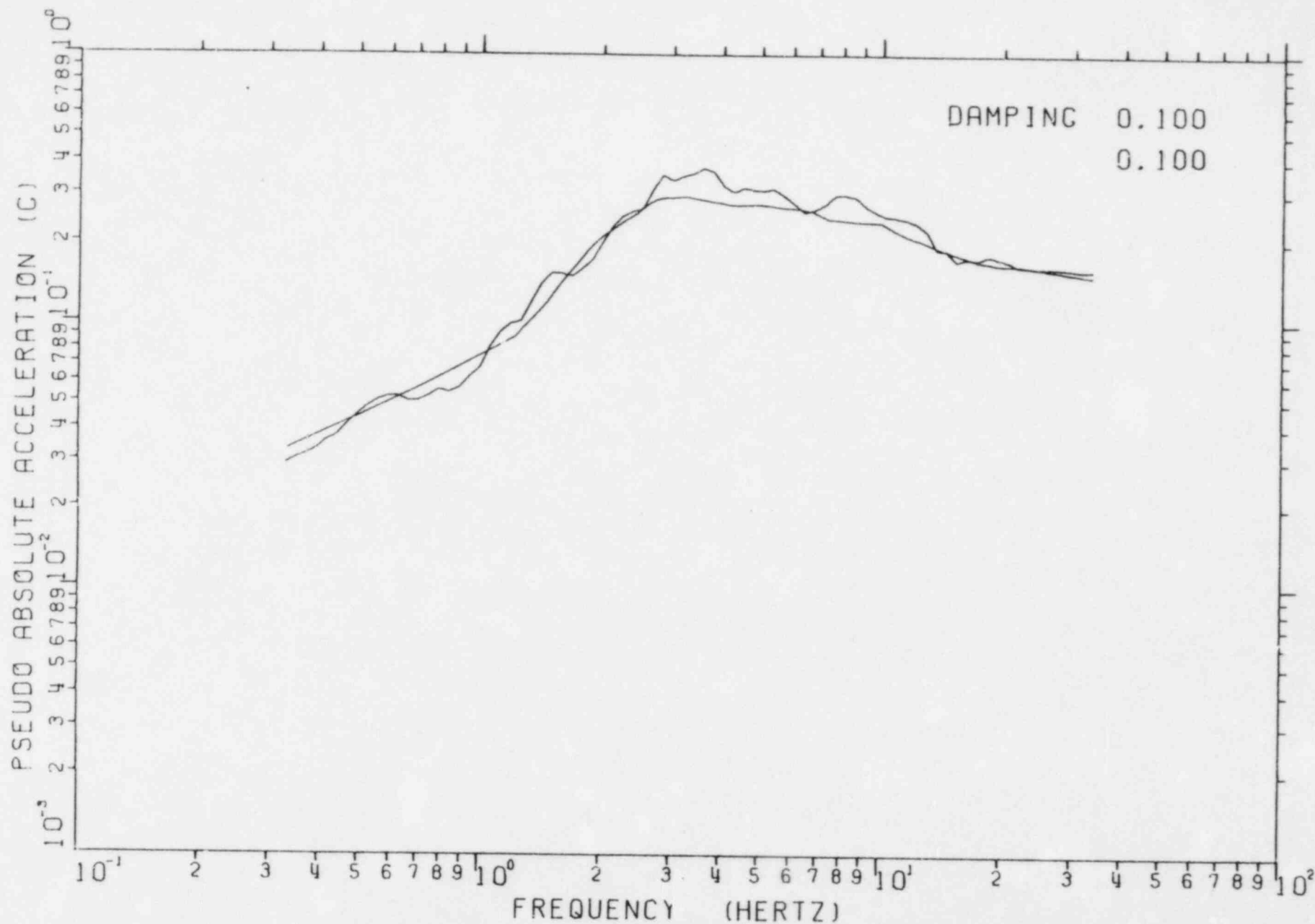


FIGURE I-2-14. COMPARISON OF SYNTHETIC TIME HISTORY AND SME ENVELOPE RESPONSE SPECTRA
TOP OF FILL - 10% DAMPING

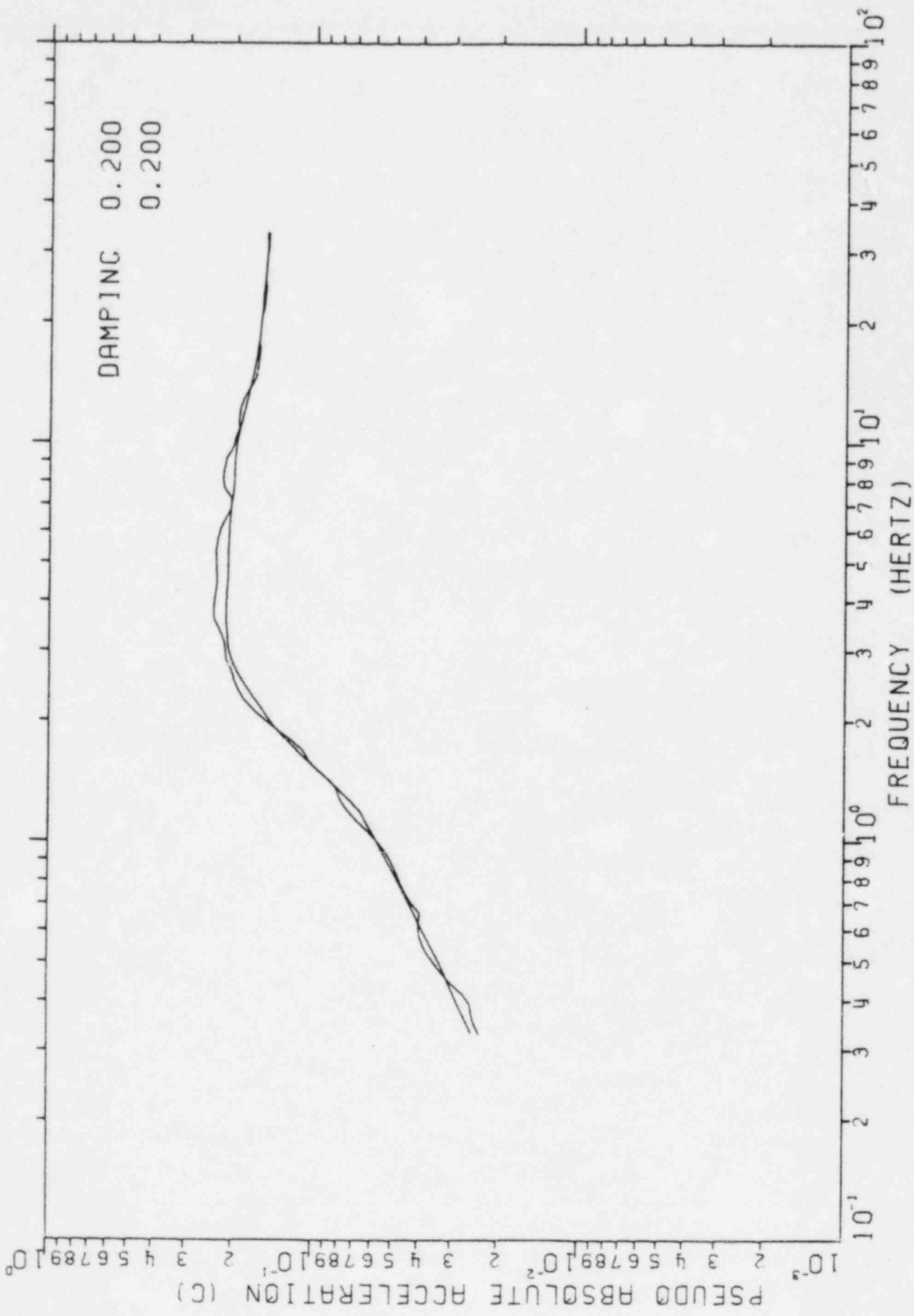


FIGURE I-2-15. COMPARISON OF SYNTHETIC TIME HISTORY AND SME ENVELOPE RESPONSE SPECTRA
TOP OF FILL - 20% DAMPING

I-2-19

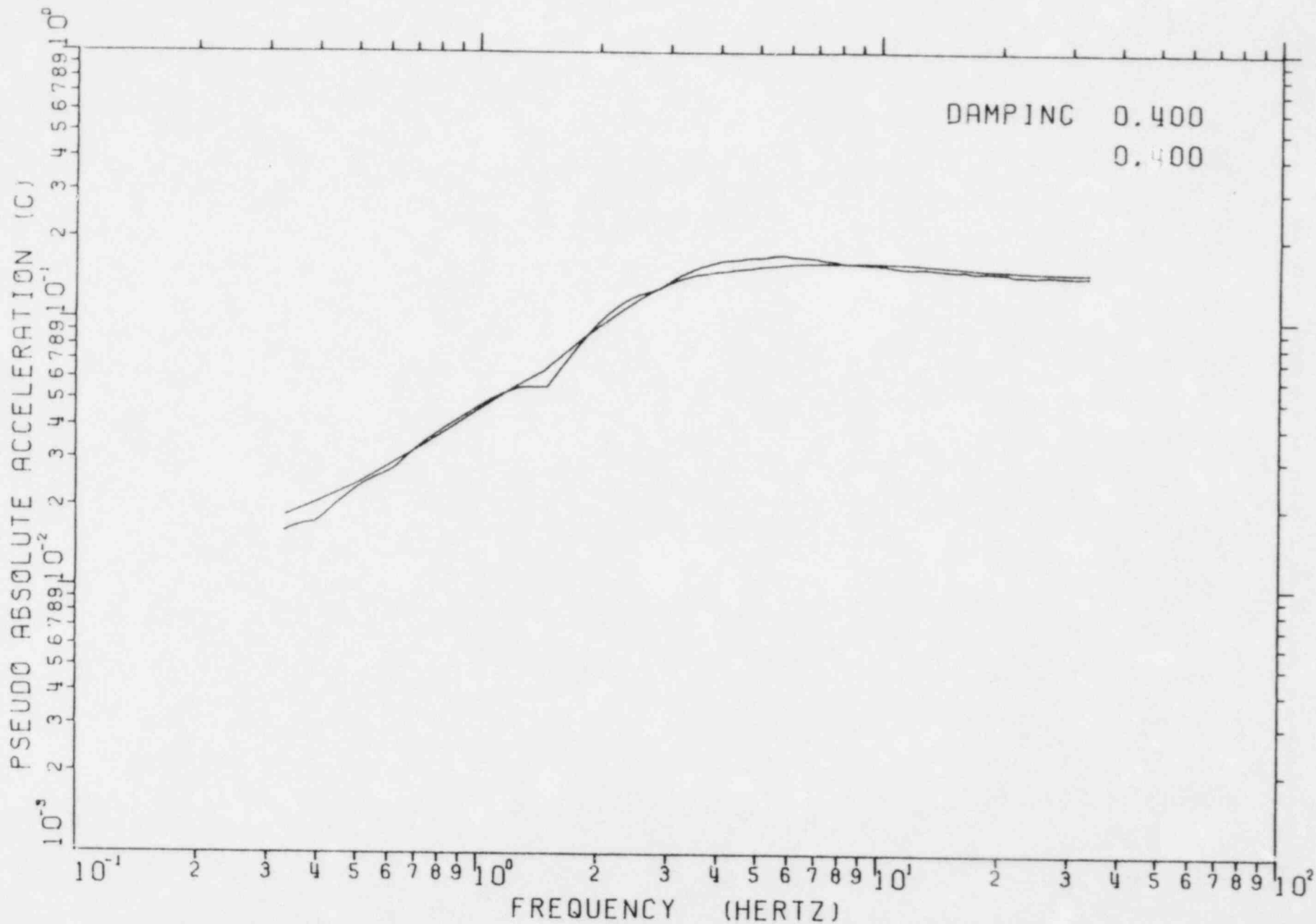


FIGURE I-2-16. COMPARISON OF SYNTHETIC TIME HISTORY AND SME ENVELOPE RESPONSE SPECTRA
TOP OF TILL - 40% DAMPING

3. MIDLAND SITE SOIL PROPERTIES

3.1 SITE CONDITIONS

The reactor building, auxiliary building, and service water pump structure (SWPS) are founded on the original material, namely glacial till deposits. The borated water storage tank (BWST) and the diesel generator building (DGB) are founded on fill just below the current grade. The geological history and characteristics of the foundation materials are described in Section 2.5 of the FSAR (Reference 1).

Geotechnical investigations have been conducted at the Midland site by both Dames & Moore, Inc. and Weston Geophysical Corporation. Subsurface investigations using techniques such as core sampling, cross-hole testing, and comparison of geologic conditions with similar sites has identified the variation of the soil properties with depth for this site. Variations of low strain shear wave velocity from about 850 fps at the top of the glacial till material to about 3000 fps at the top of the bedrock indicate that layering effects may influence the characteristics of the soil impedances developed for the structures. The soil-structure interaction techniques used in the SMR for the site considered the layered soil profile beneath each structure in determining equivalent elastic half-space soil impedance functions.

3.2 SOIL CHARACTERISTICS

Site characteristics for the Midland plant have been developed by both Dames & Moore and Weston Geophysical. Soil profiles based upon both the Dames & Moore data and Weston Geophysical results have been considered in determining soil impedances for the SME since both profiles are considered to be reasonable estimates of the site conditions.

The Dames & Moore based profile (soft site), Figure I-3-1, corresponds to information from Reference 6. Dames & Moore has specified for each of the layers the soil unit weight, W_s , Poisson's ratio, ν , and low strain shear modulus, G_{max} , from which a corresponding low strain shear wave velocity, V_s , has been determined. The strain degradation effects were estimated using the procedure discussed in Section 3.3 below in order to develop the degraded shear modulus, G_{SME} , for the SME ground motion levels.

The Weston Geophysical profile (stiff site), Figure I-3-2, corresponds to the soil layering presented in Reference 3. Soil properties for each of the layers were specified by Weston Geophysical. Strain degradation effects for these layers were estimated using the procedure discussed in Section 3.3. Although the two profiles have different values, both are considered to be reasonable estimates of the site conditions given the usual uncertainty in the data.

The low strain shear modulus, G_{max} , can differ by as much as a factor of 6 to 7 between these two profiles for some layers. Because of the differences between these two soil profiles, an intermediate soil profile (intermediate site) was developed in order to evaluate structural response that might fall between the results obtained for the other two soil profiles. The intermediate soil profile (shown in Figure I-3-3) was developed as a reasonable compromise between the soft site profile and the stiff site profile.

3.3 STRAIN DEGRADATION EFFECTS

The soil profiles shown in Figures I-3-1 to I-3-3 were developed based on low strain shear moduli, G_{max} for the soil. The effect of earthquake-induced shear strains on the soil material properties was estimated by determining equivalent linear high strain soil shear moduli, G_{SME} , applicable at SME ground motion levels by using shear modulus degradation

relationships. Figure I-3-4 presents these strain degradation relationships considered appropriate for the Midland site. This figure has been abstracted from Reference 8.

A simplified method of estimating the peak shear strain level in the soil was used in order to determine equivalent high strain soil shear moduli for each layer. The peak soil shear strain, γ , is approximately estimated by the ratio V/v_s , where V is the peak ground velocity associated with the SME and v_s is the high strain shear wave velocity of the appropriate soil layer. Because the soft site profile (Figure I-3-1) is representative of softer site conditions than the stiff site profile (Figure I-3-2), strain degradation effects were maximized for the soft site data to ensure a conservative bias towards soft-site conditions and minimized when using the stiff site data to ensure a conservative bias towards stiffer site conditions. Peak ground velocity, V , of 2.2 in/sec was used for elevations below the original ground level (Elevation 603) and a peak ground velocity of 3.3 in/sec was used at the top-of-grade (Elevation 634). Linear interpolation was used to estimate peak ground velocities between these two levels.

The procedure followed was as follows:

1. Assume a degraded shear modulus, G_{SME} , for the layer.
2. Calculate the corresponding high strain shear wave velocity, $v_s = \sqrt{G_{SME}/\rho}$ where ρ is the mass density of the soil in the layer.
3. Calculate the maximum soil shear strain from $\gamma = V/v_s$ where V is the peak ground velocity.
4. Enter Figure I-3-4 with the soil strain determined in Step 3 above, and determine a degraded shear modulus for the layer, G_{SME} , using the low strain soil modulus for the layer, G_{max} .
5. Compare G_{SME} from Step 4 to G_{SME} assumed in Step 1. Repeat Steps 1 to 5 until convergence is obtained.

For glacial till, the recommended band of G/G_{max} shown in Figure I-3-4 was used. For dense cohesionless material, the ratio of G/G_{max} shown in Figure I-3-4 for sand was used.

Figure I-3-1 presents a soft soil profile. For the SME and this profile, the following soil degraded shear modulus estimates were made:

Elevation	$\gamma(\%)$	(G_{SME} / G_{MAX})	Lower Bound (G_{SME} / G_{MAX}) Used
550 to 603	0.018 to 0.026	0.30 to 0.60	0.29
410 to 550	0.013 to 0.018	0.35 to 0.65	0.35
260 to 410	0.008	0.80	0.67

To account for possibly larger peak ground velocities at the site and possibly higher seismic shear strain levels, a lower bound ratio of G_{SME}/G_{max} which was at or below the low end of the estimated range of this ratio was used with the soft soil profile in Figure I-3-1 to obtain the soft G_{SME} values shown.

Similarly, Figure I-3-2 presents a stiff soil profile. For the SME with this profile, the following soil degraded shear modulus estimates were made:

Elevation	$\gamma(\%)$	(G_{SME} / G_{MAX})	(G_{SME} / G_{MAX}) Used
570*to 603	0.017 to 0.024	0.30 to 0.60	0.50
463 to 570*	0.009 to 0.011	0.50 to 0.73	0.60
363 to 463	0.007 to 0.008	0.56 to 0.78	0.66
263 to 363	0.007	0.82	0.82

* At the reactor building and service water pump structure, the elevation was taken as 568 and 535, respectively.

With the intermediate profile, an average strain degradation ratio (G_{SME}/G_{max}) of 0.53 was used for all layers.

3.4 Uncertainty Range on Shear Modulus

In soil-structure interaction evaluations, the following sources of uncertainty exist:

1. Uncertainty in the low strain shear modulus, G_{max}
2. Uncertainty in the degradation ratio, G_{SME}/G_{max}
3. Uncertainty in layering effects
4. Uncertainty in modeling used to obtain soil compliances (stiffnesses and radiation damping)

Parametric studies were conducted to evaluate the effect of each of these sources of uncertainty on the soil stiffness and geometric damping impedance functions. Based upon these studies, it was estimated that a conservative lower bound on soil stiffnesses and geometric damping could be obtained by using a lower bound on the effective soil shear modulus given by:

$$G_{\text{eff lower}} = 0.6 G_{\text{eff I-3-1}} \quad (3-1)$$

where $G_{\text{eff I-3-1}}$ represents the effective soil shear modulus obtained from the soft soil profile shown in Figure I-3-1. Similarly, a reasonable upper bound on soil stiffnesses and geometric damping can be obtained by using an upper bound on the effective soil shear modulus given by:

$$G_{\text{eff upper}} = 1.3 G_{\text{eff I-3-2}} \quad (3-2)$$

where $G_{\text{eff I-3-2}}$ represents the effective soil shear modulus obtained from the stiff soil profile shown in Figure I-3-2.

Thus for the SMR, soil shear moduli were varied from 60 percent of the soft soil profile shown in Figure I-3-1 to 130 percent of the stiff soil profile shown in Figure I-3-2. This range is judged to be sufficiently wide so as to encompass the full possible range of Midland soil properties.

Elevation

634

 Top of Grade

603

 Original Ground

Glacial Till

$W_s = 135 \text{ pcf}$

$\nu = 0.47$

$V_s = 1290 \text{ fps}$

$G_{max} = 7 \cdot 10^6 \text{ psf}$

$G_{SME} = 2 \cdot 10^6 \text{ psf}$

550

Glacial Till

$W_s = 135 \text{ pcf}$

$\nu = 0.47$

$V_s = 1690 \text{ fps}$

$G_{max} = 12 \cdot 10^6 \text{ psf}$

$G_{SME} = 4.2 \cdot 10^6 \text{ psf}$

410

Dense Cohesionless Material

$W_s = 135 \text{ pcf}$

$\nu = 0.34$

$V_s = 2540 \text{ fps}$

$G_{max} = 27 \cdot 10^6 \text{ psf}$

$G_{SME} = 17.8 \cdot 10^6 \text{ psf}$

} Elevation 410

$V_s = 2970 \text{ fps}$

$G_{max} = 37 \cdot 10^6 \text{ psf}$

$G_{SME} = 25.2 \cdot 10^6 \text{ psf}$

} Elevation 260

260

Bedrock

$W_s = 150 \text{ pcf}$

$\nu = 0.33$

$V_s = 5000 \text{ fps}$

FIGURE I-3-1. SOIL LAYERING PROFILE FOR SOFT SITE

Elevation

634

 Top of Grade

603

 Original Ground

Aux.
Bldg. - 570

Glacial Till

$$W_s = 120 \text{ pcf}$$

$$\nu = 0.49$$

$$V_s = 1400 \text{ fps}$$

$$G_{\max} = 7.3 \cdot 10^6 \text{ psf}$$

$$G_{\text{SME}} = 3.65 \cdot 10^6 \text{ psf}$$

Reactor
Bldg. - 568

SWPS - 585

Glacial Till

$$W_s = 135 \text{ pcf}$$

$$\nu = 0.42$$

$$V_s = 2300 \text{ fps}$$

$$G_{\max} = 22.2 \cdot 10^6 \text{ psf}$$

$$G_{\text{SME}} = 13.3 \cdot 10^6 \text{ psf}$$

463

Glacial Till

$$W_s = 135 \text{ pcf}$$

$$\nu = 0.42$$

$$V_s = 3000 \text{ fps}$$

$$G_{\max} = 37.8 \cdot 10^6 \text{ psf}$$

$$G_{\text{SME}} = 25.0 \cdot 10^6 \text{ psf}$$

363

Dense Cohesive Material

$$W_s = 135 \text{ pcf}$$

$$\nu = 0.34$$

$$V_s = 3000 \text{ fps}$$

$$G_{\max} = 37.8 \cdot 10^6 \text{ psf}$$

$$G_{\text{SME}} = 31.0 \cdot 10^6 \text{ psf}$$

263

Bedrock

$$W_s = 150 \text{ pcf}$$

$$\nu = 0.33$$

$$V_s = 5000 \text{ fps}$$

FIGURE I-3-2. SOIL LAYERING PROFILE FOR STIFF SITE

Elevation

634

 Top of Grade

603

 Original Ground

Glacial Till

$$W_s = 110 \text{ pcf}$$

$$v = 0.49$$

$$V_s = 1500 \text{ fps}$$

$$G_{\max} = 7.7 \cdot 10^6 \text{ psf}$$

$$G_{\text{SME}} = 4.08 \cdot 10^6 \text{ psf}$$

553

Glacial Till

$$W_s = 135 \text{ pcf}$$

$$v = 0.42$$

$$V_s = 1890 \text{ fps}$$

$$G_{\max} = 15 \cdot 10^6 \text{ psf}$$

$$G_{\text{SME}} = 7.95 \cdot 10^6 \text{ psf}$$

463

Dense Cohesionless Material

$$W_s = 135 \text{ pcf}$$

$$v = 0.34$$

$$V_s = 2468 \text{ fps}$$

$$G_{\max} = 25.6 \cdot 10^6 \text{ psf}$$

$$G_{\text{SME}} = 13.6 \cdot 10^6 \text{ psf}$$

263

Bedrock

$$W_s = 145 \text{ pcf}$$

$$v = 0.33$$

$$V_s = 5000 \text{ fps}$$

FIGURE I-3-3. INTERMEDIATE SOIL PROFILE

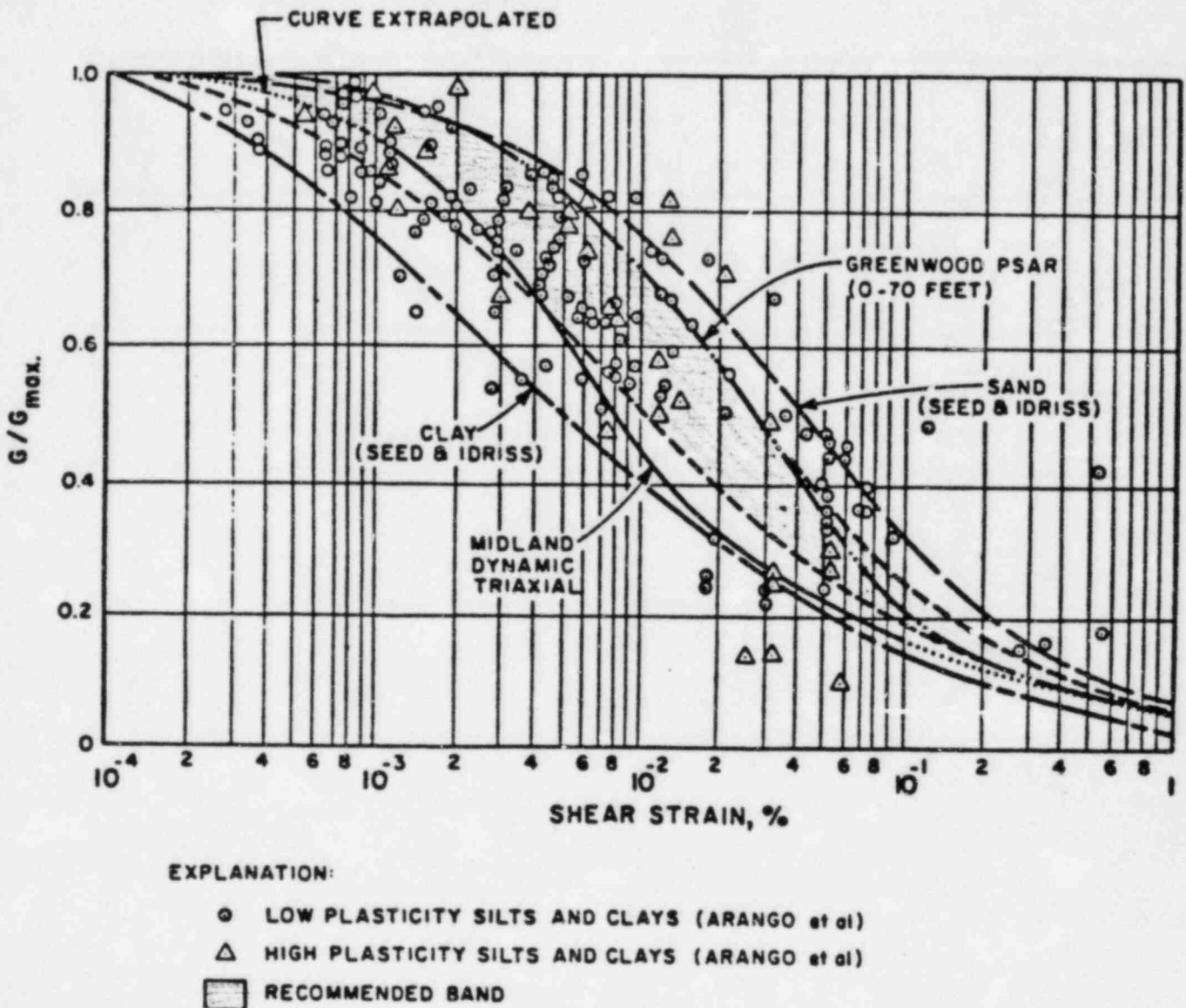


FIGURE I-3-4. STRAIN DEGRADATION RELATIONSHIPS FOR MIDLAND SITE (after Ref. 8)

4. SOIL-STRUCTURE INTERACTION

With the exception of the borated water storage tank and the diesel generator building, all structures investigated for the SME are founded on the original glacial till with varying amounts of embedment. In order to evaluate the effects of the site characteristics at Midland, equivalent elastic half-space stiffness and damping representations were developed based on a layered site analysis which could then be modified to account for embedment and non-standard shape foundation plans.

4.1 EFFECTIVE SHEAR MODULI WITH LAYERING

The soil profiles presented in Section 3.2 above were used to conduct layered site analyses using the program CLASSI (Reference 13). CLASSI develops frequency dependent soil impedances (both real and imaginary) for the structure.

In order to use CLASSI to conduct the layered site analysis, several simplifying approximations were made concerning soil-structure interaction behavior at the site. These are:

1. Equivalent linear high strain soil shear moduli, as discussed in Section 3, adequately represent the soil properties at SME strain levels.
2. Soil-structure interaction effects may be represented by soil springs and dashpots beneath the structure modeling the real and imaginary parts of soil impedance.
3. The foundation base mats for the structures behave rigidly.
4. Coupling effects between adjacent structures through the soil are not important.
5. Embedment effects due to soil surrounding the structure may be represented as a multiplier applied to the unembedded soil impedances.

6. Based upon the soil strain levels defined in Section 3, the soil material (hysteretic) damping was conservatively assumed to be five percent of critical damping (Figure I-4-1).
7. The complex foundation geometry for these structures can be modeled as an equivalent rectangle or circle.

The assumptions presented above are considered to be reasonable for the buildings studied at the Midland site.

In conducting the layered site analyses using CLASSI, idealized foundation geometries were used in the analyses for each of the structures studied. These idealized geometries closely approximated the actual foundation characteristics. For instance, Figure I-4-2 presents the actual projected foundation geometry for the auxiliary building superimposed with the dashed outlined of the idealized foundation used in the CLASSI analysis. The auxiliary building was idealized as a 140' by 236' rectangular foundation which includes the entrapped soil beneath the control tower. Similarly, the SWPS was idealized as an 89' by 106' rectangular foundation as shown in Figure I-4-3. The diesel generator idealized foundation consisted of a 77.5' by 162.5' rectangle which corresponds to the outside dimensions of the spread footings. The reactor building was idealized as a 62' radius circle which is close to the actual structure foundation configuration. The BWST was similarly idealized as a 28.75' radius circle with appropriate adjustment for the rocking degrees of freedom.

The CLASSI layered site analyses considered the structures to be unembedded with the ground surface corresponding to the bottom of the foundation base mat. The base of the foundation for each of the structures studied was determined to be:

- | | |
|------------------------------|------------------|
| 1. Auxiliary Building | - Elevation 562' |
| 2. Reactor Building | - Elevation 578' |
| 3. SWPS | - Elevation 587' |
| 4. Diesel Generator Building | - Elevation 628' |
| 5. BWST | - Elevation 628' |

Using these base mat elevations in conjunction with the general soil profiles shown in Figures I-3-1 to I-3-3, unique layered site soil profiles were determined for each structure.

Layered site analyses were run for each of the three soil profiles presented in Figures I-3-1 to I-3-3 for both the reactor building and the auxiliary building. Only the intermediate soil profile (Figure I-3-3) was used with the SWPS. Conservative soil impedances for the other two soil profiles were developed for this structure based on the auxiliary building results. Analyses for these soil profiles were conducted for the diesel generator building including provisions for the fill soil properties as discussed in Volume V of this report.

Figure I-4-4 presents typical CLASSI results obtained for the auxiliary building for the intermediate soil profile. These frequency dependent compliance functions for horizontal translation of the idealized 140' by 236' foundation in the North-South (N-S) direction correspond to stiffness and damping coefficients. Review of this figure shows that some resonance of the foundation and the underlying soil layers occurs in the 6 to 10 hertz frequency range for this stiffness term. This resonance is also reflected in the damping coefficient, but to a lesser degree.

In order to convert the CLASSI layered site soil impedances developed for the idealized foundations into soil springs and dashpots applicable to the actual structure foundation shapes accounting for both embedment effects and soil layering, effective elastic half-space shear moduli, G_{eff} , were developed. These effective shear moduli are defined as the soil shear moduli which would be required in order to obtain frequency-dependent soil stiffnesses identical to those determined by CLASSI layered site analyses using theoretical elastic half-space equations and the idealized foundation shape. The frequency-dependent elastic half-space equations (based on Reference 14) used to determine G_{eff} are presented in Table I-4-1 for rectangular and circular foundation shapes.

Using Figure I-4-4 for reference, the procedure used for determining G_{eff} for each degree-of-freedom (dof) of the structure (horizontal and vertical translation, rocking, and torsion), is as follows:

1. Estimate the fundamental soil-structure frequency, f , of the structure for the dof of interest.
2. Because of uncertainties in the evaluation of the fundamental frequency f above, determine an average layered stiffness $K(\text{CLASSI})$, over a frequency range of $0.7f$ to $1.35f$.
3. Using the frequency dependent elastic half-space equations presented in Table I-4-1, write an equation for G_{eff} where the stiffness K of the half-space is defined as $K(\text{CLASSI})$. For example, in horizontal translation

$$G_{eff} = \frac{K(\text{CLASSI})}{k_1 2(1+\nu) \beta_x \sqrt{BL}}$$

4. Estimate the frequency-dependent coefficient k_1 , from theoretical elastic half-space theory as presented in References 15, 16, 17, and 18.
5. Solve for G_{eff} for the dof in question, by estimating β_x from Table I-4-1 for the idealized foundation dimensions and estimating Poisson's ratio ν from the layered site profile.

A similar approach was used for all other dof of the soil (rocking, vertical translation, and torsion). When structural frequencies accounting for soil-structure interaction were finally developed with actual foundation geometry and embedment effects incorporated, the frequency estimate, f , used in Step 1 was checked to ensure that the assumed frequencies were compatible with the final structural frequencies. If a significant frequency shift had occurred and the results of Steps 1 to 5 were substantially modified, another iteration of the process was performed.

Using the procedures described above, effective soil shear moduli, G_{eff} , were determined for the auxiliary building and the reactor building for each of the three soil profiles presented in Figure I-3-1 to I-3-3. Effective soil shear moduli for the diesel generator building were determined for the soft site and stiff site soil profiles only. For this structure, soil shear moduli for the intermediate soil case were estimated from the results of the two bounding cases. For the BWST, three values of effective shear modulus were used. The SWPS was studied for the intermediate soil profile only and effective soil shear moduli for the soft and stiff profiles were conservatively scaled from the auxiliary building results for these two cases. Table I-4-2 presents these effective elastic half-space shear moduli, G_{eff} , for each of the structures. Layered site analysis results demonstrated that the effective shear moduli for horizontal translation and torsion could be averaged together and represented by a single value. Similarly, for rocking and vertical translation, the effective soil shear modulus may also usually be represented by one number.

Comparison of the G_{eff} values tabulated in Table I-4-2 to the layered site profiles in Figures I-3-1 to I-3-3 shows that for horizontal translation and torsion, the effective soil shear modulus is heavily influenced by the soil shear modulus in the layers close to the building foundation. For motions which involve vertical motion of the structure such as rocking and vertical translation, the effective soil shear modulus increases due to the stiffening effects of the deeper layers. The relative influence of the various layers beneath the structure varies considerably with layer depth and foundation size and geometry. In all cases, the effective elastic half-space shear modulus, G_{eff} , is heavily influenced by the soil layer immediately beneath the foundation.

4.2 ENERGY ENTRAPMENT DUE TO LAYERING

Two types of damping may be defined for the soil. The first type, known as material or hysteretic damping, is due to energy absorption by the soil due to straining of the material. For the Midland site, this damping has been conservatively estimated to be five percent of critical damping for the SME. Typical material damping (Figure I-4-1) expected at the Midland site soil strain levels would indicate higher than five

percent. Material damping is not strongly affected by layering as discussed in Section 4.5. The second type of soil damping, known as radiation or geometric damping, involves the wave propagation of energy through the soil away from the structure. For an elastic half-space, these waves propagate outwards to infinity. Layered soil profiles, however, tend to trap and reflect some of the energy back up towards the structure. One of the principal reasons for conducting a layered site analysis for the SME was to determine the effect of layering on geometric damping from the structures. In effect, the geometric damping for the layered profile is reduced to some percentage of the damping determined for an equivalent elastic half-space. This decrease in geometric damping may be determined through the use of a factor defined as

$$F_{\text{Layer}} = \frac{C(\text{CLASSI Layered Site Analysis})}{C(\text{Theoretical Elastic Half-Space})}$$

This ratio is indicative of the amount of energy entrapped beneath the structure due to layering.

The layering factor may be determined from the CLASSI layered site analyses results for each dof. Using Figure I-4-4 as an example, the layering factor, F_{Layer} is determined in the following manner:

1. Using the same estimate of the fundamental structure frequency, f , and a frequency range from $0.7f$ to $1.35f$ as discussed in Section 4.1 above, determine the average CLASSI damping, $C^*(\text{CLASSI})$. The damping coefficient determined from CLASSI incorporates the five percent soil material damping in addition to geometric damping effects.

2. Remove the frequency normalization from the CLASSI damping coefficient by:

$$C'(\text{CLASSI}) = \frac{C^*(\text{CLASSI})}{2\pi}$$

3. Remove the five percent soil material damping from the CLASSI result to determine the layered site geometric damping by:

$$C(\text{CLASSI}) + C'(\text{CLASSI}) - 0.1 \frac{K(\text{CLASSI})}{2\pi f} \quad (4-1)$$

where $K(\text{CLASSI})$ is the corresponding layered site stiffness at frequency f as discussed in Section 4.1 above.

4. Determine the equivalent theoretical elastic half-space (EHS) damping coefficient using the equations presented in Table I-4-1. These coefficients are of the form:

$$C(\text{EHS}) = C_j \frac{K_{\text{static}} R_{\text{eq}}}{v_s} \quad (4-2)$$

where:

C_j = Frequency-dependent coefficient determined from an appropriate reference such as References 15, 16, 17, or 18.

K_{static} = Static stiffness of the equivalent half-space determined by $K(\text{CLASSI})/k_j$ with these terms having the same definitions as given in Section 4.1 above.

R_{eq} = Equivalent radius of the foundation based on stiffness equivalence between rectangular and circular foundations.

v_s = $\sqrt{G_{\text{eff}}/\rho}$ where G_{eff} is determined from Table I-4-2 for the appropriate dof and ρ is the mass density of the soil beneath the structure.

5. Calculate the layering factor, F_{Layer} , by:

$$F_{\text{Layer}} = \frac{C(\text{CLASSI})}{C(\text{EHS})} \quad (4-3)$$

A similar approach was used for all the degrees-of-freedom of the structure.

Layering factors for damping were determined for all three soil cases for both the auxiliary and reactor buildings. For the diesel generator building, layering factors were determined for the soft and stiff soil profiles. For this building, layering factors for the intermediate soil profile were estimated from these results. For the SWPS, layering factors were determined for the intermediate soil profile only. Layering factors for the soft and stiff soil profiles were conservatively developed based on auxiliary building results.

The layering factors have been conservatively limited to an upper bound of 75 percent of theoretical elastic half-space damping. This limitation is consistent with a conservative interpretation of experimental results from other nuclear power plant sites (References 19 and 20) and has been recommended as a standard procedure for existing nuclear power plant seismic evaluation (Reference 21).

The layering factors, F_{Layer} , for the structures are presented in Table I-4-3. A single set of layering factors were justified for each of the three soil profiles studied for the auxiliary building, reactor building, and the SWPS. The diesel generator building, however, required an individual set of layering factors for each soil profile. The diesel generator building and BWST are founded on top of a layer of fill underlain by glacial till. Significant impedance mismatches occur at the fill to glacial till interface. For a structure with large foundation dimensions such as the diesel generator building (77.5' by 162.5'), soil stresses due to soil-structure interaction propagate below the bottom of the fill layer. Consequently, elastic energy radiating outward from the structure is trapped at the fill to glacial till interface and reflects back up toward the structure foundation. This energy entrapment is shown in the layering factors determined for the diesel generator building. Different layering factors were required for each of the soil profiles studied for this structure because of significant variation in the magnitude of the impedance mismatch at the fill to glacial till interface. For a structure with smaller foundation dimensions, layering factors would approach theoretical elastic half-space damping because of lesser influence of this interface.

4.3 DEVELOPMENT OF UPPER AND LOWER BOUND SHEAR MODULI

The effective shear moduli values listed in Table I-4-2 are for the soil profiles shown in Figures I-3-1 (soft), I-3-2 (stiff), and I-3-3 (intermediate). These ranges of effective shear moduli do not incorporate all of the sources of uncertainty defined in Section 3.4. Based upon parameter studies, it was determined to define conservative lower and upper bound values of G_{eff} by:

$$G_{\text{eff lower}} = 0.6 G_{\text{eff soft}} \quad (4-4)$$

$$G_{\text{eff upper}} = 1.3 G_{\text{eff stiff}} \quad (4-5)$$

Table I-4-4 presents lower and upper bounds on G_{eff} for each of the buildings based upon Equations 4-4 and 4-5 and Table I-4-2. The resultant range on G_{eff} is very broad and accounts for the full range of uncertainty on the effective shear moduli.

4.4 SOIL STIFFNESSES

Soil springs representing the stiffness of the soil for all degrees-of-freedom of the structure (horizontal and vertical translation, rocking, and torsion) were developed for the auxiliary building, the reactor building, the diesel building, and the SWPS based on the effective soil shear moduli, G_{eff} , presented in Table I-4-4 for each of the soil cases studied. The unembedded, frequency-dependent, elastic half-space impedance functions were evaluated for each structure based on actual foundation geometry. For foundations which contain entrapped soil such as the auxiliary building and SWPS (Figures I-4-2 and I-4-3), the horizontal and torsional impedances were based on the entire area enclosed within the foundation perimeter, while for vertical and rocking only the foundation contact area was used. Actual foundation geometries for these structures were transformed into equivalent rectangles by maintaining equivalence of area and moments of inertia. The details of the development of the equivalent rectangle geometries are presented in the volumes of this report covering the individual structures. A circular base mat with a radius of 62 feet was used in all cases for the reactor building. For the BWST, a circular base mat with a radius of 28.75 feet was used for the vertical and horizontal translation impedances. For rocking, the impedances developed for a 24-foot radius circular base mat were subtracted from the 28.75-foot rocking impedances to develop equivalent ring foundation impedances.

The frequency-dependent, elastic half-space equations presented in Table I-4-1 were used to develop soil stiffnesses for each structure. Tables I-4-5 through I-4-8 present the unembedded soil stiffnesses for the lower bound, intermediate, and upper bound soil cases for the auxiliary building SWPS, reactor building, and diesel generator building.

The auxiliary building/control tower, the reactor buildings and the SWPS are all embedded to varying degrees. The diesel generator building and BWST were considered to be unembedded. These embedment effects were considered to be applied as a multiplier to the frequency dependent elastic half-space impedances discussed above. Embedment increases both the damping and stiffness of soil-structure systems. Multipliers applied to unembedded stiffnesses and dashpots accounting for embedment effects were developed based on methodology presented in Reference 10. The embedment effect applied to the unembedded soil stiffness is of the form:

$$F_{emb_i} = \left[1 + (\alpha_i - 1) \frac{G_1}{G_2} j \right] \quad (4-6)$$

The embedment coefficient for damping is similar.

The coefficient α_i represents the embedment for degree-of-freedom i for full embedment of the structure to a depth H below the ground surface assuming complete lateral perimeter contact with the surrounding soil. The ratio of high strain side soil shear modulus (G_1) to the soil shear modulus for soil beneath the foundation (G_2) is a correction accounting for the differences in soil properties surrounding the structure. The coefficient j in the above equation is a correction term which accounts for partial embedment effects. The coefficient α_i is based on the assumption the structure is fully bonded to the surrounding soil. However, for a structure oscillating under earthquake loadings, separation of the structure and side soil may occur after a few cycles. Because of the limited ability of the soil to transmit tension, only the

portion of embedded soil in compression can then be reliably counted on to provide additional stiffening effects. The coefficient j accounts for side soil separation from the structure. In addition, this term also accounts for the fact that the structure may not be fully embedded on all sides of its perimeter. A typical plot of α_i is shown in Figure I-4-5 (from Reference 10). The details of the embedment stiffness coefficients used in the SME evaluation are presented in the appropriate volumes for the individual structures. Figure I-4-6 shows the plot of the impedance correction factor.

Tables I-4-5 through I-4-7 present the embedment factors and corresponding embedded soil stiffnesses for the auxiliary building, reactor building, and SWPS. As shown by these tables, the embedment factors for this site are relatively small and represent increases of 10 to 20 percent over the unembedded soil stiffnesses. The soil stiffnesses for the DBG and BWST are not affected by embedment as shown in Tables I-4-8 and I-4-13, respectively.

4.5 SOIL ENERGY DISSIPATION

Soil dashpots accounting for both geometrical and material damping were developed for all degrees-of-freedom of the structures. These soil impedances accounted for the actual foundation geometry of the structures, frequency dependent effects, and reduction of the soil geometrical damping due to layering effects. Embedment effects were considered to be applied as a multiplier to the unembedded dashpots determined from the elastic half-space equations presented in Table I-4-1.

The fundamental equation for calculating an unembedded dashpot accounting for geometric damping is:

$$C^* = C_i \frac{K_T (\text{Static}) R_{eq}}{v_w} F_{\text{Layer}} \quad (4-7)$$

In this formulation, C_i is the frequency-dependent coefficient determined from References 15, 16, 17, or 18 as discussed in Section 4.2 above, R_{eq} is the equivalent radius of the foundation, and v_s is the high strain shear wave velocity corresponding to the effective soil shear modulus, G_{eff} . The soil stiffness, K_T (static), represents the unembedded soil spring stiffness presented in Tables I-4-5 through I-4-8 divided by the appropriate frequency-dependent coefficient, k_i , as defined by Section 4.1 above. The layering factor, F_{Layer} , represents the reduction in radiation damping due to energy entrapment from soil layering. These layering factors have been previously presented in Table I-4-3. Tables I-4-9 through I-4-11 present the unembedded dashpots calculated for the auxiliary building, reactor building, and SWPS.

Using an approach similar to that discussed for the stiffness calculations, embedment factors were calculated which were applied as a multiplier to the unembedded soil damping coefficient, C^* . The embedment factors for damping were calculated based on the procedure presented in Reference 10 and are shown in Tables I-4-9 through I-4-11 for each of the structures studied which were determined to have significant embedment.

Soil material damping of five percent of critical was added to the damping coefficients after the soil embedment factors had been applied. The five percent soil material damping is defined as:

$$C(5\%) = 0.1 \frac{K_T \text{ (embedded)}}{2\pi f} \quad (4-8)$$

where K_T (embedded) is the embedded soil stiffness for the structure determined from Tables I-4-5 through I-4-8 and the frequency, f , is the estimate of the fundamental soil-structure frequency as discussed in Section 4.1 above. The total embedded soil dashpot was calculated by:

$$C = C^* \cdot F_{emb} \text{ (damping)} + C(5\%) \quad (4-9)$$

where F_{emb} (damping) is the embedment coefficient applicable to damping as previously discussed. Tables I-4-9 through I-4-13 present the final soil dashpots used in the SMR for all three soil cases studied.

TABLE I-4-1

Frequency Dependent Elastic Half-Space Impedance

Direction of Motion	Equivalent Spring Constant For Rectangular Footing	Equivalent Spring Constant For Circular Footing	Equivalent Damping Coefficient
Horizontal	$k_x = k_1 2(1+\nu)GB_x \sqrt{BL}$	$k_x = k_1 \frac{32(1-\nu)GR}{7-8\nu}$	$c_x = c_1 k_x(\text{static})R \sqrt{\rho/G}$
Rocking	$k_\psi = k_2 \frac{G}{1-\nu} B_\psi B^2 L$	$k_\psi = k_2 \frac{8GR^3}{3(1-\nu)}$	$c_\psi = c_2 k_\psi(\text{static})R \sqrt{\rho/G}$
Vertical	$k_z = k_3 \frac{G}{1-\nu} B_z \sqrt{BL}$	$k_z = k_3 \frac{4GR}{1-\nu}$	$c_z = c_3 k_z(\text{static})R \sqrt{\rho/G}$
Torsion	—————	$k_\theta = k_4 \frac{16}{3} GR^3$	$c_t = c_4 k_t(\text{static})R \sqrt{\rho/G}$

in which:

ν = Poisson's ratio of foundation medium,

G = shear modulus of foundation medium,

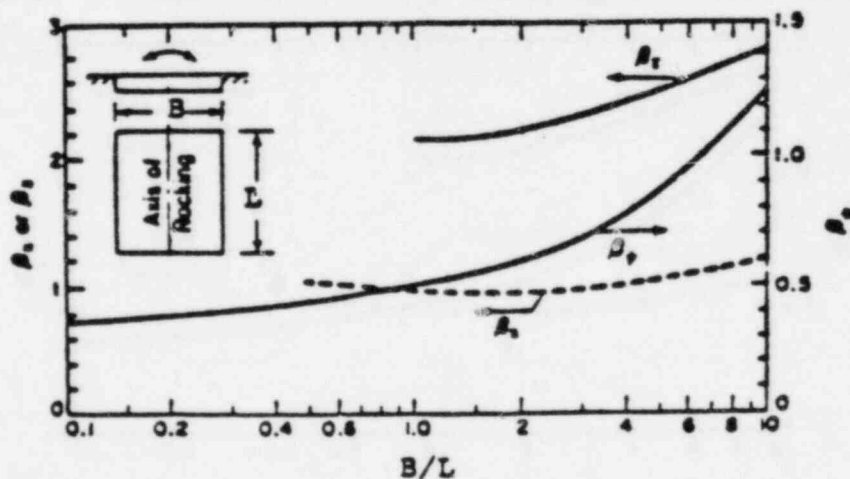
R = radius of the circular base mat,

ρ = density of foundation medium,

B = width of the base mat in the plane of horizontal excitation,

L = length of the base mat perpendicular to the plane of horizontal excitation,

k_1, k_2, k_3, k_4
 c_1, c_2, c_3, c_4 = frequency dependent coefficients modifying the static stiffness or damping.



Constants β_x , β_ψ and β_z for

TABLE I-4-2

Equivalent Elastic Half-Space Shear Moduli For Midland
Soil Profiles

Building	Structure DOF	Dynamic Soil Shear Modulus, G_{eff} (Ksf)		
		Soft Soil Profile	Intermediate Soil Profile	Stiff Soil Profile
Auxiliary	Horizontal Trans- lation, Torsion	3,200	7,100	13,900
	Vertical Trans- lation, Rocking	4,000	8,600	14,900
Reactor	Horizontal Trans- lation	2,400	5,300	7,800
	Vertical Trans- lation, Rocking	2,800	7,300	11,800
SWPS	Horizontal Trans- lation, Torsion	2,200	4,900	13,900
	Vertical Trans- lation, Rocking	2,900	6,200	14,900
DGB	Horizontal Trans- lation	830	950	1,100
	Vertical Trans- lation	1,650	2,800	3,500
	Rocking	1,300	1,700	2,100
BWST	All Degrees of Freedom	690	1,150	1,900

TABLE I-4-3

LAYERING FACTORS FOR DAMPING FOR MIDLAND STRUCTURES

Direction	$F_{\text{Layer}} = \frac{C \text{ (CLASSI Layered Site Analysis)}}{C \text{ (Theoretical Elastic Half Space)}}$					
	Auxiliary Building*	Reactor Building*	SWPS*	Diesel Generator Building		
				Soft Soil	Intermediate Soil	Stiff Soil
Horizontal Translation	0.75	0.50	0.75	0.50	0.30	0.20
Vertical Translation	0.75	0.75	0.75	0.50	0.30	0.20
Rocking	0.50	0.25	0.50	0.20	0.10	0.05
Torsion	0.75	NA	0.75	NA	NA	NA

*The same layering factor was justified for all three soil profiles for these structures.

TABLE I-4-4

Equivalent Elastic Half-Space Shear Moduli
For Range of Soil Properties Used in SME

Building	Structure Dof	Dynamic Soil Shear Modulus, G_{eff} (Ksf)		
		Lower Bound Soil Case	Intermediate Soil Case	Upper Bound Soil Case
Auxiliary	Horizontal Trans- lation, Torsion	1,900	7,100	18,100
	Vertical Trans- lation, Rocking	2,400	8,600	19,400
Reactor	Horizontal Trans- lation	1,400	5,300	10,100
	Vertical Trans- lation, Rocking	1,700	7,300	15,300
SWPS	Horizontal Trans- lation, Torsion	1,300	4,900	18,100
	Vertical Trans- lation, Rocking	1,750	6,200	19,400
DGB	Horizontal Trans- lation	500	950	1,400
	Vertical Trans- lation	1,000	2,800	4,600
	Rocking	770	1,700	2,700
BWST	All Degrees of Freedom	690	1,150	1,900

TABLE I-4-5

AUXILIARY BUILDING SOIL STIFFNESSES

Motion	Non-Embedded Soil Stiffness			Embedment Factor	Embedded Soil Stiffness		
	Lower Bound Soil	Intermediate Soil	Upper Bound Soil		Lower Bound Soil	Intermediate Soil	Upper Bound Soil
Translational							
North-South	$0.90 \cdot 10^6$	$3.21 \cdot 10^6$	$8.18 \cdot 10^6$	1.11	$1.00 \cdot 10^6$	$3.56 \cdot 10^6$	$9.08 \cdot 10^6$
East-West	$0.93 \cdot 10^6$	$3.36 \cdot 10^6$	$8.54 \cdot 10^6$	1.10	$1.02 \cdot 10^6$	$3.70 \cdot 10^6$	$9.40 \cdot 10^6$
Vertical	$1.18 \cdot 10^6$	$3.64 \cdot 10^6$	$8.07 \cdot 10^6$	1.09	$1.28 \cdot 10^6$	$3.97 \cdot 10^6$	$8.80 \cdot 10^6$
Rotational							
North-South	$1.14 \cdot 10^{10}$	$3.73 \cdot 10^{10}$	$8.41 \cdot 10^{10}$	1.24	$1.41 \cdot 10^{10}$	$4.63 \cdot 10^{10}$	$10.4 \cdot 10^{10}$
East-West	$0.87 \cdot 10^{10}$	$2.85 \cdot 10^{10}$	$6.25 \cdot 10^{10}$	1.22	$1.06 \cdot 10^{10}$	$3.48 \cdot 10^{10}$	$7.63 \cdot 10^{10}$
Torsional	$0.94 \cdot 10^{10}$	$3.48 \cdot 10^{10}$	$8.92 \cdot 10^{10}$	1.21	$1.13 \cdot 10^{10}$	$4.21 \cdot 10^{10}$	$10.9 \cdot 10^{10}$

- NOTES: 1. Units for Translational Soil Springs are K/ft.
 2. Units for Rotational Soil Springs are K-ft./rad.

TABLE I-4-6

SERVICE WATER PUMP STRUCTURE SOIL STIFFNESSES

Motion	Non-Embedded Soil Stiffness			Embedment Factor	Embedded Soil Stiffness		
	Lower Bound Soil	Intermediate Soil	Upper Bound Soil		Lower Bound	Intermediate	Upper Bound
Translational							
North-South	$3.48 \cdot 10^5$	$1.26 \cdot 10^6$	$4.66 \cdot 10^6$	1.05	$3.69 \cdot 10^5$	$1.34 \cdot 10^6$	$4.94 \cdot 10^6$
East-West	$3.53 \cdot 10^5$	$1.28 \cdot 10^6$	$4.74 \cdot 10^6$	1.06	$3.74 \cdot 10^5$	$1.36 \cdot 10^6$	$5.02 \cdot 10^6$
Vertical	$3.52 \cdot 10^5$	$1.46 \cdot 10^6$	$4.58 \cdot 10^6$	1.06	$4.79 \cdot 10^5$	$1.55 \cdot 10^6$	$4.85 \cdot 10^6$
Rotational							
North-South	$8.54 \cdot 10^8$	$2.77 \cdot 10^9$	$8.65 \cdot 10^9$	1.14	$9.73 \cdot 10^8$	$3.15 \cdot 10^9$	$9.86 \cdot 10^9$
East-West	$8.55 \cdot 10^8$	$2.78 \cdot 10^9$	$8.63 \cdot 10^9$	1.17	$1.00 \cdot 10^9$	$3.24 \cdot 10^9$	$1.01 \cdot 10^{10}$
Torsional	$8.96 \cdot 10^8$	$3.94 \cdot 10^9$	$1.25 \cdot 10^{10}$	1.16	$1.04 \cdot 10^9$	$3.94 \cdot 10^9$	$1.45 \cdot 10^{10}$

Notes: 1. Units for Translational Soil Springs are K/ft.

2. Units for Rotational Soil Springs are K-ft/rad.

TABLE I-4-7

REACTOR BUILDING SOIL STIFFNESSES

Motion	Non-Embedded Soil Stiffnesses			Embedment Factor	Embedded Soil Stiffnesses		
	Lower Bound Soil	Intermediate Soil	Upper Bound Soil		Lower Bound Soil	Intermediate Soil	Upper Bound Soil
Translational							
North-South	4.55×10^5	1.65×10^6	3.16×10^6	1.06	4.83×10^5	1.75×10^6	3.35×10^6
East-West	4.55×10^5	1.65×10^6	3.16×10^6	1.06	4.83×10^5	1.75×10^6	3.35×10^6
Vertical	6.00×10^5	2.65×10^6	5.38×10^6	1.04	6.24×10^5	2.76×10^6	5.60×10^6
Rotational							
North-South	1.96×10^9	6.90×10^9	1.50×10^{10}	1.13	2.21×10^9	7.78×10^9	1.69×10^{10}
East-West	1.96×10^9	6.90×10^9	1.50×10^{10}	1.13	2.21×10^9	7.78×10^9	1.69×10^{10}

- Notes: 1. Units for Translational Soil Springs are K/ft.
 2. Units for Rotational Soil Springs are K-ft/rad.

TABLE I-4-8

DIESEL GENERATOR BUILDING SOIL STIFFNESSES

Motion	Soil Stiffness		
	Lower Bound Soil	Intermediate Soil	Upper Bound Soil
Translational			
North-South	1.50×10^5	2.80×10^5	4.10×10^5
East-West	1.47×10^5	2.75×10^5	4.02×10^5
Vertical	2.87×10^5	7.69×10^5	1.25×10^6
Rotational			
North-South	3.94×10^8	9.12×10^8	1.43×10^9
East-West	1.03×10^9	2.44×10^9	3.84×10^9

Notes: 1. Units for Translational Soil Springs are K/ft.

2. Units for Rotational Soil Springs are K-ft/rad.

TABLE I-4-9

AUXILIARY BUILDING DAMPING CONSTANTS

Motion	Non-Embedded Dashpot			Embedment Factor	Embedded Dashpot (3)		
	Lower Bound Soil	Intermediate Soil	Upper Bound Soil		Lower Bound Soil	Intermediate Soil	Upper Bound Soil
Translational							
North-South	$6.02 \cdot 10^4$	$1.12 \cdot 10^5$	$1.77 \cdot 10^5$	1.25	$8.33 \cdot 10^4$	$1.60 \cdot 10^5$	$2.58 \cdot 10^5$
East-West	$6.46 \cdot 10^4$	$1.22 \cdot 10^5$	$1.91 \cdot 10^5$	1.24	$8.82 \cdot 10^4$	$1.69 \cdot 10^5$	$2.76 \cdot 10^5$
Vertical	$1.41 \cdot 10^5$	$2.54 \cdot 10^5$	$3.74 \cdot 10^5$	1.11	$1.64 \cdot 10^5$	$2.97 \cdot 10^5$	$4.42 \cdot 10^5$
Rotational							
North-South	$2.17 \cdot 10^8$	$4.53 \cdot 10^8$	$5.65 \cdot 10^8$	1.44	$4.25 \cdot 10^8$	$9.07 \cdot 10^8$	$1.24 \cdot 10^9$
East-West	$2.80 \cdot 10^7$	$2.03 \cdot 10^8$	$2.55 \cdot 10^8$	1.46	$2.27 \cdot 10^8$	$5.01 \cdot 10^8$	$6.84 \cdot 10^8$
Torsional	$2.08 \cdot 10^8$	$3.79 \cdot 10^8$	$6.35 \cdot 10^8$	1.49	$4.01 \cdot 10^8$	$8.03 \cdot 10^8$	$1.39 \cdot 10^9$

- NOTES: 1. Units for Translational Dashpots are K-sec/ft.
 2. Units for Rotational Dashpots are K-sec-ft./rad.
 3. Includes 5% Soil Hysteretic Damping.

TABLE I-4-10

SERVICE WATER PUMP STRUCTURE DAMPING CONSTANTS

Motion	Non-Embedded Dashpot			Embedment Factor	Embedded Dashpot (3)		
	Lower Bound Soil	Intermediate Soil	Upper Bound Soil		Lower Bound Soil	Intermediate Soil	Upper Bound Soil
Translational							
North-South	$1.57 \cdot 10^4$	$2.94 \cdot 10^4$	$5.65 \cdot 10^4$	1.12	$1.99 \cdot 10^4$	$3.73 \cdot 10^4$	$7.16 \cdot 10^4$
East-West	$1.62 \cdot 10^4$	$3.04 \cdot 10^4$	$5.84 \cdot 10^4$	1.14	$2.09 \cdot 10^4$	$3.91 \cdot 10^4$	$7.51 \cdot 10^4$
Vertical	$2.79 \cdot 10^4$	$4.80 \cdot 10^4$	$8.50 \cdot 10^4$	1.09	$3.29 \cdot 10^4$	$5.66 \cdot 10^4$	$1.00 \cdot 10^5$
Rotational							
North-South	$8.61 \cdot 10^6$	$1.48 \cdot 10^7$	$2.62 \cdot 10^7$	1.30	$1.69 \cdot 10^7$	$2.94 \cdot 10^7$	$5.15 \cdot 10^7$
East-West	$7.74 \cdot 10^6$	$1.33 \cdot 10^7$	$2.35 \cdot 10^4$	1.37	$1.65 \cdot 10^7$	$2.88 \cdot 10^7$	$5.03 \cdot 10^7$
Torsional	$1.24 \cdot 10^7$	$2.41 \cdot 10^7$	$4.63 \cdot 10^7$	1.36	$2.35 \cdot 10^7$	$4.56 \cdot 10^7$	$8.76 \cdot 10^7$

- Notes: 1. Units for Translational Dashpots are K-sec/ft
 2. Units for Rotational Dashpots are K-sec-ft/rad
 3. Includes 5% Soil Hysteretic Damping

TABLE I-4-11

REACTOR BUILDING DAMPING CONSTANTS

Motion	Non-Embedded Dashpot			Embedment Factor	Embedded Dashpot (3)		
	Lower Bound Soil	Intermediate Soil	Upper Bound Soil		Lower Bound Soil	Intermediate Soil	Upper Bound Soil
Translational							
North-South	1.77×10^4	3.06×10^4	4.23×10^4	1.15	2.28×10^4	4.33×10^4	5.95×10^4
East-West	1.77×10^4	3.06×10^4	4.23×10^4	1.15	2.28×10^4	4.33×10^4	5.95×10^4
Vertical	4.96×10^4	1.06×10^5	1.49×10^5	1.07	5.36×10^4	1.16×10^5	1.66×10^5
Rotational							
North-South	5.02×10^6	8.48×10^6	1.48×10^7	1.37	2.81×10^7	6.42×10^7	1.01×10^8
East-West	5.02×10^6	8.48×10^6	1.48×10^7	1.41	2.81×10^7	6.42×10^7	1.01×10^8

- Notes: 1. Units for Translational Dashpots are K-sec/ft
 2. Units for Rotational Dashpots are K-sec-ft/rad
 3. Includes 5% Soil Hysteretic Damping

TABLE I-4-12

DIESEL GENERATOR BUILDING DAMPING CONSTANTS

Motion	Dashpot		
	Lower Bound Soil	Intermediate Soil	Upper Bound Soil
Translation			
North-South	1.07×10^4	8.97×10^4	8.01×10^3
East-West	9.42×10^3	8.18×10^3	7.49×10^3
Vertical	2.76×10^4	2.64×10^4	2.48×10^4
Rotational			
North-South	5.62×10^6	5.94×10^6	6.66×10^6
East-West	2.60×10^7	2.70×10^7	2.94×10^7

- Notes: 1. Units for Translational Dashpots are K-sec/ft.
 2. Units for Rotational Dashpots are K-sec-ft/rad.
 3. Includes 5% Soil Hysteretic Damping.

TABLE I-4-13

BORATED WATER STORAGE TANK STIFFNESS AND DAMPING CONSTANTS

Motion	Stiffness			Dashpot(Radiation Damping)			Radiation Damping Plus Soil Material Damping (% of Critical)
	Lower Bound Soil	Intermediate Soil	Upper Bound Soil	Lower Bound Soil	Intermediate Soil	Upper Bound Soil	All Soils
Horizontal Translation	0.98×10^5	1.63×10^5	2.72×10^5	3.97×10^3	5.13×10^3	6.62×10^3	56
Rocking	2.16×10^7	3.60×10^7	6.01×10^7	5.84×10^5	7.54×10^5	9.74×10^5	39
Vertical Translation	0.99×10^5	1.65×10^5	2.76×10^5	0.81×10^4	1.05×10^4	1.35×10^4	88

- NOTES: 1. Units for Translational Soil Springs K/ft
 2. Units for Rotational Soil Springs K-ft/rad
 3. Units for Translational Dashpots K-sec/ft
 4. Units for Rotational Dashpots K-sec-ft/rad
 5. Percent of Critical Damping Includes 5% Soil Hysteretic Damping

I-4-27

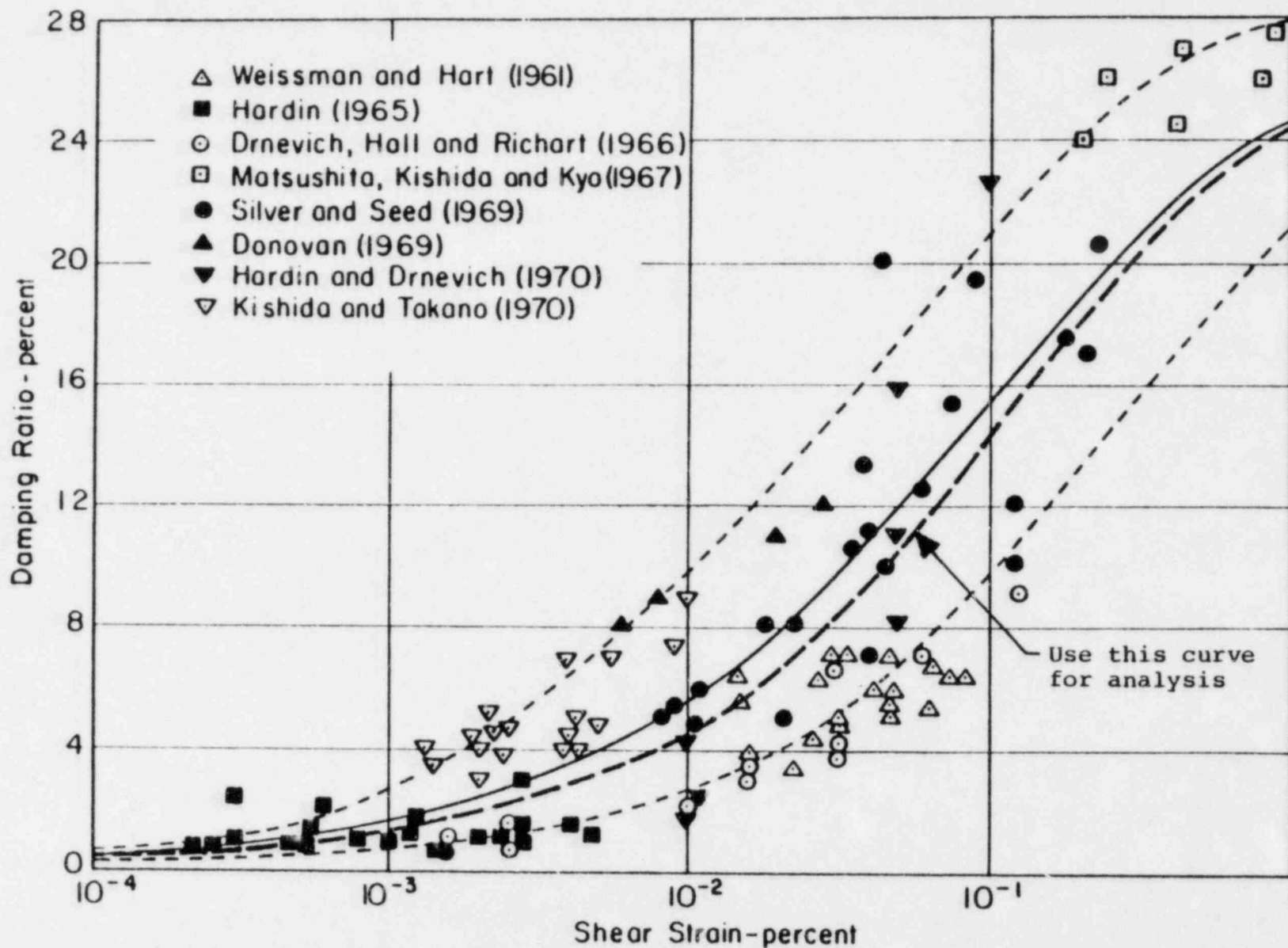


FIGURE I-4-1. DAMPING RATIOS FOR SANDS (after Reference 22)

I-4-28

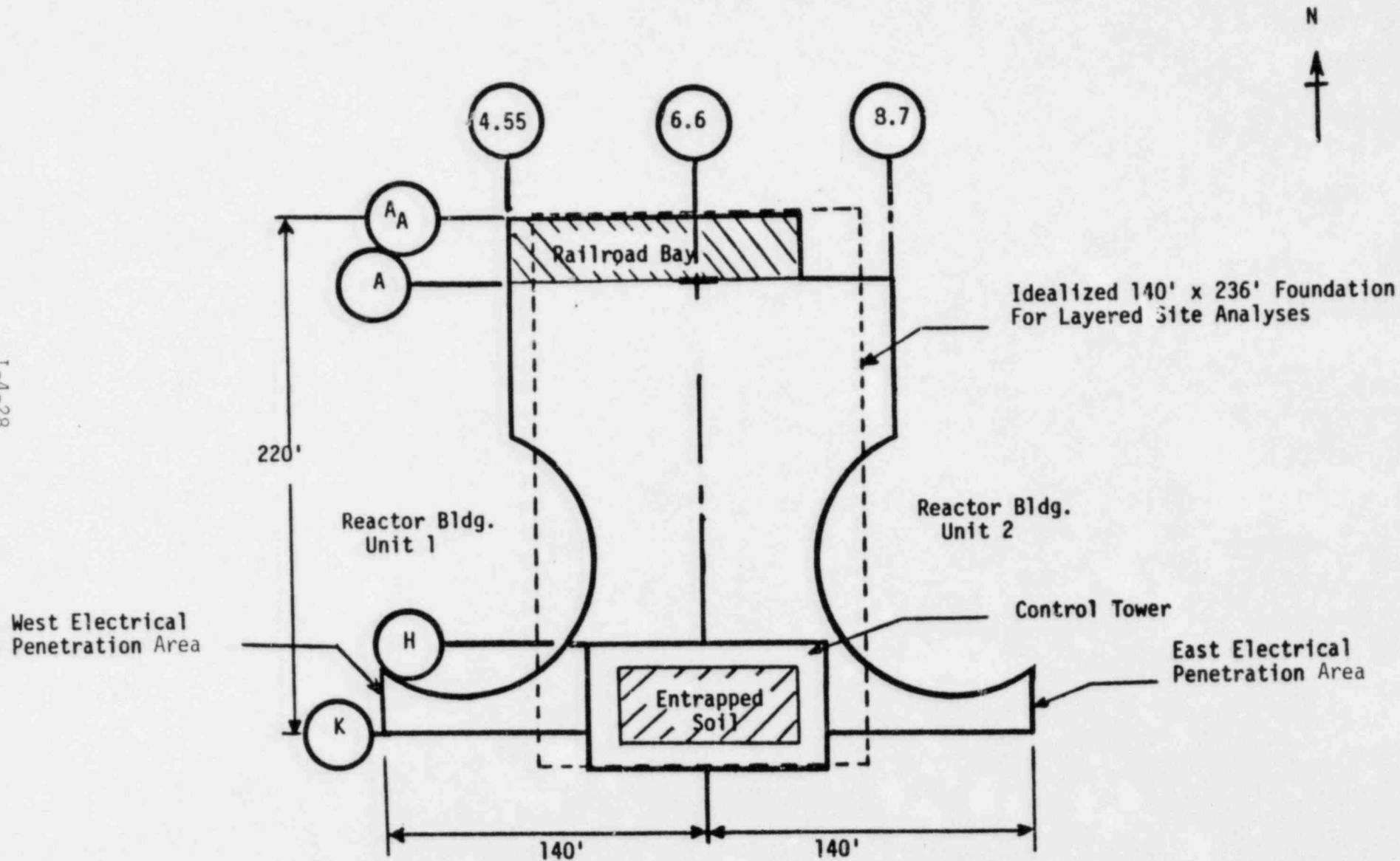


FIGURE I-4-2. SCHEMATIC REPRESENTATION OF AUXILIARY BUILDING FOUNDATION SHOWING IDEALIZED FOUNDATION USED IN LAYERED SITE ANALYSES

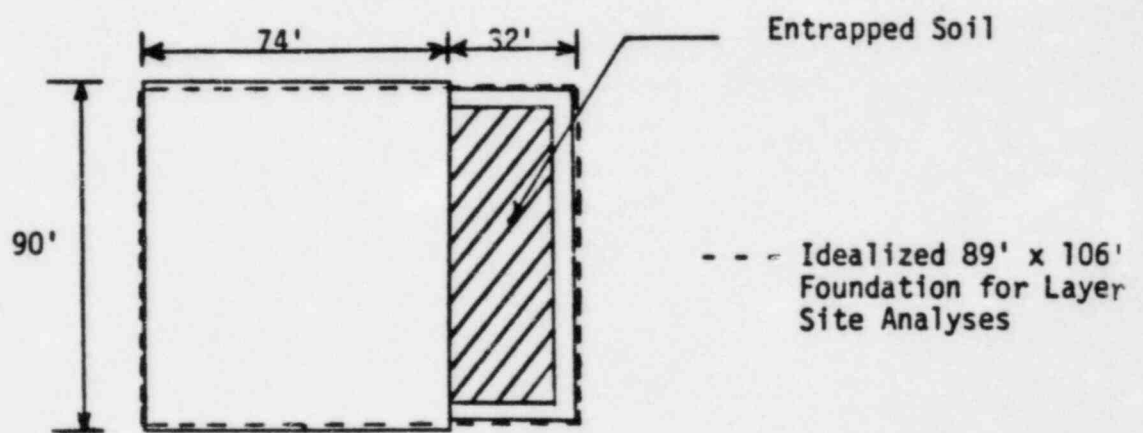


FIGURE I-4-3. SCHEMATIC REPRESENTATION OF SERVICE WATER PUMP STRUCTURE FOUNDATION SHOWING IDEALIZED FOUNDATION USED IN LAYERED SITE ANALYSES.

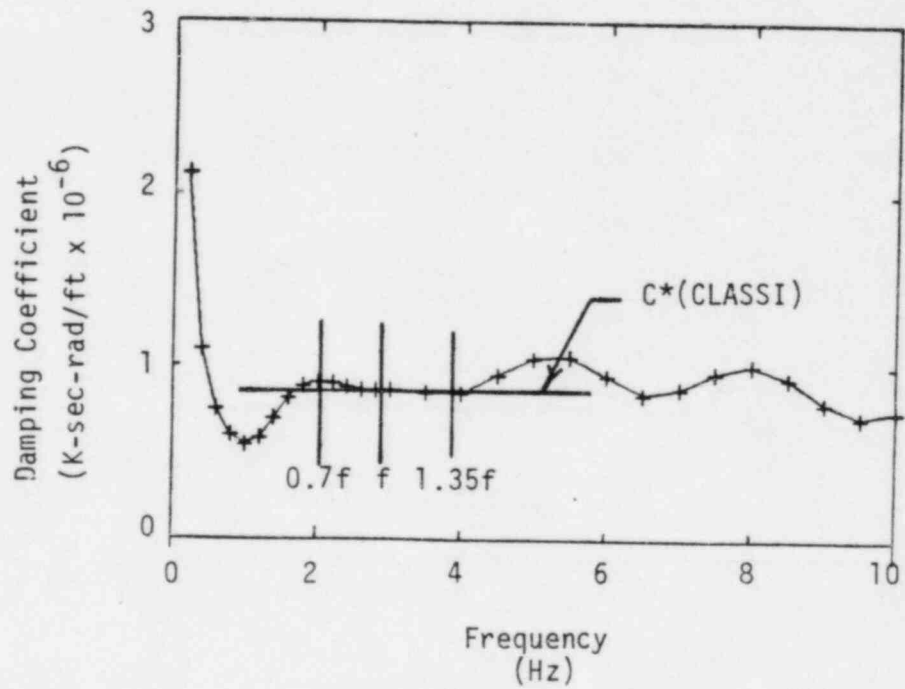
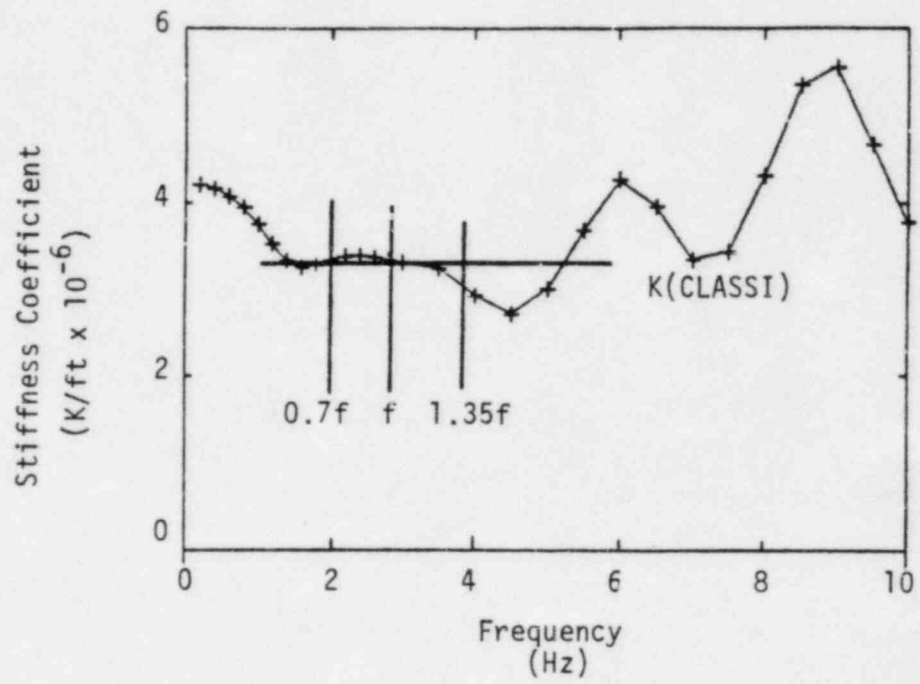


FIGURE I-4-4. TYPICAL CLASSI LAYERED SITE IMPEDANCES DEVELOPED FOR NORTH-SOUTH TRANSLATION OF THE AUXILIARY BUILDING, INTERMEDIATE SOIL PROFILE

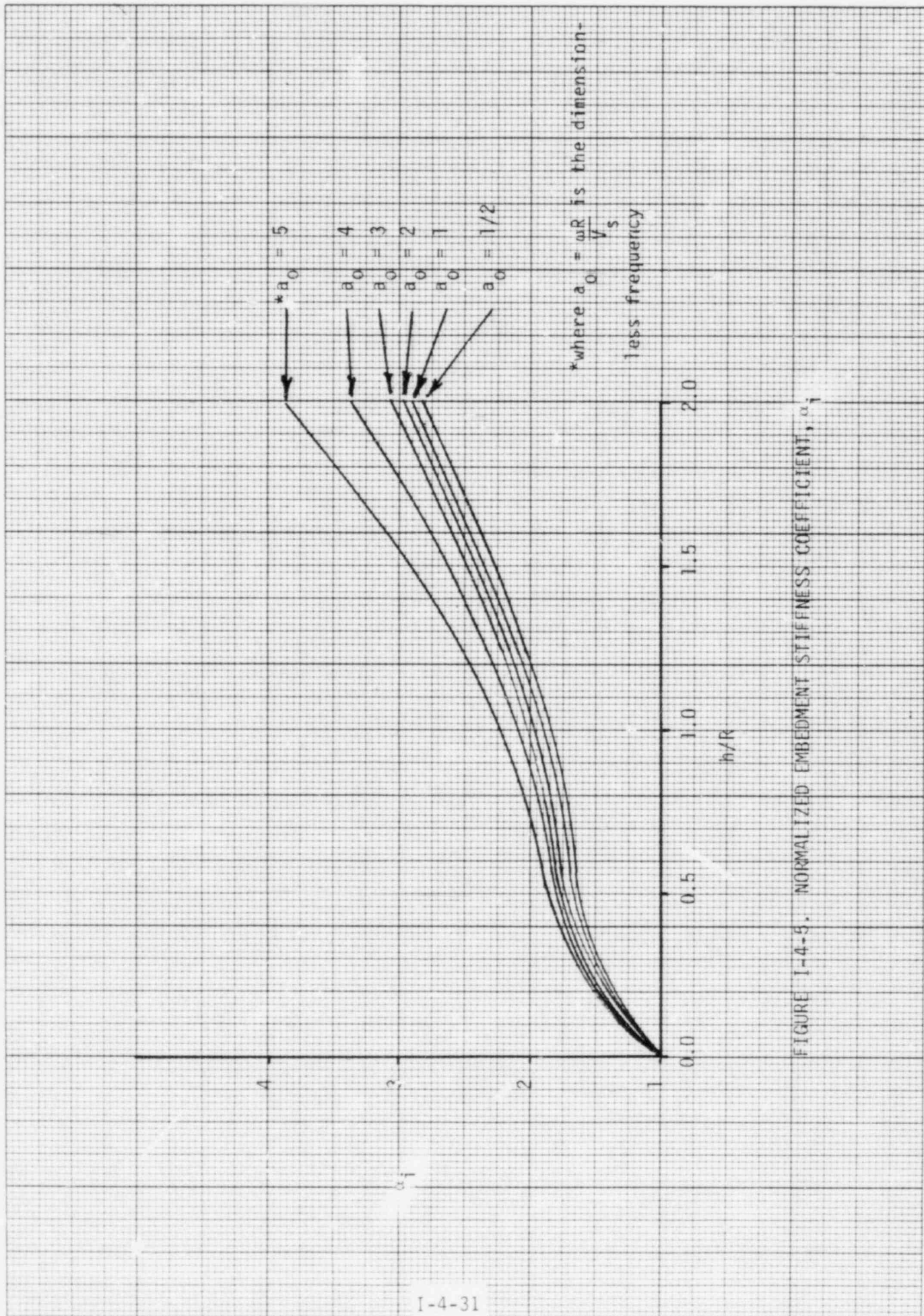
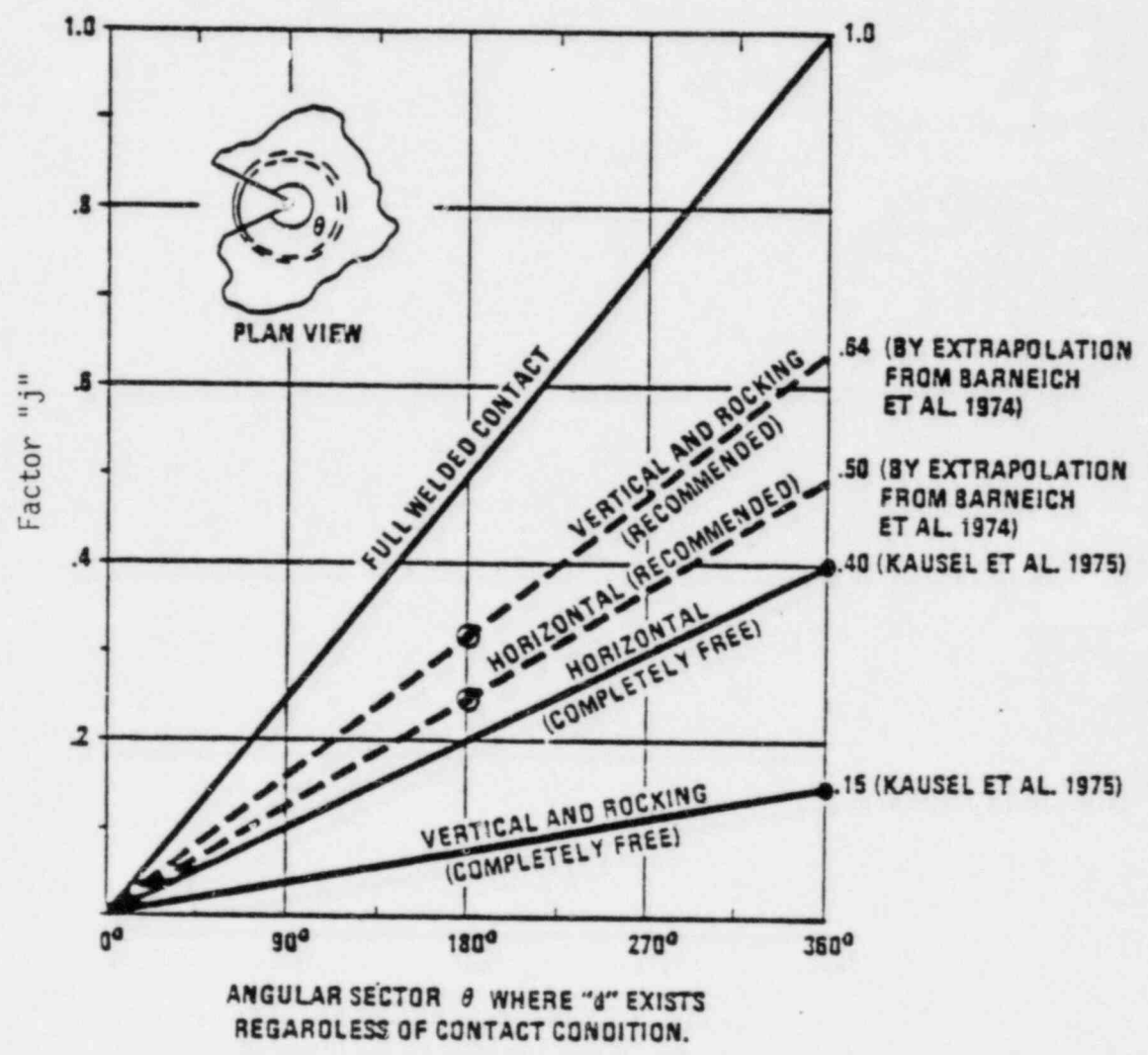
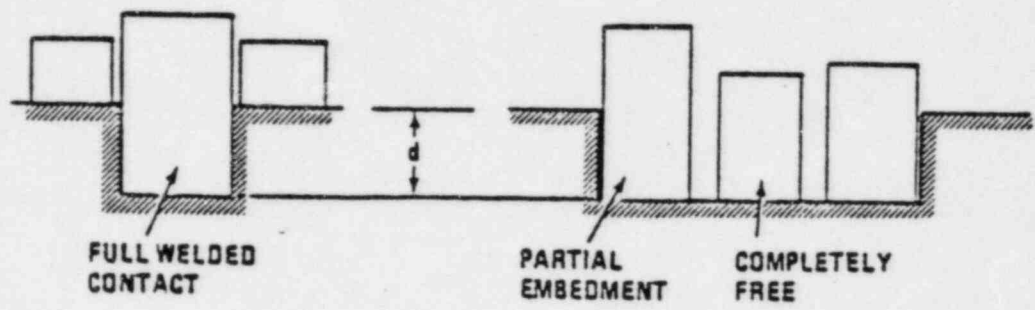


FIGURE I-4-5. NORMALIZED EMBEDMENT STIFFNESS COEFFICIENT, α_1



© FROM BARNEICH ET AL. (1974)

FIGURE I-4-6. EMBEDDED FOUNDATIONS, IMPEDANCE CORRECTION FACTOR j for SHALLOW EMBEDMENT

5. STRUCTURE ANALYTICAL MODELS

5.1 SME STRUCTURES MODEL APPROACH

For the Reactor Building, Auxiliary Building and Control Tower, Service Water Pump Structure, and the Diesel Generator Building, existing design models developed by Bechtel (References 9-12) for the structures were used for the SMR. For the BWST analysis, a new model was developed. In general, the analytical models consist of lumped masses connected by massless elements representing the structure stiffness. In locations such as the auxiliary building electrical penetration wings and underpinning walls where additional detail was required, plate finite elements were incorporated in the model. Both two and three-dimensional models of the structures were used as required. For the three-dimensional models, the center of mass and center of rigidity were modeled separately in order to account for the torsional response.

The models were reviewed for general method of approach and adequacy, but the detailed calculations used to develop these models were not checked as part of the SMR. However, in order to assure consistency between the structure models used in design and the SME calculations, all models were first run for either a fixed base condition or with design values for the soil springs, and the frequencies and mode shapes were compared with the design values.

With the exception of heavy components such as the Nuclear Steam Supply System (NSSS), equipment was not specifically modeled in the dynamic models of the Midland structures. The overall dynamic models of the auxiliary building, reactor building, SWPS, and diesel generator building included the mass of the equipment lumped at the appropriate floor in the structures but no dynamic characteristics of the equipment were included. For light, floor-mounted equipment which has negligible influence on the overall dynamic characteristics of the structure, this is an acceptable modeling assumption.

5.2 STRUCTURE MODEL DESCRIPTION

This section presents a brief description of the structure models used in the SMR. Detailed mass, stiffness, eigenvalue, and damping information for the individual structures is presented in subsequent volumes, together with the response results.

The dynamic lumped mass model for the reactor building is shown in Figure I-5-1. Since the structure is essentially symmetric a two-dimensional model is considered adequate. The model includes representations of the containment vessel shell, the concrete internals structure, the steam generators, and the reactor vessel. Soil compliance functions for the SME site characteristics including embedment were developed separately and added to the model.

The auxiliary building structure is considerably more complex. A sketch of the external configuration is shown in Figure I-5-2. This sketch shows only the exterior concrete outline and does not include the steel superstructure of the auxiliary building or the underpinning walls beneath the control tower and electrical penetration wings. The dynamic model of the auxiliary building includes the underpinning walls. The structure is essentially symmetric about the N-S axis. However, in order to adequately model the torsional response introduced by E-W excitation, a three-dimensional model is necessary. In addition, a combination of lumped mass and flat plate finite elements were incorporated to more accurately treat the electrical penetration wings and underpinning. The dynamic model used for the auxiliary building is shown in Figure I-5-3. Centers of mass and stiffness were offset as required. The element stiffnesses comprising massless elements of the sticks were computed accounting for the different shear wall orientations at the stories. Concrete block wall stiffnesses were not considered to contribute to the primary structure stiffness.

A vertical section view of the service water pump structure together with the lumped mass model is shown in Figure I-5-4. Although this is a much simpler structure than the auxiliary building, a three-dimensional model was also developed for this building. The mass of the water for horizontal response was distributed between the nodes located from the base slab through Elevation 620'. The mass of the water for vertical response was concentrated at the base slab. The service water pump structure model also includes the underpinning walls for the soils remedial design.

The diesel generator building dynamic model is presented in Figure I-5-5. Because this structure is essentially symmetric, a two dimensional lumped mass model is considered adequate for calculating dynamic response. The lumped mass degree-of-freedom (dof) for the model shown represents the mass of the footings, diesel generator pedestals and diesel generators, walls, and major floors. Massless stiffness elements were used to represent the shear walls in this structure. This model assumes the building, entrapped soil, and diesel generators are coupled and respond in-phase.

In addition, to conservatively bound the diesel generator building response, a second independent dynamic model of the structure was developed. This new model assumes the structure and diesel generators are uncoupled. The base mat mass and soil stiffnesses are assumed to be located at Elevation 634'-6". Entrapped soil, spread footings, diesel generator pedestals, and diesel generator masses are not included in this model. Dynamic responses from both models were evaluated in determining peak loads and floor response spectra for the SME margin study.

A new analytical model including the structure mass and stiffness, soil impedance functions, and fluid effects including sloshing was developed for the BWST.

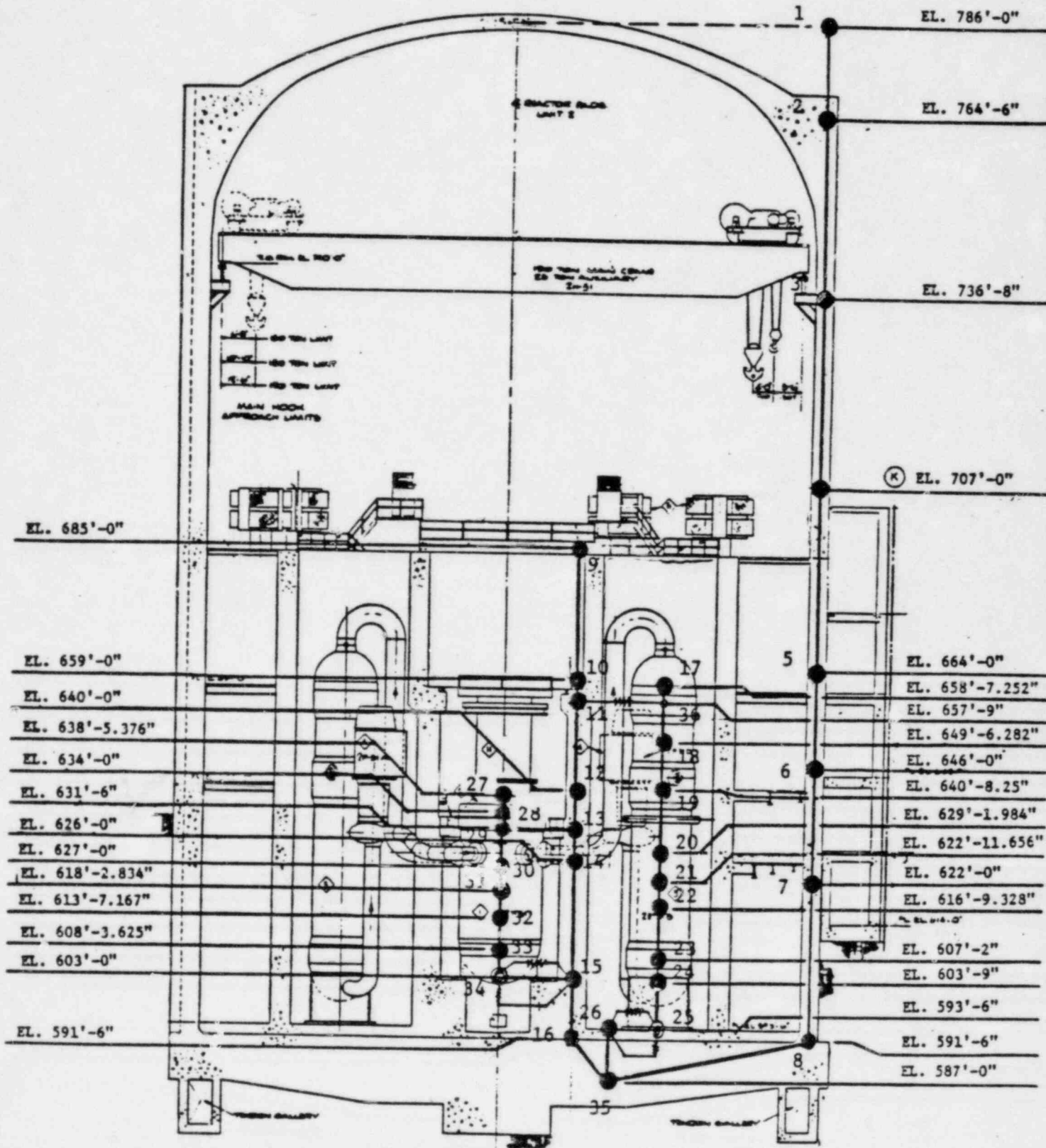


FIGURE I-5-1. REACTOR BUILDING LUMPED MASS MODEL

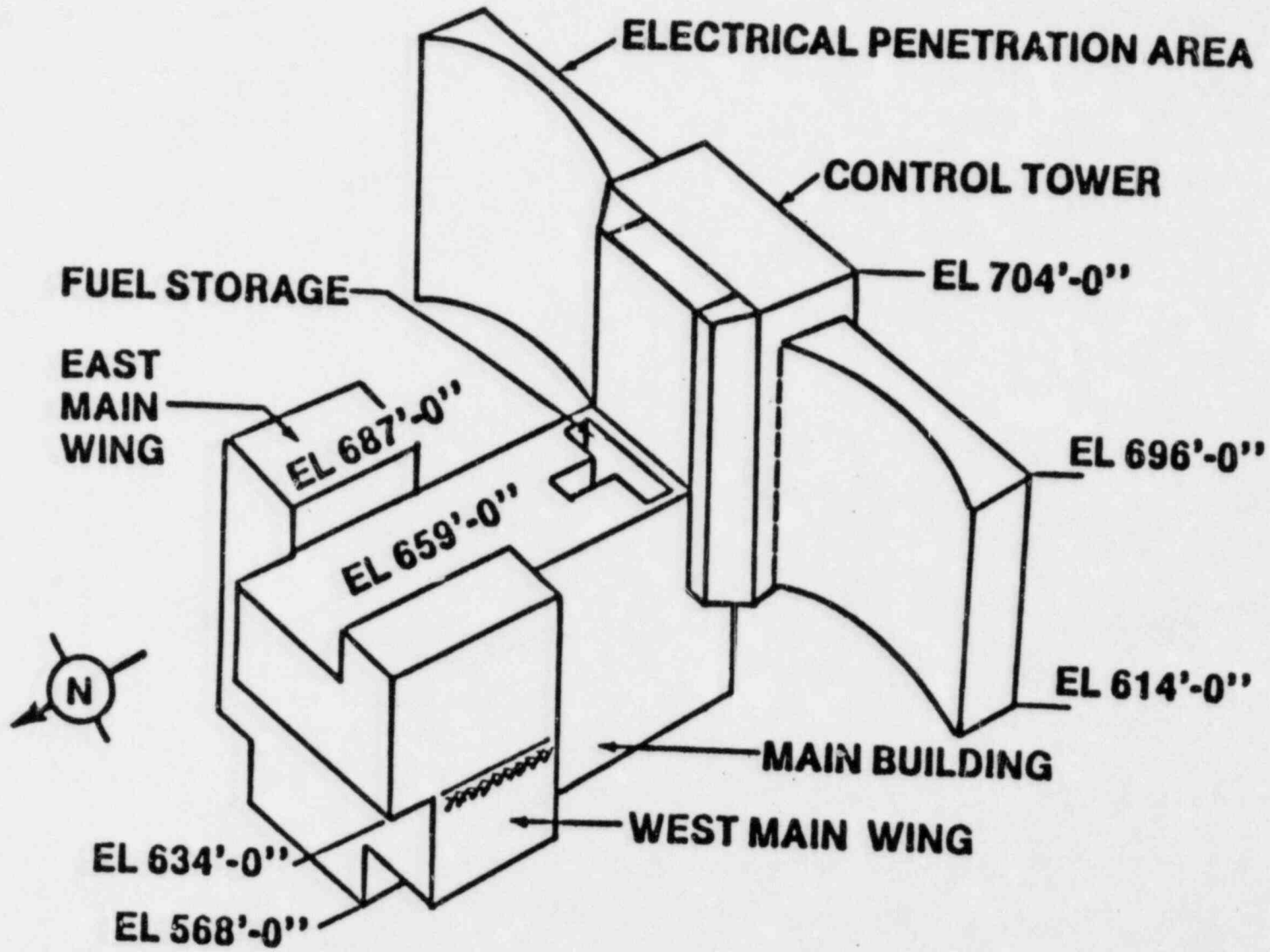


FIGURE I-5-2. AUXILIARY BUILDING/CONTROL TOWER CONFIGURATION

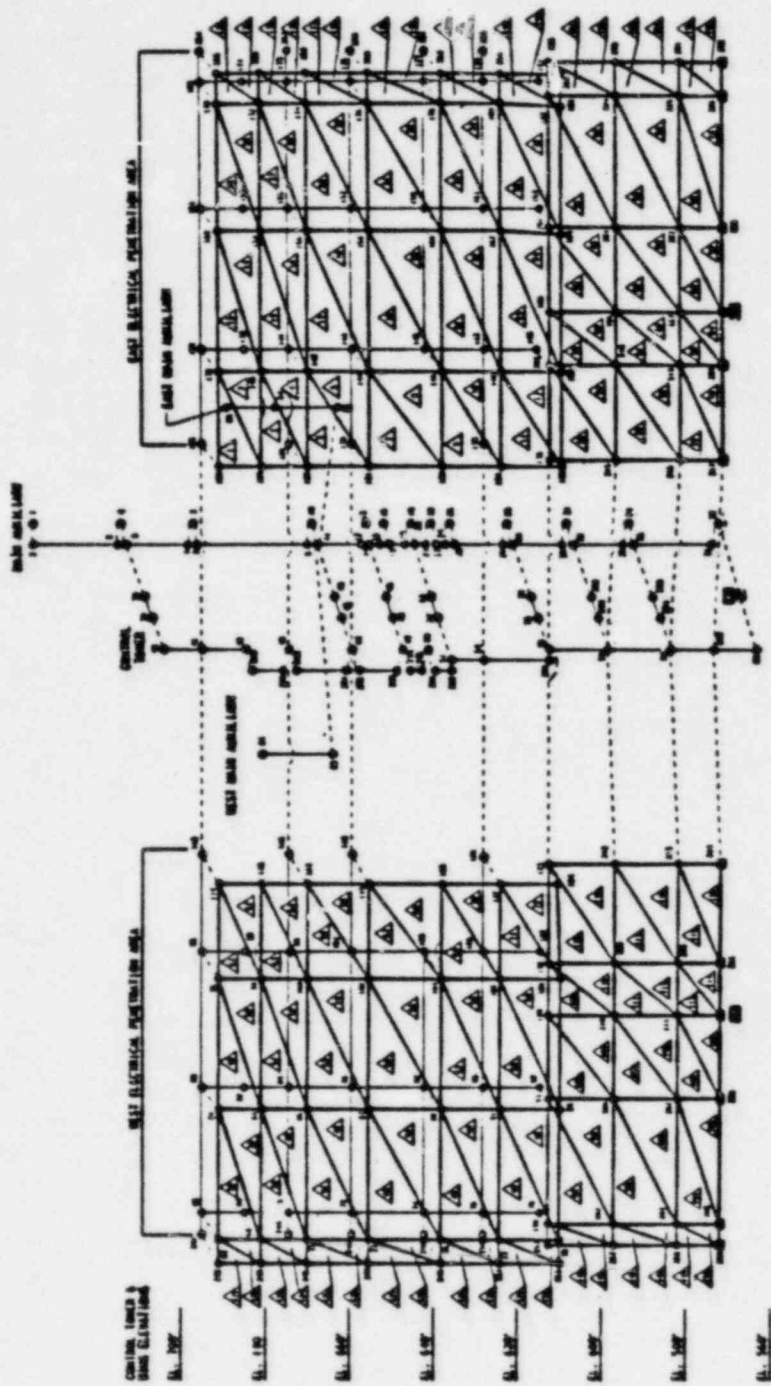


FIGURE I-5-3 . AUXILIARY BUILDING DYNAMIC MODEL

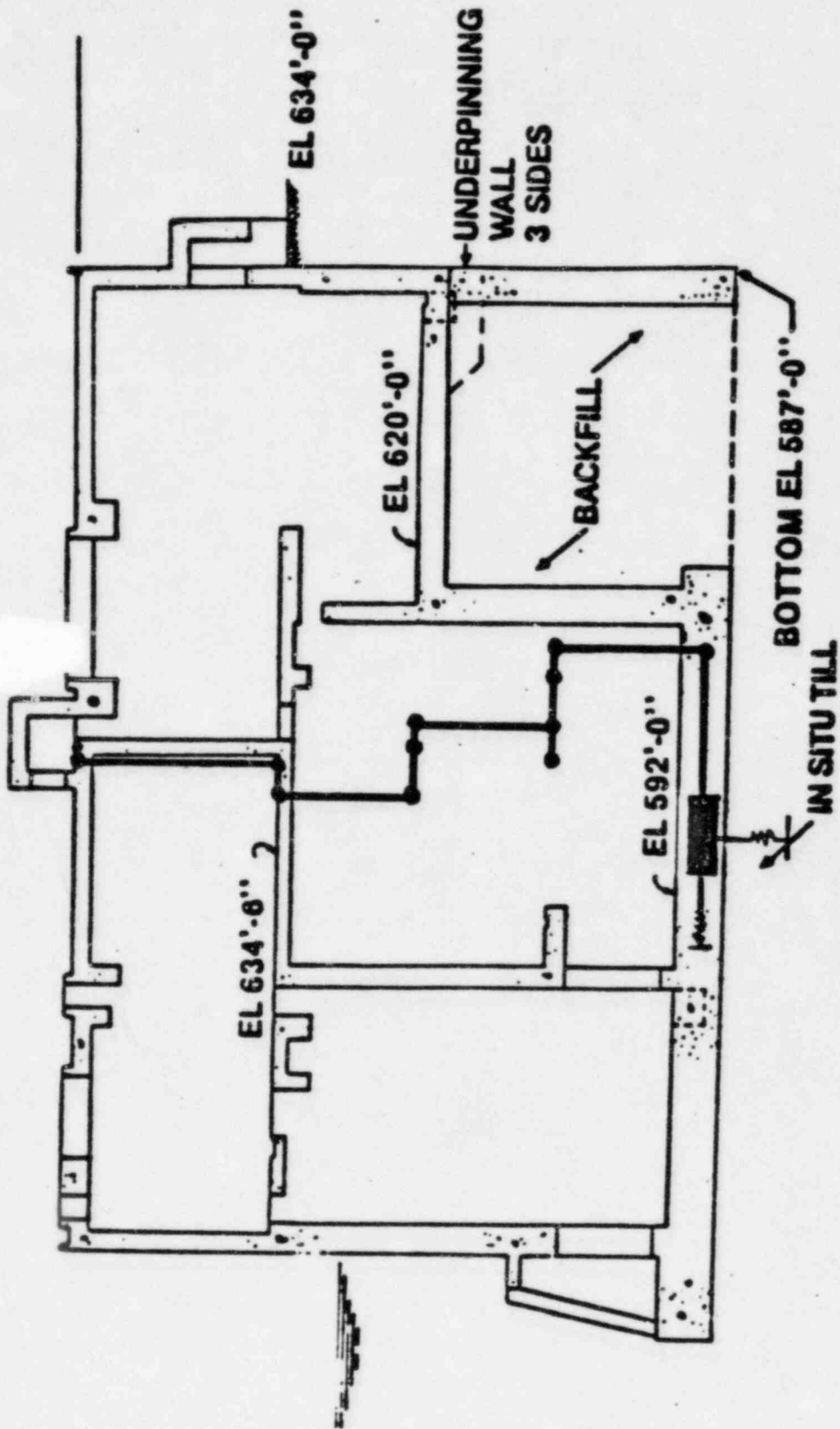
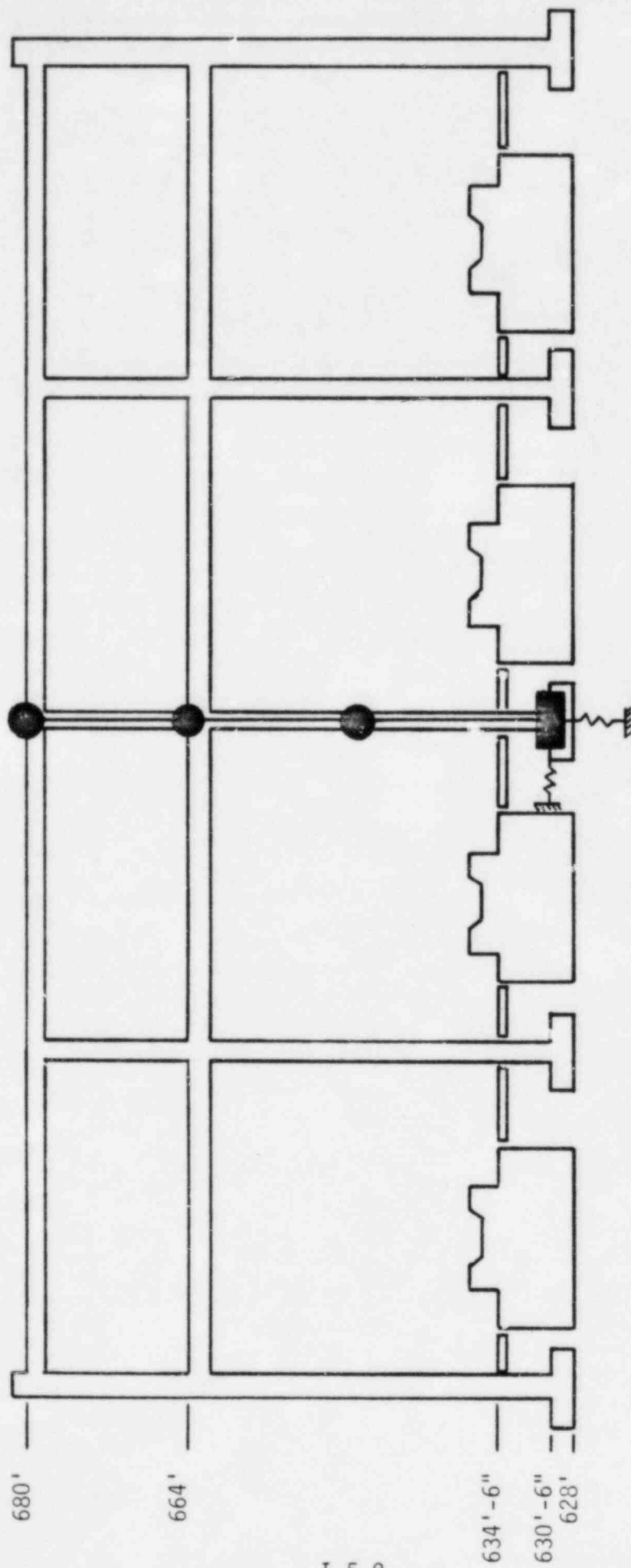


FIGURE I-5-4. SERVICE WATER PUMP STRUCTURE LUMPED MASS MODEL



I-5-8

FIGURE I-5-5. DIESEL GENERATOR BUILDING LUMPED MASS MODEL

6. STRUCTURES SEISMIC RESPONSE

6.1 SEISMIC ANALYSIS PROCEDURE

The generation of the SMR structure loads and in-structure response spectra was conducted with the design basis models of the structures with new soil compliance functions, and using the SME ground motions described in Section 2 as input. A simplified flow chart of the analysis process is shown in Figure I-6-1. In order to assure that the design models were properly interpreted and implemented for use for the SME analysis, a comparison of frequencies and mode shapes was made with the corresponding results generated by Bechtel. Depending on the assumptions made in the individual models received from Bechtel, the check was for either the fixed base condition or one of the design soil cases.

A review of the design basis models which included methods of lumping mass procedures for computing element stiffnesses, and general level of detail required to characterize the seismic response was conducted. Where any significant uncertainties existed concerning assumptions in modeling or levels of detail in the design models, parametric studies were conducted or additional analyses were pursued. Examples of parametric studies conducted are the modeling assumptions used in determining the relative soil stiffness under the electrical penetration wings of the auxiliary building control tower structure (Volume III), the vertical amplification of floor slabs (Appendix I-A), and different assumptions of the diesel generator building entrapped soil (Volume V). Therefore, detailed checks of the design calculations used to develop the models were not conducted for the SMR.

Both time history and response spectrum analyses were conducted for the SME. Time history analyses were used to develop the in-structure response spectra used as input to floor mounted equipment. Response spectrum analyses were used to generate the seismic response loads in the

structures. By using response spectrum analyses to determine seismic response loads, excess conservatism was avoided since the SME ground response spectra are smooth and do not have the peaks and valleys associated with the spectra generated by the synthetic time histories.

6.2 COMPOSITE MODAL DAMPING

Response spectrum analysis techniques assume the structure has classical normal modes. In other words, the equations of motion are assumed to be uncoupled and the response of the structure can be calculated as the superimposed response of a series of single degree-of-freedom systems. For structures with more than 10 to 20 percent critical damping, the structure does not possess classical normal modes. Structural response can be rigorously computed only by a step-by-step technique such as direct integration time history analysis. However, by appropriately selecting modal damping values, a normal mode method such as response spectrum analysis can be used to generate reasonably accurate results.

For structures on a soil site such as the Midland Plant, soil-structure interaction is an important consideration. Typically the fundamental frequencies of these structures are in the 2 to 4 Hz range with the primary response mode being a combined soil-structure mode. These fundamental soil modes are often highly damped with damping values for horizontal translational response as high as the 20 to 30 percent critical damping range. Vertical translational damping values can be as much as 60 percent critical damping. The damping used for each mode in a normal mode analysis represents a combination of both damping due to the soil in the form of soil hysteresis and energy waves propagating outward from the structure, and damping in the structure. Combined soil geometric and material damping ratios are normally several times as large as structural damping. For structural response modes which are combined soil and structure, it is necessary to assign modal damping to each combined mode of the structure in order to assure accurate yet conservative levels of seismic response.

Various techniques are available for computing composite modal damping accounting for both soil damping and structural damping. These include empirically derived methods such as stiffness and mass proportional damping. With these methods, the degree of approximation between a normal mode solution using damping values computed by these techniques and a rigorous solution cannot be predicted. Frequently, these methods overpredict the modal damping and consequently can seriously underpredict structural response. Underprediction of response can become quite serious at locations high in the structure. This underprediction of response is normally prevented by cutting off the maximum modal damping predicted by these methods at an arbitrary damping level. The degree of conservatism this arbitrary cutoff introduces normally is not known.

In order to avoid underpredicting the seismic response, a technique developed by Tsai (Reference 23) was used to develop the composite modal damping for the Midland structures. The basic principal of this technique is, at the flexible base structural frequencies, to match the rigorous and normal mode solutions of the transfer function at critical locations in the structure. Matching of the transfer function normally is done high in the structure at a location like the top floor where response is sensitive to damping. In this method, the structure model is excited by a unit harmonic input and the structural response transfer function for a particular location is determined throughout the frequency range of interest. Flexible base modes of the structure are then determined including the effect of soil flexibility. The structure transfer function for the normal mode solution is then developed from the uncoupled equations of motion. By iterating on the modal damping used in the normal mode solution, the transfer functions from the normal mode solution and harmonically excited complex solution can be equated at all frequencies of interest and conservative composite modal damping calculated for all important modes. Comparisons of normal mode solutions using damping based on this technique and rigorous solutions shows excellent agreement (Reference 22).

Composite modal damping values based on the Tsai approach were calculated using the program SOILST (Reference 24) for all structures considered in the SMR. This program is an extension of the work presented in Reference 23 to three dimensions. For each soil case studied in the SMR, locations in the various structures were chosen which were expected to be sensitive to damping. Composite modal damping values were determined at these different locations in the structure for excitation in each of the three principal directions. Composite modal damping values predicted by SOILST were tabulated for each location on a mode by mode basis. Damping values for each mode were chosen based on a conservative fit of all data.

In order to ensure that the composite modal damping values were conservatively chosen, comparisons of structural response predicted by direct integration time history analysis using concentrated dashpots to model the soil geometric and material damping and seismic response predicted using composite modal damping were conducted. Acceleration levels throughout each of the structures were calculated from direct integration time history analyses during the development of floor response spectra. These zero period accelerations are directly related to the maximum seismic response loads on the structure. A similar set of response accelerations in the structure was calculated by using modal superposition time history analysis with modal damping values corresponding to the composite modal damping determined in the manner described above. The same input time history was used in both the direct integration and modal superposition analyses in making these comparisons. By comparing zero period accelerations throughout the structure and checking that the zero period accelerations determined using composite modal damping approximately met or exceeded those from direct integration time history analysis, confidence in the calculated composite modal damping values was developed. The actual composite modal damping values determined for each structure and soil case are presented in the separate volumes for each structure presenting SMR results.

6.3 STRUCTURE SEISMIC LOADS

Structure shear, moment, and axial loads were developed using response spectrum analysis techniques. The computer program MODSAP (Reference 25) was used to develop the flexible base modes required for the response spectra analysis. MODSAP is an updated version of SAP IV and is directly compatible with the Bechtel version of SAP IV used in the design analysis. The appropriate SME spectra presented in Section 2 of this report were then used in conjunction with the composite modal damping values and flexible base modes discussed above to determine seismic response loads in the structure.

6.4 DETERMINATION OF NUMBER OF MODES

For a particular soil case, enough flexible base modes were determined for each structure to ensure the overall seismic response was accurately defined. The number of modes required for a particular soil case was determined by the criteria that for any nodal location k on the structures enough modal mass must be participating to ensure:

$$0.85 \leq \sum_{j=1}^m PF_{ij} \phi_{k,ij} \leq 1.15 \quad (6-1)$$

where m is the number of modes, PF_{ij} is the earthquake participation factor for excitation direction i , mode j , and $\phi_{k,ij}$ is the eigenvector for node k , degree-of-freedom i , and mode j . This criteria ensures no less than 85 percent and no more than 115 percent of the structure mass is participating in the modal solution. These limitations are generally considered to be adequate for determining the seismic response of structures.

6.5 COMBINATION OF MODAL RESPONSES

Seismic response of SMR structures was evaluated for ground motion in each of the three earthquake components (two horizontal and one vertical) acting independently. Combination of individual modal responses was done in accordance with U.S. NRC Regulatory Guide 1.92 (Reference 26). Modes of the structure which were considered to be randomly phased were combined by square-root-sum-of-the-squares (SRSS). Closely-spaced modes for which random phasing was not a valid assumption were combined by the ten percent grouping method defined by U.S. NRC Regulatory Guide 1.92. For any response value R which is desired, the representative maximum value of the particular response for a particular earthquake component is given by:

$$R = \left[\sum_{k=1}^N R_k^2 + 2 \sum_{i \neq j} |R_i R_j| \right]^{1/2} \quad (6-2)$$

where R_k is the peak response value due to the k the mode, and N is the number of significant modes considered in the modal response combination. The second summation accounts for all i and j modes which are closely spaced to each other and can be considered to be in phase. Closely spaced modes are defined by:

$$\left. \begin{array}{l} \frac{\omega_j - \omega_i}{\omega_i} = 0.10 \\ \text{also } 1 \leq i \leq j \leq N \end{array} \right\} \quad (6-3)$$

6.6 COMBINATION OF THE THREE COMPONENTS OF MOTION

Structural response loads to seismic excitation were determined for each of the three earthquake components acting independently. Stresses at all critical locations in the structure were determined for each earthquake component considered separately. Stresses due to all three earthquake components considered simultaneously were calculated using the square-root-sum-of-the-squares of individual responses. Overall structural moments, shears, axial loads, and displacements were calculated based on a square-root-sum-of-the-squares of directional responses.

6.7 DISTRIBUTION OF LOADS TO STRUCTURE ELEMENTS

Overall seismic loads were developed from the SME response spectrum analyses conducted for each of the structures. For lumped mass structures whose stiffnesses were represented by vertical stick elements, these loads consist of axial forces, horizontal shears, torsional moments, and overturning moments. To conduct the structures capacities evaluation, it is necessary to distribute these overall structure seismic loads to the individual elements that compose the load-resisting system. The load distribution methods employed were selected as being appropriate for the different load-resisting systems evaluated in this study.

The lateral load-resisting systems for the auxiliary building, service water pump structure, and diesel generator building consist primarily of concrete shear walls interconnected by concrete floor slabs. The floor slabs act as diaphragms distributing horizontal seismic inertial loads to the shear walls which transmit these loads down through the structure to the foundation. If the diaphragm is nearly rigid, the shear walls of a story are constrained to displace laterally as a unit and the horizontal loads can be distributed to the walls in proportion to their relative rigidities. The rigid diaphragm approximation is commonly employed in the design of concrete wall/floor slab structures. It is expected to lead to reasonable estimates of structure element loads and was used to define the load distributions within the concrete portions of the auxiliary building (main auxiliary building and control tower), service water pump structure, and diesel generator building.

Equations used to calculate individual wall horizontal shear loads based on wall relative rigidities are presented in Reference 27. The total element shear load consisted of contributions from overall structure story shears and torsional moments. For conservatism, the contribution from torsional moment was always taken to increase the total element shear since relative signs of the overall story shear and torsional moment are lost by the SRSS modal combination. Overall story shears and torsional moments used as load input to the load distribution equations were those generated by the structure response spectrum analysis. For symmetric structures, minimum torsional moments were defined as the product of the story shear acting in the direction of ground motion and an eccentricity equal to five percent of the maximum structure plan dimension at that story. As noted in Section 6.6, element forces were determined for overall loads due to each of the three earthquake directional components acting separately, then combined by SRSS.

Overall structure overturning moments are defined at the nodes of the dynamic model. The incremental change in overturning moment in a story (difference in overturning moment between the top and bottom floors of the story) was distributed to the walls in the same proportion as the distribution of horizontal shears to the walls. This approach is specified by References 28 and 29. In effect, the overturning moment increments were distributed to the walls in proportion to their relative rigidities. To account for additional load due to torsion, an incremental overturning moment equal to the product of the horizontal shear due to torsional moment and the story height was included for each wall. The total wall overturning moment at a particular elevation was taken as the sum of the incremental changes in wall overturning moment for the stories from the top of the wall to that elevation.

Determination of wall relative rigidities requires estimates of the element story stiffnesses in the directions of lateral loading. Structural members considered effective in resisting seismic loads were

identified in the calculations performed by Bechtel to develop the dynamic model stiffnesses for the auxiliary building, SWPS, and diesel generator building. For the auxiliary building (main auxiliary building and control tower) and service water pump structure, the seismic load-resisting walls at a story were discretized into separate elements rectangular in plan. Story stiffnesses for these elements were calculated in both horizontal directions. In-plane wall stiffnesses considered both shear and flexural deformations while out-of-plane wall stiffnesses considered flexural deformations only. These stiffnesses were based on a condition of rotational fixity at the top and bottom floors of the stories. In general, all concrete walls were included in the dynamic models. Some walls were modeled by a series of elements rather than a single continuous element. Major openings were included as discontinuities in the element layout. Masonry walls were not considered to be seismic load-resisting shear walls.

For the auxiliary building and the service water pump structure, the element story stiffnesses presented as part of the dynamic model properties calculations were used to determine element relative rigidities. Story stiffnesses for the walls of the diesel generator building were calculated in a similar manner. Out-of-plane wall stiffnesses were not included so that conservative in-plane loads would be produced. When necessary, some of the wall story stiffnesses were modified to provide better correlation to the actual structural conditions. When a single wall was defined by a series of elements, the total load acting on that wall was taken as the sum of the element loads. When a single element was used to model a length of wall actually consisting of a series of piers separated by significant openings, the total shear load was distributed to the individual piers in proportion to their relative rigidities.

Concrete structures which are not composed of conventional shear wall/floor slab lateral load-resisting systems include the containment building and internal structures. These structures do not

have floor diaphragms to distribute the seismic loads to the vertical elements so the relative rigidities approach adopted for the auxiliary building is not as directly applicable. The dynamic model stiffness properties of the containment and internal structures were represented by elastic beam properties consisting of axial and shear areas and moments of inertia. The seismic stress distributions are expected to be predicted with sufficient accuracy by elementary elastic beam theory. For the containment wall, being a shell, the horizontal seismic responses generated by beam elements translate primarily into tangential shear and meridional membrane stresses. These stresses were distributed around the shell wall according to a first harmonic. Axial responses generated on the beam elements representing the containment shell from the vertical seismic analyses result in uniformly distributed wall meridional membrane stress. Membrane and bending stresses due to the seismic response of the base mat and dome were estimated through classical solutions. The seismic load-resisting walls of the reactor building internal structure are sufficiently tied together to behave as a single vertical beam member. Calculations performed to determine the equivalent beam properties for the dynamic model identified which walls were considered to be seismic load-resisting. Overall horizontal shears from the response spectrum analyses were distributed to the walls in proportion to their shear areas. Vertical stresses due to vertical load and overturning moment were determined by elementary elastic beam theory with the walls occurring at a particular elevation combined to form a single beam cross-section.

The only steel framed structure expected to be significantly stressed by seismic loads occurs above Elevation 659'-0 in the auxiliary building. Resistance to seismic loading consists primarily of moment-resisting frames in the E-W direction and braced frames in the N-S direction. Seismic design forces in the structural steel members due to the OBE were determined by static finite element analyses. The finite element model is able to account for the effects of seismic inertial

loads and differential displacements between the main auxiliary building and the control tower on the structural steel member forces. Member forces due to the SME were determined by increasing the OBE forces from the static analyses by scale factors. These scale factors were defined as the ratios of the SME responses to the OBE responses in the elements of the dynamic model.

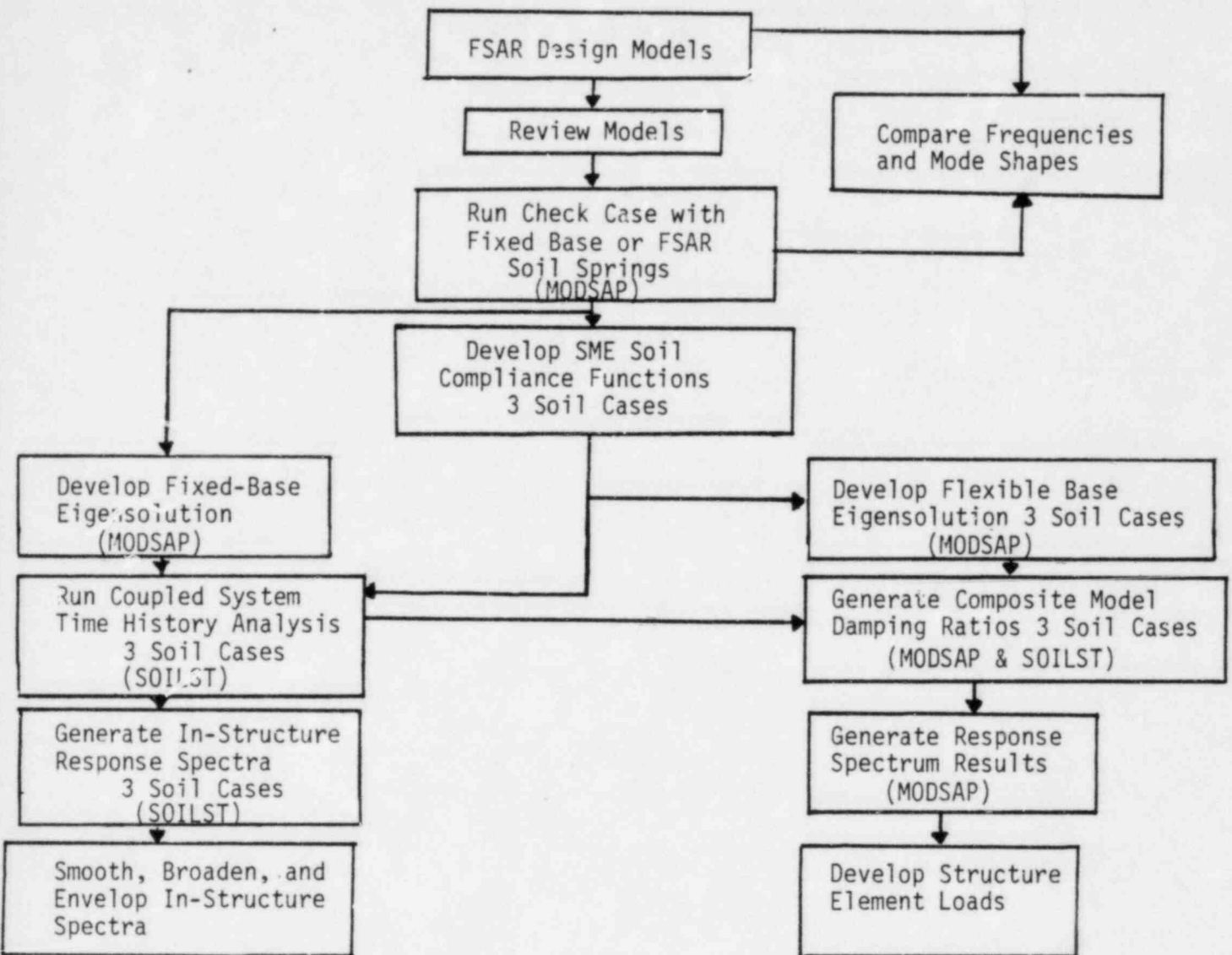


FIGURE I-6-1. SEISMIC ANALYSIS PROCEDURE

7. MARGIN EVALUATION OF STRUCTURES

7.1 LOAD COMBINATIONS

The structures seismic margin review was conducted for the following load combination:

$$U = 1.0D + 1.0T + 1.0L + kE_{sm}$$

where: U = Limiting load on the structure
D = Dead load (Including equipment)
L = Operating live load during normal operation plus any live load occurring as a direct result of earthquake loading.
T = Loads due to differential settlement, if any
E_{sm} = Seismic Margin Earthquake load
k = Ductility reduction factor

In addition, the load combination for the reactor containment building includes the design basis pressure and temperature for this condition.

$$U = 1.0D + 1.0F + 1.0L + 1.0P + 1.0T_A + KE_{sm}$$

where: F = Prestress
P = Design Basis Pressure (Reference 1)
T_A = Design Basis Temperature (Reference 1)

Member forces due to dead and live loads were based on the results of existing design basis analyses or calculations by Bechtel. In cases where live or settlement loads were found to reduce the effects of dead and seismic loads, structural member capacities were checked without the presence of the live and settlement loads. For structures which could conceivably be above yield as a result of the SME, provisions are made to include the effects of inelastic energy dissipation by means of the ductility reduction factor, k. The ductility reduction factor is a means of accounting for the inherent seismic resistance of a system above that expected based on elastic analysis. Nonlinear behavior of a ductile system limits the imposed forces and accompanying stresses. A

ductility reduction factor less than unity would be expected for ductile post-yield behavior. The derivation and limitation on the use of ductility reduction factors is described in Appendix B of this volume.

The seismic margin review is primarily concerned with reporting code margins (margins against current code allowables). For code margins:

$$k = 1.0$$

In other words, no ductility reduction factor was used in any code margin. Provision is made to compute a failure margin in any case where the code margin is calculated to be less than unity. In developing failure margins, a ductility reduction factor less than unity may be used. Where k less than unity is used, the value used is clearly defined. In general, for failure margins:

$$k = 0.8$$

For certain failure modes discussed in Appendix B, a value of k of unity is used even for failure margins. A value of k less than 0.8 is used only when justified by special studies.

7.2 ACCEPTANCE CRITERIA

The acceptance criteria adopted for evaluation of the structural elements conform to the applicable codes currently specified by the Standard Review Plan (SRP) for design of concrete containments, concrete internal structures, and other Seismic Category I structures.

7.2.1 Concrete Structures

For the concrete containment, the provisions specified by Article CC-3000 of the ASME Section III, Division 2, "Code for Concrete Reactor Vessels and Containments" (Reference 30) were followed. Stresses in the concrete, steel reinforcement, and prestress tendons were limited

to the allowable stresses for factored loads. In addition, the tangential shear stress in the prestressed containment wall was limited to that value causing a principal tensile stress of $4\sqrt{f'_c}$ where f'_c is the concrete compressive strength in psi. This requirement is specified in subsection II.5 of Section 3.8.1 of the Standard Review Plan. For the concrete internal structures and concrete portions of the other Seismic Category I structures, the section strength available for resisting loads was based on the ultimate strength design methods contained in ACI 349-80, "Code Requirements for Nuclear Safety Related Concrete Structures" (Reference 31).

The code allowable values were based on the as-built configurations for the elements evaluated. The evaluation of selected concrete elements included a check for the reinforcing cutting allowance delineated in Reference 32. These criteria provide that one bar each way, each face, may be cut no closer than five feet or equivalent for selected locations. No cutting was allowed in the containment shell, near steel lined surfaces, in congested locations or bundle bars, #14 or #18 bars, or other critical locations. In addition, non-conformance reports were reviewed in order to identify any other discrepancies existing in the elements selected for the SME evaluation.

7.2.2 Steel Structures

Stresses in members of the steel structures were calculated elastically and were typically limited to 1.6 times the allowable stresses specified in Part 1 of the AISC "Specification for the Design, Fabrication, and Erection of Structural Steel for Buildings" (Reference 33). Shear stresses were limited to 0.55 times the minimum specified material yield stress in accordance with Section 2.5 of the AISC Specifications. This stress limit is that specified in the Standard Review Plan for steel structures subjected to a load combinations consisting of normal operating and extreme environmental loads. The one-third increase in allowable stresses for steel members was not permitted. Determination of the allowable stresses or ultimate strengths was conservatively based on the minimum specified material yield or crushing strengths.

8. INPUT TO EQUIPMENT

8.1 DEVELOPMENT OF IN-STRUCTURE RESPONSE SPECTRA

In-structure response spectra were developed based on the dynamic structures models used in the SMR. Development of these spectra considered the effects of multidirectional earthquake excitation, the different soil profiles evaluated for the SME, torsional response of the structures, and floor slab vertical amplification. This section presents the methodology used in developing in-structure response spectra for the SME. Actual spectra generated for the critical structures studied in this evaluation are presented in the separate volumes for each structure.

In-structure response spectra were generated at specified locations in the SMR structures. Typically, one set of in-structure response spectra which considered both the effects of multidirectional earthquake excitation and torsional response were developed for each excitation direction at a specific elevation for each structure analyzed. For the main auxiliary building, floor response spectra were generated at critical floor elevations in the control tower, throughout the main auxiliary building, and at the eastern end of the east electrical penetration wing. Examination of auxiliary building modal response and symmetry considerations demonstrated that response of the west electrical penetration wing was virtually identical to the east electrical penetration wing and separate response spectra were not required. In the reactor building, in-structure response spectra were generated at the structure base mat for the internal reactor vessel-steam generator support structure, and at the crane support level on the containment. In-structure response spectra were generated at the base mat and at all major floors for both the service water pump structure and the diesel generator building.

Structural damping values defined by US NRC Regulatory Guide 1.61 (Reference 33) for the SSE were used for the major concrete structures. It was verified that for each structure the SME stress levels exceeded one-half yield stress so that these damping values were justified. For reinforced concrete structures, such as the auxiliary building, diesel generator building, service water pump structure, and reactor building internal structure, structural damping was assumed to be 7 percent of critical damping. The prestressed concrete containment for the reactor building was taken to be at 5 percent critical damping. Stresses in both the reactor vessel and steam generator were considered to be below one-half yield stress and a corresponding lower damping value of 2 percent of critical was used for these large pieces of equipment to reflect the lower stresses.

Stiffness proportional damping was used in conjunction with the fixed-base eigensolution for the reactor building to define modal damping for all modes. In this formulation, the equivalent modal damping $\bar{\beta}_j$ for the jth mode is defined by:

$$\bar{\beta}_j = \frac{\langle \phi_j \rangle [\bar{K}] \{ \phi_j \}}{\langle \phi_j \rangle [K] \{ \phi_j \}} \quad j = 1, \dots, n \quad (8-1)$$

where: $\{ \phi_j \}$ is the mode shape for the jth mode,

$\langle \phi_j \rangle$ is the transpose of $\{ \phi_j \}$

$[\bar{K}]$ is the modified stiffness matrix constructed from the product of the modal damping ratio and the element stiffness matrix for each member.

$[K]$ is the stiffness matrix

The fixed-base mode shapes and corresponding stiffness proportional modal damping values were used as input to the program SOILST for determining time history response.

For a set of soil impedances corresponding to each soil case, the appropriate artificial time history (either original ground surface or top-of-fill) from Section 2 was used as input to the structure dynamic model considered. The structure was excited by each earthquake component acting independently and response time histories were calculated throughout the structure for all translation degrees-of-freedom and rotation about the vertical axis.

Response spectra were generated for each of the three excitation directions including torsion. These spectra were generated for 2, 3, 4, and 7 percent of critical equipment damping at the frequency intervals outlined in US NRC Regulatory Guide 1.122 (Reference 34).

For the SMR analysis, much of the equipment is expected to be at stress levels exceeding one-half yield due to seismic loadings. Higher damping levels are considered to be appropriate for evaluating equipment at these higher stresses. Table I-8-1 presents the damping levels used for determining both the code margin capacity and failure margin capacity (if necessary) for structures and equipment analyzed in the SMR.

Since several of the structures studied in the SMR are asymmetric, structural excitation in one direction will excite response for other degrees-of-freedom. Translational floor response spectra for each response direction (two horizontal and one vertical) were developed by taking the square-root-sum-of-the-squares (SRSS) of the contributions to the spectral ordinates from the vertical and the two horizontal ground motions. Rotational in-structure response spectra for rotations about the vertical structure axis at the center of rigidity of each floor were developed in a similar fashion.

In developing the SMR in-structure response spectra, inclusion of the torsional response of the structures was required when equipment was not located at the center of rigidity (rotation) of the floor. The procedure to incorporate torsional response into the SMR spectra can be

visualized using Figure I-8-1, which presents a schematic representation of a typical structure floor showing critical equipment items at distances R_1 and R_2 from the center of rigidity. Both translational and torsional in-structure response spectra were developed at the center of rigidity of each floor accounting for all three excitation directions as described above. For floors of a structure which have significant torsional response, the Y direction translational spectrum for an equipment item located at a distance R_1 (Figure I-8-1) from the center of rigidity may have a significant translational component due to rotation about the center of rigidity. This translational component can be conservatively included in the in-structure spectra for Y excitation by adding the absolute sum of the moment arm R_1 times the rotational spectra at the floor center of rigidity to the Y direction translational spectra at the center of rigidity. By choosing this location such that the distance in the X direction from the center of rigidity is maximized, conservative spectra in the Y direction are defined for the floor. Development of the in-structure response spectra in the X direction is similar. In this case, a distance R_2 representing the maximum distance in the Y direction that a critical piece of equipment is located from the center of rigidity is used to define the translational component of X response due to rotation. Translational response in the vertical direction, due to rotations about the two horizontal building axes, was determined to be unimportant for all SMR structures and was not considered in the development of vertical in-structure response spectra.

The approach described above to include torsional response in the translational response spectra is conservative. Adding the absolute sum of the rotational spectra times a moment arm assumes that worst possible phasing is occurring at all times. By maximizing the distance R from the center of rigidity to critical equipment on the floor, torsional effects are maximized.

8.2 IN-STRUCTURE FLOOR RESPONSE SPECTRA SMOOTHING AND BROADENING

To account for variabilities in structural frequencies due to uncertainties in material properties, soil profiles, and approximations in modeling techniques, the peaks of the spectra from the three soil cases were broadened by $\pm 10\%$. Uncertainty in the knowledge of the site soil characteristics is covered by the broad range of soil shear moduli used in the SMR evaluation. The $\pm 10\%$ broadening is considered to conservatively cover the uncertainty introduced by structural modeling assumptions and variations in material properties and is in conformance with USNRC Regulatory Guide 1.122 (Reference 35). Where additional uncertainties were considered possible, additional parametric analyses were conducted, and worst case response results were used for the in-structure response spectra. The peak broadening of $\pm 0.10 f_j$ on structure frequency j , is shown in Figure I-8-2. This broadening procedure was done for all specified response locations using a computerized broadening technique.

Final SME in-structure response spectra were then developed as an envelope of the broadened spectra for the different soil cases at each location. This development of the enveloped spectra considered possible shifting of structure frequencies due to uncertainty in actual site soil properties. The enveloped spectra were further smoothed to remove minor valleys. A typical example of this enveloping procedure is shown in Figure I-8-3.

8.3 VERTICAL AMPLIFICATION OF FLOOR SLABS

Enveloped vertical floor response spectra were developed in accordance with the procedures presented in this section. These vertical design spectra are applicable for equipment located close to the shear walls and for floors which have frequencies high enough to be considered rigid. However, for equipment centrally located on larger, more flexible floor slabs, these vertical floor response spectra can be unconservative since additional amplification of the ground motion due to slab vertical flexibility may occur.

The vertical seismic input to piping and equipment may exceed that which would otherwise be computed from an overall soil-structure interaction model which neglects vertical floor slab flexibility. The dynamic models used in the original design did not include a provision for vertical floor slab flexibility. In order to evaluate the effect of vertical floor slab flexibility on vertical seismic input to piping and equipment, representative floor slabs on which critical equipment and piping were located were selected for analysis.

The selection of the floor slabs for evaluation was based on a general review of the individual structures. Emphasis was placed on slabs with long spans and/or high loads. Finite element models of the slabs were developed including plate element representation of the slab together with consideration of the beams, girders, and cut-outs. These models included the weights of attached equipment items and non-loadbearing masonry walls. A total of five slabs located throughout the main auxiliary building, control tower, and electrical penetration wings were analyzed in the auxiliary building structure and one each in the SWPS and diesel generator building. Fundamental frequencies in the range from 11 Hz to over 33 Hz were calculated. Relatively low stress levels resulting from combined seismic and dead-weight loads were computed, so that uncracked section properties were used in the analysis. Consistent with these low stress levels, structural damping in the slabs was limited to 4% of critical.

In-structure response spectra were generated at the centers of the slabs and were then compared to spectra near the wall at the corresponding locations throughout the structure. From these comparisons, a vertical amplification factor (VAF) was developed which was used to determine the increased input to equipment located near the floor slab centers. The VAF is a function of both equipment frequency and damping and permits including a conservative representation of the floor slab vertical amplification effects without the need to analyze every slab in the structure. The details of this evaluation are included in Appendix I-A of this report.

TABLE I-8-1

DAMPING VALUES - PERCENT CRITICAL TO BE USED IN THE
SEISMIC MARGINS REVIEW FOR PASSIVE COMPONENTS⁽⁴⁾

Structure or Component	Percent Critical Damping	
	Code Margin	Failure Margin
Large diameter piping systems Pipe diameter \geq 12 in.	3.0	4.0(1)
Small diameter piping systems Pipe diameter < 12 in.	2.0	3.0(1)
Welded Steel Structures	4.0	4.0(3)
Bolted Steel Structures	7.0	7.0(3)
Welded Steel Components	3.0	4.0(2)
Bolted Steel Components	3.0	7.0(2)
Reinforced Concrete Structures	7.0	7.0(3)
Prestressed Concrete Structures	5.0	5.0(3)

-
- (1) These values are based on test performed by Westinghouse Electric Co. (References 35, 36).
- (2) These damping values are consistent with damping values defined for welded and bolted structures and by review of existing test data (Reference 36).
- (3) R.G. 1.61 OBE damping levels shall be used as structural damping in generation of floor response spectra where total calculated stresses in the structure for the SME do not exceed one-half yield.
- (4) Damping values used in evaluation of active components shall be reduced in the same proportion of OBE to SSE damping values as defined in Table 1 of R.G. 1.61.

⊗ - Critical Equipment Locations on Floor

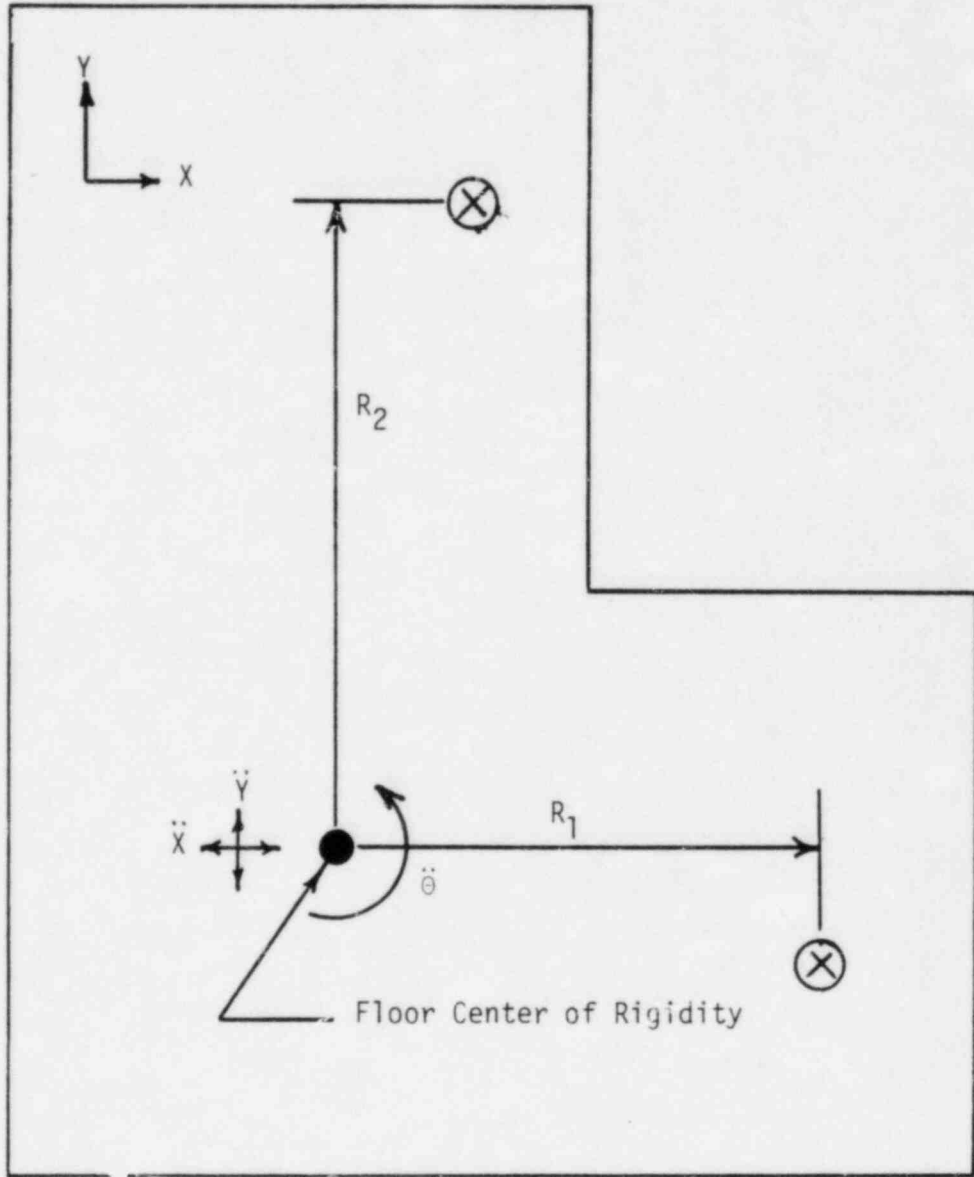


FIGURE I-8-1. SCHEMATIC REPRESENTATION OF TYPICAL FLOOR SHOWING CRITICAL EQUIPMENT LOCATIONS RELATIVE TO THE FLOOR CENTER OF RIGIDITY

6-8-1

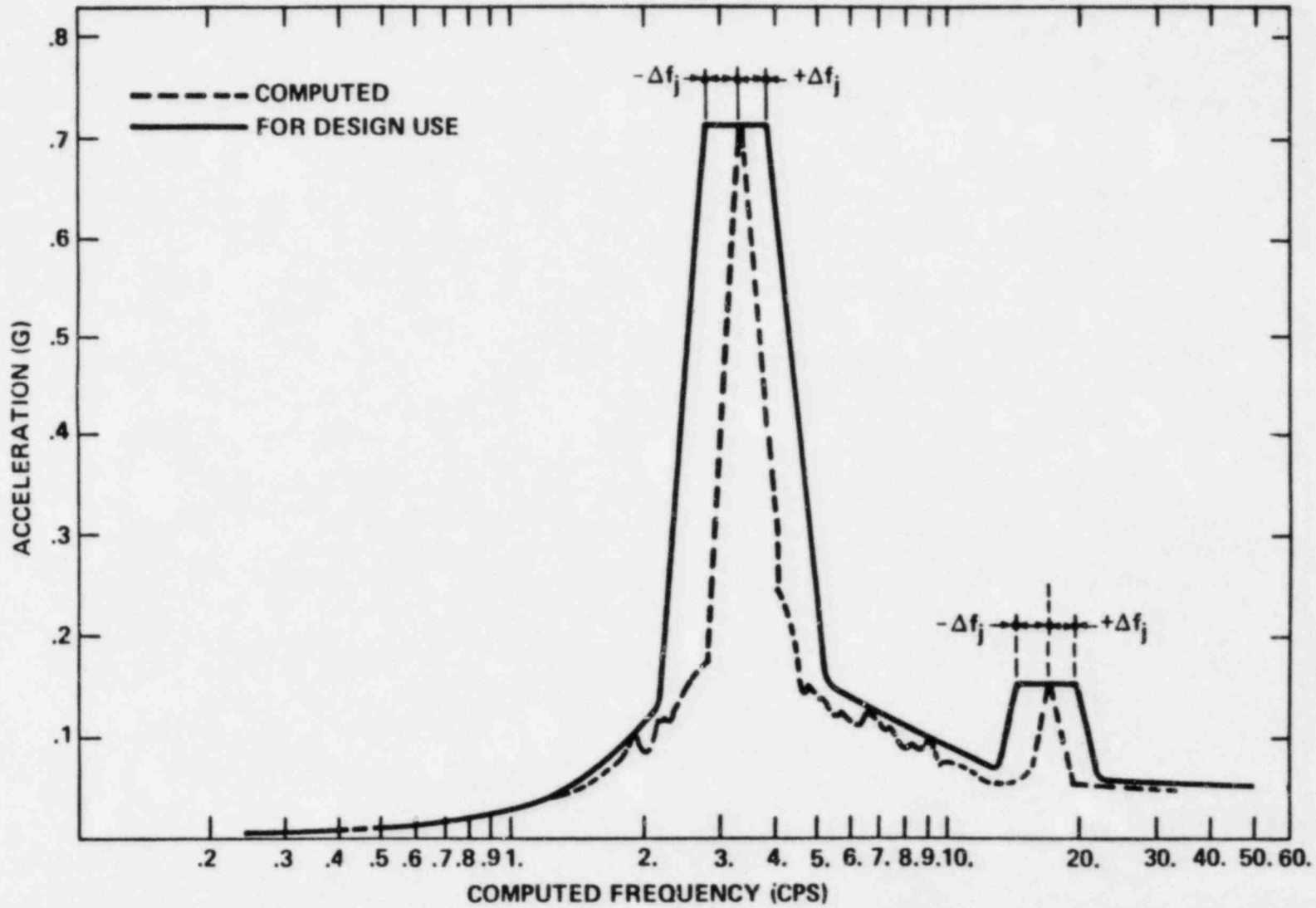


FIGURE I-8-2. RESPONSE SPECTRUM PEAK BROADENING AND SMOOTHING (FROM REFERENCE 28)

01-8-1

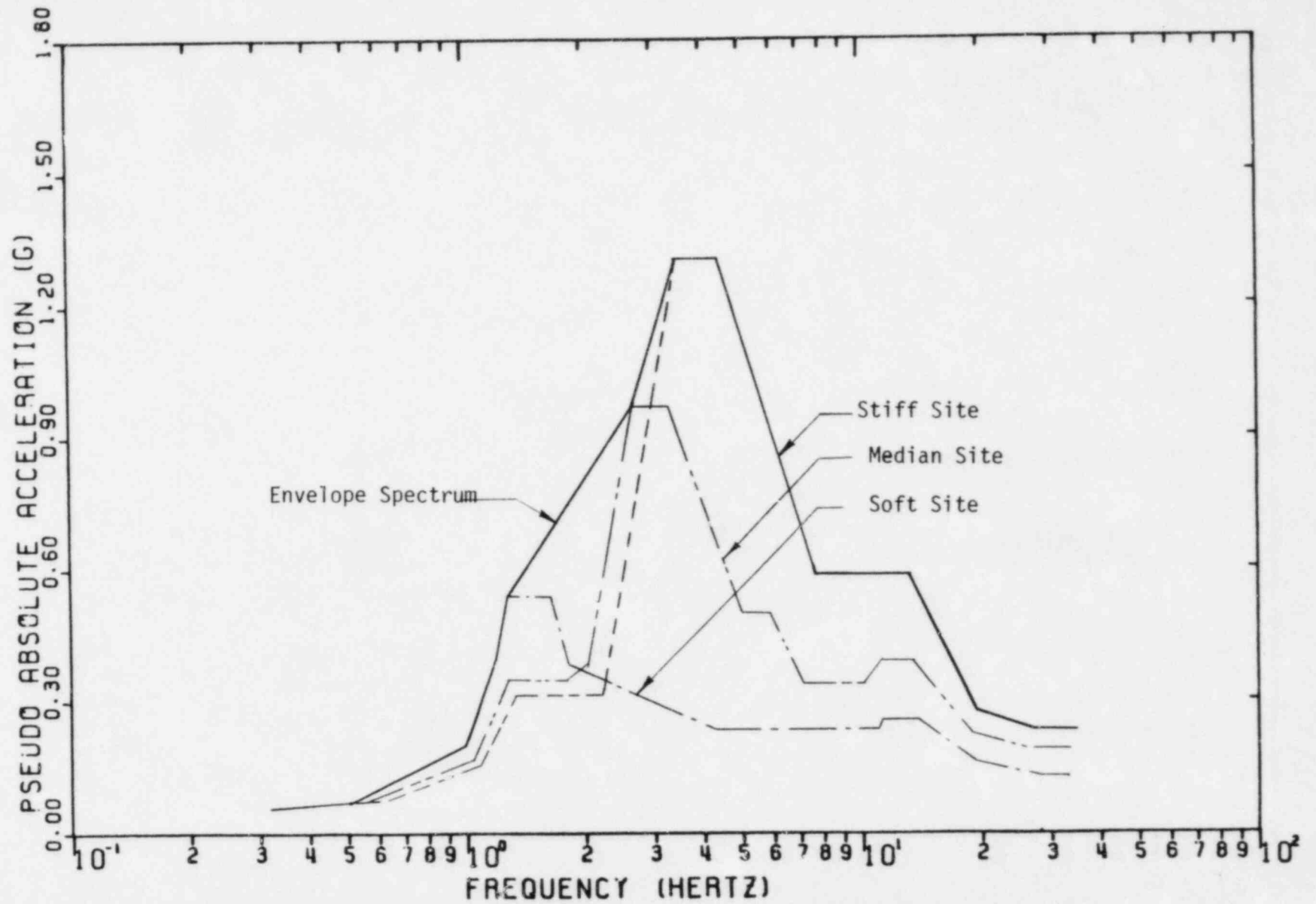


FIGURE I-8-3. DEVELOPMENT OF ENVELOPE IN-STRUCTURE RESPONSE SPECTRA

9. SME SEISMIC MARGIN EVALUATION METHODS AND ACCEPTANCE
CRITERIA FOR EQUIPMENT AND SUPPORTS

A carefully selected sample of equipment was evaluated for the SME. The evaluation was conducted in accordance with methodology and acceptance criteria comparable to current NRC licensing criteria. In the event that the acceptance criteria were not met, margins against failure were calculated in order to assess the magnitude of actual margins for the SME loading.

Equipment acceptance criteria vary, depending upon the governing design code, Regulatory Guide and Standard Review Plan criteria. Some equipment were qualified by test to demonstrate functionality as well as structural integrity while other equipment and their supports were qualified for seismic service by analytical methods only. The following general categories of equipment and supports are addressed in the Seismic Margin Review Study:

- NSSS Piping, Vessels and Supports
- Reactor Internals
- ASME Code Class 1 Balance-of-Plant Piping
- ASME Code Class 2 and 3 Balance-of-Plant Piping
- ASME Code Class 1 Balance-of-Plant Equipment
- ASME Code Class 2 and 3 Balance-of-Plant Equipment
- Component Supports for ASME Code Class 1 Piping and Equipment
- Component Supports for ASME Code Class 2 and 3 Piping and Equipment
- Emergency Power Supplies
- Cable Trays and Supports
- HVAC Ducting and Supports
- Electrical Conduit and Supports
- Component Support Anchorage
- Electrical, Instrumentation and Control Equipment

Load combinations for evaluation of piping, components and component supports were limited to the combination of normal operating plus SME loads. Load combinations and stress acceptance criteria were based on the requirements of governing codes and standards for plant faulted loading conditions.

Figure I-9-1 shows a flow diagram of the step-by-step process for determining the margins against code or against failure for active and passive components qualified by analysis and the margin against the achieved test level for active and passive components qualified by test.

9.1 SELECTION OF EQUIPMENT

Equipment most vital to achieve a safe shutdown of the reactor was selected for independent evaluation for loading resulting from the SME. The selection process took into consideration criticality of function, location in the structure, resulting stresses from FSAR design load combinations and engineering judgment as to the types of components most sensitive to seismic loading. The selection process encompassed a review of the FSAR, equipment layout drawings, a comparison of SME to SSE floor spectra and a review of stress summaries provided by Bechtel. In addition, plant walk downs were conducted in order to finalize the selection. The selection process and resulting samples are believed to be sufficient to demonstrate that adequate margin exists to assure function of all safe shutdown equipment in the event of a SME. Following is a summary of the selection procedure for each of the generic equipment categories previously listed.

9.1.1 NSSS System (Piping, Vessels, Supports and Reactor Internals)

All critical areas of the NSSS system were examined for effects of the SME combined with normal operating loads. Babcock and Wilcox conducted seismic response analyses for the SME and provided the resulting responses along with responses for the SSE, LOCA and normal operating loads to SMA. Also provided, were computed stresses for governing critical areas of the reactor internals for SSE and LOCA loading. All potentially critical areas were examined by SMA for compliance to code acceptance criteria.

9.1.2 ASME Code Class 1, 2 and 3 Balance-of-Plant Piping and Supports

A summary of stress response for all seismic Category 1 piping systems was provided by Bechtel Associates Power Corporation. From this comprehensive list, several Class 1, 2 and 3 piping systems were selected for independent analysis for the SME. Only the highest stressed lines, where the maximum faulted condition stress response was dominated by the SSE, were chosen. These lines were considered to be the most sensitive to changes in seismic loading. All supports associated with these lines were selected for independent evaluation.

9.1.3 ASME Code Class 1 Balance-of-Plant Equipment

All ASME Class 1 active valves within the ASME Class 1 Balance-of-Plant (BOP) piping systems chosen for independent analyses were included in the SME study. There are no other ASME Class 1 BOP components, besides some additional valves in lines that were not independently evaluated, that are required for a safe shutdown.

9.1.4 ASME Code Class 2 and 3 Balance-of-Plant Equipment and Supports

The selection of ASME Class 2 and 3 BOP equipment was conducted principally on the basis of criticality of function. All major pumps, heat exchangers and vessels necessary for a safe shutdown were evaluated for SME loading. Active valves within the piping systems chosen for independent analysis were evaluated for the SME. All component supports for the selected piping and equipment were included in the study.

9.1.5 Emergency Power Supplies

The diesel generators and all of their engine-mounted and floor and wall-mounted supporting equipment were evaluated. The 125 VDC batteries and their racks were evaluated. Thus, all emergency power supply sources were included in the study.

9.1.6 Cable Trays and Supports

Cable tray systems were selected on an engineering judgment basis. Systems selected were mounted at high elevations in their respective supporting structures and were in locations where a comparison of SME

to SSE in-structure response spectra indicated the greatest potential exceedance in frequency ranges deemed most applicable to cable tray systems. A walk down of the plant was further conducted to finalize the selection. Systems selected are considered to be representative of the more critical systems in the plant. All supports on the tray runs selected were included in the evaluation.

9.1.7 HVAC Ducting and Supports

The control room HVAC ducting and Diesel Generator cooling ducting were determined to be the most critical to safe shutdown and were selected for independent evaluation. All supports of the ducting systems selected were included.

9.1.8 Electrical Conduit and Supports

A generic evaluation of Bechtel's support spacing criteria for electrical conduit was conducted. This generic evaluation encompassed all Category 1 electrical conduit.

9.1.9 Component Support Anchorage

Grouted and expansion-type anchor bolts were evaluated for all piping and equipment supports included in the SME Margin Study.

9.1.10 Electrical, Instrumentation and Control Equipment

Electrical, instrumentation and control cabinets were selected on the basis of their functional criticality and location within the structures. All essential 4160 V switchgear and 480 V motor control centers were included in the sample size. Additional critical control panels located at higher elevations in the structures were selected. The additional cabinets included but are not limited to the Emergency Safety Features Actuation Cabinets, Auxiliary Shutdown Panels, BOP Logic Cabinets, HVAC control cabinets for the auxiliary and diesel generator buildings and the diesel engine and generator control panels.

9.2 PROCEDURES USED TO COMPUTE MARGINS

Margins against code allowables or established functional acceptance criteria were derived by several means. Where practical and justifiable, existing analyses were conservatively scaled to determine upper bounds on SME response. The margins relative to the applicable acceptance criteria were then computed. In other cases, new analyses were utilized to determine responses to the SME. When new analyses were conducted, they were performed using state-of-the-art analytical methods. When original qualification analyses were extrapolated to obtain SME responses, the method of analysis used by the equipment vendor was evaluated and if deemed unconservative relative to current practice, appropriate and conservative factors were applied to assure an upper bound prediction of SME response.

The seismic margin, F_{SME} , was defined as the factor by which the SME would have to be increased to reach the maximum allowable stress or the achieved qualification test level under normal plant operating conditions.

9.2.1 Procedures Used for New Analysis

When new analyses were performed, they were conducted in accordance with current regulatory guide and Standard Review Plan (Reference 40) requirements. For the most part, analyses were conducted using finite element multimode dynamic response computer programs. The response spectrum method was used for all dynamic analyses of BOP equipment and subsystems. Analyses of the NSSS system, conducted by Babcock and Wilcox, employed both the response spectrum and time history methods of analyses. Some analyses of rigid systems or simple flexible systems were conducted using the equivalent static coefficient approach. When new analyses were conducted, the margin against code allowable was computed from the relationship:

$$F_{SME} = \frac{\sigma_A - \sigma_N}{\sigma_{SME}} \quad (9-1)$$

where

σ_A = allowable stress from governing code

σ_N = stress due to normal operating loads

σ_{SME} = stress due to the SME

If margins against failure were computed, the allowable stress, σ_A , was replaced with the failure stress, σ_f .

9.2.1.1 Damping

In conducting new analyses for developing margins against code, responses to the SME were based upon the damping values specified in Regulatory Guide 1.61, Reference 34. In the event that code margins were not met, increased damping values were considered, where justified, in the determination of margins against failure. Table I-8-1 shows Regulatory Guide 1.61 damping values used for code margin analyses and increased damping values for use in failure margin analyses.

9.2.1.2 Combination of Modal Responses

Modal responses were combined by the SRSS method except for closely spaced modes. In all computer programs used, closely spaced modes were combined by one of the acceptable methods specified in Regulatory Guide 1.92, Reference 26. In conducting response spectrum analyses, non-participating mass was accounted for per Standard Review Plan requirements stated in Section 3.7.2 II B1 a(5). The NUPIPE computer code (Reference 39) utilized for piping analyses automatically computes the amount of mass participation on a mode-by-mode and degree-of-freedom basis and adds in the non-participating mass as rigid body modes. The MODSAP (Reference 25) and STARDYNE (Reference 45) computer codes used for analysis of cable trays, ducting and component supports did not have an automatic feature to add in the non-participating mass. In using these codes, modal responses were computed to 33 Hz or greater. The non-participating mass was then conservatively enveloped by applying an additional static load equal to the zero period acceleration times the system weight. This upper bound on non-participating mass was added to the dynamic solution modal responses by the SRSS method.

9.2.1.3 Combination of Earthquake Components

When new analyses were conducted, the requirements of Regulatory Guide 1.92 for earthquake component combinations were incorporated. Analyses were conducted for the three independent directional inputs and the resulting end items of interest was combined by the SRSS method. If stresses were the item of interest, resulting stresses from the three independent runs were combined by SRSS. If support reactions were the end item of interest, the three reactions were combined by SRSS.

9.2.1.4 Analytical Procedures

Finite element methods were employed to compute component and subsystem responses for normal static loading and SME dynamic loading. The degree of complexity of the finite element models varied with the degree of sophistication warranted for the analysis. New analyses were conducted for, the NSSS system, BOP piping systems, cable tray systems and HVAC systems.

9.2.1.4.1 NSSS System - The NSSS system analysis was conducted by Babcock and Wilcox (B&W) for SME base mat input motion defined by Structural Mechanics Associates, Inc. (SMA). B&W utilized their existing NSSS loop model and the response spectrum analysis technique to compute NSSS piping loads and NSSS equipment support loads. The loop model is a complex model of one-half of the complete NSSS system and includes the RPV, one steam generator, two primary coolant pumps, the pressurizer and all interconnecting piping. The model is described in Reference 46. Response spectra at BOP piping/NSSS interface points were generated by B&W from the loop model using the time history method of analysis. B&W also developed SME loading for the RPV intervals using their existing RPV isolated model and the time history method analysis. The RPV isolated model is also described in Reference 46. All SME response results along with results for the SSE and LOCA were transmitted to SMA via Reference 47.

NSSS components and component support reactions from the SME plus normal operating loads were compared by SMA to SSE plus normal loading and the faulted load combinations of normal plus SSE plus LOCA. Positive margins for the SME were derived from load comparisons without further analyses. For RPV internals, existing stress analyses conducted by B&W were reviewed and scaled by SMA to derive stress levels for the combination of normal operating plus SME loads. Margins were derived for the internals by Equation 9-1.

9.2.1.4.2 BOP Piping Systems - BOP piping analyses were conducted using the NUPIPE computer code, Reference 39. NUPIPE is a proprietary finite element computer code developed by the Quadrex Corporation and offered for use on a service bureau basis through several computer companies. The Control Data Corporation system was used in the application of NUPIPE.

NUPIPE computational procedures are formulated to meet all applicable requirements of ASME Codes, Regulatory Guides and the Standard Review Plan, including the earthquake component combination and multimodal response combination requirements of Regulatory Guide 1.92 and the inclusion of non-participating mass per Standard Review Plan requirements of Section 3.7.2 II B1 a(5).

Piping supports were modeled as rigid except in the case of some large lines in the service water system. For these lines, the flexibility and mass of the supports was included in the finite element model.

Support reactions obtained from the piping analyses were utilized in hand calculations or in static finite element models to compute support stresses.

9.2.1.4.3 Cable Tray Systems - Cable tray systems were modeled in two ways. For the simpler systems, the trays were modeled as beam elements and the individual supports were modeled as boundary element springs. Support stiffnesses were computed using static finite element models of

each support. System response was computed from the system models to determine internal forces and moments and boundary forces. The internal forces and moments were compared to acceptance criteria for the tray systems. Boundary forces were applied to the static support computer models and support stresses were computed from these models.

The MODSAP computer program (Reference 25) was used for all static and dynamic analyses of tray systems conducted in this manner. MODSAP is a modified and expanded version of the program SAP IV originally developed at the University of California, Berkeley. The program was modified under a jointly-funded program between the Energy Research and Development Administration and General Atomic Company and is available in the public domain. This code has been used extensively by SMA for general purpose structural analysis and has been thoroughly verified for the types of analyses conducted in this study.

For some cable tray systems, complex coupled models were constructed for the tray runs and supports. Static and dynamic responses were computed for specified normal loading and the SME. Combined responses in the tray runs and the support elements were compared to the applicable acceptance criteria.

For the coupled models, the STARDYNE computer program (Reference 45) was utilized. STARDYNE is a general purpose static and dynamic computer code developed by Mechanics Research Incorporated and marketed on a service bureau basis. The Control Data Corporation version of the code was used for these analyses.

9.2.1.4.4 HVAC Systems - HVAC ducting and supports were analyzed primarily by the equivalent static coefficient method. The ducting is rigid and the supports are in most cases rigid. Support stiffnesses were computed using static finite element models. Tributary duct weights and the support stiffnesses were used to develop equivalent single-degree-of-freedom (SDOF) models for computation of natural frequency and corresponding

spectral acceleration. Resulting SDOF responses were applied to the static support models to develop support stresses and to simple beam models of the ducting to obtain ducting stresses.

9.2.1.5 Multiple Support Equipment and Subsystems

Where piping, cable tray and HVAC ducting models were supported at different elevations in a structure, the SME spectra for an elevation equal to or greater than the highest support elevation were used for analysis. This is conservative since the spectral acceleration amplitudes increase with elevation in all of the structures. In evaluating BOP Class 1 piping, multiple spectra techniques were used. Interface spectra at the Class 1 BOP piping/NSSS interface were generated by Babcock and Wilcox Company for the SME. Reactor building response spectra were generated by Structural Mechanics Associates, Inc. The shape and magnitude of the NSSS versus reactor building spectra were quite different making the use of multiple spectra input desirable. The NUPIPE computer code has an option for conducting multiple spectra analysis. Supports were separated into groups and modal responses were computed separately for the response spectrum applicable to each group. The resulting modal responses for each support group were then conservatively combined by the absolute sum method.

9.2.2 Procedures Used for Existing Design Analyses

For vendor supplied equipment qualified by analysis, margins were determined by extrapolating data in existing qualification reports to reflect SME response in lieu of SSE response. The equipment evaluated responded predominantly in a single mode and was always stiff enough that the lowest fundamental frequency was on the stiff side of the applicable SME spectral peak. Seismic response determined by the vendor was scaled by the ratio of the SME spectral acceleration to the SSE spectral acceleration taken at the equipment fundamental frequency. The seismic margin against code allowable was computed from Equation 9-1.

In some cases, the qualification reports did not contain sufficient information to separate out the stress contribution of normal operating loads from the SSE induced loads. In these cases, one of two approaches was used to conservatively bound the SME margin.

If the SME spectral acceleration exceeded the SSE spectral acceleration, the lower bound margin was computed as:

$$F_{SME} \geq \frac{\sigma_A}{\sigma_T} \quad (9-2)$$

where

$$\sigma_T = \frac{S_{a_{SME}}}{S_{a_{SSE}}} (\sigma_{SSE} + \sigma_N) \quad (9-3)$$

$S_{a_{SME}}$ and $S_{a_{SSE}}$ are the spectral accelerations for the SME and SSE respectively, defined at the equipment fundamental frequency and $(\sigma_{SSE} + \sigma_N)$ is the total computed stress response for the specified SSE plus normal loading. The resulting margin is conservative when computed in this manner since the normal loading stress response is scaled upward along with the SSE stress response.

If the SME spectral acceleration was less than the SSE spectral acceleration, no scaling was done, as scaling the SSE plus normal load response downward would be non-conservative. In this case, the SME margin is bounded by the margin computed for the SSE.

$$F_{SME} > \frac{\sigma_A}{\sigma_D} \quad (9-4)$$

where σ_D is the combined SSE plus normal loading stress from the vendor's design analysis.

9.2.3 Procedure Used for Equipment Qualified by Test

For active equipment which must undergo a motion to provide its functional contribution to safe shutdown, testing rather than analysis was usually employed in the qualification process. In some cases, a combination of analysis and test was employed wherein analysis was conducted to develop internal loads in supporting members and seismic responses at active components of the subsystem under consideration. Testing of the active components was then conducted to verify their function under the computed responses at the mounting locations in the subassembly.

The tests may have been static or dynamic. In most cases, the component or subsystem assemblies were complex and dynamic testing was conducted. However, when the components are simple or are rigid, static tests could have been performed. Valves have sometimes been qualified by lateral static test loading of the operators while the valve was opened or closed under operating pressure and temperature conditions. The procedures used to determine margins for the SME consequently differ depending upon the test method.

9.2.3.1 Equipment Qualified by Dynamic Testing

When equipment was qualified by dynamic testing, the general procedure was for a required response spectrum, RRS, applicable for the equipment location to be provided to the equipment supplier. The supplier then tested the equipment with an input motion that resulted in a test response spectrum, TRS, which met or exceeded the RRS throughout the applicable frequency range. Typically, in random motion or complex waveform spectral testing, the TRS closely followed the RRS in the low-frequency regime (< 5 Hz) but greatly exceeded the RRS in the higher frequency ranges; thus, components with fundamental frequencies greater than about 5 Hz were typically overtested by a substantial amount.

Testing procedures for seismic qualification of equipment have varied considerably for equipment purchased in the early to mid-1970's. Current criteria for testing is defined in IEEE 344, 1975, Reference 42

and Regulatory Guide 1.100, Reference 43. Earlier criteria were specified in IEEE 344, 1971. For the most part, testing procedures reviewed by SMA and utilized for Midland equipment qualification meet current criteria. Most tests conducted were biaxial random motion or complex waveform spectral tests that simultaneously excited multiple modes and multiple directions. In a few instances, the test inputs were single axis, single frequency tests of the sine beat, sine sweep or sine dwell type. Many times such tests are justified if the components respond predominantly in a single direction and a single mode.

In evaluating equipment qualified by dynamic testing, a thorough review of the test report was conducted to determine the type of test, the frequencies of the equipment and the presence of multiaxial coupling. For multiaxial tests or for single axis, single frequency tests where the test data indicated that the responses would be predominantly single frequency and uncoupled from multiaxes inputs, the margin against qualification level was determined by comparison of the TRS with the SME-RRS at the equipment fundamental frequency.

$$F_{SME} = \frac{TRS}{SME-RRS} \quad (9-5)$$

If it was determined that the single axis, single frequency tests were not applicable because of multimode and coupled response, the TRS was scaled downward for comparison to the SME-RRS. The scaling factors were developed on a case-by-case basis after a thorough review of the test reports and are described in detail where applied in Volume VII, Section 7.0, dealing with electrical power, control and instrumentation equipment.

If the test reports contained insufficient data to develop multimode and multiaxes coupling scale factors, a worst-case scale factor was developed assuming 100% coupling of the three-directional inputs and an assumed upper bound factor of 1.5 for multimode response. The coupling

scale factor assuming 100% coupling depends upon the specified input (RRS) for each of the three directions. As an upper bound, considering 100% coupling between each of the three orthogonal directions and equal spectral acceleration input for each direction (RRS is equal for each direction), the scale factor was taken as $\sqrt{3}$.

9.2.3.2 Equipment Qualified by Static Testing

The first step in developing margins for equipment qualified by static testing was to determine if the SME loading exceeded the loading specified for qualification. For instance, valves are required to be rigid and be qualified for 3g acceleration in each direction. If computed valve accelerations did not exceed 3g, then the margin was defined as the required acceleration level divided by the calculated acceleration level. If the minimum required qualification level was exceeded, the qualification report was examined in detail to determine the achieved test level. The SME margin was then defined as the achieved test level divided by the calculated input level appropriate for the SME response.

9.3 LOAD COMBINATIONS AND ACCEPTANCE CRITERIA

For each of the equipment categories considered in the Seismic Margin Study, applicable load combinations and acceptance criteria were established. Effective code dates used in the original design and in the Seismic Margin Study varied, depending upon the component under consideration. The effective code date selected was that which essentially was closest to the original design criteria but which reflected the general intent of current code criteria. In most cases, there is little technical difference between the specified design code and current criteria and effective code dates for the SME study are close to the specified design code date.

9.3.1 ASME Code Class 1 NSSS and Balance-of-Plant Piping

The load combination applicable for all Class 1 piping consisted of pressure plus deadweight plus SME inertial loading. Calculated stresses from this load combination were compared to ASME code faulted condition allowables. Table I-9-1 summarizes the load combination and faulted condition code stress acceptance criteria.

Internal loading for Class 1 piping within the NSSS scope of work was developed by Babcock and Wilcox (B&W) for SME base mat input motion defined by Structural Mechanics Associates, Inc. (SMA). B&W utilized their existing NSSS loop model and the response spectrum analysis technique to compute NSSS piping loads. Note that seismic anchor motion loading is inherently included in the NSSS piping analysis for the SME since the loop model couples all NSSS components and piping together. Thus, piping reactions to differential movement of the RPV, steam generator and primary coolant pumps is included in the analysis output.

Class 1 BOP piping analyses were conducted by SMA for selected systems using models uncoupled from the NSSS systems. Load combinations applicable to the Class 1 BOP systems consisted of normal operating loads plus the SME inertial loads. The same models were used to compute thermal expansion and seismic anchor motion loads. These loads were combined with pressure, deadweight and SME loading in order to develop embedment loads at seismic supports. Restraint of thermal expansion and seismic anchor motion loading are not, however, applicable to faulted condition load combinations for Class 1 piping evaluation.

9.3.2 ASME Code Class 2 and 3 Balance-of-Plant Piping

Selected samples of Class 2 and 3 BOP piping were analyzed for SME and normal operating loads and results were compared to ASME code faulted condition criteria. From these same models, thermal expansion and seismic anchor motion cases were also run. Results were combined with pressure, weight and SME inertial loading in order to develop embedment loads at piping supports. Load combinations and faulted condition stress acceptance criteria for Class 2 and 3 piping are summarized in Table I-9-2.

9.3.3 ASME Class 1 Vessels, Pumps and Valves

Components required for safe shutdown that are included in this category are the reactor pressure vessel, steam generators, primary coolant pumps, pressurizer and Class 1 valves in Class 1 Balance-of-Plant (BOP) lines connecting to the NSSS.

All SME loading for these components, except for BOP valves, was developed by B&W from either their loop model using response spectrum methods or from their Reactor Vessel Isolated Model using the time history method of analysis. Critically stressed areas were identified by Babcock and Wilcox and stress response information for the faulted condition design basis loading was provided to SMA. SME stress response was computed by scaling stresses computed for the faulted condition design basis by the ratio of the SME loading to the faulted condition design basis loading. Scaled SME stress results were combined with pressure and deadweight stresses and compared to ASME code faulted condition allowables to develop code margins.

Accelerations at Class 1 valves in the Class 1 BOP piping systems were computed from selected SMA piping models and compared to original valve qualification criteria to derive margins for valve function. Operation of the primary coolant pumps is not necessary for a safe shutdown, thus, evaluation of the pumps was confined to the pressure boundary.

Acceptance criteria and applicable load combinations are summarized in Table I-9-3.

9.3.4 ASME CODE CLASS 2 AND 3 EQUIPMENT

New analyses were not conducted for Class 2 and 3 BOP equipment. Selected equipment reports were reviewed and seismic stresses were scaled by the ratio of the SME spectral acceleration to the design basis spectral acceleration at the equipment fundamental frequency. Stress results from loading due to pressure, weight, operating mechanical loads and SME were then combined and compared to the ASME code faulted condition stress criteria. Load combinations and stress acceptance criteria are summarized in Table I-9-4.

9.3.5 COMPONENT SUPPORTS FOR ASME CODE CLASS 1 PIPING AND EQUIPMENT

Component support reactions for the load combination of dead-weight plus operating mechanical loads plus SME were compared to the faulted condition loadings used in the component support designs. In the

event that the faulted condition design basis loading was exceeded, an independent stress check was made to determine the margin against code. ASME Code Class 1 faulted condition component support criteria and the applicable load combination are presented in Table I-9-5.

Restraint of free-end thermal displacements and seismic anchor motion loading are not required by code to be included in the faulted condition acceptance criteria for component supports. These loadings are, however, included in the evaluation of component support anchorage.

NSSS component support skirts were designed to ASME Code Class 1 vessel criteria as their design preceded ASME codification of component supports. For those component supports designed to vessel criteria, the faulted condition vessel criteria of Table I-9-3 were applied rather than the component support criteria of Table I-9-5.

Other NSSS component supports were designed to the criteria of the 1969 AISC code, Reference 41. These include the steam generator upper lateral support, RPV upper lateral support and the pressurizer upper and lower supports. Acceptance criteria for the SME is based upon the original design code with a working stress increase factor of 1.6 for faulted condition loading. Table I-9-6 summarizes the acceptance criteria for these supports.

9.3.6 Component Supports for ASME Code Class 2 and 3 Piping and Equipment

The Class 2 and 3 component support margin evaluation procedure and load combination are identical to the Class 1 criteria except for the faulted condition acceptance criteria. Code Class 2 and 3 faulted condition acceptance criteria for linear, plate and shell and component standard supports are defined in Table I-9-7.

9.3.7 Cable Trays and Supports

Cable trays for Midland were qualified by static load testing in the lateral and vertical directions and by classic stress and buckling analysis techniques for the longitudinal direction. Tests were run to failure and the allowable equivalent static loading was determined to be the lesser of two-thirds the ultimate load or one-half the deflection at ultimate failure. Lower bound natural frequencies for the lateral and vertical directions were derived from the load-deflection relationships as were equivalent moments of inertia. The original design acceptance criteria for the trays were established by limiting acceleration in each of three directions. The acceleration acceptance criteria were based upon the allowable equivalent static loading derived from test data. An interaction formula was used to combine 1g dead load with the g loading for the three-directional components of earthquake. In the design analyses, tributary weights of cable trays were added to individual supports and system fundamental frequencies and resulting spectral accelerations were derived. These spectral accelerations were assumed to be uniform along the tray and were compared to the acceleration acceptance criteria derived from static tests.

For the SME evaluation, detailed finite element beam models were utilized to obtain SME responses. Since internal moments in the trays were computed from these models, an alternate tray acceptance criteria was derived from the test data. Instead of basing the acceptance criteria on acceleration, which varies along the length of the trays, allowable moments were derived from the static load test data and an interaction equation based upon allowable moments was derived. Table I-9-8 summarizes the load combination and acceptance criteria for cable trays use in the SME study.

Stress acceptance criteria for cable tray supports is that defined by the latest version of the AISC Code, Reference 33, Part 2, plastic design as supplemented by the Standard Review Plan, Section 3.8.4 II E5. Stress acceptance criteria for cable tray supports is shown in Table I-9-9.

9.3.8 HVAC Ducting and Supports

HVAC ducting support spacing in Midland is specified so that the ducting is considered rigid (frequency greater than 33 Hz). In most instances, the supports are also rigid. Consequently, the evaluating of ducting and supports could be carried out by static analyses methods. Stress acceptance criteria for HVAC ducting supports are identical to that for cable tray supports and are summarized in Table I-9-9.

Rectangular ducting, because of the large, flat sheet sections, is more buckling critical than stress critical. Compressive stresses in the ducting due to external pressure and beam bending were computed and compared to buckling criteria developed for thin, rectangular simply-supported panels. A factor of at least 2.0 was maintained for the combination of external pressure plus deadweight plus SME loading.

External pressure tests conducted on similar ducting, References 48, 49 and 50, verify that the buckling acceptance criteria developed from classical buckling equations for simply-supported plates are conservative. Table I-9-10 summarizes the ducting acceptance criteria.

9.3.9 Component Support Anchorage

Embedded anchorage criteria for component supports is governed by appropriate civil codes and the Standard Review Plan. For steel embeddings in concrete, either the steel ultimate capacity or the concrete pullout capacity will govern. Current concrete pullout capacity and appropriate load combinations are governed by the ACI-349 Code, Reference 31, as supplemented by the Standard Review Plan, Section 3.8.4. Current ultimate steel capacity and load combinations are governed by the AISC code (Reference 33) as supplemented by the Standard Review Plan, Section 3.8.4. These acceptance criteria and load combinations are summarized in Table I-9-11.

For grouted and shell-type expansion anchors, acceptance criteria developed from test data, and applying appropriate and conservative factors of safety, are defined in Bechtel Specifications 7220-C-305Q, Reference 51, and 7220-C-306Q, Reference 52. Support reactions at support/anchorage interfaces were compared to the allowable loads as defined in the Bechtel Specifications to determine code margins. These acceptance criteria are summarized in Table I-9-11.

TABLE I-9-1

LOADING COMBINATIONS AND STRESS LIMITS FOR CLASS 1 PIPINGLoading Combinations for
Faulted Conditions:

Operating Pressure + Deadweight + Seismic
Margin Earthquake Loads (SME)

Code Stress Acceptance Criteria

$$B_1 \frac{P D_o}{2t} + B_2 \frac{D_o}{2I} M_i \leq 3.0 S_m \quad (1)$$

Where:

- B_1, B_2 = primary stress indices for the specific product under investigation (NB-3680)
 P = Design Pressure, psi
 D_o = outside diameter of pipe, in (NB-3683)
 t = nominal wall thickness of product, in. (NB-3683)
 I = moment of inertia, in.⁴ (NB-3683)
 M_i = resultant moment due to a combination of Design Mechanical Loads (Dead Wt.+SME)
 S_m = allowable design stress intensity value, psi (Tables I-1.0)

Notes:

1. Faulted condition criteria per 1974 ASME Boiler and Pressure Vessel Code, Section III, Subsection NB, with no addenda.

TABLE I-9-2

LOADING COMBINATIONS AND STRESS LIMITS FOR CLASS 2 & 3 PIPINGLoading Combination forFaulted Conditions:

Operating Pressure + Deadweight + Seismic
Margin Earthquake Loads (SME)

Stress Acceptance Criteria

$$\frac{P_{\max} D_o}{4t_n} + 0.75i \left(\frac{M_A + M_B}{Z} \right) \leq 2.4 S_h \quad (1)$$

Where:

- P_{\max} = peak pressure, psi
 D_o = outside diameter of pipe, in.
 t_n = nominal wall thickness, in.
 M_A = resultant moment loading on cross section due to weight and other sustained loads, in.lb.
 M_B = resultant moment loading on cross section due to earthquake inertial loads.
 Z = section modulus of pipe, in.³(NC-3652.4)
 i = stress intensification factor [NC-3673.2(b)]. The product of 0.75i shall never be taken as less than 1.0.
 S_h = basic material allowable stress at operating temperature, psi

Note:

1. Faulted condition stress criteria per 1974 ASME Code, Section III, with Winter 1976 Addenda.

TABLE I-9-3

LOADING COMBINATION AND STRESS LIMITS
FOR CLASS 1 VESSELS, PUMPS AND VALVES

<u>Loading Combination</u>	<u>Stress Limit</u> ^{1,2,3,4}
$P_N + D + OML + SME$	$\left. \begin{array}{l} P_m \leq 2.4 S_m \\ \leq 0.7 S_u \end{array} \right\}$ $\left. \begin{array}{l} P_L + P_b \leq 3.6 S_m \\ \leq 1.05 S_u \end{array} \right\}$
	For Materials in Table I-1.2
	$\left. \begin{array}{l} P_m \leq 0.7 S_u \\ P_L + P_b \leq 1.05 S_u \end{array} \right\}$
	For Materials in Table I-1.1

Where:

P_N = Normal operating pressure

D = Deadweight

OML = Operating mechanical loads from connecting piping including earthquake anchor motion and restraint of free end thermal displacement

SME = Seismic Margin Earthquake Inertial Loading

S_m = Allowable stress value from ASME Code, 1974 edition with Addenda through Winter 1976, Table I-i

P_m = General membrane stress intensity produced by pressure and other mechanical loads

P_L = Local membrane stress intensity produced by pressure and other mechanical loads

P_b = Primary bending stress intensity produced by pressure and other mechanical loads

Notes:

1. Stress limits apply to extended support structures for valves.
For active valves, the extended operator support structure primary stress is limited to S_y .
2. Faulted condition stress criteria per 1974 ASME Code, Section III, with Winter 76 Addenda.
3. Use lesser of limits specified.
4. Valve operator acceleration is limited to 3g in any direction.

TABLE I-9-4

LOADING COMBINATIONS AND STRESS LIMITS FOR
CLASS 2 & 3 VESSELS, PUMPS AND VALVES

<u>Loading Combination</u>	<u>Stress Limit</u> ^{1,2}
$P_N + D + OML + SME$	$\sigma_m \leq 2.0 S$
	$\sigma_L + \sigma_b \leq 2.4 S$

Where:

- P_N = Normal operating pressure
- D = Deadweight
- OML = Operating mechanical loads including earthquake anchor motion and restraint of free-end thermal displacement loading from connecting piping
- SME = Seismic Margin Earthquake Inertial Loading
- S = Allowable stress value from ASME Code, 1974 edition with Addenda through Winter 1976, Tables I-7 or I-8
- σ_m = General membrane stress produced by pressure and other mechanical loads
- σ_L = Local membrane stress produced by pressure and other mechanical loads
- σ_b = Primary bending stress produced by pressure and other mechanical loads

Notes:

1. Stress limits apply to extended support structures for valves. For active valves, the extended operator support structure primary stress is limited to S_y .
2. Faulted condition stress criteria per 1974 ASME Code, Section III, with Winter 76 Addenda.
3. Valve operator acceleration is limited to 3.0g in any direction.

TABLE I-9-5

LOADING COMBINATIONS AND STRESS LIMITS FOR
ASME CLASS 1 COMPONENT SUPPORTS

Loading Combination	Linear Type Support Limits ^{1,2,3,7}	Component Standard Linear Supports Designed by Load Rating	Plate and Shell ³ Support Limit
D + OML + SME	Within Lesser of: $\frac{1.2 S_y}{F_t} \text{ or } \frac{0.7 S_u}{F_t}$ Times Normal Operating Stress Limit, F_{all} .	$0.8 L_t$	$\left. \begin{aligned} P_m &\leq \begin{matrix} 1.5 S_m \\ 1.2 S_y \end{matrix} \\ P_m + P_b &\leq \begin{matrix} 2.25 S_m \\ 1.8 S_y \end{matrix} \end{aligned} \right\} \begin{matrix} 4,5 \\ 4,6 \end{matrix}$

where:

- D = Deadweight
- OML = Operating Mechanical Loads
- SME = Seismic Margin Earthquake Loading
- S_y = Material yield strength at temperature
- S_u = Material ultimate strength at temperature
- F_t = Allowable tensile stress per ASME Section III, Appendix XVII at temperature
- F_{all} = Allowable stress value from ASME Code, Appendix XVII, XVII-1100
- L_t = Ultimate Collapse Load as defined in ASME Code, Appendix F, F1370(d)
- P_m = Primary membrane stress intensity produced by mechanical loads
- P_b = Primary bending stress intensity produced by mechanical loads
- S_m = Allowable stress intensity from ASME Code, Appendix I

Notes:

1. Compressive axial member loads should be kept to less than 0.67 times the critical buckling load.
2. Includes Component Standard Supports designed by analysis.
3. Component support analyses and material allowables per ASME Code, Section III, 1974 edition with Winter 1976 Addenda.
4. Use greater of values specified.
5. Not to exceed $0.7 S_u$.
6. Not to exceed $1.05 S_u$.

TABLE I-9-6

LOADING COMBINATION AND STRESS LIMITS FOR
NSSS COMPONENT SUPPORTS DESIGNED TO THE AISC CODE

<u>Loading Combination</u>	<u>Stress Limit</u> ⁽¹⁾
D + OML + SME	1.6 f_s

where:

D = Dead Load

OML = Operating Mechanical Loads

SME = Seismic Margin Earthquake Loading

f_s = Allowable stress from Part 1 of the AISC Specification
for Design, Fabrication and Erection of Structural Steel
for Buildings, 7th Edition

Notes:

1. Shear Stress is limited to 0.5 F_y where F_y is the specified yield strength of the material

TABLE I-9-7

LOADING COMBINATIONS AND STRESS LIMITS FOR
CLASS 2 AND 3 COMPONENT SUPPORTS

Loading Combination	Linear Type Support Limits ^{1,2,3}	Component Standard Linear Supports Designed by Load Rating	Plate and Shell ³ Support Limit
D + OML + SME	Within Lesser of: $\frac{1.2 S_y}{F_t}$ or $\frac{0.7 S_u}{F_t}$ Times Normal Operating Stress Limit, F_{all} .	$0.8 L_t$	$\sigma_1 \leq 1.5 S^4$ $\sigma_1 + \sigma_2 \leq 2.25 S^5$ $\sigma_3 \leq 0.5 S$

where:

- D = Deadweight
- OML = Operating Mechanical Loads
- SME = Seismic Margin Earthquake Loading
- S_y = Material yield strength at temperature
- S_u = Material ultimate strength at temperature
- F_t = Allowable tensile stress per ASME Section III, Appendix XVII at temperature
- F_{all} = Allowable stress value from ASME Code, Appendix XVII, XVII-1100
- L_t = Ultimate Collapse Load as defined in ASME Code, Appendix F, F1370(d)
- σ_1 = Average membrane stress produced by mechanical loads
- σ_2 = Primary bending stress produced by mechanical loads
- σ_3 = Maximum tensile stress at contact surface of welds in through thickness direction of plates and rolled sections
- S = Allowable stress from ASME Code, Appendix I

Notes:

1. Compressive axial member loads should be kept to less than 0.67 times the critical buckling load.
2. Includes Component Standard Support designed by analysis.
3. Component support analyses and material allowables per ASME Code, Section III, 1974 edition with Winter 1976 Addenda.
4. Not to exceed $0.4 S_u$.
5. Not to exceed $0.6 S_u$.

TABLE I-9-8

LOADING COMBINATION AND ACCEPTANCE
CRITERIA FOR CABLE TRAYS

Load Combination

Acceptance Criteria^{1,2}

D + SME

$$\frac{M_D}{M_{UV}} + \left[\left(\frac{M_V}{M_{UV}} \right)^2 + \left(\frac{M_T}{M_{UT}} \right)^2 + \left(\frac{E_L}{Y_L} \right)^2 \right]^{1/2} \leq 1$$

where:

- D = Dead Weight of Tray and Contents
- SME = Seismic Margin Earthquake Inertial Loading
- M_D = Bending Moment due to Dead Weight
- M_V = Bending Moment in the Vertical Plane from the SME
- M_T = Bending Moment in the Transverse Plane from the SME
- M_{UV} = Allowable Moment in the Vertical Plane
- M_{UT} = Allowable Moment in the Transverse Plane
- E_L = Axial Load in Tray from the SME
- Y_L = Allowable Axial Load in Tray

Note:

1. M_{UV} and M_{UT} are derived from ultimate load tests and are based on the lessor of 2/3 the maximum collapse moment or the moment at a displacement equal to 1/2 the ultimate load displacement.
2. Y_L is 2/3 of the ultimate load capacity.

TABLE I-9-9

LOADING COMBINATION AND
ACCEPTANCE CRITERIA FOR HVAC AND
CABLE TRAY SUPPORTS

Load Combination	Allowable Stress*
D + L + To + SME	1.6 S or Y

Where:

- D = Dead Load
- L = Live Load
- To = Loading from Restraint of Free-End Thermal Displacement
- SME = Loading from Seismic Margin Earthquake Including Inertial Effects and Differential Anchor Motion
- S = Working Stress Allowable from AISC Code, 8th Edition, 1980
- Y = Section Strength Required to Resist Design Loads and Based on Plastic Design Methods Described in Part 2 of the AISC Code

*Allowable Stress Based upon AISC Code, 8th Edition, Part 2, Plastic Design and NUREG-0800

TABLE I-9-10

LOADING COMBINATION AND STRESS LIMITS
FOR HVAC DUCTING

<u>Loading Combination</u>	<u>Stress Limit</u>
P + D + SME	$0.5 \sigma_{cr}$

where:

- P = Design pressure acting externally on duct
- D = Dead Weight
- SME = Seismic Margin Earthquake
- σ_{cr} = Critical buckling stress computed for thin sheet simply supported on all edges and subjected to biaxial compressive stresses resulting from P, D and SME

TABLE I-9-11

LOADING COMBINATIONS AND STRESS LIMITS FOR
COMPONENT SUPPORT ANCHORAGE^{1,2}

Loading (1) Combination	(2,3,4) Embedded Anchors	Grouted Anchors	Expansion Anchors
D+L+To+Ro+SME	Lesser of U or 1.6S	Allowable loads per Bechtel Specifica- tion 7220-C-306Q	Allowable loads per Bechtel Specification 7220-C-305Q

where:

- D = Dead loads from attached equipment or piping
- L = Live loads from attached equipment or piping
- To = Restraint of free-end thermal displacement of attached equipment or piping
- Ro = Pipe and equipment reactions during normal operating or shutdown conditions not already included in D+L+To (i.e., piping reactions on vessel which are transmitted to vessel anchors)
- SME = Load effects of Seismic Margin Earthquake including effects of differential anchor movement.
- U = Ultimate pullout strength per ACI 349-80, Appendix B
- S = Allowable working stress per AISC Code, 8th edition, 1980.

NOTES:

1. Load combinations are consistent with NUREG-0800 Standard Review Plan, Section 3.8.4; ACI 349-1980, Section 9.2, and Regulatory Guide 1.142
2. Strength criteria are consistent with NUREG-0800, Standard Review Plan, Section 3.8.4; ACI 349-1980, Appendix B and AISC Part 2, eighth edition, 1980.
3. The faulted stress limit for the reactor vessel anchor studs is 75 ksi (See Reference 43)
4. The faulted stress limits for LAQT bolts will be provided later.

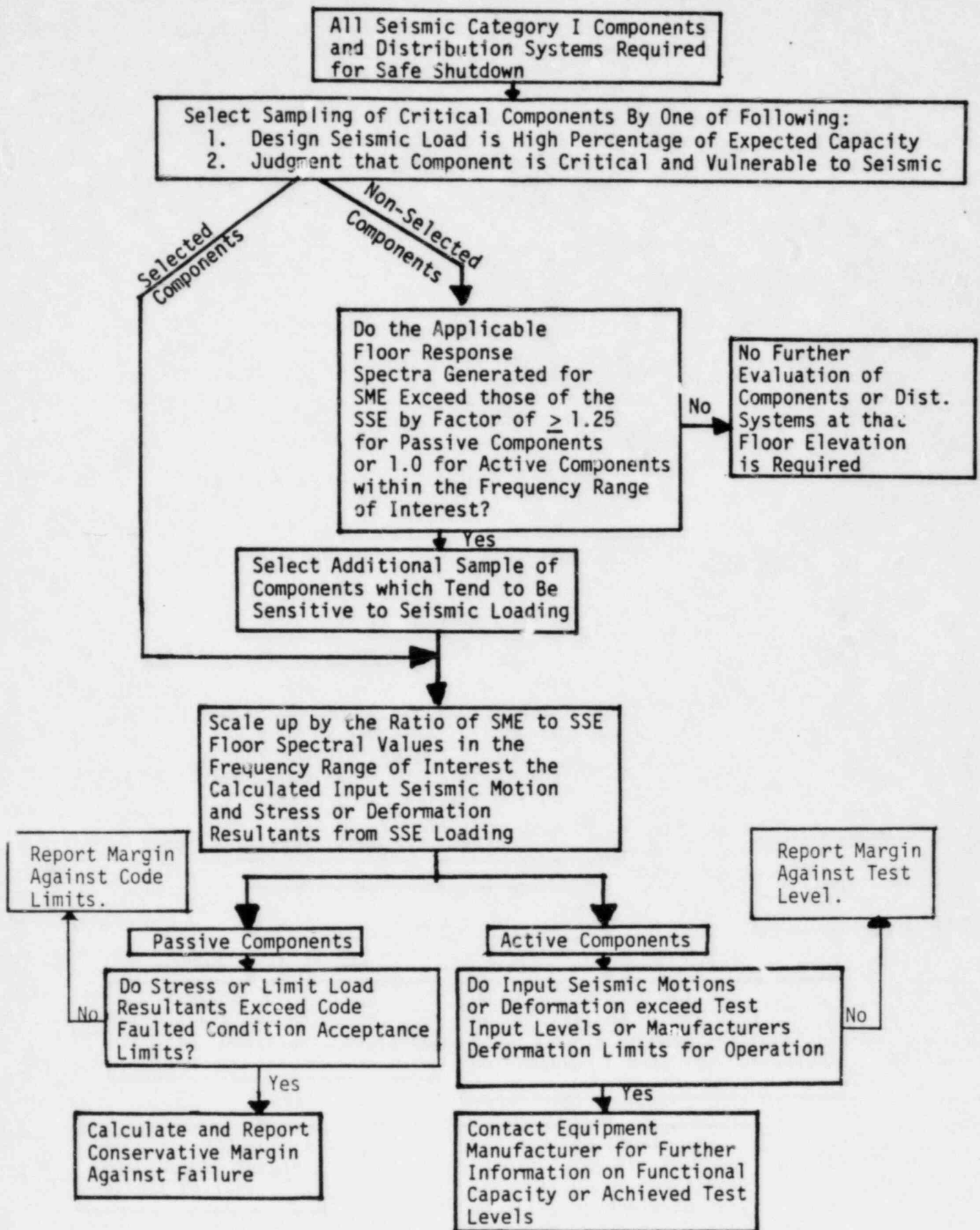


FIGURE I-9-1: PROCESS TO SELECT COMPONENTS AND DISTRIBUTION SYSTEMS FOR SEISMIC SAFETY MARGIN EVALUATION AND DEVELOP MARGINS

REFERENCES

1. Final Safety Analysis Report (FSAR), Midland Plant - Units 1 and 2, Consumers Power Company.
2. TID-7024, Nuclear Reactors and Earthquakes, Lockheed Aircraft Corporation and Holmes and Narver, Inc., August, 1963.
3. Site Specific Response Spectra, Midland Plant - Units 1 and 2, Part I, Response Spectra - Safe Shutdown Earthquake, Original Ground Surface, Weston Geophysical Corporation, prepared for Consumers Power Company, February, 1981.
4. Site Specific Response Spectra, Midland Plant - Units 1 and 2, Part II, Response Spectra - Applicable for the Top-of-Fill Material at the Plant Site, Weston Geophysical Corporation, prepared for Consumers Power Company, April, 1981.
5. Draft, Site Specific Response Spectra, Midland Plant - Units 1 and 2, Part III, Seismic Hazard Analysis, Weston Geophysical Corporation, prepared for Consumers Power Company, Revision 1, May, 1982.
6. Letter correspondence dated March 25, 1982 from M. L. Kiefer (Dames & Moore) to L. H. Curtis (Bechtel), Subject "Recommended Soil Dynamic Moduli - Soil Dynamic Modulus Study - Consumers Power Company, Midland Units 1 and 2", March 25, 1982.
7. Johnson, D. K. and D. M. Trujillo, "STUF", Holmes & Narver, Inc., February 6, 1975.
8. "Soil Dynamic Modulus Study Midland Units 1 and 2 Consumers Power Company", Dames & Moore, Inc., Dames & Moore Job No. 05697-039-07, February 19, 1982.
9. Letter correspondence dated February 23, 1982 from E. M. Hughes (Bechtel) to R. P. Kennedy (SMA), Subject: "Seismic Model Properties for the Reactor Building Midland Units 1 and 2".
10. Bechtel submittal to NRC "Auxiliary Building Seismic Model Revision 3 for Midland Plant Units 1 and 2 Consumers Power Company", September 28, 1981.
11. Bechtel submittal to NRC, "Service Water Pump Structure Seismic Model Revision 2 for Midland Plant Units 1 and 2 Consumers Power Company", November 24, 1981.
12. Letter correspondence dated November 25, 1981 from L. H. Curtis (Bechtel) to R. Kennedy (SMA), Subject "Soil Spring Summary for Diesel Generator Building" November 25, 1981.

REFERENCES (Continued)

13. Wong, H. L. and J. E. Luco, "Soil-Structure Interaction: A Linear Continuum Mechanics Approach (CLASSI), Report, CE, Department of Civil Engineering, University of Southern California, Los Angeles, California, 1980.
14. Richart, F. E., Hall, J. R. and R. A. Woods, Vibrations of Soils and Foundations, Prentice-Hall, Inc., New Jersey, 1970.
15. Kausel, E., and R. Ushijima, "Vertical and Torsional Stiffness of Cylindrical Footings", Massachusetts Institute of Technology, Research Report R79-6, February, 1979.
16. Veletsos, A. S., and Y. T. Wei, "Lateral and Rocking Vibration of Footings", Journal of the Soil Mechanics and Foundations Division, Proceedings of ASCE, EM5, pp 1381-1395, October, 1971.
17. Luco, J. E., and R. A. Westmann, "Dynamic Response of Circular Footings", Journal of the Engineering Mechanics Division, Proceedings of ASCE, EM5, pp 1381-1395, October, 1971.
18. Veletsos, A. S., and B. Verbic, "Basic Response Functions for Elastic Foundations", Journal of the Engineering Mechanics Division, EM2, April, 1974, pp. 189-202.
19. Woodward-McNeill and Associates, "Development of Soil-Structure Interaction Parameters Proposed Units 2 and 3, San Onofre Nuclear Generating Station, "San Onofre, California, January, 1974.
20. Tsai, N. C., "A Review of Experimental Soil-Structure Interaction Damping", Transactions of the 6th International Conference on Structural Mechanics in Reactor Technology, Volume K, August, 1981, Article K3/10.
21. Newmark, N. M., W. J. Hall, R. P. Kennedy, R. C. Murray, and J. D. Stevenson, "SSRT Guidelines for SEP Soil-Structure Interaction Review", Submittal to W. T. Russel, U.S. Nuclear Regulatory Commission, December 8, 1980.
22. Seed, H. B. and Idriss, I. M., "Soil Moduli and Damping Factor for Dynamic Response Analysis", Earthquake Engineering Research Center, Report No. 70-10, University of California, Berkeley, California, December, 1970.

REFERENCES (Continued)

23. Tsai, N. C., "Modal Damping for Soil-Structure Interaction", Journal of Engineering Mechanics Division, ASCE, Vol. 100, No. EM2, pp 323-341, April, 1974.
24. Johnson, J. J., "SOILST - A Computer Program for Soil-Structure Interaction Analyses", General Atomic Company, GA-A15067, April, 1979.
25. Johnson, J. J., "MODSAP - A Modified Version of the Structural Analysis Program SAP-IV for the Static and Dynamic Response of Linear and Localized Nonlinear Structures", General Atomic Company, GA-A14006, June, 1976.
26. USNRC Regulatory Guide 1.92, Combining Responses and Spatial Components in Seismic Response Analysis, Rev. 1, February 1976.
27. Derecho, A. T., et. al., "Analysis and Design of Small Reinforced Concrete Buildings for Earthquake Forces", Portland Cement Association, 1974.
28. "Uniform Building Code - 1982 Edition", International Conference of Building Officials, 1982.
29. "Tentative Provisions for the Development of Seismic Regulations for Buildings", National Bureau of Standards Special Publication 510, Applied Technology Council.
30. ASME Boiler and Pressure Vessel Code, Section III, Division 2, "Code for Concrete Reactor Vessels and Containments", American Society of Mechanical Engineers, 1980.
31. ACI 349-80, "Code Requirements for Nuclear Safety Related Concrete Structures", American Concrete Institute, 1980.
32. Bechtel Associates Professional Corporation, "Technical Specifications for Forming, Placing, Finishing and Curing of Concrete for the Consumers Power Company Midland Plant - Midland, Michigan", Spec. 7220-C-231Q, Revision 21, September 28, 1981
33. AISC, "Specification for the Design, Fabrication, and Erection of Structural Steel for Buildings", American Institute of Steel Construction, 8th Edition, 1980.

REFERENCES (Continued)

34. USNRC Regulatory Guide 1.61, Damping Values for Seismic Design of Nuclear Power Plants, October, 1973.
35. USNRC Regulatory Guide 1.122, Development of Floor Design Response Spectra for Seismic Design of Floor-Supported Equipment or Components, September, 1976.
36. Bohm, G. J., "Damping for Dynamic Analysis of Reactor Coolant Systems", presented at the National Topic Meeting, Water Reactor Safety of the American Nuclear Society, Salt Lake City, Utah, 26-28 March, 1973.
37. Morrone, A., "Damping Values of Nuclear Power Plant Components", Report WCAP-7921 Westinghouse Nuclear Energy Systems, November, 1972.
38. Stevenson, J. D., "Structural Damping Values as a Function of Dynamic Response Stress and Deformation Levels", Nuclear Engineering and Design, Vol. 60, 1980.
39. NUPIPE II/TRHEAT, Piping Analysis Programs, User Information Manual, Rev. I, Control Data Corporation and Nuclear Service Corporation, 1981.
40. NUREG-0800, Standard Review Plant, U.S. Nuclear Regulatory Commission, July, 1981.
41. AISC, "Specification for Design, Fabrication and Erection of Structural Steel for Buildings, 7th Edition, American Institute of Steel Constructions, 1969.
42. IEEE 344-1975, "IEEE Recommended Practices for Seismic Qualification of Class 1E Equipment for Nuclear Power Generating Stations, January 31, 1975, Institute of Electrical Engineers, New York.
43. USNRC Regulatory Guide 1.100, Seismic Qualification of Electrical Equipment for Nuclear Power Plants, Rev. 1, August, 1977.
44. Consumers Power Company Submittal to NRC, "Reactor Vessel Support Modification for Midland Nuclear Power Plant, Report No. 3, Revision 1", December, 1981.
45. MRI/STARDYNE 3, Static and Dynamic Structural Analysis Systems, Users Information Manual, Control Data Corporation, Revision B, April, 1978.

REFERENCES (Continued)

46. Babcock and Wilcox Functional Specifications 18-1235000012-09 for Reactor Coolant System Supports and Foundation Loading, October, 1982.
47. Babcock and Wilcox Report 86-1139259-00, "Consumers Seismic Margin Study Report for Midland Units 1 & 2.
48. Structural Design of Class I Seismic HVAC Ducts based on Analysis and Testing for Philadelphia Electric Co., Limerick Generating Station, Units 1 & 2, Job 8031, Bechtel Power Corporation, Volume I, April, 1976.
49. Report on Testing of Class I Seismic HVAC Duct Specimens for Philadelphia Electric Co. Limerick Generating Station, Units 1 & 2, Job 8031, Bechtel Power Corporation, Volume II, April, 1976.
50. Final Test Report of Results on HVAC Ducts - Phase II Vol. 1, Limerick Generating Station, Units 1 & 2, Philadelphia Electric Co., Hales Testing Lab, Report No. OM83-11, Lab No. 46704A, Revision 1, February 25, 1976.
51. Bechtel Technical Specification 7220-C-305Q, Rev. 14, for Design Furnishing Installations and Testing of Expansion Type Concrete Anchors for the Consumers Power Company Midland Plant, Units 1 and 2.
52. Bechtel Technical Specifications 7220-C-306Q, Rev. 8, for Design, Furnishing and Installation of Grouted Anchor Bolts for the Consumers Power Company, Midland Plant, Units 1 and 2, Midland, Michigan.
53. Scanlan, R. H. and K. Sachs, "Earthquake Time Histories and Response Spectra", Journal of Engineering Mechanics, ASCE, August, 1974.

APPENDIX I-A

EFFECTS OF FLOOR SLAB FLEXIBILITY
ON THE VERTICAL SEISMIC INPUT TO
PIPING AND EQUIPMENT

APPENDICES I-A AND I-B
(VOLUME I)

TABLE OF CONTENTS

<u>Section</u>	<u>Title</u>	<u>Page</u>
I-A	EFFECTS OF FLOOR SLAB FLEXIBILITY ON THE VERTICAL SEISMIC INPUT TO PIPING AND EQUIPMENT	
A-1	INTRODUCTION	I-A-1-1
A-2	CALCULATION OF FUNDAMENTAL VERTICAL FLOOR FREQUENCIES	I-A-2-1
	A-2.1 General Analytical Modeling Approach . . .	I-A-2-1
	A-2.2 Auxiliary Building Floors	I-A-2-3
	A-2.2.1 Elevation 584'-0" between Column Lines A, B, 6.2, and 6.9	I-A-2-4
	A-2.2.2 Elevation 614'-0" between Column Lines B, C, 6.2, and 6.9	I-A-2-4
	A-2.2.3 Elevation 646'-0" between Column Lines J, K, 5.9, and 6.6	I-A-2-5
	A-2.2.4 Elevation 685'-0" between Column Lines H, K, 5.3, and 7.8	I-A-2-6
	A-2.2.5 Elevation 642'-7" West of Column Line 4.1 of the West Electrical Penetration Wing	I-A-2-7
	A-2.3 Reactor Building Floors	I-A-2-7
	A-2.4 Service Water Pump Structure Floors . . .	I-A-2-8
	A-2.5 Diesel Generator Building Floors	I-A-2-9
A-3	DEVELOPMENT OF VERTICAL IN-STRUCTURE RESPONSE SPECTRA INCLUDING FLOOR FLEXIBILITY	I-A-3-1
	A-3.1 Auxiliary Building Response Spectra . . .	I-A-3-1
	A-3.2 Service Water Pump Structure Response Spectra	I-A-3-6
	A-3.3 Diesel Generator Building Response Spectra.	I-A-3-8
A-4	SUMMARY	I-A-4-1

I-A REFERENCES

APPENDICES I-A AND I-B (Continued)
(Volume I)

TABLE OF CONTENTS

<u>Section</u>	<u>Title</u>	<u>Page</u>
I-B	USE OF NONLINEAR BEHAVIOR TO MODIFY SEISMIC DESIGN LOADS	
B.1	EFFECT OF NONLINEAR RESPONSE AND DUCTILITY REDUCTION FACTORS	I-B-1
B.2	DEFINITION OF DUCTILITY	I-B-2
B.3	DERIVATION OF DUCTILITY REDUCTION FACTOR FORMULAS	I-B-2
B.4	LIMITATIONS ON THE USE OF THE DUCTILITY REDUCTION FACTOR, k , AND THE DUCTILITY, μ	I-B-3
I-B	REFERENCES	

A-1. INTRODUCTION

Typical lumped-mass models used in the seismic analysis of nuclear power plant structures and generation of the seismic input for qualification of piping and equipment are based on the overall mass and stiffness of the structure. These models often do not include the local flexibility of individual elements such as floor slabs to which piping and equipment is attached. In the plane of the slab such as horizontal motion of floor slabs, this introduces essentially no error due to the high in-plane stiffness. However, the out-of-plane stiffness may be relatively low, especially for slabs with large spans and major openings. Vertical floor amplification may be significant for slabs with relatively low frequencies, especially if the fundamental frequency of the floor is close to a vertical frequency of the overall soil-structure system. For these slabs, the vertical seismic input to piping and equipment may exceed that which would otherwise be computed from an overall soil-structure interaction model which neglects the floor slab flexibility.

The structural models received by SMA from Bechtel were developed to compute the overall building seismic response and, therefore, did not include any provision for vertical floor slab flexibility. In order to determine the effect of the floor slab flexibility on the vertical seismic input to piping and equipment, representative floor slabs in the Seismic Category I buildings were selected for analysis based on the following screening and evaluation program presented in Reference A-1. Following this program, the floor slabs of the auxiliary building, reactor building internal structure, service water pump structure, and diesel generator building were reviewed to determine the variations in structural conditions. Consideration was given to slab thickness, spans, and reinforcement, structural steel framing, support conditions, large slab openings, supported mass, and location within the structure. The floor slabs of each structure were examined and those expected to exhibit the maximum amount of vertical

amplification were selected for more detailed evaluation. A finite element model of each selected floor slab was created using the program MODSAP (Reference A-2) to provide an accurate representation of the structural conditions and out-of-plane behavior. Vertical floor frequencies were determined from an eigenvalue/eigenvector analysis performed for each model. Hand calculations were used together with classical plate theory models to provide an independent check of the finite element models.

For base slabs and other floor slabs founded directly on soil, a much higher equivalent plate stiffness occurs so that vertical amplification of these slabs is negligible. Also, for equipment mounted on metal gratings, the stiffness of the grating and support frame is often included in the component analytical model. Consequently, vertical amplifications of slabs founded on soil and grating supported by steel framing were not considered in the screening program.

Single-degree-of-freedom (SDOF) lumped mass models were created for the selected floor slabs, each system having a fundamental vertical frequency equal to that of the actual slab as determined by the more detailed MODSAP analysis. In all cases investigated, the fundamental vertical slab frequency was found to be well above the fundamental vertical soil-structure interaction frequencies. Therefore, the higher frequency floor modes are not expected to have significant effect on floor response. The SDOF models for the floors of the service water pump structure and the diesel generator building were included in the overall soil-structure analytical models while the SDOF models of the auxiliary building floor slabs were not. Within the containment, no slabs subject to vertical amplification could be which were not included in the equipment support analytical models. Vertical in-structure response spectra were generated at the floor slab masses and the masses of the overall analytical model corresponding to the slab supports. For the auxiliary building, comparisons of these response spectra were conducted to develop factors to be used to conservatively derive response spectra

including the effects of floor flexibility from response spectra not including these effects. For the service water pump structure and the diesel generator building, response spectra generated from the SDOF floor models were used directly in the SME equipment evaluation.

Section A-2 of this report contains the fundamental frequencies of the floors selected for evaluation. Included in this section are descriptions of the general analytical modeling techniques, the physical conditions of the selected floors, and additional modeling details necessary for individual floors. Section A-3 presents in-structure response spectra generated in this study. Comparisons are made between response spectra with and without floor flexibility and between SSE design spectra and SME spectra with floor flexibility. A procedure to apply the results of this study to floors of the auxiliary building that were not evaluated is included in this section. A summary of the conclusions of this study is contained in Section A-4.

A-2. CALCULATION OF FUNDAMENTAL VERTICAL FLOOR FREQUENCIES

Following the screening process outlined in Reference A-1, a number of floor slabs in the Seismic Category I structures were selected to study the influence of floor flexibility on vertical in-structure response spectra. The floor slabs chosen, based on a review of the structural conditions, were those expected to show the maximum amount of vertical amplification. The vertical floor frequencies were determined using finite element computer models representing the actual structural conditions. Vertical in-structure response spectra accounting for local floor flexibility were generated from single degree of freedom lumped mass models having frequencies equal to those of the floor slab systems using the response of the overall soil-structure analytical model as input. This section describes the floors selected to study possible vertical amplification and the manner in which these floors were modeled analytically. Fundamental vertical floor frequencies are reported for each selected floor.

A-2.1 GENERAL ANALYTICAL MODELING APPROACH

The selected floor slabs generally correspond to single bays bounded by vertical supports composed of load-bearing concrete walls and/or structural steel girders connected to columns. These boundaries, with appropriate boundary deformation conditions, permit the creation of refined finite element models providing an accurate representation of the actual floor structural conditions. As an example, a schematic plan of the finite element mesh for the auxiliary building floor at Elevation 584'-0" is shown in Figure A-2-1 (see Section A-2.2.1).

Translations and rotations at the boundaries of each floor panel were constrained depending on the presence of walls or adjacent floor panels with steel framing. In general, the stiffnesses of the load-bearing walls were found to be much greater than the stiffnesses of the floors being analyzed. Walls were thus taken to impose a condition

of fixity against translation and rotation, both in-plane and out-of-plane, at the boundaries where they occur. Steel columns also prevent translation of the floor panels in the vertical direction. Adjacent floor panels were generally assumed to vibrate nearly in-phase with the floor panels being analyzed with vertical translations being approximately equal. A condition of symmetry exists at a floor panel boundary corresponding to an interface with an adjacent floor panel and out-of-plane floor rotations about an axis through the interface as well as in-plane translations were suppressed. The stiffnesses of steel girders at the boundaries were appropriately reduced to reflect the influence of mass from adjacent floor panels causing increased girder deformations.

The concrete slab of each floor panel was represented in the finite element model by the plate elements of MODSAP (Reference A-2). These elements generate both the in-plane and out-of-plane stiffnesses of the slab. The presence of major slab openings was included in the finite element models to accurately represent their influence on floor vibrational behavior. A uniform thickness was assigned to each plate element. For concrete slabs poured on metal deck, the additional stiffness associated with the deck and concrete confined within the deck ribs was conservatively neglected. The above procedure is considered to provide a realistic representation of the actual structural conditions.

The out-of-plane stiffness of a concrete floor slab is dependent on the extent of cracking under load. For cracked members, an effective moment of inertia can be calculated using Equation 9-7 of Reference A-3. This effective moment of inertia is a function of the cracked and uncracked moments of inertia, the cracking moment corresponding to a modulus of rupture of $7.5 \sqrt{f'_c}$ (f'_c being the concrete compressive strength), and the maximum moment to which the member is subjected. Based on a comparison of expected moments due to vertical floor loading

at operating conditions including vertical seismic response versus cracking moments, the stiffnesses of the slabs analyzed in this study were found to be adequately represented by the gross, uncracked stiffness.

Steel and concrete beams and girders were represented by the beam elements of MODSAP (Reference A-2). Appropriate support conditions, typically fixed against translation and free to rotate for the steel members, were assigned to the beam elements. Under vertical seismic excitation, the concrete floor slab and the steel framing will vibrate together as a combined system. Rigid links connecting the nodes of the beam and plate elements were included in the finite element models to force these elements to displace together in the vertical direction.

Mass of the structural elements, non-load bearing interior concrete and masonry walls, and attached equipment was incorporated in the finite element models developed. Structural mass included that of the concrete slab, metal deck, and steel or concrete beams and girders. Some of the floor panels evaluated support non-load bearing interior concrete or concrete block walls which can significantly contribute to the total mass. Estimated masses associated with light attached equipment, cable trays, electrical conduit, and piping were typically uniformly distributed over the entire floor panel. Masses estimated for heavier equipment such as tall electrical cabinets or large tanks were typically distributed over the actual plan area with which they are in contact with their slabs below.

A-2.2 AUXILIARY BUILDING FLOORS

Because of the wide diversity of floor configurations within the auxiliary building, several floor panels were selected from this structure for evaluation. The sampling includes floor panels from the main auxiliary building, the control tower, and the electrical penetration wings, each of which is represented by a different portion of the overall soil-structure analytical model. The structural configurations and fundamental vertical frequencies for the selected floor panels are reported in the following sections.

A-2.2.1 Elevation 584'-0" Between Column Lines A, B, 6.2, and 6.9

This floor panel, shown in Figure A-2-2, was selected for evaluation to represent a floor located at the lower elevations of the main auxiliary building. It supports one of the large boron recovery system receiver tanks, and this large mass was expected to cause a greater amount of vertical amplification than other floor panels at similar locations. The slab consists of 27 inches of concrete poured on metal deck. The 3'-0" by 5'-0" openings located at the northeast and northwest corners of the floor panel were included in the finite element model in order to account for their reduction in slab stiffness. The W36 x 280 girders on Lines 6.2 and 6.9 support W33 x 141 beams spanning in the East-West (E-W) direction. The top portion of each beam is embedded in the concrete slab with holes burned in the web to permit passage of every other bottom slab reinforcement bar oriented normal to the beam. Load-bearing walls border this floor panel on Lines A and B. The interior concrete walls on Lines 6.2 and 6.9 are discontinued at Elevation 584'-0" and do not span down to the base mat below. However, these walls should still provide some boundary stiffness and, along with the steel girders and adjacent floor panels, can be expected to impose fixed boundary conditions for both translations and rotations. Using the finite element model developed for this panel (Figure A-2-1), a fundamental vertical frequency of 35 Hz was calculated.

A-2.2.2 Elevation 614'-0" Between Column Lines B, C, 6.2, and 6.9

This floor panel was selected to represent a floor at an elevation higher in the main auxiliary building than the case previously described in Section A-2.2.1. A sketch of this floor panel is shown in Figure A-2-3. Equipment supported includes the load center and other electrical gear. The slab consists of 12 inches of concrete poured on metal deck. W14 steel columns support steel floor framing at the southeast and southwest panel corners along Line C. The W36 x 182 girders on Lines 6.2 and 6.9 are simply connected to the columns and at beam pockets in the wall on Line B. Beams span in the E-W direction

between the girders and, at the south boundary, between the columns. A 0.75" x 6.5" plate was field welded to the bottom flange of each W18 x 60 beam. Boundary conditions were prescribed as noted in Section A-2.1 except at the south boundary. The region to the south of Line C contains an equipment hatch and a stairway. Due to the lack of an adjacent floor slab providing rotational restraint, out-of-plane slab rotations were permitted along the boundary at Line C. A fundamental vertical frequency of 14 Hz was determined using the finite element model developed for this floor panel.

A-2.2.3 Elevation 646'-0 Between Column Lines J, K_C, 5.9, and 6.6

This floor panel is expected to exhibit the greatest amount of vertical amplification of the floors at the lower elevations of the control tower. A sketch of the floor structure is shown in Figure A-2-4. Elevation 646'-0" of the control tower contains the lower cable spreading rooms. Slab openings for electrical and heating and ventilating chases occur along nearly the entire length of the south control tower wall. These openings were expected to significantly contribute to the vertical floor flexibility and were included in the finite element model developed for this floor panel.

The slab of the lower cable spreading room consists of 12 inches of concrete poured on metal deck. W14 steel columns support framing at the northeast and northwest panel corners along Line J. The W30 x 172 girders along Lines 5.9 and 6.6 are simply connected to the columns and at beam pockets in the south control tower wall. W18 x 77 beams span in the E-W direction between the girders and, at the north boundary, the columns. A concrete buttress separates two electrical chases near Line 5.9. Six #9 reinforcement bars tie the concrete slab to this buttress. In the finite element model, the buttress was taken to provide vertical support for the slab with out-of-plane slab rotations conservatively permitted. The mass of the concrete block wall on Line 6.6 and along the edge of the electrical chases were included in the model. A fundamental vertical frequency of 14 Hz was determined using the finite element model developed for this floor panel.

A-2.2.4 Elevation 685'-0" Between Lines H, K_C, 5.3, and 7.8

This floor is expected to exhibit the greatest amount of vertical amplification of the floors at the higher elevations of the control tower. A sketch of this floor is shown in Figure A-2-5. HVAC equipment and related control panels are attached to the slab. Floor flexibility is increased by the presence of slab openings for heating and ventilating chases along the south wall of the control tower. Also, steel columns do not support the steel framing as at floors lower in the control tower. Instead, girders span the full distance between the north and south control tower walls. The reduction in out-of-plane floor stiffness is expected to increase the amount of vertical amplification relative to the other floors in the upper portion of the control tower.

The slab at Elevation 685'-0" consists of 15 inches of concrete poured on metal deck. The slab openings for the heating and ventilating chases were included in the finite element model. The W36 x 300 girders are simply supported at beam pockets in the north and south control tower walls. Headed studs welded to the top flange of each girder enable composite action to be developed between the girder and the concrete slab for resisting vertical loads. W18 x 60 beams span in the E-W direction between the girders. Non-load bearing concrete and concrete block walls serve as enclosures for the heating and ventilating chases and as room partitions. The mass of these walls was included in the finite element model.

To calculate the plate vibrational behavior of this floor, the boundaries of the finite element model were established at the exterior walls of the control tower. This permits the stiffening effect of the east and west walls to be accounted for. To model the composite girder-slab behavior, rigid links forcing the nodes of the beam and plate elements to displace vertically and rotate about the E-W axis together were included. Rather than model the beams as discrete elements, the stiffness of the plate elements representing the slab was increased for

rotations about the N-S axis to compensate. Boundary conditions at the end of the buttresses similar to those employed at Elevation 646'-0" (see Section A-2.2.3) were used. A fundamental vertical floor frequency of 11 Hz was calculated with this finite element model.

A-2.2.5 Elevation 642'-7" West of Column Line 4.1 of the West Electrical Penetration Wing

This floor panel is expected to exhibit the maximum amount of vertical amplification of the floors in the electrical penetration wings. A sketch of this floor is shown in Figure A-2-6. The power supply and transfer cabinets for the control rod drive mechanism are mounted to the slab at this area of the penetration wings. More vertical amplification is expected for this floor panel compared to other panels in the penetration wings due to the relatively high plan aspect ratio, support flexibility at the north boundary adjacent to the reactor building, and the supported mass of the relatively heavy electrical cabinets.

The slab of this floor panel consists of 12 inches of concrete poured on metal deck. Load-bearing walls form the south, east, and west panel boundaries. W14 steel columns along Line J support steel framing beneath the metal deck. The north boundary of the panel is separated from the reactor building containment wall by a two inch wide expansion joint. Vertical support at this boundary consists only of the relatively flexible steel floor beams spanning between the columns and the west wall. Out-of-plane slab rotations were permitted in the finite element model. A fundamental vertical frequency of 29 Hz was determined using the finite element model developed for this floor.

A-2.3 REACTOR BUILDING FLOORS

Most of the critical equipment in the reactor building is not located on floor slabs which are expected to exhibit significant amplification. The NSSS is supported for the most part on the base slab or on massive individual supports. Other slabs are used primarily to support equipment during refueling

One of the core flooding tanks is supported on the slab at Elevation 640'-0" and another core flooding tank is supported on steel framing at the same elevation. However, the flexibility of both the slab and the framing was included in the design analysis of the tanks. For other equipment supported on steel framing and grating within the reactor building, the flexibility of the steel was also included in the analysis of the component. The base slab varies between 9 and 13 feet thick and rests on soil so that equipment items supported on this slab are not expected to be affected by slab amplification. On the basis of this review, no analysis of floor slab amplification within the reactor building was conducted, and it is concluded that the vertical in-structure response spectra determined from the overall soil-structure interaction model may be used as seismic input for equipment evaluation.

A-2.4 SERVICE WATER PUMP STRUCTURE FLOORS

Most of the safety-related equipment in the Service Water Pump Structure (SWPS) is located on the floor at Elevation 634'-6". The service water pumps are mounted adjacent to a load-bearing wall on a floor expected to show minimal vertical amplification. The SWPS floor selected for evaluation is shown in Figure A-2-7. Motor control centers, load centers, and other electrical equipment are mounted to this floor. This is the floor in the SWPS supporting safety-related equipment that is expected to have the most vertical amplification.

The concrete floor slab in this region is 18 inches thick. 2'-0" by 3'-6" concrete beams spanning in the N-S direction were cast integrally with the slab. To properly model the behavior of the T-beam system including the effects of shear lag, these beams were represented by beam elements in the finite element model. Rigid links were included to force the beam and plate nodes to displace vertically and rotate about the E-W axis together. The east and west boundaries of the model were formed by the exterior walls of the SWPS. The influence of these walls on out-of-plane floor response was conservatively modeled by permitting slab rotations about the N-S axis at these boundaries. Out-of-plane

rotational stiffnesses of the exterior walls, neglecting restraint due to the soil, were represented by the boundary elements of Program MODSAP (Reference A-2). The south boundary of the floor panel was formed by the E-W wall below Elevation 634'-6" as shown in Figure A-2-7. The rotational stiffness of this wall was treated similar to the east and west walls, with a reduction taken to account for the presence of large openings near the base mat. The rotational stiffness of the floor slab south of this wall was conservatively neglected since the openings shown in Figure A-2-7 significantly reduce its effectiveness. The north boundary of the floor panel was formed by the wall, shown in Figure A-2-7, spanning above Elevation 634'-6" to the roof. A note on the construction drawings indicates that the floor slab shoring was not to be removed until this wall had attained its full strength. The stiffness of this wall, compared to other vertical slab supports, is expected to be such that the wall will behave as a beam spanning between the east and west end walls. Accordingly, this wall was modelled by beam elements having stiffness against vertical loads. Appropriate additional masses acting on this wall from the roof and the adjacent floor slab were included in the model. N-S walls intersecting the north boundary wall eight feet from either side of the SWPS centerline provide additional resistance to vertical displacement. For conservatism, only the vertical stiffness of the wall east of the centerline was included, as the other wall does not span down to the base mat and its effectiveness as a vertical support is expected to be less significant. Using the finite element model developed for this floor, a fundamental vertical frequency of 25 Hz was determined.

A-2.5 DIESEL GENERATOR BUILDING FLOORS

The diesel generator units are mounted on concrete pedestals bearing on the soil at the lowest story of the diesel generator building. Most of the other safety-related equipment is attached to the slab-on-grade at Elevation 634'-6". Floors founded directly on soil are not expected to exhibit any vertical amplification. The diesel fuel oil day tanks and some other equipment items are located on the floor at Elevation 664'-0", so this floor was selected for evaluation.

The diesel generator building is composed of four nearly identical bays separated by concrete walls, each containing a diesel generator unit and related equipment. A sketch of the floor for one of these bays is shown in Figure A-2-8. The concrete slab is 24 inches thick including the metal deck at the bottom face. Openings occur in the slab towards the north and south exterior walls as shown in Figure A-2-8. Structural steel beams span in the E-W direction between pockets in the N-S load bearing exterior and interior walls. The walls forming the boundaries of the floor panel along with the adjacent floor panels will tend to enforce the boundary conditions noted in Section A-2.1. The nearly 2:1 plan dimension aspect ratio for this panel is such that two-dimensional plate action is expected to be less significant compared to a square panel. Also, the openings will tend to reduce the effectiveness of the north and south exterior walls acting as supports. For conservatism then, only a single steel beam with tributary width of slab was represented by the finite element model developed for this floor. The north and south edges of this model were permitted to displace vertically but not to rotate about the E-W axis. A fundamental frequency of 17 Hz was determined for this floor.

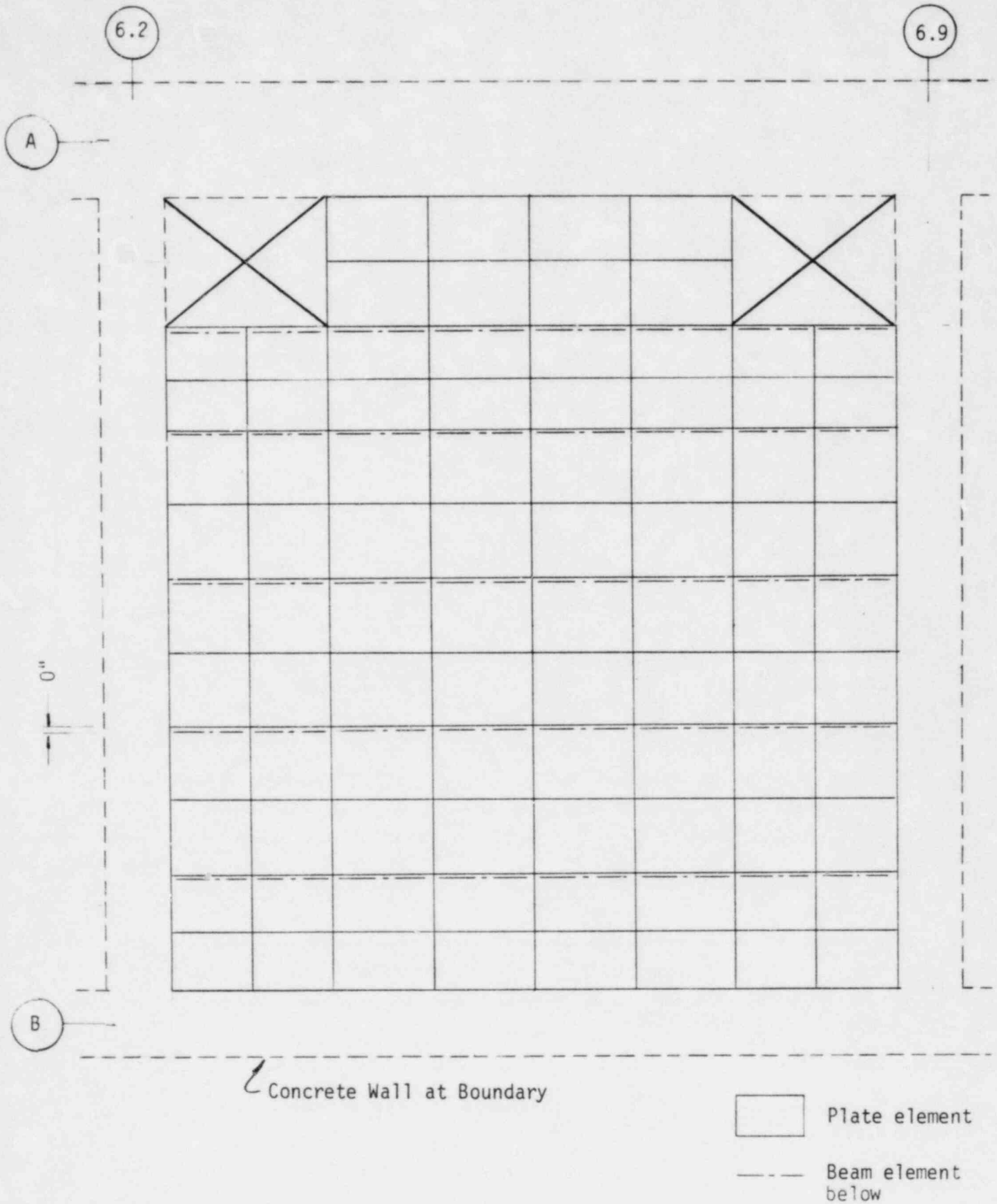


FIGURE A-2-1. FINITE ELEMENT MESH OF AUXILIARY BUILDING FLOOR AT ELEVATION 584'-0"

I-A-2-11

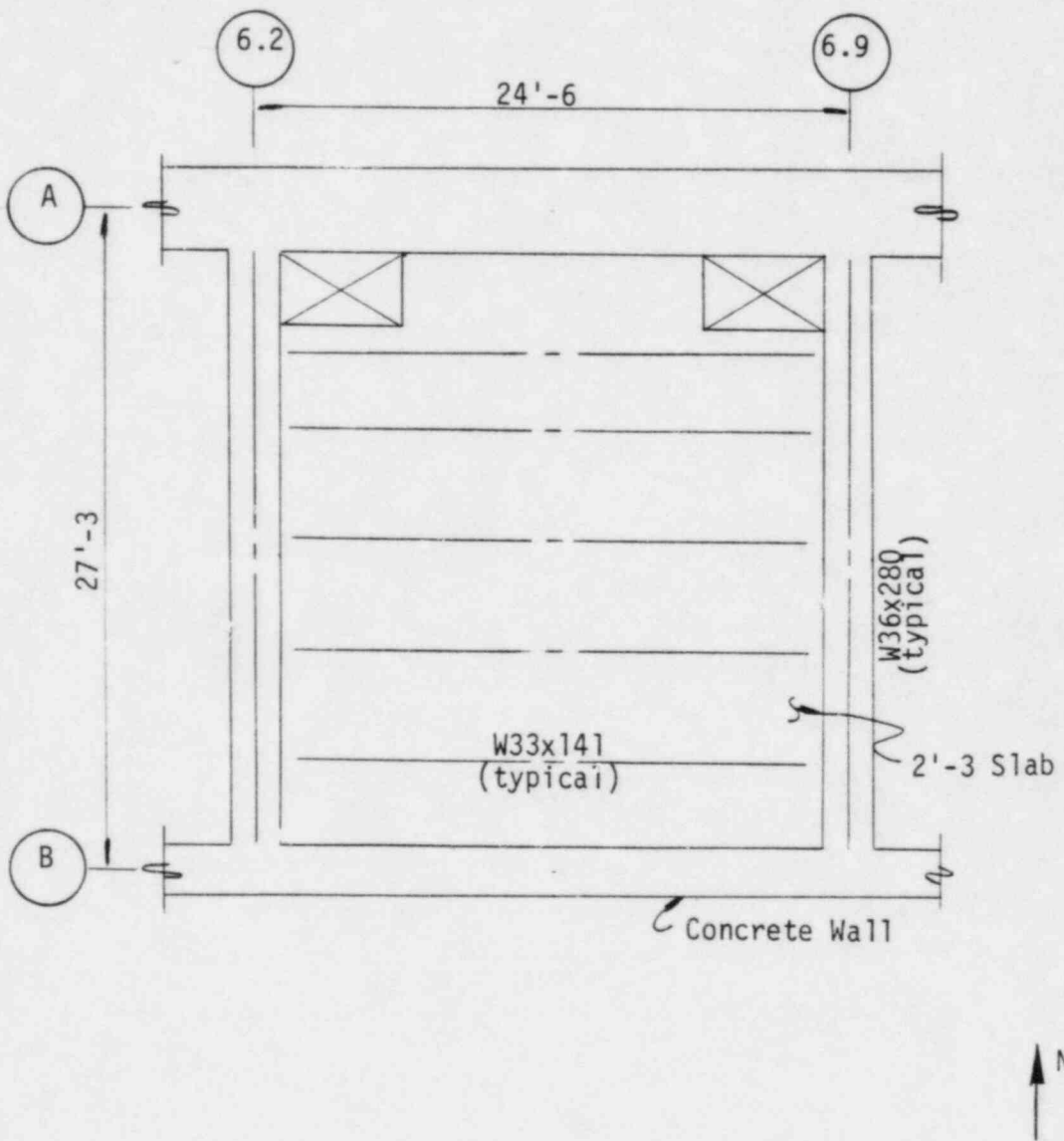


FIGURE A-2-2. AUXILIARY BUILDING FLOOR AT ELEVATION 584'-0

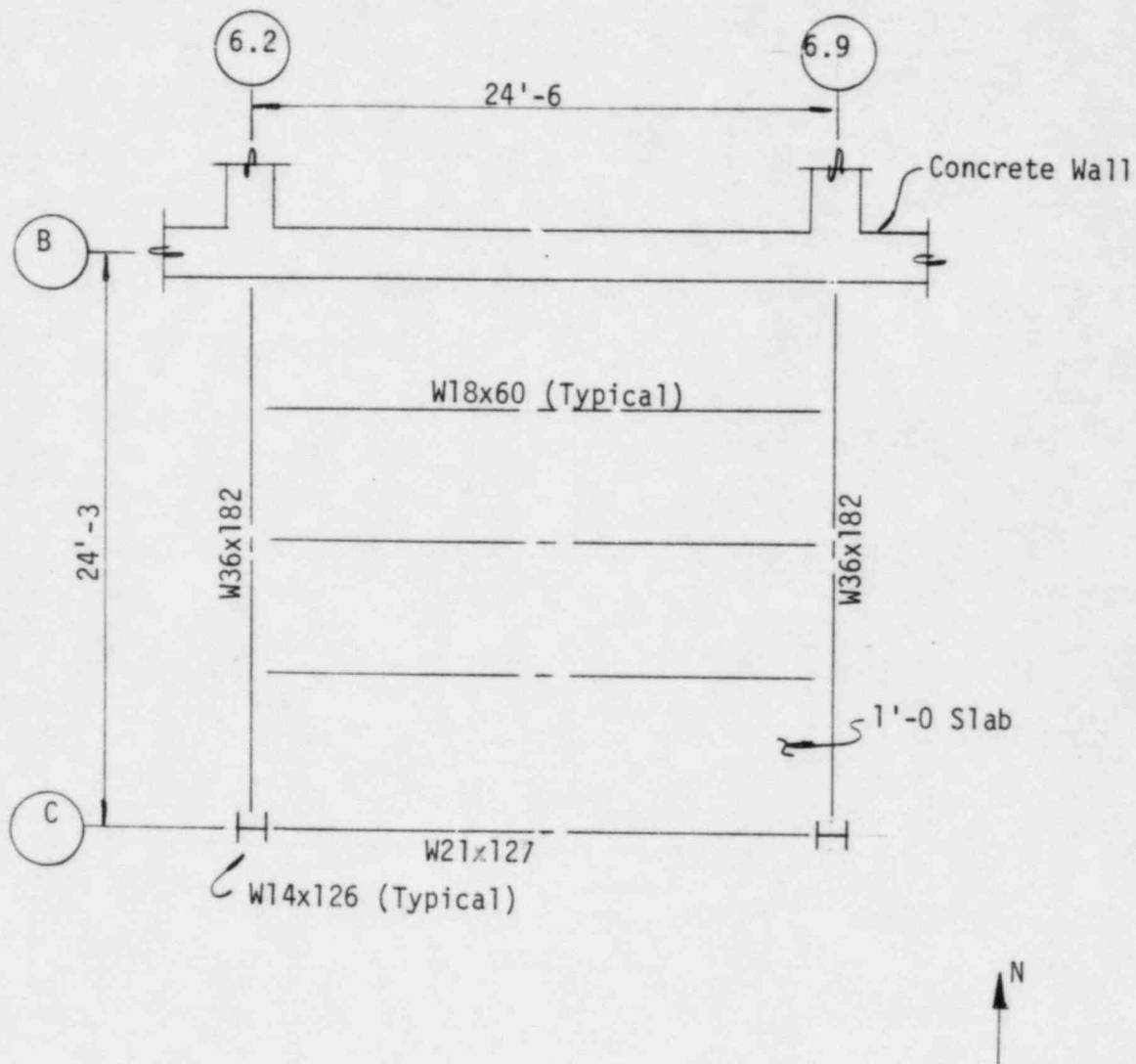


FIGURE A-2-3. AUXILIARY BUILDING FLOOR AT ELEVATION 614'-0

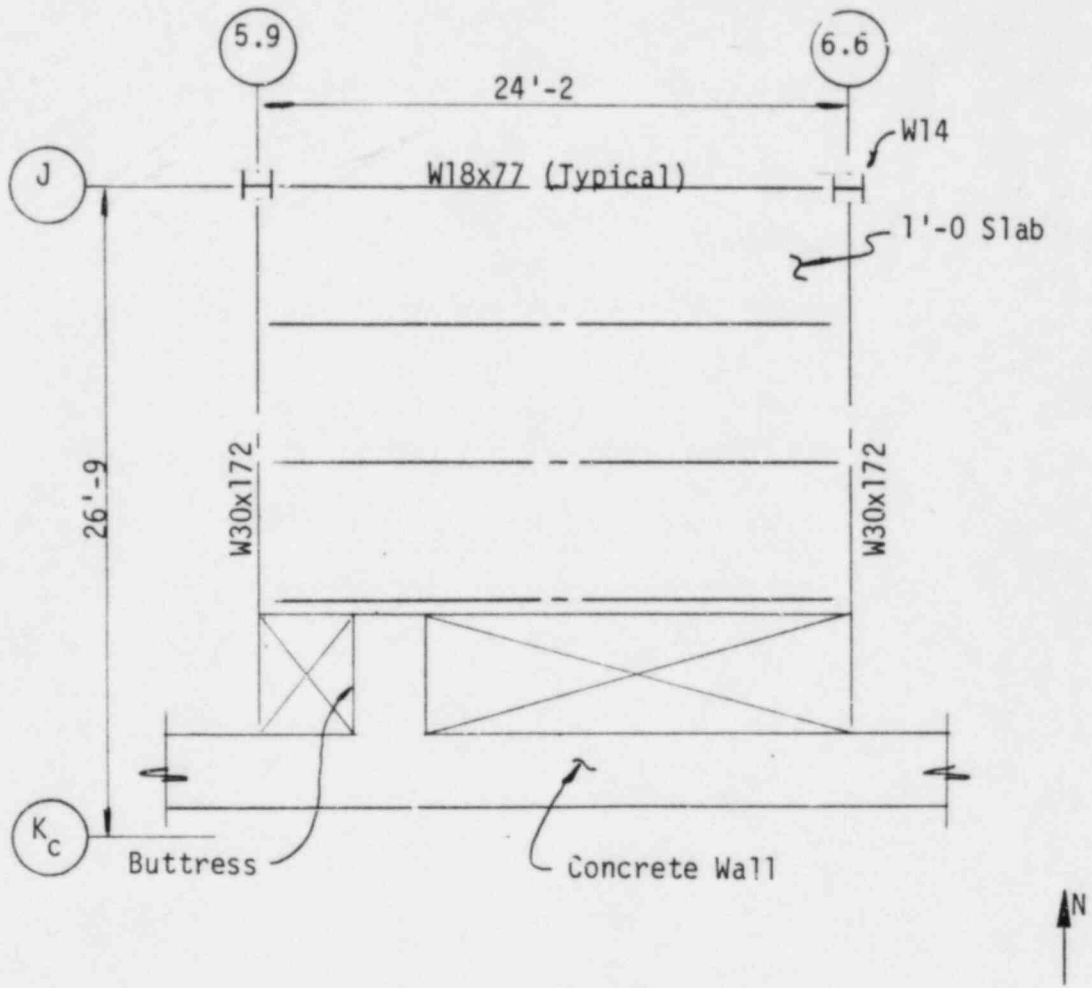


FIGURE A-2-4. AUXILIARY BUILDING FLOOR AT ELEVATION 646'-0"

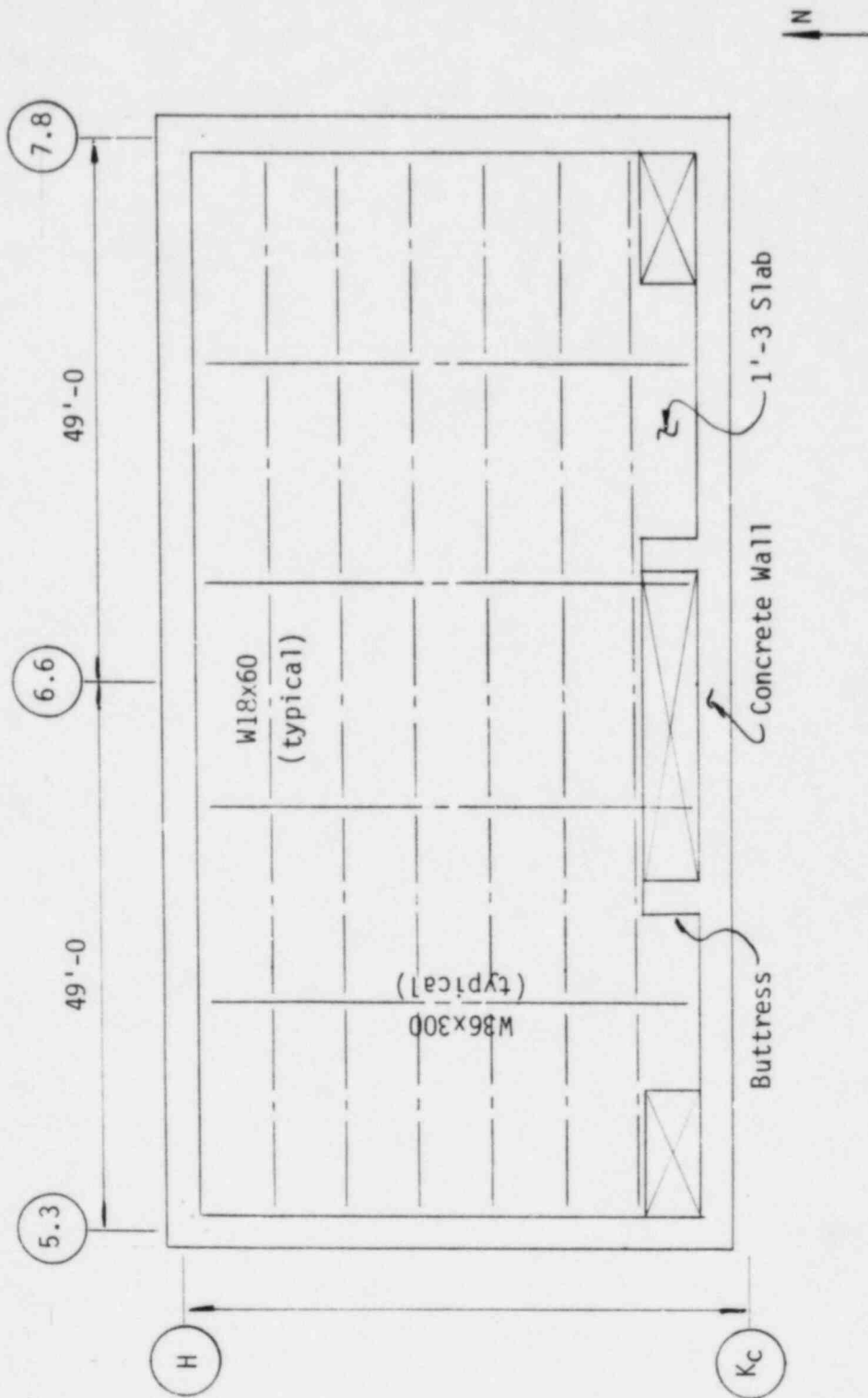


FIGURE A-2-5. AUXILIARY BUILDING FLOOR AT ELEVATION 685'-0

I-A-2-16

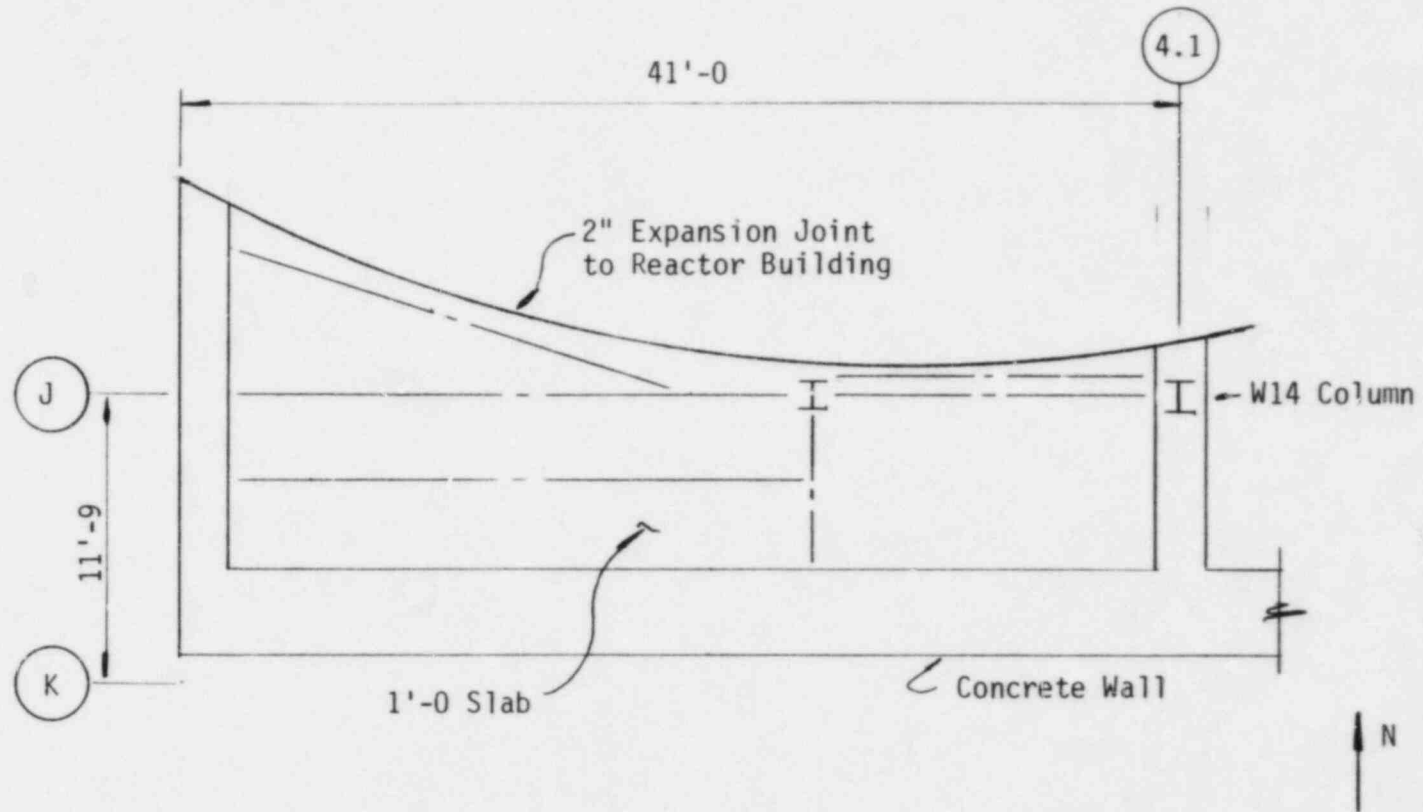


FIGURE A-2-6. AUXILIARY BUILDING FLOOR AT ELEVATION 642'-7 (WEST ELECTRICAL PENETRATION WING)

I-A-2-17

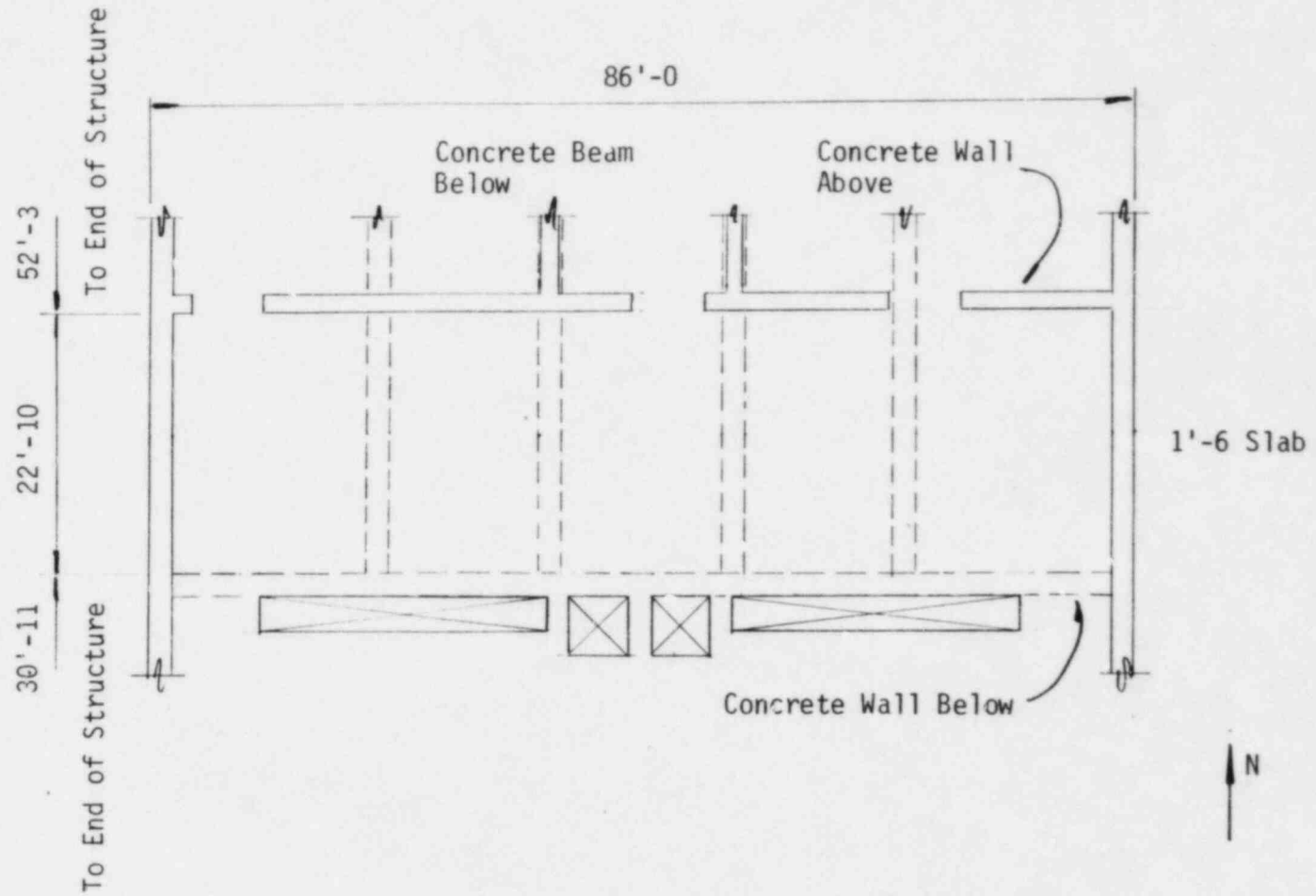
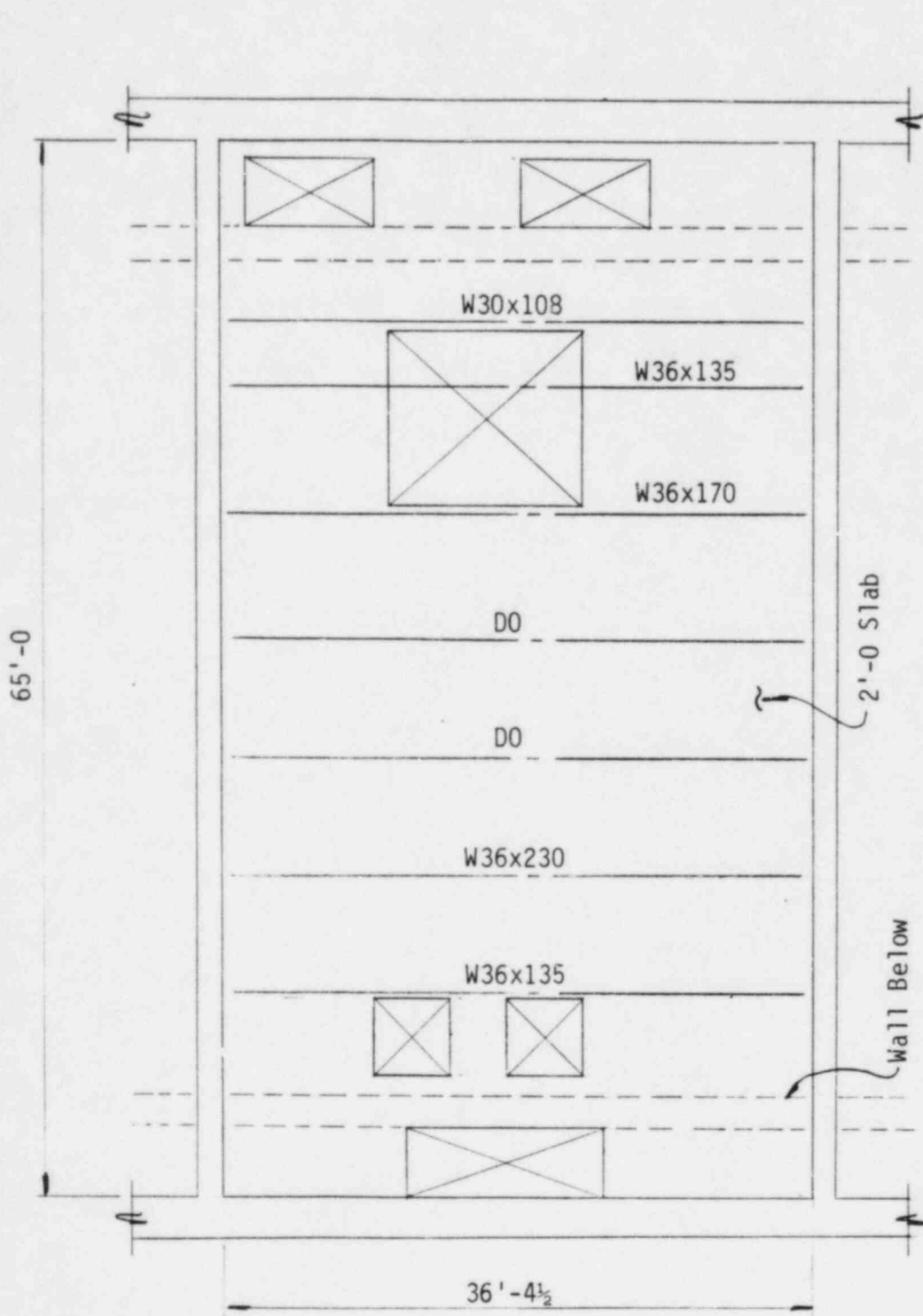


FIGURE A-2-7. SERVICE WATER PUMP STRUCTURE FLOOR
AT ELEVATION 634'-6



Note: Some walls and framing not shown for clarity.

FIGURE A-2-8. DIESEL GENERATOR BUILDING FLOOR AT ELEVATION 664'-0"

A-3. DEVELOPMENT OF VERTICAL IN-STRUCTURE RESPONSE SPECTRA INCLUDING FLOOR FLEXIBILITY

Fundamental vertical frequencies for each of the floors selected for study were calculated by finite element models as noted in Section A-2. To develop vertical in-structure response spectra including the effects of flexible floor vibration, single degree of freedom (SDOF) lumped mass models having the calculated vertical frequencies reported in Section A-2 were created. For the auxiliary building, these SDOF models were uncoupled from the structure. Seismic input consisted of vertical earthquake acceleration time-histories generated by the overall soil-structure dynamic analysis. Resulting seismic response of the SDOF models tuned to the derived slab frequencies were used to generate in-structure response spectra. The SDOF models for the service water pump structure and diesel generator building floors were included in the overall soil-structure models and vertical seismic response of the floors generated directly as a part of the overall structure dynamic analysis. This section reports the resulting response spectra when floor flexibility is included.

A-3.1 AUXILIARY BUILDING RESPONSE SPECTRA

The auxiliary building SDOF floor models were subjected to vertical acceleration time-histories generated by the overall soil-structure dynamic analysis for the upper bound soil case. The upper bound soil case is expected to cause the greatest amount of floor response since a larger portion of the structure mass participates at the higher frequencies which approach those of the floor panels. Four percent of critical damping, appropriate to reinforced concrete members responding at low stress levels, was assigned to the floors based on stresses predicted by the finite element models. The resulting uncoupled floor vertical acceleration time-histories were used to develop in-structure response spectra including floor flexibility at 2, 3, 4 and 7 percent equipment damping ratios. Response spectra not including floor flexibility were previously calculated from the acceleration time-histories generated by the overall soil-structure dynamic analysis.

For the floors described in Section A-2.2, the unbroadened vertical response spectra including floor flexibility are compared to the broadened spectra not including floor flexibility for the upper bound soil case at 2 and 7 percent equipment damping in Figures A-3-1 to A-3-5. The vertical spectra for 3 and 4 percent damping are not shown for clarity. The influence of the inclusion of floor flexibility is apparent from these comparisons. Spectral accelerations at equipment frequencies approaching the fundamental floor frequencies considering floor flexibility exceed those calculated when floor flexibility is neglected. The difference can be very significant when the floor frequencies are 11 or 14 Hz. The increase in spectral accelerations carries over through the higher frequency range of the response spectrum with at least some amplification in the Zero Period Acceleration (ZPA). Through the lower equipment frequency range, (less than about 5 Hz), the broadened spectra not including floor flexibility essentially envelopes the spectra with floor flexibility considered.

To provide a numerical comparison of the effect of floor flexibility on equipment response spectra, a vertical amplification factor (VAF) is defined:

$$\text{VAF} = \frac{\text{(Unbroadened spectral acceleration at frequency } f \text{ including floor flexibility)}}{\text{(Broadened spectral acceleration at frequency } f \text{ not including floor flexibility)}}$$

VAF's for the five auxiliary building floors evaluated in this study are listed in Tables A-3-1 to A-3-4 for 2, 3, 4, and 7 percent equipment damping ratios. For a particular floor, the maximum VAF occurs at the fundamental floor frequency with magnitudes as large as five for the 11 and 14 Hz floor frequency cases. The 11 and 14 Hz cases were selected as the floors most likely to exhibit significant amplification. The remaining floors throughout the structure are expected to show lower amplification. Values less than unity are due to broadening of the spectra not including floor flexibility. Maximum VAF's typically decrease as equipment damping increases.

As a part of the Seismic Margin Earthquake (SME) equipment evaluation, design response spectra at design damping levels developed by Bechtel for the Safe Shutdown Earthquake (SSE) are compared to response spectra developed for the SME at SME evaluation damping levels. For the auxiliary building floors included in this study, vertical SME response spectra including floor flexibility and enveloping all three soil cases are compared to SSE design spectra in Figures A-3-6 to A-3-10. The SME damping value depends on the component being analyzed and whether a code margin or failure margin evaluation is being conducted. However, it is appropriate to compare 0.5 and 1 percent SSE design spectra to 2 and 3 percent SME spectra and 2 percent SSE design spectra to 4 percent SME spectra. As shown in Figures A-3-6 to A-3-10, the SSE design spectra generally envelope corresponding SME spectra. However, SME spectra including floor flexibility may significantly exceed the SSE design spectra at equipment frequencies approaching the fundamental floor frequencies. This is especially true for the 11 and 14 Hz floor frequency cases.

Based on the results of this study, it is apparent that the effects of floor flexibility should be incorporated in the vertical response spectra used in the SME equipment evaluation. One manner in which this can be conservatively accomplished is by increasing the vertical response spectra which do not include floor flexibility by an envelope VAF function for floor slab frequencies in excess of 14 Hz. For a given equipment frequency and damping, the envelope VAF is defined as the maximum VAF predicted by the results of this study. The envelope VAF is a maximum at the center of the slab and unity at the vertical supports. At intermediate locations, it is assumed to vary sinusoidally to conservatively account for amplifications due to higher modes.

Due to the likely existence of floor slabs having fundamental frequencies in the 15 Hz to 30 Hz range, additional SDOF models having frequencies of 20 Hz and 25 Hz were created and subjected to the acceleration time-histories at Elevation 614'-0" of the main auxiliary building

and Elevation 685'-0 of the control tower. Calculated VAF's for these cases are listed in Tables A-3-5 to A-3-8. Based on the VAF's compiled in Tables A-3-1 to A-3-8, the envelope VAF functions presented in Figure A-3-11 for 2, 3, 4, and 7 percent equipment damping were developed. These functions were broadened by 10 percent consistent with the development of response spectra for the SME evaluation. Some of the amplitudes were conservatively adjusted to simplify the envelope VAF function shapes for application. In addition, because of the unique conditions of the floor at Elevation 685'-0" of the control tower, the 11 Hz frequency is not expected to occur at any other floor panel in the structure. The amplifications for this case were not included in developing the envelope VAF functions.

If the fundamental frequency of a particular floor panel is known, some of the conservatism inherent in the use of the envelope VAF's plotted in Figure A-3-11 can be eliminated. Based on the data listed in Tables A-3-1 to A-3-8, envelope VAF's can be determined as a function of fundamental floor frequency as shown in Figures A-3-12 to A-3-14 for 14 Hz, 20 Hz, and 25 Hz frequencies. The envelope VAF function shapes were derived similar to those on Figure 3-11 as noted above.

Based on the results of this study, the following approach will be used to define vertical in-structure response spectra for use in the SME auxiliary building equipment evaluation:

1. For equipment not mounted at the locations noted in 2 and 3 below:
 - a. The maximum VAF as a function of equipment frequency and damping will be taken from Figure A-3-11.

$VAF_m(f, \beta) =$ Maximum VAF from Figure A-3-11

$f =$ Equipment frequency

$\beta =$ Equipment damping

- b. Since this maximum VAF is applicable only for equipment at the center of the floor, a reduction accounting for the actual equipment location will be taken.

$$VAF'_m(f, \beta) = [VAF_m(f, \beta) - 1] \sin \frac{\pi x}{L_x} \sin \frac{\pi y}{L_y} + 1$$

x, y = Distances in the two horizontal directions from the equipment to the vertical supports

L_x, L_y = Total floor spans between vertical supports

- c. Equipment will be evaluated using the maximum vertical response spectra including floor flexibility.

$S_{am}'(f, \beta)$ = Maximum vertical spectral acceleration including floor flexibility

$$= S_a(f, \beta) VAF'_m(f, \beta)$$

$S_a(f, \beta)$ = Spectral acceleration not including floor flexibility (generated from the acceleration time-history from the auxiliary building dynamic analysis).

- d. For equipment not meeting the acceptance criteria under the modified vertical spectrum $S_{am}'(f, \beta)$, the actual fundamental floor frequency will be calculated. The envelope VAF function can then be determined from Figures A-3-12 to A-3-14, depending on the floor frequency.

$VAF(f, \beta, F)$ = VAF from Figures A-3-12 to A-3-14, depending on the actual floor frequency

F = Actual fundamental floor frequency

- e. The VAF function accounting for actual floor frequency will then be reduced to account for equipment location as in b above.

$$VAF'(f, \beta, F) = [VAF(f, \beta, F) - 1] \sin \frac{\pi x}{L_x} \sin \frac{\pi y}{L_y} + 1$$

- f. Equipment will then be evaluated using the vertical response spectrum including the actual floor frequency.

$$S_a'(f, \beta, F) = S_a(f, \beta) VAF'(f, \beta, F)$$

2. For equipment mounted at Elevation 685'-0" of the control tower:

- a. Since the 11 Hz frequency of this floor is not expected to occur at any other floor, its amplifications were not included in Figure A-3-11. Equipment mounted on this floor can be evaluated using the broadened spectra including floor flexibility plotted in Figure A-3-9, with a reduction accounting for equipment location as in Step 1b above.

$S_a(f, \beta) =$ Spectral acceleration including floor flexibility and equipment location

$$= \left[S_{am}(f, \beta) - S_a(f, \beta) \right] \sin \frac{\pi x}{L_x}$$

$$\sin \frac{\pi y}{L_y} + S_a(f, \beta)$$

$S_{am}(f, \beta) =$ Maximum spectral acceleration including floor flexibility (from Figure A-3-9)

$S_a(f, \beta) =$ Spectral acceleration not including floor flexibility

3. For equipment mounted in the penetration wings:

- a. The 29 Hz fundamental frequency calculated for Elevation 642'-7" is expected to be the lowest occurring in the penetration wings. As noted in Tables A-3-1 to A-3-4, this case exhibits little amplification. Vertical amplification of the response spectra in the penetration wings can therefore be neglected.

A-3.2 SERVICE WATER PUMP STRUCTURE RESPONSE SPECTRA

For the Service Water Pump Structure (SWPS), the lumped mass model for the vertical response of the floor at Elevation 634'-6 was included in the overall soil-structure model. Model properties consisted of the effective modal mass for the fundamental floor mode as calculated by the finite element analysis and a vertical stiffness corresponding to the fundamental floor frequency of 25 Hz and the given mass. Mass included in the SDOF floor model was deducted from the vertical mass of the structure model at Elevation 634'-6 to preserve the total mass at

this location. Material damping of four percent of critical, appropriate to reinforced concrete members responding at low stress levels, was assigned to the vertical floor vibration. Vertical acceleration time-histories were generated by the overall soil-structure dynamic analysis for all three soil conditions at the floor mass and the structure mass to which the floor model was attached. In-structure response spectra at 2, 3, 4, and 7 percent equipment damping including floor flexibility were generated using the acceleration time-histories at the floor model mass while spectra not including floor flexibility were generated using the acceleration time-histories at the structure mass.

Unbroadened vertical response spectra including floor flexibility are compared to broadened spectra not including floor flexibility for 2 and 7 percent equipment damping in Figure A-3-15 for the upper bound soil case. Vertical amplification factors, as defined in Section A-3.1, of approximately 2.2 and 1.6 for 2 and 7 percent equipment damping, respectively, occur near the fundamental floor frequency. The VAF's decrease from these maximum values towards the low frequency end to unity at an equipment frequency of about 10 Hz. Towards the higher frequencies, the VAF's decrease from the maximum to a value of 1.0 at the ZPA. The maximum values and variation of the VAF's appear to be reasonably consistent with results for auxiliary building floors having frequencies of 25 Hz (See Figure A-3-14).

SSE design spectra at design damping values are compared to broadened SME spectra at SME evaluation damping values including floor flexibility in Figure A-3-16. It is seen that the SME spectra including floor flexibility exceed the SSE design spectra over a frequency range of approximately 15 to 27 Hz. This can be attributed to the increase in response near the fundamental floor frequency of 25 Hz.

Much of the safety-related equipment in the SWPS is located on the floor evaluated in this study. Other equipment is typically mounted on or adjacent to walls and are expected to show little vertical amplification. The in-structure response spectra including floor

flexibility in Figure A-3-16 are appropriate for equipment located near the center of the floor panel while the response spectra not including floor flexibility are appropriate for equipment located adjacent to the rigid vertical supports. As a conservative first step, all equipment at this floor can be evaluated using the response spectra including floor flexibility in Figure A-3-16 since these spectra contain the maximum vertical amplifications. For equipment not meeting the acceptance criteria based on these conservative spectra, spectral accelerations accounting for actual equipment location can be calculated using the interpolation procedure described in Section A-3.1 for Elevation 685'-0 of the control tower.

A-3.3 DIESEL GENERATOR BUILDING RESPONSE SPECTRA

For the diesel generator building, the lumped mass model of the floor at Elevation 664'-0 was included in the overall soil-structure model. Derivation of the model properties for the 17 Hz fundamental floor frequency and generation of the in-structure response spectra including floor flexibility were performed similar to the service water pump structure floor as described in Section A-3.2.

Unbroadened vertical response spectra including floor flexibility are compared to broadened spectra not including floor flexibility for 2 and 7 percent equipment damping in Figure A-3-17. This comparison is made for response spectra generated by the diesel generator building upper bound soil base model giving the highest equipment response at frequencies near that of the floor (See Section A-4.2 for description of different diesel generator building models). Maximum vertical amplification factors of approximately 2.4 and 1.6 for 2 and 7 percent damping, respectively, occur near the fundamental floor frequency. The VAF's decrease down to unity towards the low frequency end of the response spectra at an equipment frequency of approximately 3 Hz. Towards the higher frequencies, the VAF's decrease to a value of 1.1 at the ZPA. The VAF's appear to be reasonably consistent with results for the auxiliary building floors with fundamental frequencies approaching the 17 Hz

frequency for this floor. SSE design spectra at design damping values are compared to the broadened SME spectra including floor flexibility at SME damping values in Figure A-3-18.

Much of the safety-related equipment in the diesel generator building is attached to slabs or concrete pedestals bearing directly on the soil. This equipment is expected to experience no vertical amplification. Any other safety-related equipment is located on the floor evaluated in this study. Equipment mounted at the center of this floor can be analyzed using the response spectra including floor flexibility shown in Figure A-3-18. Response spectra not including floor flexibility are applicable to equipment mounted on or near the walls. Spectral accelerations for equipment mounted at intermediate locations on the floor can be determined using the equation presented in Section A-3.2.

TABLE A-3-1

AUXILIARY BUILDING VERTICAL AMPLIFICATION FACTORS2% Equipment Damping

Location	Floor Frequency (Hz)	Equipment Frequency							
		5 Hz	8 Hz	11 Hz	14 Hz	20 Hz	25 Hz	29 Hz	33 Hz
El. 584'-0", Main Auxiliary Bldg.	35	1.0	0.89	0.96	0.79	0.95	1.1	1.3	1.6
El. 614'-0", Main Auxiliary Bldg.	14	1.1	1.3	2.3	5.2	1.9	1.8	1.9	1.8
El. 646'-0", Control Tower	14	1.2	1.1	1.8	3.4	1.1	1.3	1.4	1.4
El. 685'-0", Control Tower	11	1.3	1.7	5.0	2.1	1.6	2.0	2.0	2.0
El. 642'-7", West Penetration Wing	29	1.0	0.96	0.87	1.1	0.98	1.1	1.3	1.1

I-A-3-10

TABLE A-3-2

AUXILIARY BUILDING VERTICAL AMPLIFICATION FACTORS

3% Equipment Damping

Location	Floor Frequency (Hz)	Equipment Frequency							
		5 Hz	8 Hz	11 Hz	14 Hz	20 Hz	25 Hz	29 Hz	33 Hz
El. 584'-0", Main Auxiliary Bldg.	35	0.99	0.83	0.99	0.79	0.96	1.1	1.3	1.6
El. 614'-0", Main Auxiliary Bldg.	14	1.1	1.2	2.4	4.5	1.9	1.8	1.9	1.8
El. 646'-0", Control Tower	14	1.1	1.1	1.8	2.9	1.1	1.3	1.4	1.4
El. 685'-0", Control Tower	11	1.2	1.5	4.8	2.3	1.7	2.0	2.0	2.0
El. 642'-7", West Penetration Wing	29	1.0	0.88	0.92	1.0	0.99	1.1	1.2	1.1

I-A-3-11

TABLE A-3-3

AUXILIARY BUILDING VERTICAL AMPLIFICATION FACTORS4% Equipment Damping

Location	Floor Frequency (Hz)	Equipment Frequency							
		5 Hz	8 Hz	11 Hz	14 Hz	20 Hz	25 Hz	29 Hz	33 Hz
El. 584'-0", Main Auxiliary Bldg.	35	0.98	0.85	1.0	0.79	0.97	1.1	1.2	1.5
El. 614'-0", Main Auxiliary Bldg.	14	1.1	1.2	2.4	4.0	2.0	1.9	1.9	1.8
El. 646'-0", Control Tower	14'	1.1	1.0	1.8	2.6	1.2	1.3	1.4	1.4
El. 685'-0", Control Tower	11	1.2	1.6	4.6	2.4	1.7	2.0	2.0	2.1
El. 642'-7", West Penetration Wing	29	1.0	0.86	0.94	1.0	1.0	1.1	1.2	1.1

I-A-3-12

TABLE A-3-4

AUXILIARY BUILDING VERTICAL AMPLIFICATION FACTORS7% Equipment Damping

Location	Floor Frequency (Hz)	Equipment Frequency							
		5 Hz	8 Hz	11 Hz	14 Hz	20 Hz	25 Hz	29 Hz	33 Hz
El. 584'-0", Main Auxiliary Bldg.	35	0.97	1.0	1.1	0.78	1.0	1.1	1.2	1.3
El. 614'-0", Main Auxiliary Bldg.	14	1.1	1.4	2.4	3.3	2.1	1.9	1.9	1.8
El. 646'-0", Control Tower	14	1.1	1.3	1.7	2.2	1.2	1.4	1.4	1.4
El. 685'-0", Control Tower	11	1.3	1.9	4.0	2.7	1.9	2.0	2.1	2.1
El. 642'-7", West Penetration Wing	29	1.0	1.0	0.96	1.1	1.1	1.1	1.1	1.1

I-A-3-13

TABLE A-3-5

ADDITIONAL AUXILIARY BUILDING VERTICAL AMPLIFICATION FACTORS2% Equipment Damping

Location	Assumed Floor Frequency (Hz)	Equipment Frequency							
		5 Hz	8 Hz	11 Hz	14 Hz	20 Hz	25 Hz	29 Hz	33 Hz
El. 614'-0", Main Auxiliary Bldg.	20	1.1	0.99	1.2	1.2	2.5	1.3	1.3	1.2
El. 685'-0", Control Tower	20	1.1	0.95	1.0	0.98	2.8	1.5	1.3	1.3
El. 614'-0", Main Auxiliary Bldg.	25	1.0	0.93	1.1	0.91	1.2	1.6	1.1	1.1
El. 685'-0", Control Tower	25	1.0	0.90	0.91	0.38	1.2	1.8	1.2	1.1

I-A-3-14

TABLE A-3-6

ADDITIONAL AUXILIARY BUILDING VERTICAL AMPLIFICATION FACTORS3% Equipment Damping

Location	Assumed Floor Frequency (Hz)	Equipment Frequency							
		5 Hz	8 Hz	11 Hz	14 Hz	20 Hz	25 Hz	29 Hz	33 Hz
El. 614'-0", Main Auxiliary Bldg.	20	1.0	0.92	1.3	1.1	2.2	1.3	1.3	1.2
El. 685'-0", Control Tower	20	1.0	0.89	1.1	1.0	2.4	1.5	1.4	1.3
El. 614'-0", Main Auxiliary Bldg.	25	1.0	0.87	1.1	0.91	1.2	1.6	1.1	1.1
El. 685'-0", Control Tower	25	1.0	0.97	0.95	0.89	1.2	1.7	1.2	1.1

I-A-3-15

TABLE A-3-7

ADDITIONAL AUXILIARY BUILDING VERTICAL AMPLIFICATION FACTORS

4% Equipment Damping

Location	Assumed Floor Frequency (Hz)	Equipment Frequency							
		5 Hz	8 Hz	11 Hz	14 Hz	20 Hz	25 Hz	29 Hz	33 Hz
El. 614'-0", Main Auxiliary Bldg.	20	1.0	0.92	1.3	1.1	2.1	1.3	1.3	1.2
El. 685'-0", Control Tower	20	1.0	0.87	1.1	1.0	2.1	1.5	1.4	1.3
El. 614'-0", Main Auxiliary Bldg.	25	1.0	0.87	1.1	0.90	1.2	1.5	1.1	1.1
El. 685'-0", Control Tower	25	1.0	0.82	0.97	0.90	1.2	1.6	1.2	1.1

I-A-3-16

TABLE A-3-8

ADDITIONAL AUXILIARY BUILDING VERTICAL AMPLIFICATION FACTORS7% Equipment Damping

Location	Assumed Floor Frequency (Hz)	Equipment Frequency							
		5 Hz	8 Hz	11 Hz	14 Hz	20 Hz	25 Hz	29 Hz	33 Hz
El. 614'-0", Main Auxiliary Bldg.	20	1.0	1.1	1.3	0.99	1.7	1.4	1.3	1.2
El. 685'-0", Control Tower	20	1.1	1.1	1.1	1.1	2.0	1.5	1.4	1.3
El. 614'-0", Main Auxiliary Bldg.	25	0.99	1.1	1.1	0.87	1.2	1.3	1.1	1.1
El. 685'-0", Control Tower	25	1.0	1.0	1.0	0.96	1.2	1.4	1.2	1.1

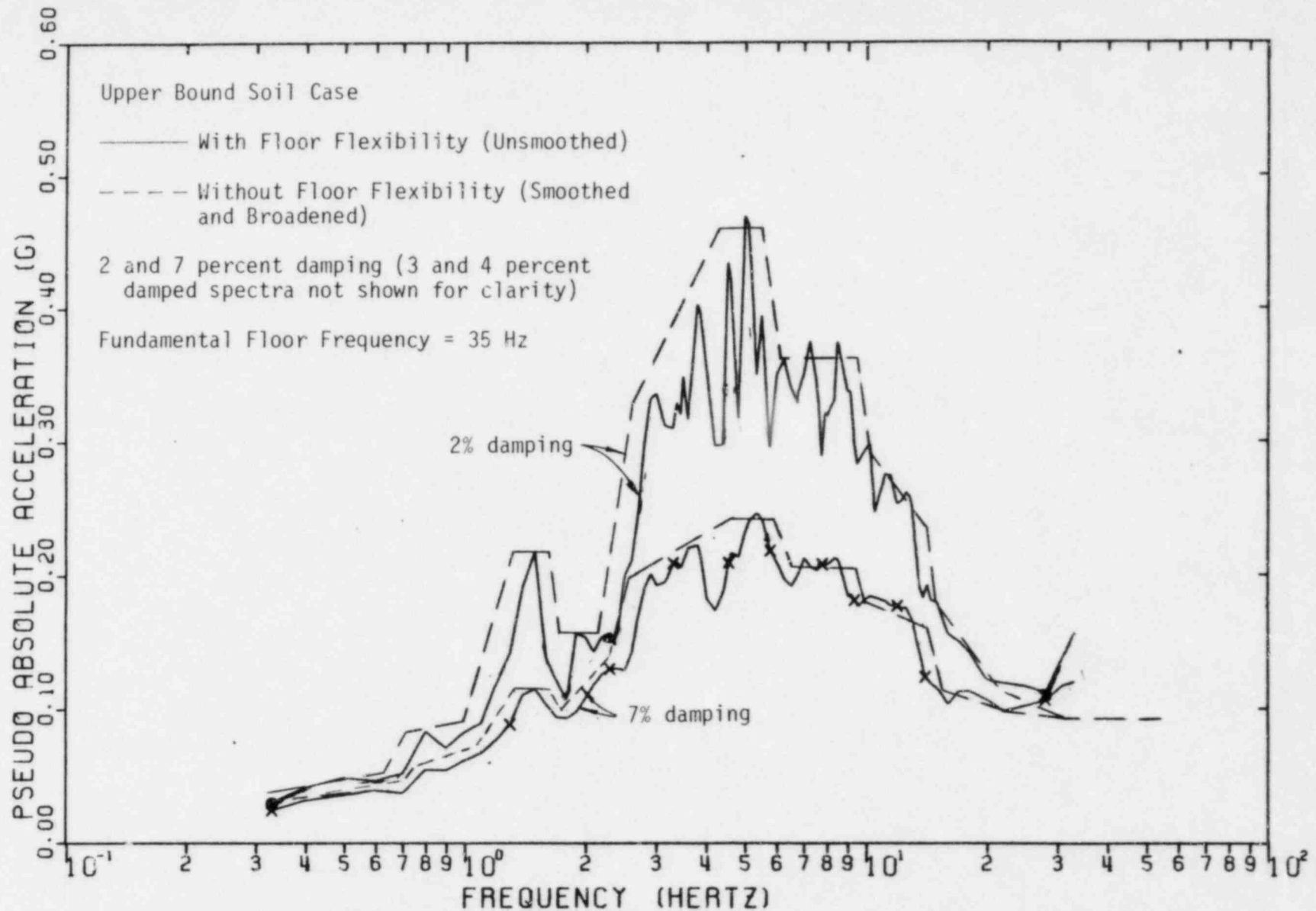


FIGURE A-3-1. COMPARISON OF VERTICAL SPECTRA WITH AND WITHOUT FLOOR FLEXIBILITY AT ELEVATION 584'-0", MAIN AUXILIARY BUILDING

I-A-3-19

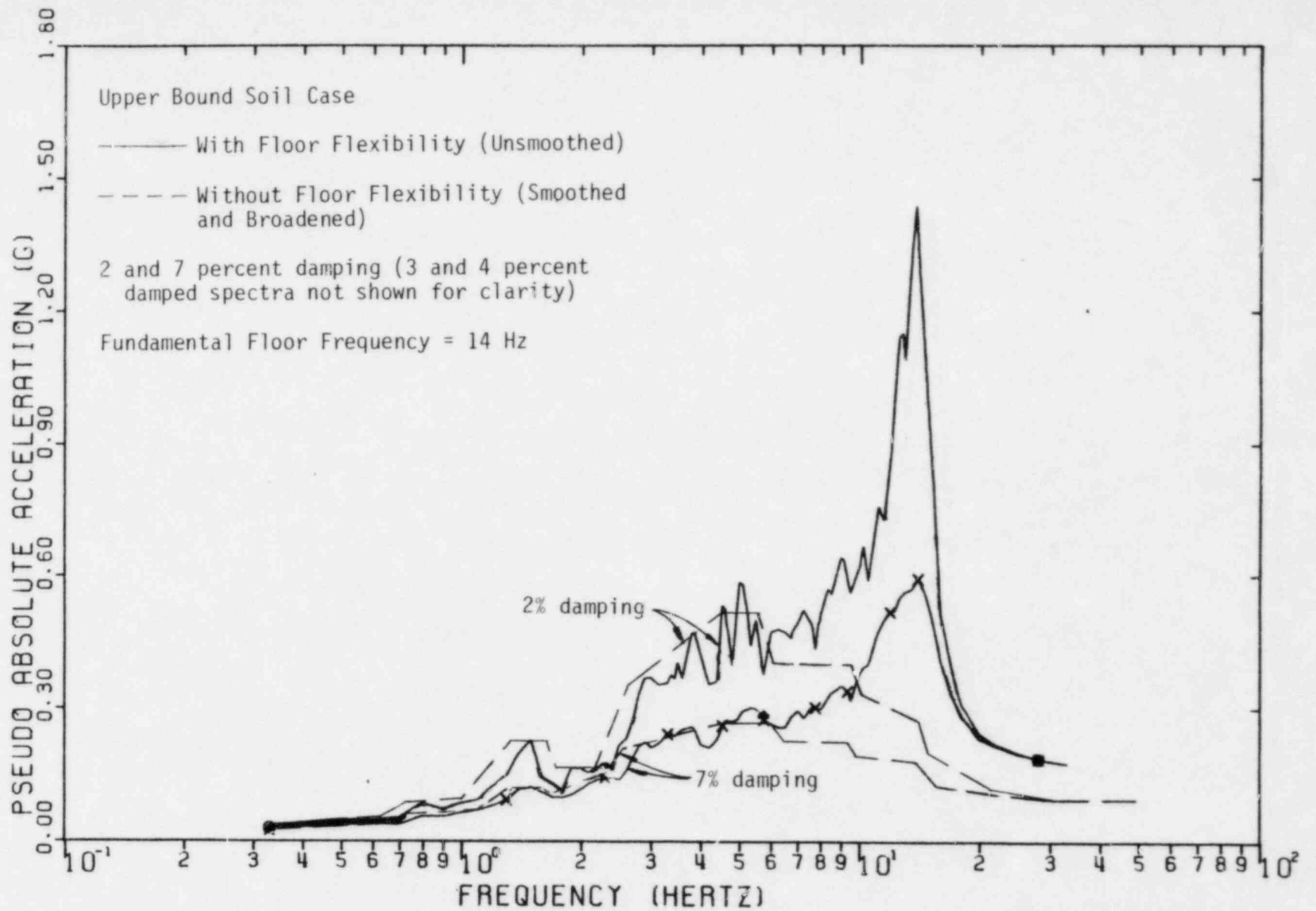


FIGURE A-3-2. COMPARISON OF VERTICAL SPECTRA WITH AND WITHOUT FLOOR FLEXIBILITY AT ELEVATION 614'-0", MAIN AUXILIARY BUILDING

I-A-3-20

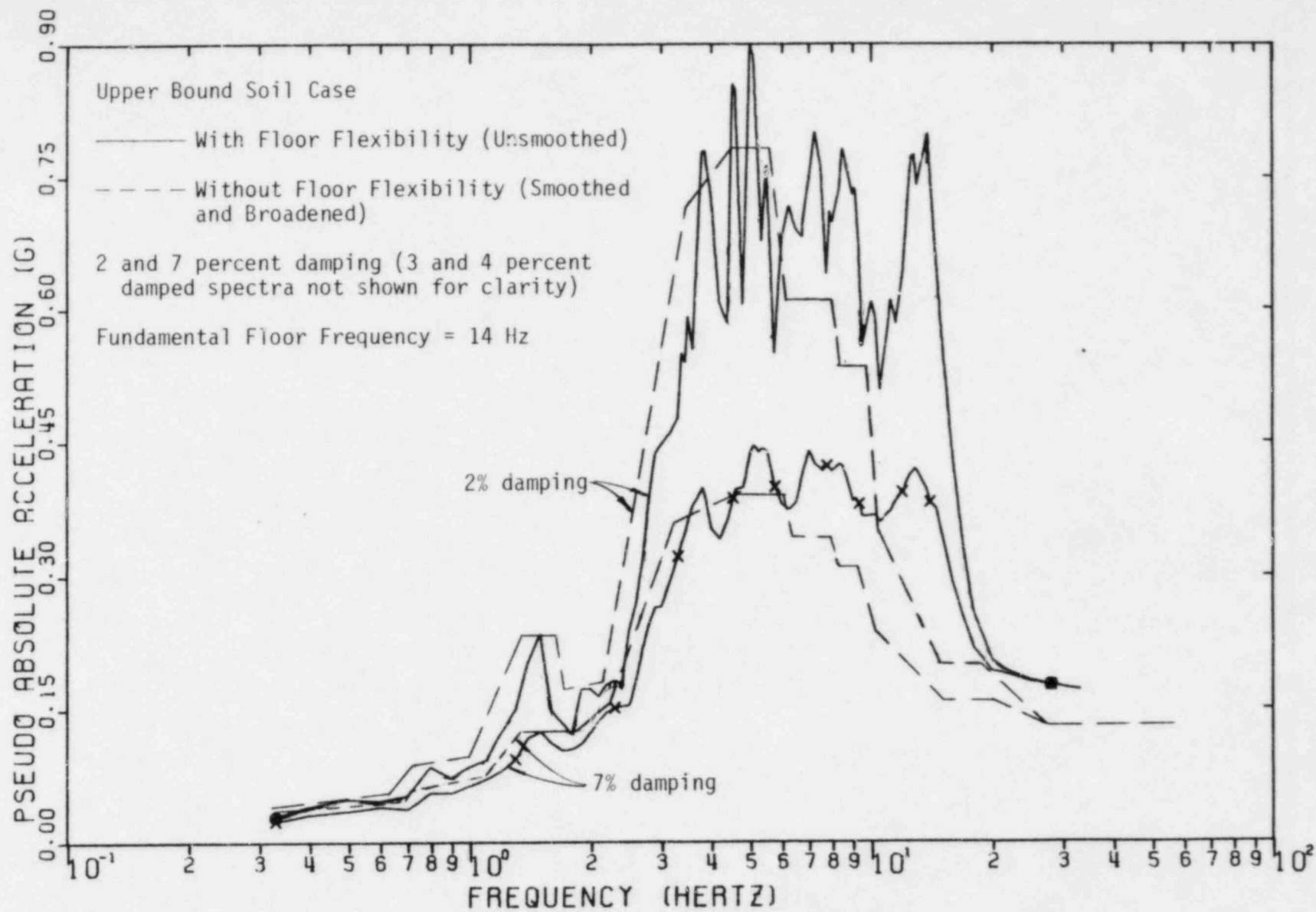


FIGURE A-3-3. COMPARISON OF VERTICAL SPECTRA WITH AND WITHOUT FLOOR FLEXIBILITY AT ELEVATION 646'-0", CONTROL TOWER

I-A-3-21

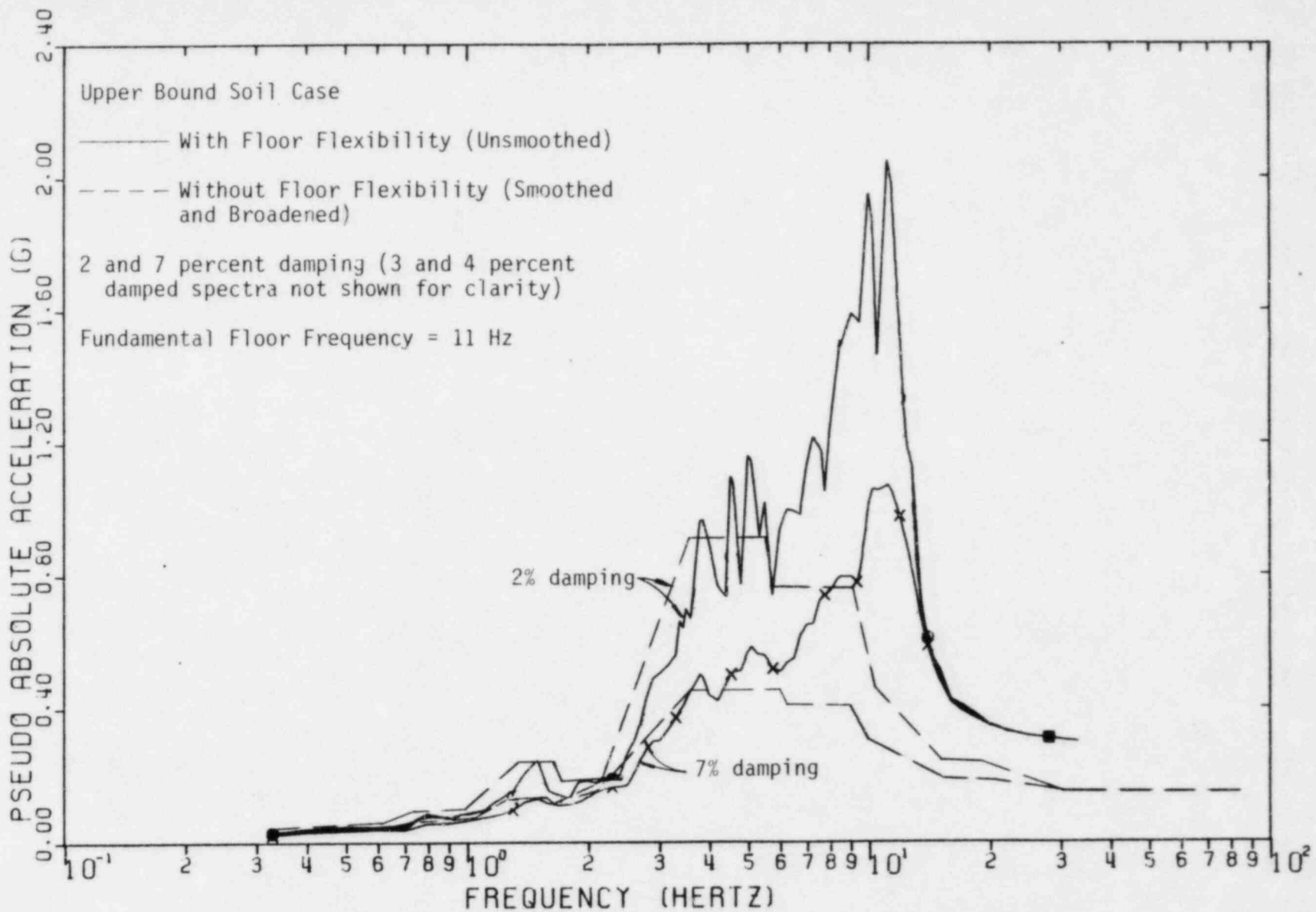


FIGURE A-3-4. COMPARISON OF VERTICAL SPECTRA WITH AND WITHOUT FLOOR FLEXIBILITY AT ELEVATION 685'-0", CONTROL TOWER

I-A-3-22

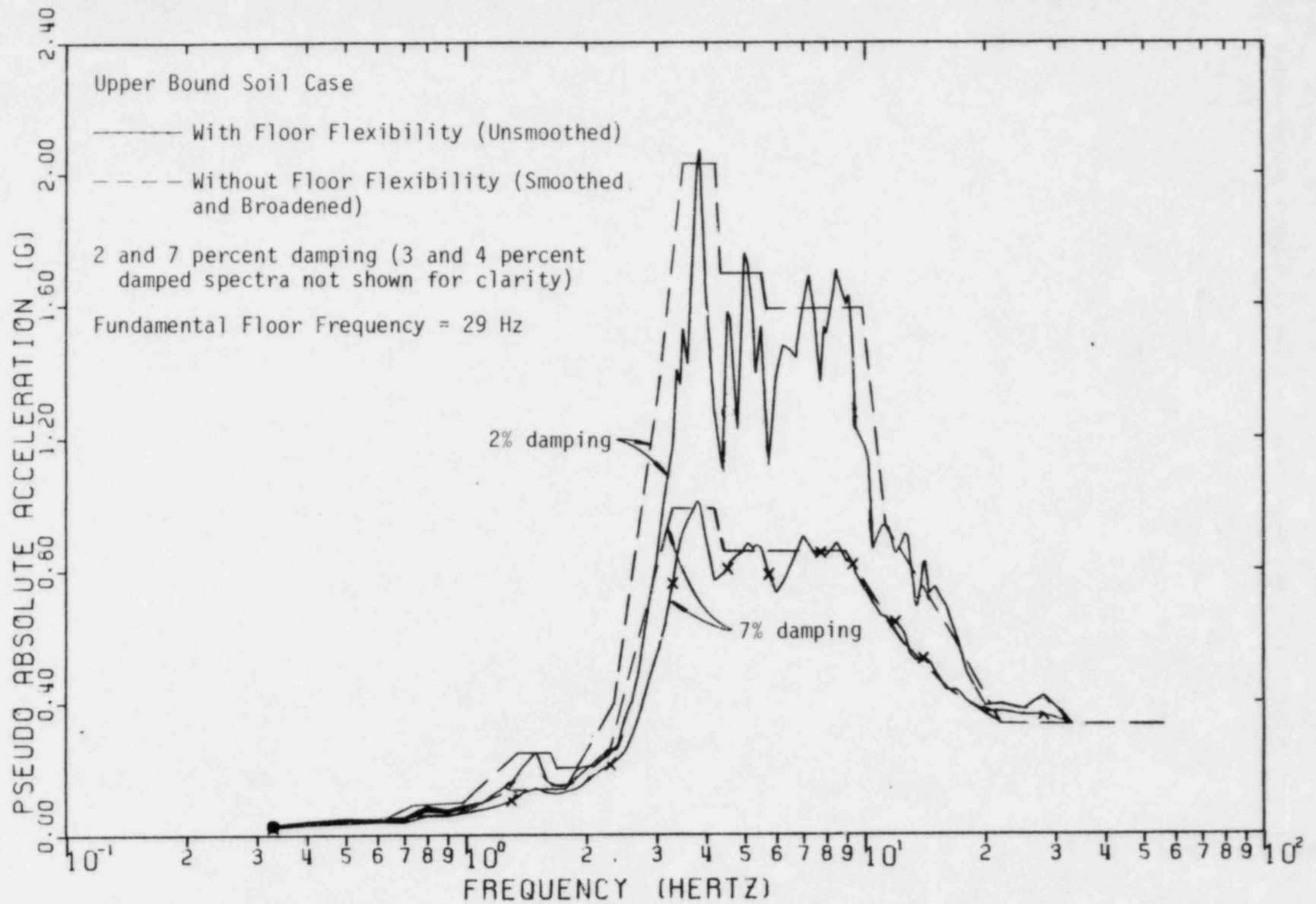


FIGURE A-3-5. COMPARISON OF VERTICAL SPECTRA WITH AND WITHOUT FLOOR FLEXIBILITY AT ELEVATION 642'-7", PENETRATION WING

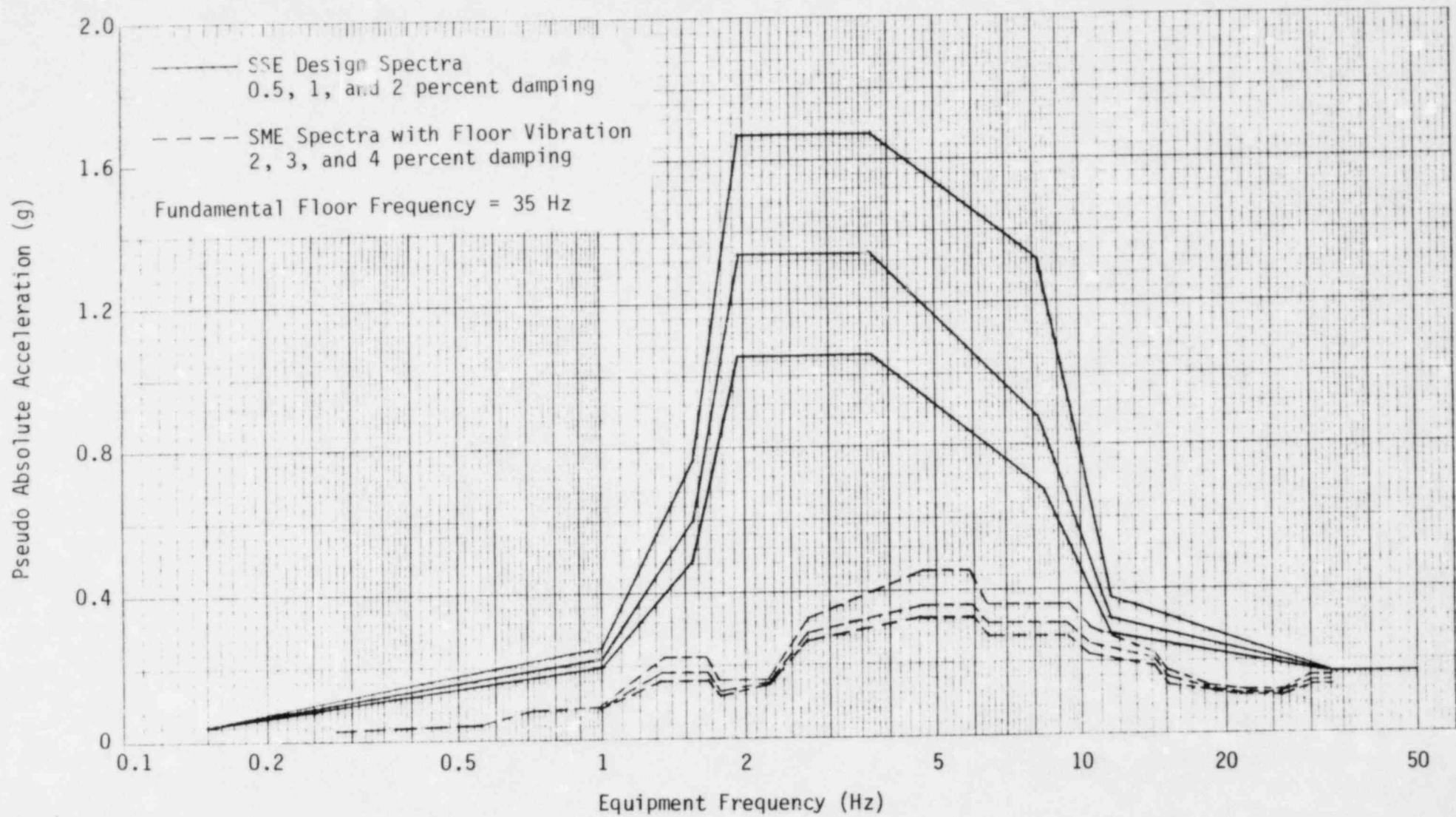


FIGURE A-3-6. COMPARISON OF SSE DESIGN AND SME VERTICAL SPECTRA AT ELEVATION 584'-0", MAIN AUXILIARY BUILDING

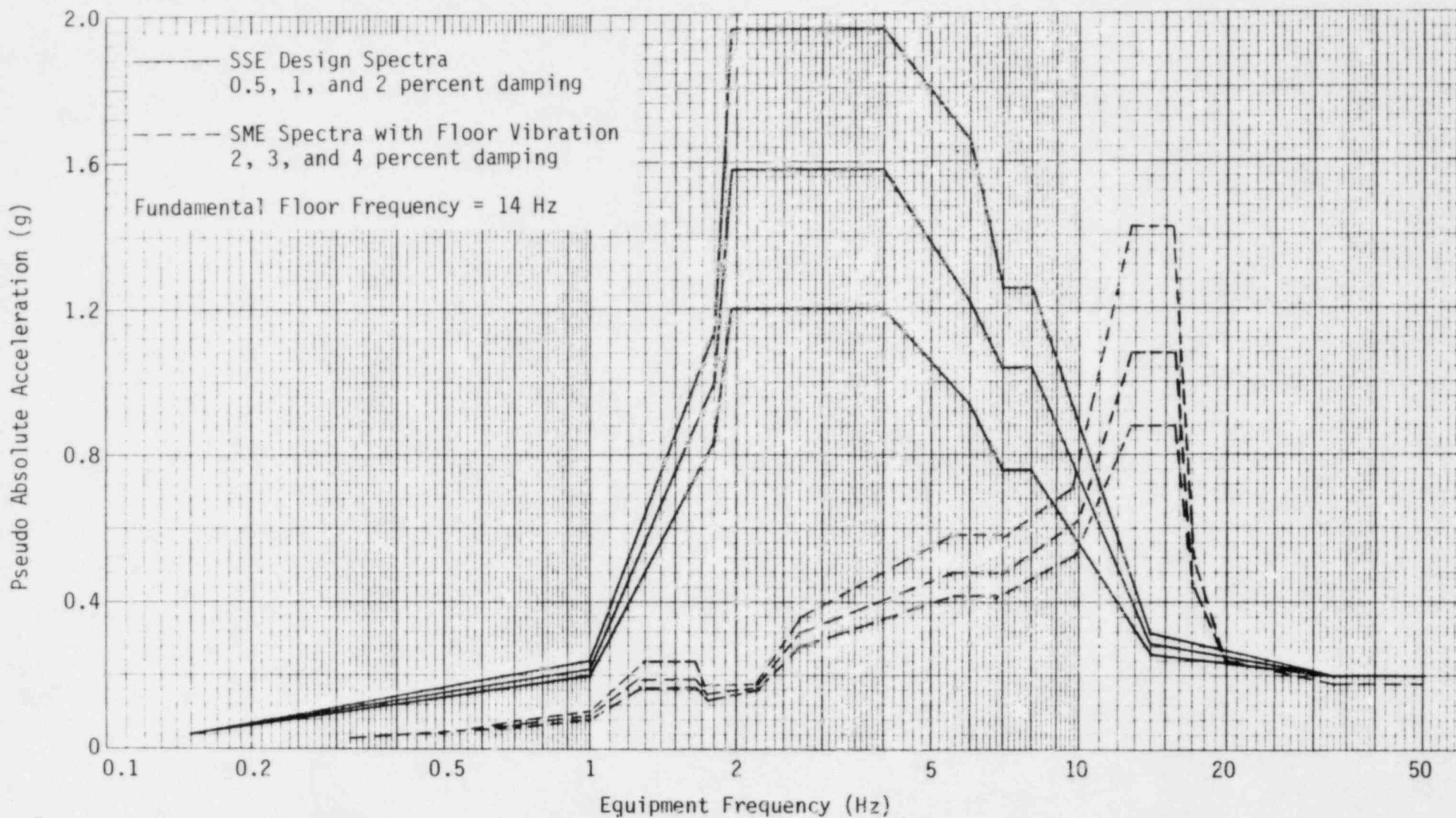


FIGURE A-3-7. COMPARISON OF SSE DESIGN AND SME VERTICAL SPECTRA AT ELEVATION 614'-0", MAIN AUXILIARY BUILDING

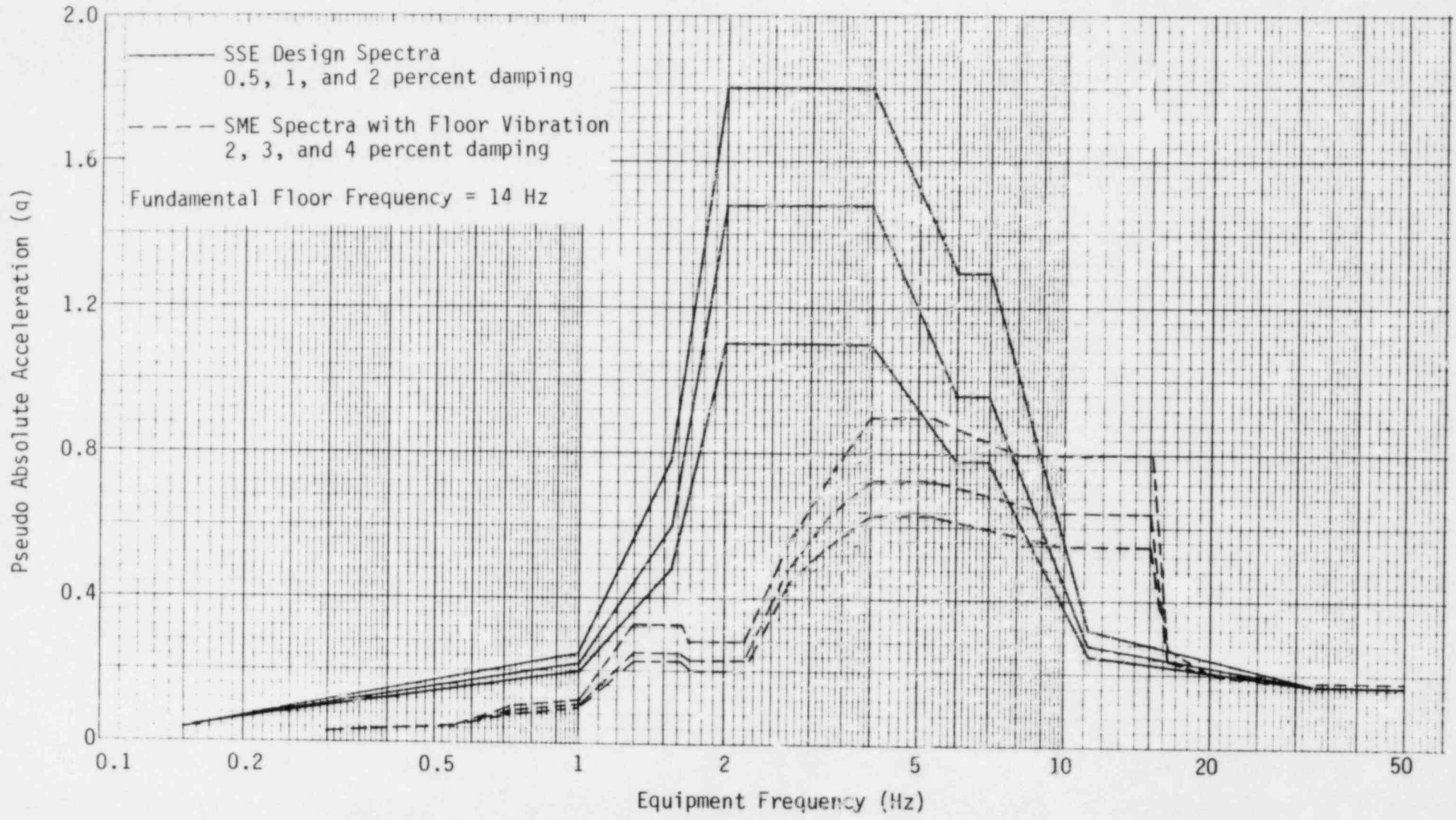


FIGURE A-3-8. COMPARISON OF SSE DESIGN AND SME VERTICAL SPECTRA AT ELEVATION 646'-0", CONTROL TOWER

I-A-3-25

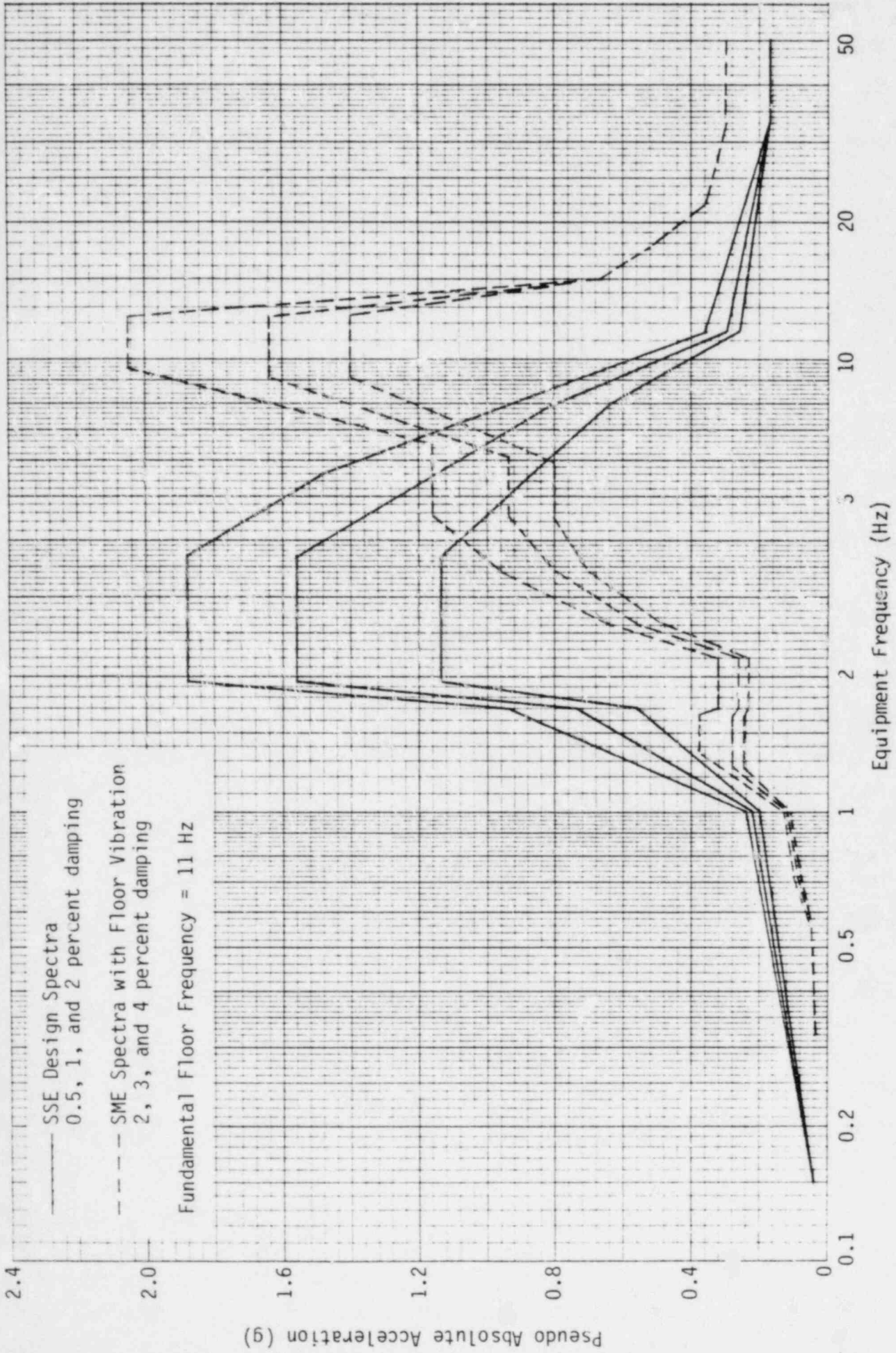


FIGURE A-3-9. COMPARISON OF SSE DESIGN AND SME VERTICAL SPECTRA AT ELEVATION 685'-0", CONTROL TOWER

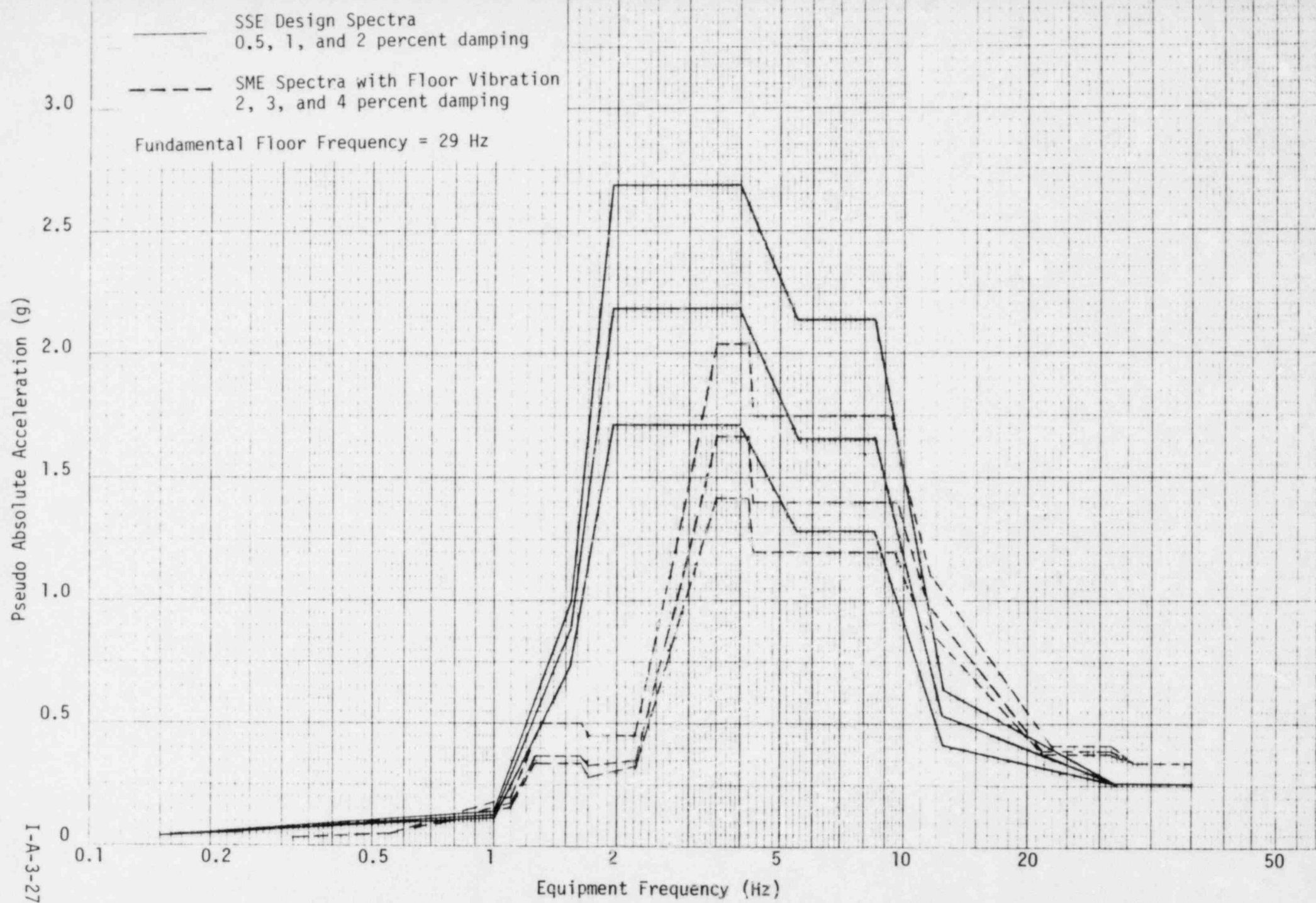


FIGURE A-3-10. COMPARISON OF SSE DESIGN AND SME VERTICAL SPECTRA AT ELEVATION 642'-7", PENETRATION WING

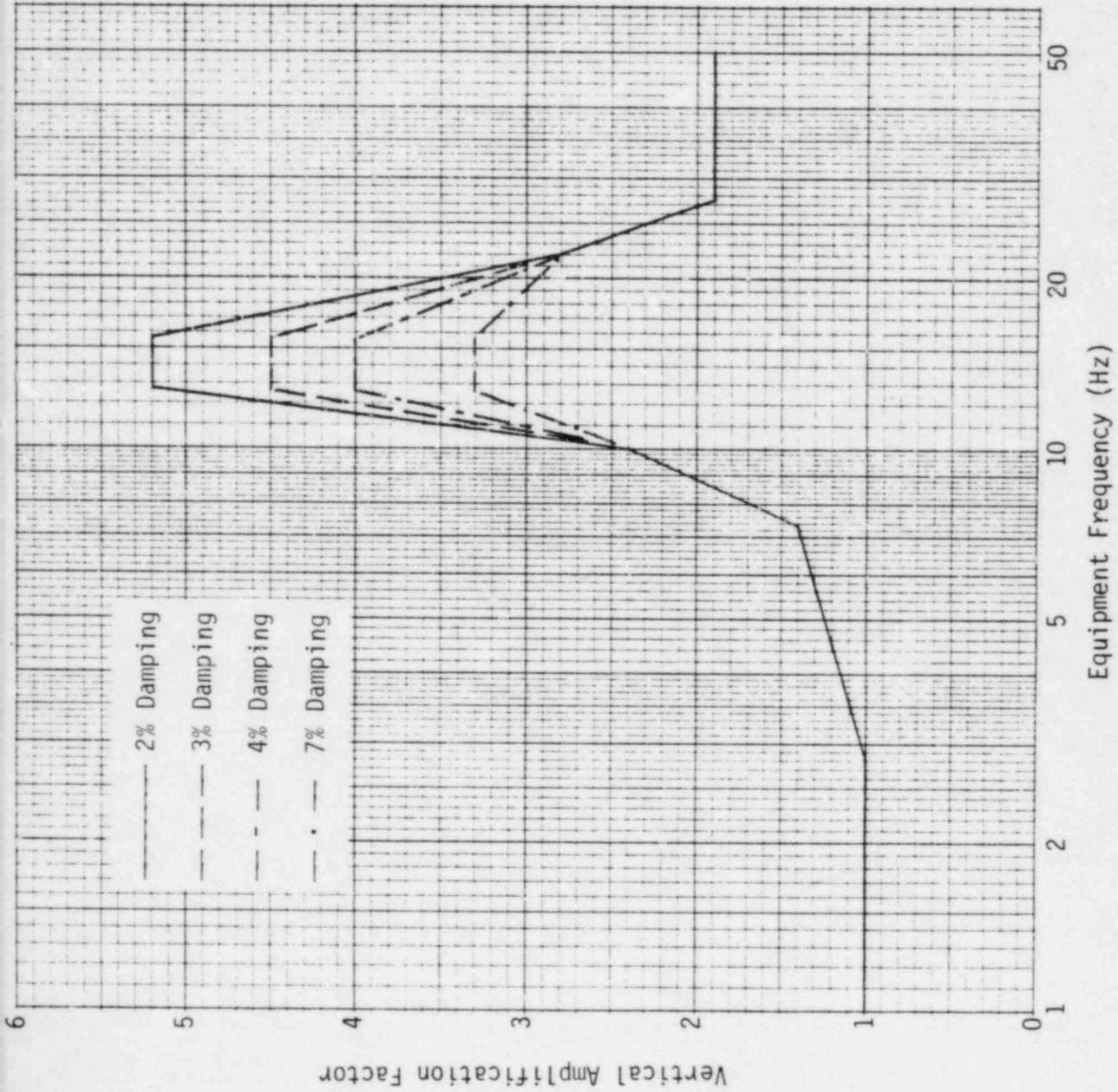


FIGURE A-3-11. ENVELOPE VERTICAL AMPLIFICATION FACTORS FOR AUXILIARY BUILDING

I-A-3-29

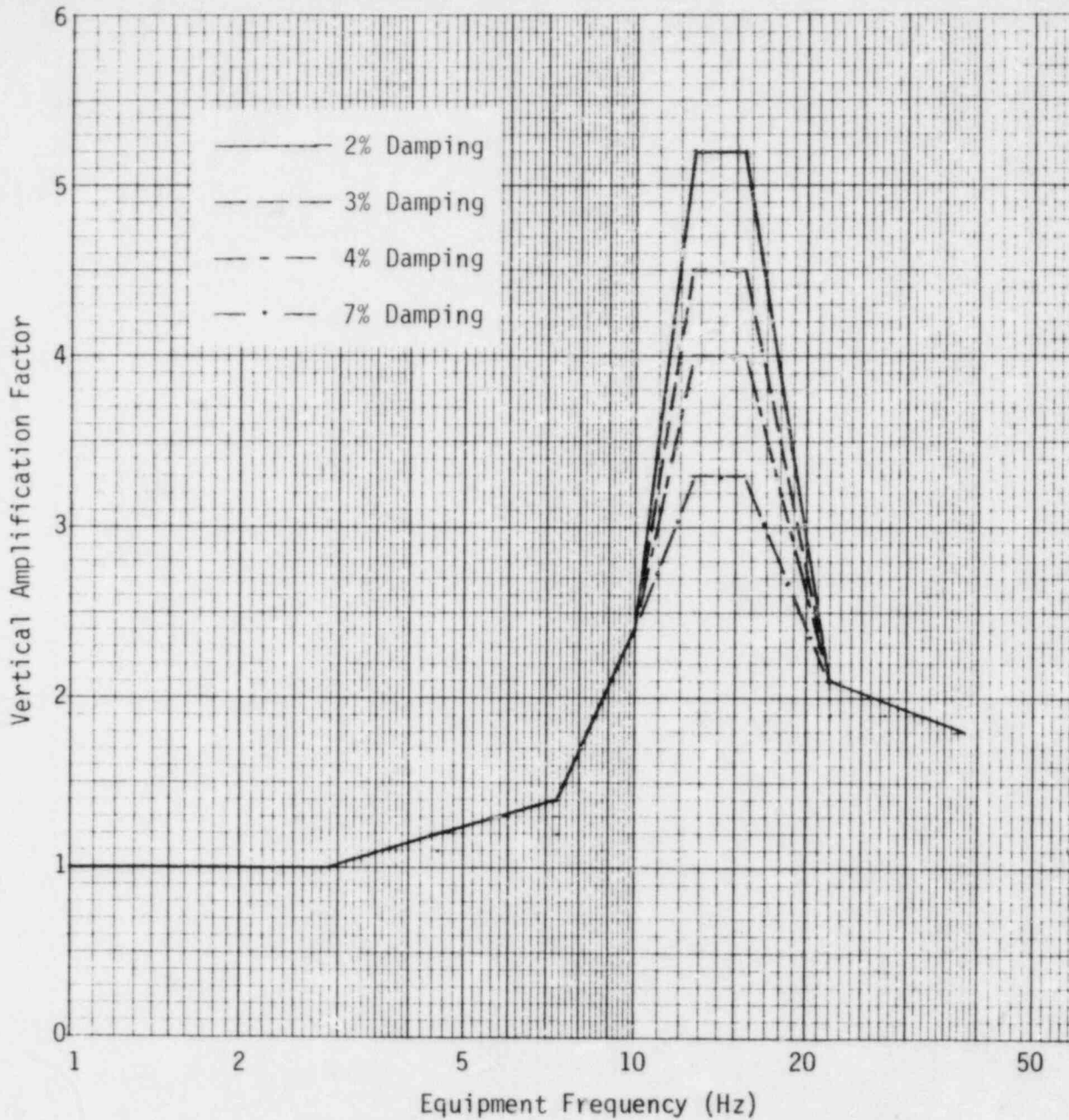


FIGURE A-3-12. VERTICAL AMPLIFICATION FACTOR FUNCTIONS FOR 14 Hz FUNDAMENTAL FREQUENCY FLOORS FOR AUXILIARY BUILDING

I-A-3-30

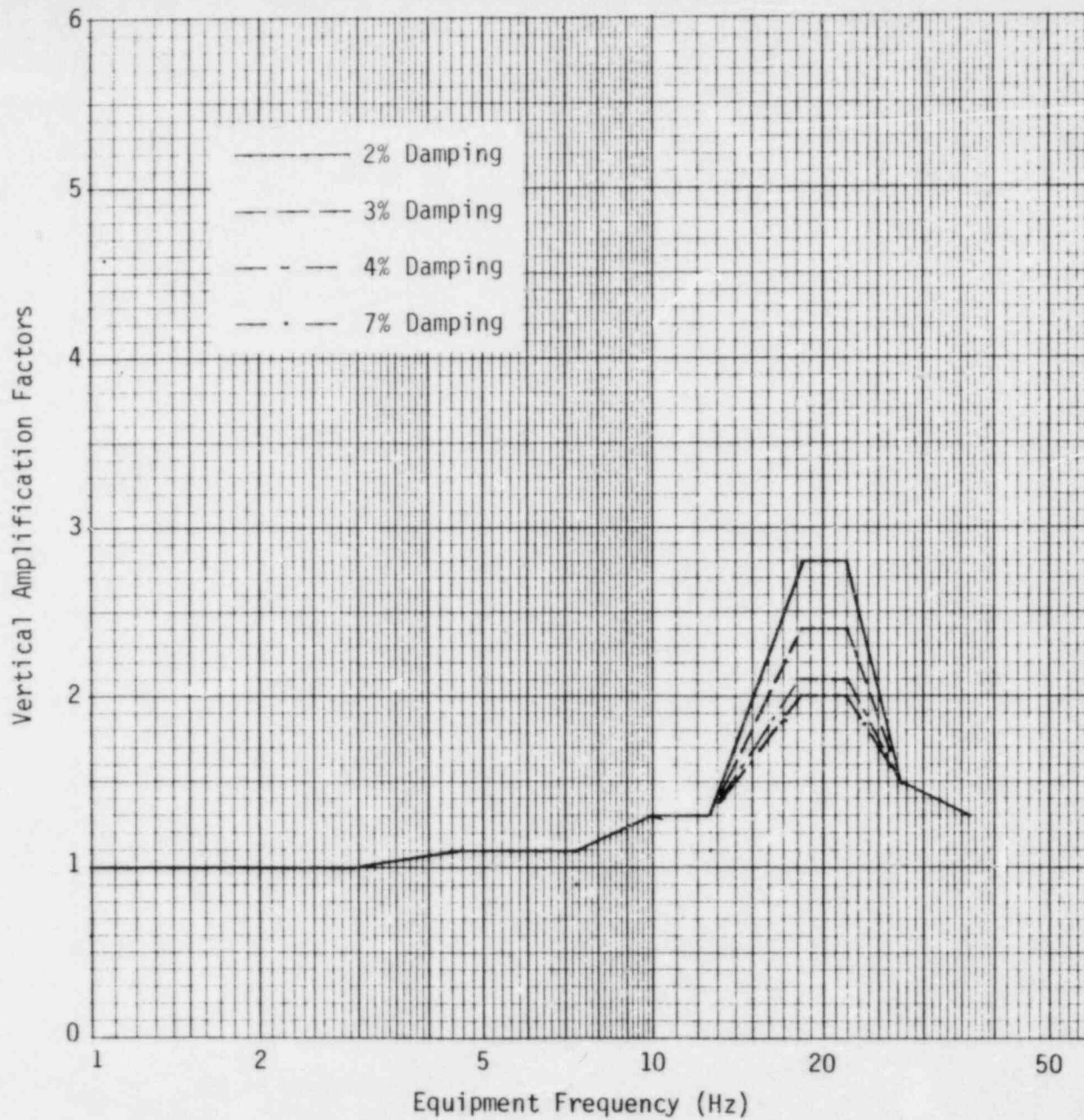


FIGURE A-3-13. VERTICAL AMPLIFICATION FACTOR FUNCTIONS FOR 20 Hz FUNDAMENTAL FREQUENCY FLOORS FOR AUXILIARY BUILDING

I-A-3-31

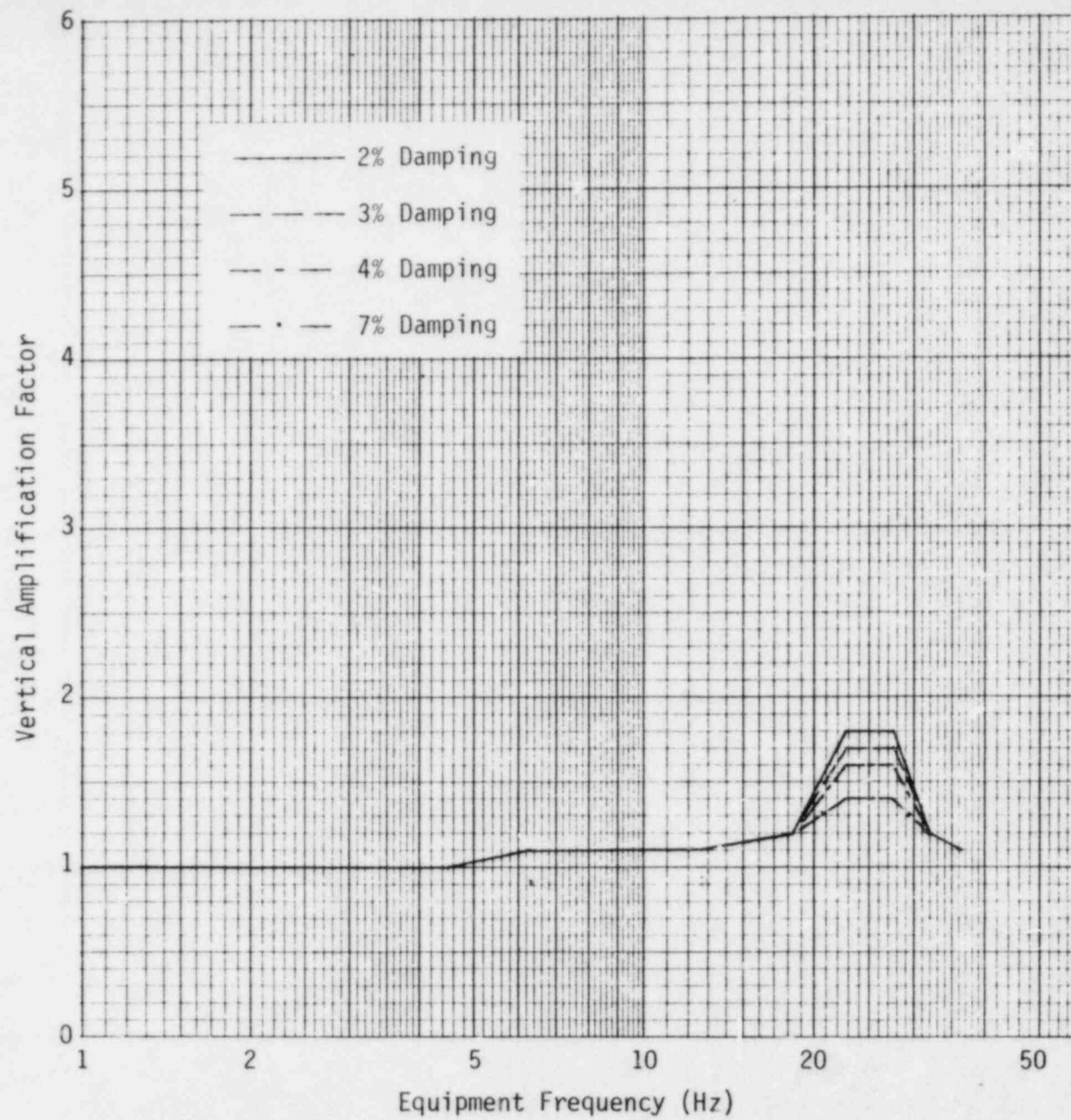


FIGURE A-3-14. VERTICAL AMPLIFICATION FACTOR FUNCTIONS FOR 25 Hz FUNDAMENTAL FREQUENCY FLOORS FOR AUXILIARY BUILDING

I-A-3-32

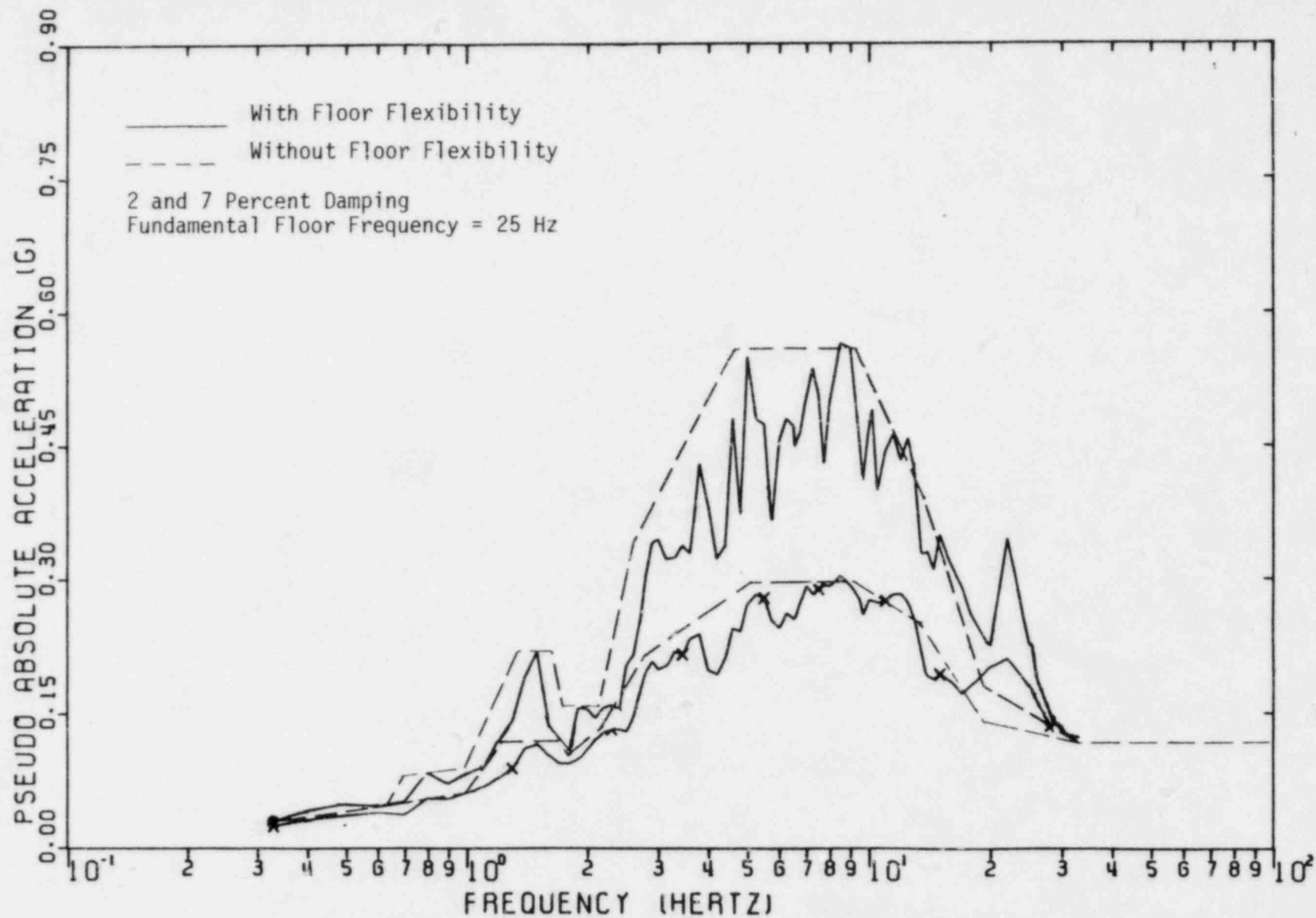


FIGURE A-3-15. COMPARISON OF VERTICAL SPECTRA WITH AND WITHOUT FLOOR FLEXIBILITY AT ELEVATION 634'-0", SERVICE WATER PUMP STRUCTURE

— SSE Design Spectra
 0.5, 1, and 2 percent damping
 - - - SME Spectra with Floor Vibration
 2, 3, and 4 percent damping
 Fundamental Floor Frequency = 25 Hz

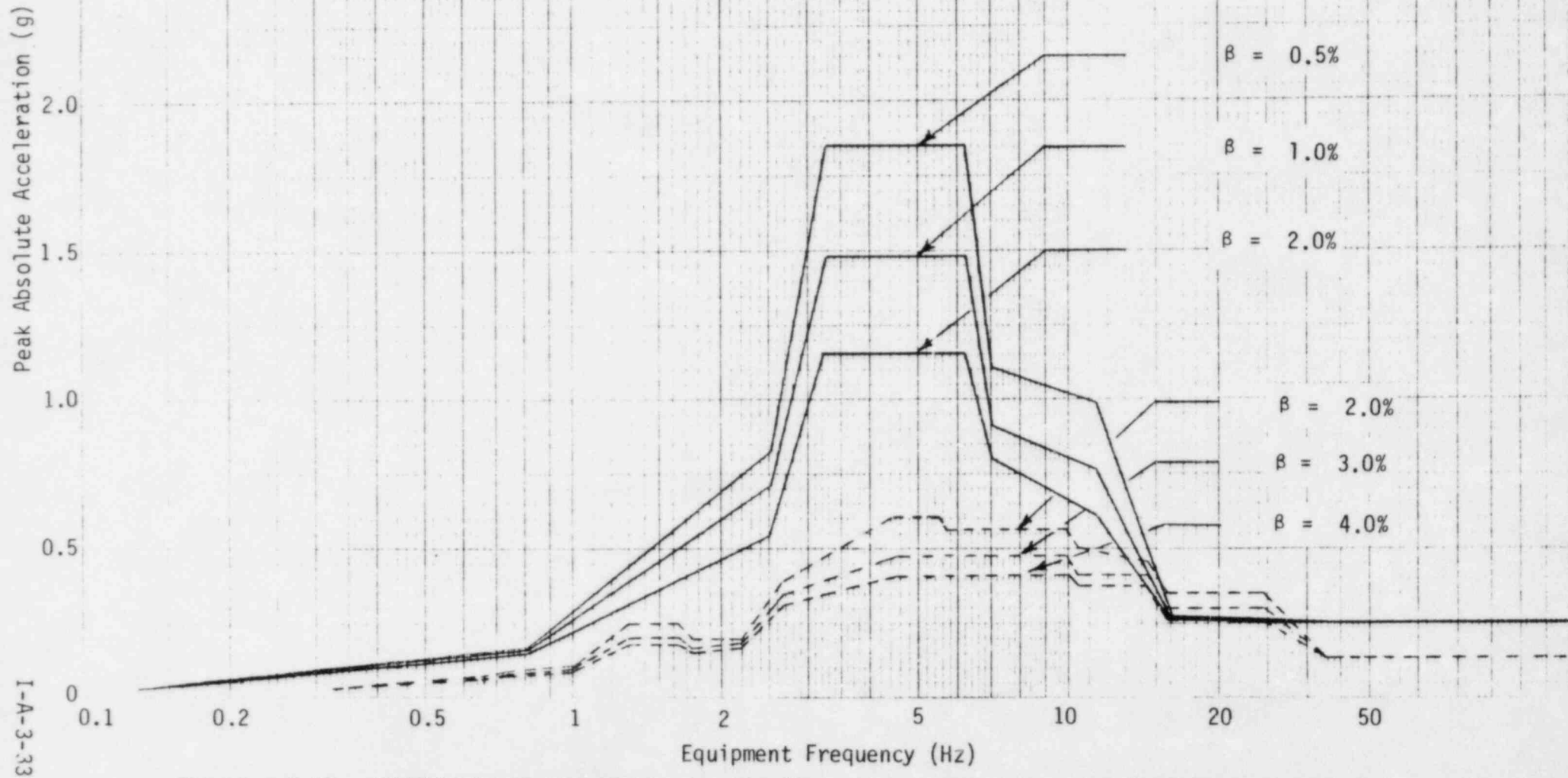


FIGURE A-3-16. COMPARISON OF SSE DESIGN AND SME (INCLUDING FLOOR FLEXIBILITY) VERTICAL SPECTRA AT ELEVATION 634'-6, SERVICE WATER PUMP STRUCTURE

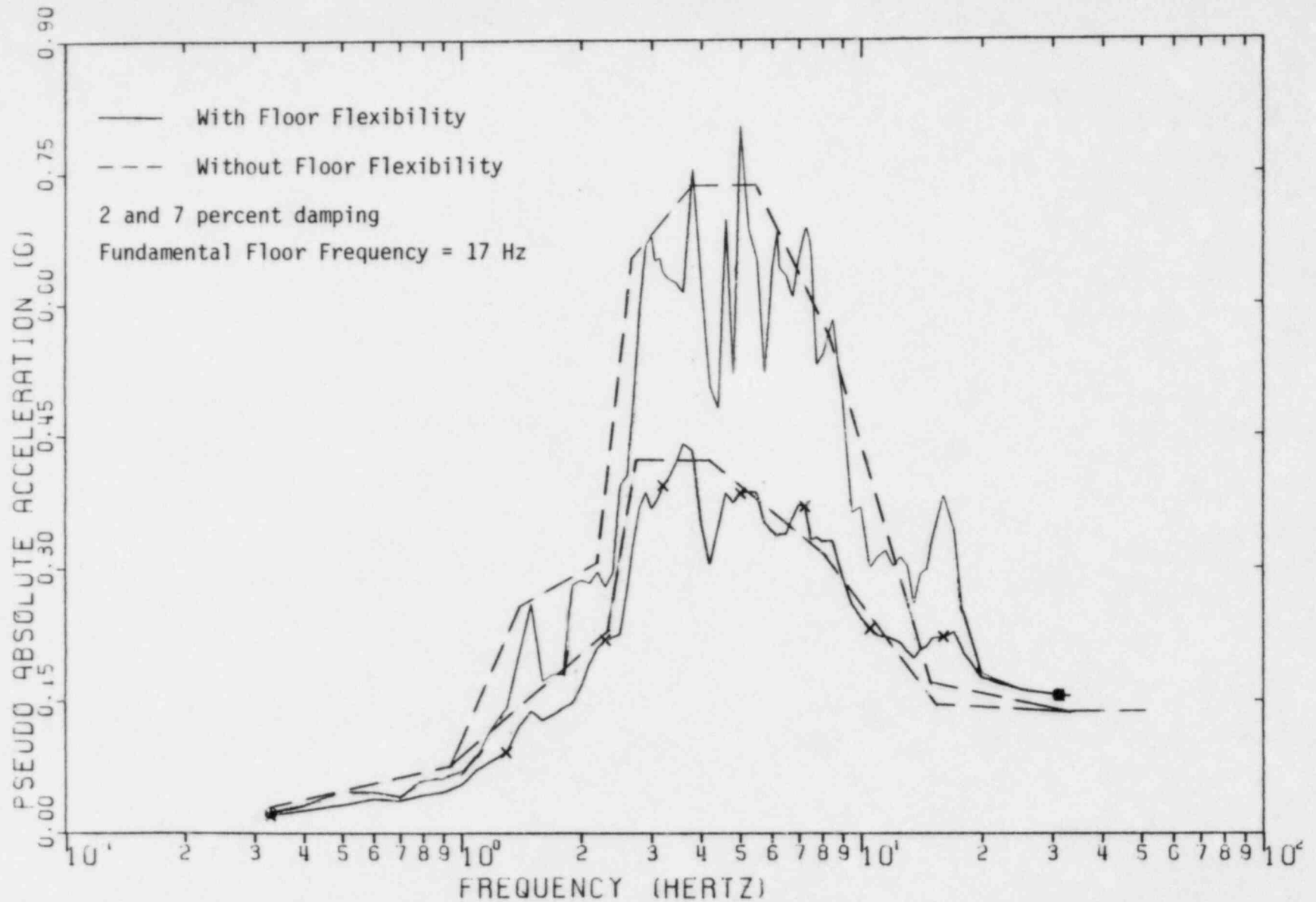


FIGURE A-3-17. COMPARISON OF VERTICAL SPECTRA WITH AND WITHOUT FLOOR FLEXIBILITY. ELEVATION 664'-0", DIESEL GENERATOR BUILDING

— SSE Design Spectra
 0.5, 1, and 2 percent damping

- - - SME Spectra with Floor Vibration
 2, 3, and 4 percent damping

Fundamental Floor Frequency = 17 Hz

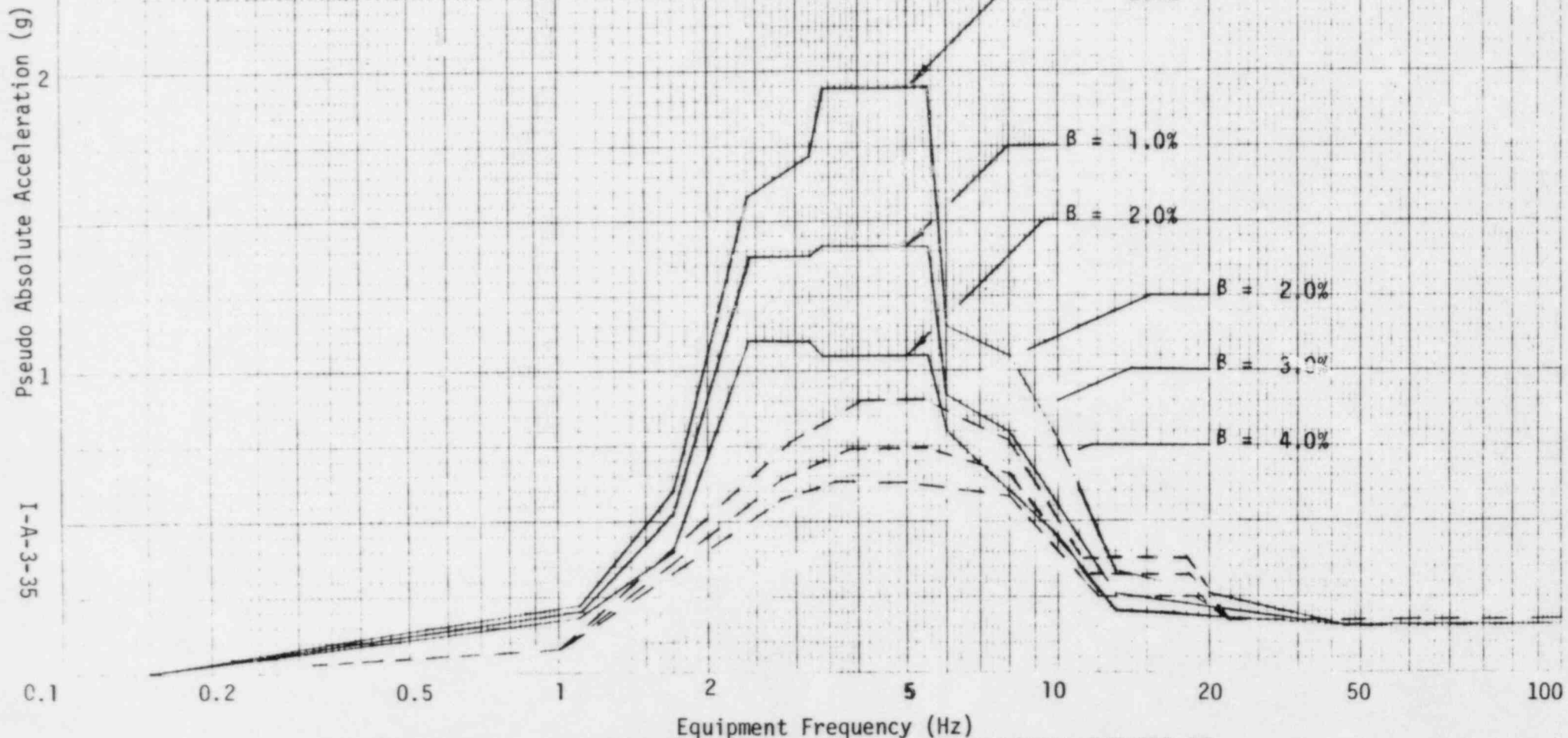


FIGURE A-3-18. COMPARISON OF SSE DESIGN AND SME VERTICAL SPECTRA AT ELEVATION 664'-0", DIESEL GENERATOR BUILDING

A-4. SUMMARY

This appendix describes the study conducted to evaluate the effects of vertical floor slab flexibility on the in-structure response spectra to be used in the SME evaluation of the Midland Plant. Lumped mass models developed for the seismic analysis of nuclear power plant structures often do not consider the local flexibility of floor slabs in the generation of seismic input to floor-mounted equipment and piping. For in-plane slab behavior, this treatment introduces little error since floor slabs generally have large in-plane stiffnesses. However, the out-of-plane stiffnesses may be relatively low, particularly if the slabs have significant openings or must span long distances between vertical supports. If the fundamental out-of-plane floor frequency is low enough, the in-structure response spectra may significantly exceed those generated by neglecting floor flexibility in the vertical direction. The seismic models received by SMA did not account for floor slab flexibility, so this study was undertaken to evaluate the influence of vertical floor amplification on the in-structure response spectra.

A screening process, described in Reference A-1, was conducted to select floor slabs in each of the Seismic Category 1 Midland structures for detailed evaluation. The floors chosen were those expected to exhibit the greatest amount of vertical amplification. Finite element models were created to determine the fundamental vertical frequency of each floor. Model boundaries, with appropriate boundary conditions, were generally established at locations of vertical support. Concrete slabs were represented by plate elements and concrete and steel beams and girders by beam elements. Mass of the structural elements, non-load bearing interior walls, and any attached equipment was accounted for in the models. Static analyses were performed to determine concrete stresses under normal operating loads including vertical seismic response. Results of these analyses indicated that significant slab cracking was unexpected and that the slabs could be adequately represented by their gross stiffnesses.

Single-degree-of-freedom (SDOF) lumped mass models having frequencies calculated by the finite element models were created for each of the floors. The SDOF models of the auxiliary building floors were uncoupled from the overall soil-structure model. Acceleration time-histories generated by the overall model were used as seismic input to the SDOF floor models. Resulting time-histories were used to generate in-structure response spectra including floor flexibility. Significant increases in the response spectra were indicated for the floors having the lower fundamental frequencies (11 to 14 Hz) at equipment frequencies approaching those of the floors. In addition, increases to a lesser degree in the zero period acceleration were found for these more flexible floors. By defining vertical amplification factor functions from the auxiliary building response spectra including floor flexibility, an approach was devised to develop response spectra to be used in the SME equipment evaluation for floors not included in this detailed study. Spectral accelerations including floor flexibility can be determined for given floor frequencies and equipment frequencies, dampings, and locations.

Both the Service Water Pump Structure (SWPS) and the diesel generator building were expected to have only a single floor supporting safety-related equipment which exhibits significant vertical amplification. The SDOF lumped mass floor models for these structures were incorporated in the overall soil-structure models. Floor response acceleration time-histories were generated directly as a part of the overall structure response analysis. A comparison of the response spectra with and without floor flexibility revealed the same trends as those described above for the auxiliary building. The magnitudes of the vertical amplification factors for the SWPS and the diesel generator building were reasonably consistent with those for the auxiliary building.

APPENDIX I-A

REFERENCES

- A-1. Wesley, D. A., Letter to Dr. Thiru Thiruvengadam, Consumers Power Company, 1945 West Parnall Road, Jackson, Michigan, January 6, 1982.

- A-2. Johnson, J. J., "MODSAP-A Modified Version of the Structural Analysis Program SAP IV for the Static and Dynamic Response of Linear and Localized Nonlinear Structures", GA-A14006, UC-77, June, 1976.

- A-3. "Code Requirements for Nuclear Safety Related Concrete Structures (ACI 349-80) and Commentary - ACI 349R-80", American Concrete Institute, Detroit, Michigan, 1980.

APPENDIX I-B

USE OF NONLINEAR BEHAVIOR TO MODIFY SEISMIC DESIGN LOADS

APPENDIX I-B

B.1 EFFECT OF NONLINEAR RESPONSE AND DUCTILITY REDUCTION FACTORS

It has long been recognized that the inherent seismic resistance of a well designed and constructed system is usually much greater than that expected based on elastic analysis largely because nonlinear behavior is mobilized to limit the imposed forces and accompanying deformations. To consider this effect rigorously, it would be necessary to perform time-history nonlinear analysis which is still the fringe of the state-of-the-art for real structures and components. Newmark and Hall (Reference B-1) have suggested the use of a modified elastic response spectra as a tractable solution to the problem. In this criteria a Ductility Reduction Factor, k , is developed as suggested by Villanueva (Reference B-2) and applied directly to elastically derived seismic loads.

Ductility reduction factor formulas are mathematically derived by assuming either: (1) that displacements are equal whether the structure behaves in an elastic or elasto-plastic manner or, (2) that the energy absorbed in an elastic system equals that of an elasto-plastic system. Then, multiply each earthquake force in the member by the ductility reduction factor with the earthquake force in the member being computed from a pseudo-static or full dynamic linear analysis. Use these "reduced" earthquake forces to design the members. The underlying principle used here is that stress in a member will not continue to increase once it reaches its yield point.

B.2 DEFINITION OF DUCTILITY

Ductility as used herein is defined as the ratio of the maximum displacement to the displacement at yield point.

$$\mu = \frac{\delta_{\max}}{\delta_y} \quad (\text{B-1})$$

The term ductility generally implies strain values within the elasto-plastic range, and in this range ductility, μ , values are greater than one.

B.3 DERIVATION OF DUCTILITY REDUCTION FACTOR FORMULAS

There are two formulas commonly used to calculate the ductility reduction factor, k . The derivation of these two formulas is shown below. Each is derived using the following respective assumptions:

Assumption 1 - Applicable for frequencies below 2 Hz. For the same structure and loading, the maximum displacements of a nonlinear elasto-plastic analysis equal those obtained if a linear elastic (no yield limit) analysis were made (Reference B-3).

From Figure B.1 the actual (yield) force equation is:

$$f_y = \frac{\delta_y}{\delta_{\max}} f_{\max} \quad (\text{B-2})$$

Clearly the ductility reduction factor equation is:

$$k = \frac{1}{\mu} \quad (\text{B-3})$$

Assumption 2 - Applicable for frequencies in the 2-8 Hz range. For the same structure and loading, the energy absorbed is the same for both the elasto-plastic system and the elastic system.

Equating equivalent energies $E_e = E_p$ as shown in Figure B.2 and B.3, we have:

$$\frac{1}{2} k \delta_y^2 + (\delta_{\max} - \delta_y) K \delta_y = \frac{1}{2} K \bar{\delta}_{\max}^2 \quad (B-4)$$

Dividing by the stiffness k and the square of the deformation at yield δ_y and substituting $\mu = \delta_{\max} / \delta_y$, the above equation can be rewritten as

$$2\mu - 1 = \frac{\bar{\delta}_{\max}}{\delta_y^2} \quad (B-5)$$

or

$$\bar{\delta}_{\max} = \sqrt{2\mu - 1} \delta_y \quad (B-6)$$

Since $f = k\delta$, the ductility reduction factor is:

$$k = \frac{1}{\sqrt{2\mu - 1}} \quad (B-7)$$

For frequencies above 8 Hz the value of k increases linearly to the value of 1.0 at 33 Hz.

B.4 LIMITATIONS ON THE USE OF THE DUCTILITY REDUCTION FACTOR, k , AND THE DUCTILITY, μ

While the use of ductility reduction factor, k , is a practical means for introducing the effect of nonlinear response and ductility into seismic design, it must be used with care. The ductility reduction factor, k , is based on the global or systems ductility. It is quite possible in a given structural system that local ductility demand can exceed the assumed system ductility (Reference B-4). In this criteria, the limiting system ductility, $\mu = 1.3$, has been conservatively selected to ensure local ductility demands can be met. Use of this rather conservative systems ductility factor results in a ductility reduction factor, $k \cong 0.8$ for components with dominant frequencies at and below 8 Hz and varies linearly to $k = 1.0$ between 8 and 33 Hz. In addition,

since strain softening behavior which is also characteristic of buckling behavior can result in large local ductility demands, members subject to buckling shall use $k = 1.0$. Also in cases where a brittle-type failure mode associated with shear failures is dominant, k will be limited to 1.0. Finally, in cases where the effect on local ductility demand has been assessed, k values less than 0.8 may be used.

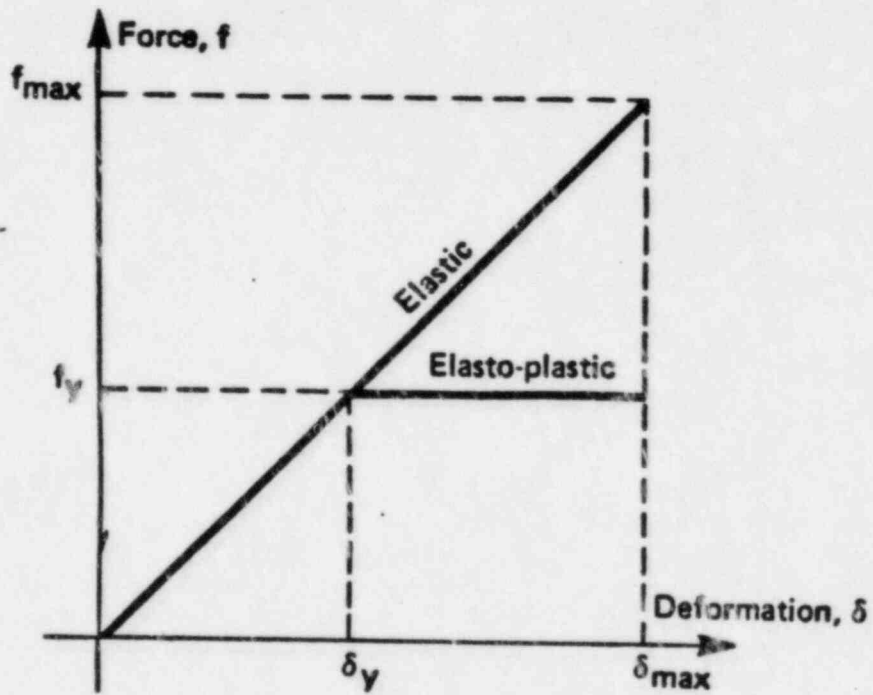


FIGURE B.1: SUPERIMPOSED FORCE - DEFORMATION DIAGRAMS

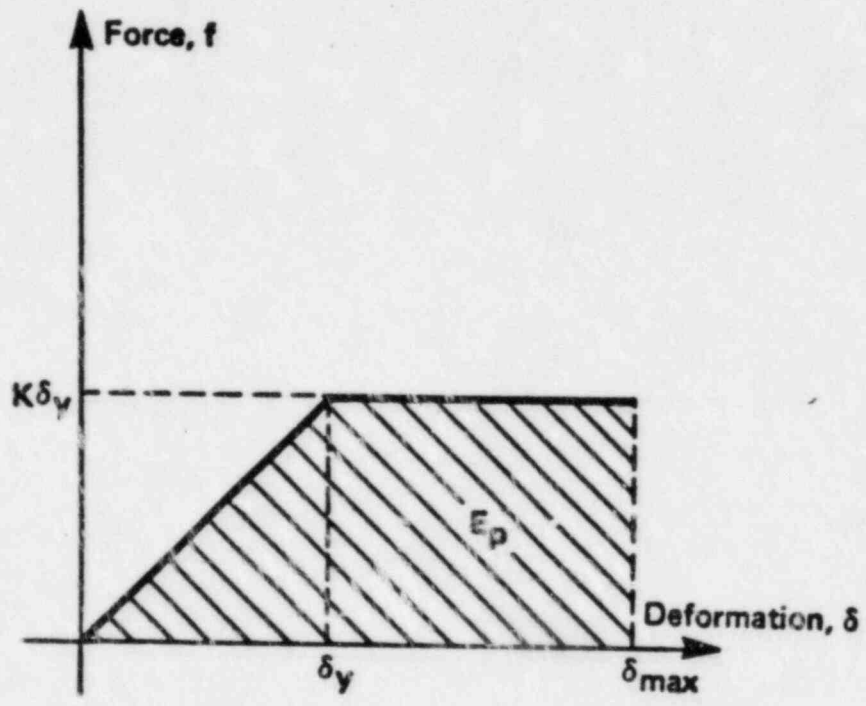


FIGURE B.2: ELASTO-PLASTIC DIAGRAM

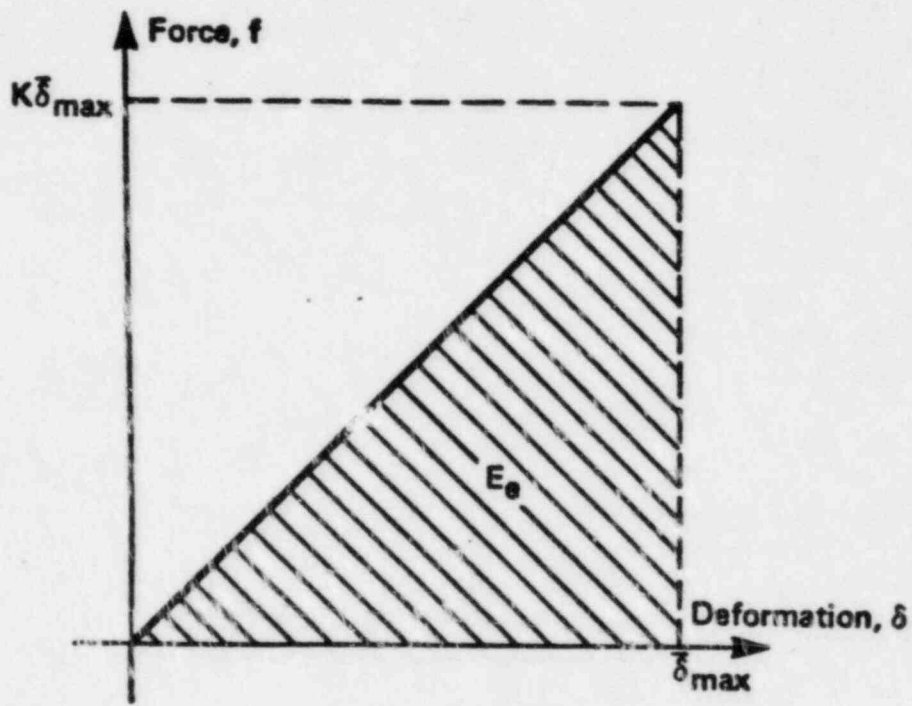


FIGURE B.3: ELASTIC (NO YIELD LIMIT) DIAGRAM

APPENDIX I-B

REFERENCES

- B-1. Newmark, N. M., and Hall, W. J., Development of Criteria for Seismic Review of Selected Nuclear Power Plants, NUREG/CR-0098, May, 1978.
- B-2. Villaneuva, A. S., "Ductility Reduction Factors for Earthquake Design," Reprint 3209, ASCE Spring Convention, Pittsburgh, Pennsylvania, 1978.
- B-3. Clough, R. W. and Penzien, J., Dynamics of Structures, McGraw-Hill Co., New York, 1975.
- B-4. Mahin, S. A. and Bertero, V. V., "An Evaluation of Inelastic Seismic Design Spectra," Reprint 3278, ASCE Convention, April, 1978.